DESIGN, SYNTHESIS AND EVALUATION OF SMALL MOLECULES FOR PROFILING THIOL PROTEOME OF MICROBES

A THESIS

SUBMITTED IN PARTIAL FULFILMENT OF THE REQUIREMENTS

OF THE DEGREE OF

DOCTOR OF PHILOSOPHY

BY

AMOGH KULKARNI

20122031

INDIAN INSTITUTE OF SCIENCE EDUCATION AND RESEARCH PUNE – 411 008

2019

Dedicated to…

My Parents

Aparna & Maheshchandra

…standing on whose shoulders I have seen way further!!!

"If I have seen further it is by standing on the shoulders of Giants." - Sir Isaac Newton

भारतीय विज्ञान शिक्षा एवं अनुसंधान संस्थान, पुणे
INDIAN INSTITUTE OF SCIENCE EDUCATION AND RESEARCH (IISER), PUNE
(An Autonomous Institution, Ministry of Human Resource Development, Govt. of India)
900 NCL Innovation Park Dr Homi Bhabha Road Pune 411008

Harinath Chakrapani, Ph.D.
Associate Professor – Chemistry
www.iiserpune.ac.in/~harinath/

CERTIFICATE

Certified that, the work incorporated in the thesis entitled, "***Design, Synthesis and Evaluation of Small Molecules for Profiling Thiol Proteome of Microbes***" submitted by ***Amogh Kulkarni*** was carried out by the candidate, under my supervision. The work presented here or any part of it has not been included in any other thesis submitted previously for the award of any degree or diploma from any other University or institution.

Date: 20th December 2019 **Dr. Harinath Chakrapani**

Pune (MH), India.

DECLARATION

I declare that this written submission represents my ideas in my own words and where others' ideas have been included; I have adequately cited and referenced the original sources. I also declare that I have adhered to all principles of academic honesty and integrity and have not misrepresented or fabricated or falsified any idea/data/fact/source in my submission. I understand that violation of the above will be cause for disciplinary action by the Institute and can also evoke penal action from the sources which have thus not been properly cited or from whom proper permission has not been taken when needed.

Date: 20th December 2019 **Amogh Kulkarni**

Pune (MH), India. **20122031**

Table of Contents

General Remarks

- ^{1}H spectra were recorded on a JEOL ECX 400 MHz or a Bruker 400 MHz spectrometer unless otherwise specified using as an internal tetramethylsilane (δ_H = 0.00). Chemical shifts are expressed in ppm units downfield to TMS.
- ^{13}C spectra were recorded on a JEOL 100 MHz or a Bruker 100 MHz spectrometer unless otherwise specified using as an internal tetramethylsilane (δ_C = 0.0).
- Chemical shifts (δ) are reported in ppm and coupling constants (*J*) in Hz.
- Mass spectra were obtained using HRMS-ESI-Q-Time of Flight LC-MS (Synapt G2, Waters) or MALDI TOF/TOF Analyser (Applied Biosystems 4800 Plus).
- FT-IR spectra were obtained using Bruker Alpha-FT-IR spectrometer and reported in cm^{-1}.
- All reactions were monitored by Thin-Layer Chromatography carried out on precoated Merck silica plates (F254, 0.25 mm thickness); compounds were visualized by UV light.
- All reactions were carried out under nitrogen atmosphere with dried solvents under anhydrous conditions and yields refer to chromatographically homogenous materials unless otherwise stated.
- All evaporations were carried out under reduced pressure on Büchi and Heildoph rotary evaporator below 45 °C unless otherwise specified.
- Silica gel 60-120 and 100-200 mesh were used for column chromatography.
- Materials were obtained from commercial suppliers and were used without further purification.
- Preparative HPLC purification was performed using high performance liquid chromatography (HPLC) with C-18 preparative column (21.2 mm × 250 mm, 10 μm; Kromasil®C-18).
- HPLC analysis data was obtained using Agilent Technologies 1260 Infinity, C18 reversed phase column (4.6 mm × 250 mm, 5 μm).
- Spectrophotometric and fluorimetric measurements were performed using Thermo Scientific Varioscan microwell plate reader.
- All SDS-PAGE gels (activity based gels and coomassie gels) were imaged on a Syngene G-Box Chemi-XRQ gel documentation system.

Abbreviations

% - Percent

χ - Electronegativity

$\Delta G^{\ddagger}$ - Gibbs Free energy

µg - Microgram

µL - Microliter

µM - Micromolar

ABP - Activity-based probe

ABPP - Activity-Based Protein Profiling

Ac - Acetyl

ACN - Acetonitrile

ADP - Adenosine diphosphate

AECs - aminoepoxycyclohexenones

AMR - antimicrobial resistance

AR - Amplex Red

ATCC - American-type culture collection

ATP - Adenosine triphosphate

au – Arbitrary unit

B. subtilis - *Bacillus subtilis*

bBBr - bibromobimane

BBR - Benzbromarone

BCA - Bichinchoninic acid

BME - β-mercaptoethanol

bs - Broad singlet

BSA - Bovine serum albumin

BSH - Bacillithiol

BTK - Bruton's Tyrosine Kinase

C. difficile - *Clostridium difficile*

Calcd – Calculated

CCDC - Cambridge crystallographic data centre

CcpA - Catabolite control protein A

$CDCl_3$ - Chloroform-D

CDNB - chloro-dinitrobenzene

CFU - Colony forming unit

$CHCl_3$ - Chloroform

ClpP - caseinolytic protein protease

Ctrl - Control

CuAAC - Copper-catalyzed Alkyne-Azide Cycloaddition

$CuSO_4.5H_2O$ – Copper sulfate pentahydrate

CV - Cyclic voltammetry

Cys - Cysteine

DAD - Diode array detector

DCF - 2',7'-dichlorodihydrofluorescein

DCM - Dichloromethane

dd - Doublet of doublet

DMF - *N*,*N*-Dimethylformamide

DMSO - Dimethylsulfoxide

DNA - Deoxyribonucleic acid

DPBS - Dulbecco's Phosphate-Buffered Saline

Dpn1 - Type IIM restriction enzyme

dt - Doublet of triplet

DTNB - 5,5'-dithiobis-(2-nitrobenzoic acid)

DTT - Dithiothreitol

E64 - *L*-trans-Epoxysuccinyl-leucylamido(4-guanidino)butane

EDG - Electron donating group

EGFRs - Epidermal growth factor receptor

equiv. - Equivalents

ESI - Electron spray ionization

ESKAPE - *E. coli, S. aureus, K. pneumonia, A. baumannii, P. aeruginosa, E. faecalis, E. faecium*

Et_2O - Diethyl ether

Et_3N - Triethylamine

etc - et cetera

EtOAc - Ethyl acetate

EtOH - Ethanol

EWG - Electron withdrawing group

FDNB - 1-Fluoro-2,4-dinitrobenzene

FLD - Fluorescence detector

FPLC - Fast protein liquid chromatography

FP-TAMRA - Fluorophosphonate-based Tetramethyl rhodamine

FT-IR - Fourier transform Infra Red spectroscopy

g - Gram

GSH - Glutathione

h - Hours

H_2DCF-DA - 2',7'-dichlorodihydrofluorescein diacetate

H_2O - Water

H_2O_2 - Hydrogen peroxide

HCl - Hydrochloric acid

Hla - α-hemolysin

HPLC - High performance liquid chromatography

HRMS - High-resolution mass spectrometry

HRP - Horseradish peroxidase

HSQC - Heteronuclear single quantum coherence spectroscopy

Hz - Hertz

IAA - iodoacetamide alkyne

IAM - Iodoacetamide

IC_{50} - Half maximal inhibitory concentration

INDQE - Indole-based naphthoquinone epoxide

in situ - describes a process involving compound treatment in live cells followed by the profiling of the proteins from the lysates

^{i}Pr - isopropyl

IPTG - Isopropyl-β-D-1-thiogalactopyranoside

IR - Infrared

IUPAC - International Union of Pure and Applied Chemistry

J - Coupling constant

K_2CO_3 - Potassium carbonate

LB - Luria Bertani

LC-MS/MS - Liquid chromatography-Mass spectrometry Mass spectrometry

LDE - Lipid-derived electrophiles

LPS - Lipopolysaccharide

m - Multiplet

M. tuberculosis - *Mycobacterium tuberculosis*

m/*z* - Mass to Charge ratio

MALDI - Matrix-Assisted Laser Desorption Ionization

Mar R - Multiple antibiotic resistance regulator

mBBr - monobromobimane

Me - Methyl

MeOH - Methanol

mg - Milligram

MHB - Mueller Hinton II Broth

MHz - Megahertz

MIC - Minimum inhibitory concentration

Min. - Minutes

mL - Millilitre

mM - Millimolar

mmol - Millimoles

MRSA - Methicillin-resistant *S. aureus*

MS - Mass spectrum

MSTP - 4-(5-methanesulfonyl-[1,2,3,4]tetrazol-1-yl)-phenol

MTT - 3-(4,5-Dimethylthiazol-2-yl)-2,5-diphenyltetrazolium bromide

MurA - UDP-*N*-acetylglycosamine-1-carboxyvinyltransferase

MW - Molecular weight

Na_2SO_4 - Sodium sulphate

NaH - Sodium hydride

$NaHCO_3$ - Sodium bicarbonate

NaI - Sodium iodide

$NaNO_2$ - Sodium nitrite

NaOCl - Sodium hypochlorite

NBD-Cl - 4-chloro-7-nitrobenzofurazan

n-BuLi - *n*-butyllithium

NEM - *N*-ethylmaleimide

NH_4Cl - Ammonium chloride

Ni-NTA - Nickel-nitrilotriacetic acid

NMM - *N*-methylmaleimide

NMR - Nuclear magnetic resonance

NOESY - Nuclear Overhauser Effect Spectroscopy

NQEs - Naphthoquinone epoxides

O.D. - Optical density

oxPTM - oxidative PTM

P450 - Cytochrome P450

PBS - Phosphate Buffer Saline

PCR - Polymerase chain reaction

PDI - Protein Disulfide Isomerase

Ph - Phenyl

pH - Potential of hydrogen

pK_a - negative base -10 logarithm of the acid dissociation constant K_a

ppm - Parts per million

PTM - Post-translational Modification

RNS - Reactive nitrogen species

ROS - Reactive Oxygen Species

RSS - Reactive sulfur species

R_t - Retention time

RT - Room temperature

s - Singlet

S. aureus - *Staphylococcus aureus*

S. epidermis - *Staphylococcus epidermis*

S. typhimurium - *Salmonella typhimurium*

SAR - Structure Activity Relationship

SDS-PAGE - Sodium dodecyl sulphate polyacrylamide gel electrophoresis

SiO_2 - Silica

SLIC - sequence- and ligation-independent cloning

STEFs - semi-oxamide vinylogous thioesters

t - Triplet

TBHP - *tert*-butyl hydroperoxide

TBTA - Tris(benzyltriazolylmethyl)amine

TCEP - Tris(2-carboxyethyl)phosphine hydrochloride

TCI - Targeted covalent inhibitors

TDAE - tosyl-substituted doubly activated ene

TF - Transcriptional factors

TFA - Trifluoroacetic acid

THF - Tetrahydrofuran

TLC - Thin layer chromatography

TMS - Tetramethylsilane

TrX - Thioredoxin

UV - ultraviolet

VISA - Vancomycin-intermediate *Staphylococcus aureus*

VRSA - Vancomycin-resistant *Staphylococcus aureus*

WHO - World Health Organisation

Zn - Zinc

λ_{em} - Emission wavelength

λ_{ex} - Excitation wavelength

δ – Delta (in ppm)

Acknowledgements

It is always wonderful to thank the people who have contributed to your success, and a success like getting a PhD degree stands out from all other successes.

To start with, it is imperative to write about ***Hari***, my supervisor, Dr. Harinath Chakrapani. Thanking him is not something that needs to be done formally. He has been a person who has supported and guided me through the hardships of PhD, and has constantly kept motivating me to keep up the good work, not only in times of successes but more so in times of troubles and failures. I have learnt a number of things from Hari, not only in science but in life, in general. Topping the list are punctuality, professionalism and presentation skills.

The next person who has been a backbone in my thesis work is Dr. Siddhesh Kamat. ***Siddhesh*** joined the Department of Biology at IISER Pune as a Faculty when I was in my fifth year of the Integrated PhD programme. We were struggling with the INDQE project as the manuscript had been rejected twice from the Journal of Medicinal Chemistry, even after extensive Chemistry and Biology work done, both from our lab and from the lab of our collaborator, ***Dr. Sidharth Chopra*** at CDRI, Lucknow. We were looking for some help and guidance in order to push the project further. Siddhesh agreed to help us and that I feel was the turning point of my PhD.

Faculties like ***Dr. Hotha***, ***Dr. Srivatsan*** and ***Dr. Gopi*** (present Chair, Chemistry) have been an integral part of my RAC and Comprehensive Seminar Meetings, and their suggestions have contributed extensively to my Thesis work. ***Dr. C. V. Ramana*** from NCL has also been very helpful during my RAC meetings. I earnestly thank ***Dr. Amrita Hazra*** for her valuable suggestions and for helping me understand certain key biological concepts. I also thank all other Faculty members at IISER and our former director Prof. K. N. Ganesh and our present director Prof. Jayant Udgaonkar, who have contributed to my growth as a science student and a researcher. I also thank Prof. Jayakannan, former Chair, Chemistry for his infrastructural support.

Lab colleagues are like a family away from Home. I have been blessed with some fabulous people who have made significant contributions, not just to my lab work, but also to my life. I cherish my connections with these people. My senior colleagues ***Dharma***, ***Kavita*** and ***Ravi*** were very co-operative and motivating and have taken my mistakes in their stride during my first few years. They have time and again helped me learn the difficult game of PhD and have been patient with me when I have not been able to understand certain key lab skills and practices. I owe a lot to them. Dharma has been my first mentor in the lab, and he has taught me a number of things. Kavita has been very caring all through, even now, and I'm sure it will continue to be so for years to come. Ravi has been a true friend and guide throughout my PhD time and his suggestions and criticisms have always helped me in improving the standard of my work. My other

senior colleagues ***Satish***, ***Vinayak*** and ***Kundan*** have also been very helpful and I have learned a number of things from them.

Ajay and ***Preeti*** joined the lab about 8 months after I had joined and they became very close friends of mine. Ajay has been a comrade in good and bad times, and I have shared almost all my PhD problems with him. We are (were) bench partners, and I have cherished sharing things (apparatus, PJs, food, students etc.) with him. We used to plan trekking trips together and I have enjoyed each one of them with our trekking group. Preeti has also been a nice friend.

My other junior lab colleagues have made this lab a happy place to work in. ***Prerona*** has added different flavours (and smells as well, with H_2S :P) to the lab. She is a joyous girl with a lot of energy (and pitch in her voice :P) that keeps the lab vibrant almost everytime she is around. We have shared a lot of cool stuff together and it has been wonderful to have known her. ***Anand*** is a gem of a person. He has immaculate precision in whatever he does and has immense patience in handling situations. He is very calm and supportive. I have shared lot of stuff (gyan) with him over coffee and his help with my presentations and reports has always been valuable. ***Laxman*** is possibly one of the most inert yet reactive (element) person I have ever met. He is calm and almost unreactive towards difficult situations, yet is playful, laughs, and cracks jokes in the lab. It has been nice to have spent time with him. Interestingly, we shared a Theatrical project together, also entitled 'PhD' which was performed during Chemphilic Club's annual celebrations. ***Pooja*** has been a true friend in times of happiness as well as trouble, and my association with her has been very peaceful and satisfactory. She has contributed substantially to my success and has supported me on emotional grounds as well, when I have been at a very low during my PhD work. I am lucky to have found a genuine friend like her, and I cherish my friendship with her. ***Gaurav*** is a true Delhi guy and comes with a lot of broad and bold views, not only about science, lab, but also about life. He joined the lab for his lab rotation as an Integrated PhD student under my mentorship. He is a very intelligent chap and goes about things very methodically. On the other side, he enjoys his life in his own way. He has been a genuine contributor to my Research projects. ***Suman*** is another Integrated PhD student who joined Hari's lab. He is full of zeal and zest and follows his heart doing science as well as leading life. He is naive at a lot of things, but is a true rebel at injustice done to him (only outside lab :P). Suman also has been part of the 'Sea Minor production' and 'Ratra', which are two of my Theatrical ventures. During this period, we have grown closer as friends and have spent good amount of time together. His contribution has definitely helped both the productions substantially. In the lab too, he has been a good friend to me and I have thoroughly enjoyed spending my time with him. ***Farhan*** is the 'Artist' of the lab. A prolific singer and rationale thinker (uhnnn…), he is also a master at cracking pathetic jokes (God… please help :P). Spending time with him has always been interesting though!!! ***Harshit*** is the latest kid in the lab. As much as he is junior to everyone, he has all capabilities to win over arguments and verbal battles (the pulling leg ones… ;p) against anyone and everyone in the lab. But, he is a genuine guy and knows how to have fun in the lab.

Apart from the PhD and Integrated PhD students, a number of BS-MS people have been a part of my journey. Starting from ***Sharath***, he has been more like a brother to me. We have spent a lot of time together, in classes, in the lab, over Chai, on the cricket ground etc. Our wavelengths match, and we are still in good contact with each other. ***Mrutyunjay*** is someone, whom no one can ever forget. A happy, smiling chubby, MJ joined the lab after his first Semester (What motivation!). He was asked to work with me, and truly I have cherished all moments with him from the time I have known him. He is a hard worker and it has shown in his achievements from time to time. I feel proud and lucky to have been associated with him as his mentor. ***Swetha*** is my dear angel. We have been very close friends and have shared nice memories together. I have always found her caring and motivating. ***Aswin*** is another 'artist' from the lab. My association with him has been more outside the lab than inside. A prolific dancer and choreographer, he is also a very humble person and a true friend of mine. My other students ***Aditya***, ***Shreyas***, ***Ravalika***, ***Manjima*** are very talented and hard-working, and I feel blessed to have had the opportunity to mentor them. ***Viraj*** was a post-doc in the lab and like an elder sister to me. She has her lazy elegance to go with her beautiful smile. She has helped me with learning certain basics of microbiology. She continues to be one of my well-wishers and I feel good to have shared nice moments with her. ***Sankar*** and ***Abhjeet*** were wonderful companions when I started my lab work, and it has been nice to have known them. ***Sushma***, ***Charu***, ***Suraj***, ***Amal***, ***Jishnu***, ***Komal***, ***Ritu***, ***Beulaa*** have been wonderful people to work with and I have thoroughly enjoyed sharing lab space and time with them. Two new PhDs ***Bharat*** and ***Utsav*** recently joined Hari's Lab. My best wishes to them.

Apart from my lab (Dr. HC Lab), I have spent a chunk of time in Kamat Lab learning ABPP and cloning and purification and what not. I truly thank the members of Kamat Lab for helping me learn these new techniques and contributing substantially to my thesis work as well as chemical biology training. I thank ***Dhanashree, Abinaya, Alaumy, Shubham, Kaveri, Minhaj, Neha, Amol, Neelay, Sharvari*** for all their help.

On a similar note, I have spent a lot of time taking help from members of the Amrita Hazra Lab, for all kinds of biological experiments. I truly thank ***Yashwant, Rupali, Yamini, Ateek, Prathamesh*** and ***MJ*** for selflessly helping me, especially in my urgent need.

PhD (Integrated ;p) is a long time at any place. And as I am wired, I don't think I would have been able to survive this time just by doing lab work. Well, I was blessed to have a bunch of happening theatricians at IISER, with whom I have been able to perform, enjoy and cherish Theatre!!! It is difficult to thank each and everyone here (the list may easily go beyond 200!). However, there were some dear ones, with whom I have been closely associated during my stay at IISER. ***Prof. John Mathew*** has been a revelation in my life. A full of life character and a master at Theatre, I have learned innumerable values and arts from John. He becomes a friend to all and makes Theatre even more fun. He continues to be a dearie to me, and I know I can depend upon him always for any help and inputs in Theatre and Life, in general. I have been lucky to have had a close circle of very capable, proactive, sensitive and full of life people around me in the Drama

club in the last 4-5 years at IISER. ***Shweta, Sameer, Dhriti, Sukanya, Adarsh, Akanksha, Harsha, Danish, Anwesh, Aswin, Prabhat, Anshul*** have been my close buddies in Theatre and I have spent a lot of quality time and have done a lot of quality Theatre with them. They have not only contributed to my Theatrical growth, but have also helped me in leaving away all the frustrations of my PhD life away, and build and enjoy a different world altogether. I have lived a different life with these people during the rehearsals, workshops and performances that have made immense contributions to my personality. The night time was booked for Theatre, and these people along with a number of others have made it just worth the effort. I truly thank ***Prof. Sudha Rajamani,*** our Drama-Club co-ordinator, for all the motivation and support she has given all of us to freely create the grand performances on the stage. ***Sea Minor 2016, 2018*** and ***2019*** teams along with the ***Ratra*** team need special mention as well for what they have contributed to my PhD life.

It is important to have good people around you, especially in your tough times, and I am blessed to have a bunch of BFFs who have taken the toll of my PhD during my difficult times and have kept me motivated and charged on an emotional level to continue to strive hard for my work. ***Jerrin*** has been my buddy for the last 7 years. We joined the Integrated PhD programme together, and since then we have shared all our successes, failures, frustrations, fun and what not! He has been a strong support in all these 7 years and continues to be. ***Yashwant,*** or I may call him Guruji, is my elder brother at IISER. He has always been there for me, be it anything. He, even in his busiest schedules, would find time for me, for a chai, snacks, theatre ('PhD' and Sea Minor 2019), protein purification, going for a walk, going out just for fun, giving me 'gyan', cracking PJs with me, *etc etc etc.* He is one of the most optimistic and motivated people, I have ever met. He makes me smile even when I am angry, and I know I can't thank him enough for what he has been for me for all these years. ***Aditi, Sneha, Hridya, Rahi*** are my other batchmates who have been very close to me all these years. They are few of the nicest friends I have, and I have shared tonnes of things with them. Again, their contributions have helped me struggle and survive the tougher parts of my PhD. I may thank a few people again, but, it is because of the associations I have had with them outside lab or outside the Drama Club as well. **Pooja**, who has been my labmate, has been one of my best friends ever. She understands me very well, and has been a strong pillar of support during the tough phases of my PhD as well as life. ***Sukanya,*** a wonderful singer and a gem of a person at heart, has been my dear little angel. Long conversations with her have given me fresh air and new zeal to go back and work in the lab. ***Shweta,*** a wonderful actor and a genuine and honest person at heart, has been associated with me for almost all my Theatrical productions at IISER. But apart from that, she has been a close friend, philosopher and guide during tough times. Her valuable suggestions and words of motivation have helped me to rethink about critical issues with more clarity.

Sports have also been an important part of my PhD life, mainly cricket. I have been fortunate to play with ***Team Eagles*** for 5 years in the IPL (IISER Premier League ;p). I truly thank all the team members over

these 5 years and especially ***Sharath*** and ***Adarsh*** for all the wonderful memories on the cricket field. I also got the opportunity to play with ***Team Helix*** in my last year and I thank all of them as well.

I thank all the Chemistry office staff especially Mr. Mayuresh Kulkarni for his valuable support. I also thank people from the Academic Office for their help. I sincerely thank all the operators of various instruments that I have used during my PhD tenure for acquiring important data – Deepali and Chinmay (NMR), Ganesh (IR), Swati (MALDI-ToF), Nayana (HRMS), Archana (XRD). I truly thank Mr. Mahesh Jadhav for all the technical help, especially with the HPLC instrument. I thank Sachin Behra and teammates for all the help in the IT Dept. I also thank all other staff members at IISER for their timely help. I sincerely thank all the housekeeping staff for regularly keeping the workplace neat and clean and helping us in all odd chores without delays.

Finally, I thank my other friends and family members, especially my parents ***Aparna*** and ***Maheshchandra***, and my dear sister ***Anagha***, who have been with me throughout these 7 years. Their support and motivation has carried me through all the ups and downs of PhD life and help me accomplish my goals.

\- Amogh

*****

P.S. I sincerely thank all those people who made my life miserable at IISER and added to my struggle (professional or emotional). Your negative energies against me have kept me up in the fight of not only accomplishing my PhD but also becoming a better human being!!!

ABSTRACT

Thiols are biologically important molecules and play a vital role in a number of cellular processes. Cysteine is the most important biological thiol, least abundant (3.3%), yet highly conserved on the proteome. Along with other cytosolic thiols, it helps in regulating the redox balance of the cell. Any perturbation to the levels of thiols inside cells can cause redox stress that can lead to lethality. Cysteine residues are also responsible for retaining the structural stability of the protein, which ensures the smooth functioning of a number of cellular processes. They are involved in different post-translational modifications such as *S*-phosphorylation, *S*-glutathionylation, disulfide formation *etc*. Additionally, cysteine serves as the reactive nucleophile in many enzymatic biochemical reactions. The nucleophilicity of the thiol is profoundly dependent upon the microenvironment around the cysteine residue in the native state of the protein, which eventually dictates the pK_a of the thiol. Even in bacteria, thiols play important roles in maintaining redox homeostasis. For example, Bacillithiol in *Staphylococcus aureus* (*S. aureus*) and Glutathione in *Escherichia coli* (*E. coli*) essay the role of antioxidants. Cysteines are also key residues on bacterial proteins responsible for generating resistance and virulence in pathogenic bacteria. Due to all the aforementioned reasons, thiols and in particular cysteine, becomes an attractive biological target from a therapeutic and diagnostic point-of-view.

Thus, in order to target cellular thiols, we designed and evaluated the ability of Indole-based naphthoquinone epoxides (INDQEs) to react with cellular thiols *via* the opening of the epoxide ring. A series of analogues were synthesized and their reactivity with thiol was evaluated. We could propose a sterics-based model that explains that the reactivity with thiol could be tuned by varying the groups neighbouring the epoxide. The epoxide-thiol reaction resulted in an irreversible covalent modification. When tested against a panel of pathogenic bacteria, these compounds were found to inhibit Gram-positive *S. aureus* at low concentrations. The key finding was a good correlation between reactivity with a thiol and the antibacterial potency. Additionally, the kinetics of the reaction with a thiol was a major driving force in bacterial inhibition. The lead compound identified, was found to inhibit clinically acquired extremely drug-resistant strains of *S. aureus* such as Methicillin-resistant *S. aureus* (MRSA) and Vancomycin-resistant *S. aureus* (VRSA) at potent Minimum Inhibitory Concentrations (MIC). Clinically, infections caused by these drug-resistant strains are extremely difficult to treat. Daptomycin is the antibiotic of last resort against VRSA infections. Thus, development of better antibacterial candidates with novel targets is of urgent need.

In order to decipher the targets of the lead compound in *S. aureus*, INDQE alkyne probes were synthesized and Activity-Based Protein Profiling (ABPP) technique was employed to profile the thiol proteome of *S. aureus* to identify the target proteins. An active INDQE alkyne probe was identified with similar reactivity with thiol and inhibitory activity against *S. aureus* as that of the lead compound. A series of ABPP experiments were conducted using this probe to establish the selectivity of these compounds towards cysteine residues as well as the permeability specific to *S. aureus* only. Further, chemoproteomics experiments using this probe fished out certain transcriptional virulence factors as potential targets.

The identified target proteins were obtained by routine techniques of cloning and purification and were further validated using ABPP techniques. Cysteine-point mutants were generated using site-directed mutagenesis and ABPP experiments corroborated cysteine as the target site for these compounds. Two Mar R (Multiple antibiotic resistance regulator) family of proteins were identified and validated from this study. These identified targets are novel and hence targeting these can help in generating improved and more potent antibacterial agents. This development may help in reducing the burden of antibacterial resistance in the near future.

Chapter 1. INTRODUCTION

1.1. Thiols

Thiols are sulfur-containing analogs of alcohols, the term being derived from the two terms 'thio' and 'alcohol', 'thio' meaning sulfur. Thiols are also well known as mercaptans due to their strong affinity for mercury. They generally have a very pungent odour. The smell of the dreadful skunk spray can be correlated to a mixture of two thiols. Due to their distinctive smell, certain thiols are used as odorants in the detection of natural gas.

1.2. Chemistry of thiols

Compared to oxygen (χ = 3.5), sulfur (χ = 2.5) is less electronegative and nearly as electronegative as carbon (χ = 2.5). Due to the small difference in electronegativity between sulfur (χ = 2.5) and hydrogen (χ = 2.2), thiols are weakly acidic in nature. For example, thiophenol (pK_a 6.6), β-mercaptoethanol (pK_a 9.6), *L*-cysteine (pK_a 8.3)[1] *etc.*; these values suggest their ability to form thiolates in physiological pH and act as nucleophiles. By far, thiols are one of the best nucleophiles, and a number of organic reactions utilise this nucleophilic nature.

With varied chemical reactivity displayed by thiols, it is not surprising that they play a unique and vital role in biological systems. A number of thiol-addition reactions are well-known and are used extensively for thiol-recognition purposes.[2] This is important from the point of view of studying the biological roles of thiols, wherein their chemistry can be utilised and synchronised for biochemical applications.

1.3. Biology of thiols

Biologically, thiols are important molecules inside cells. Cysteine is one of the least abundant yet highly conserved residues on the proteome (Fig. 1.1). It is also by far the most reactive amino acid residue on protein surfaces. They are redox-active groups[3] and are important in a number of post-translational modifications (PTMs)[4] which are responsible in protecting the integrity of the cell. For example, in certain bacteria, *S*-glutathionation takes place in order to protect the active site cysteine in certain enzymes from getting oxidized to an irreversible sulphur oxidation state. *S*-bacillithiolation[5,6] and *S*-mycothiolation are also important defense strategies in *B. subtilis, S. aureus* and *M. tuberculosis.* In *S. aureus,* cysteine-phosphorylation,

which is a rare PTM, of certain transcriptional factors (TFs), is important for virulence development and generating resistance against vancomycin.[7]

Figure 1.1. Schematic showing the important roles of Cysteine residues of proteins

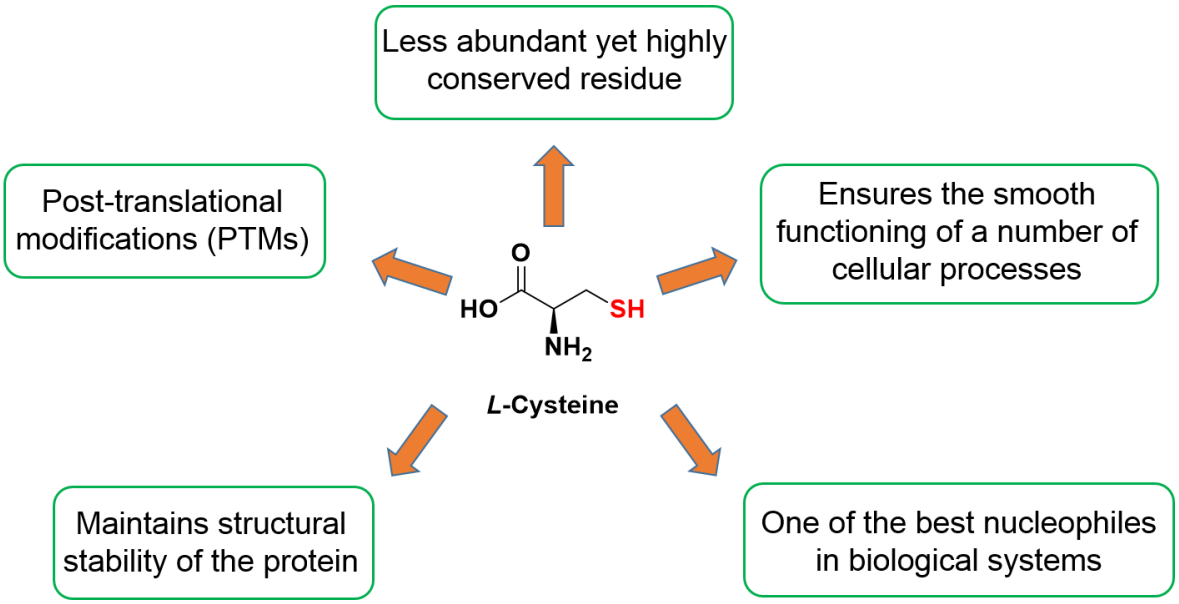

Glutathione (GSH), a cysteine-containing tripeptide (Fig. 1.2), is the major thiol found in mammalian cells that essays the role of an antioxidant. Even in bacteria, thiols are crucial to the antioxidant machinery which maintains redox balance. For example, Bacillithiol (BSH) (Fig. 1.2) in *S. aureus*.[5,8,9] Thus, any perturbation to the levels of thiols can cause a redox imbalance that can lead to stress, in turn, proving lethal for the organism. Additionally, thiols are also important biological nucleophiles and catalyze a number of biochemical reactions. The nucleophilicity of the thiol is profoundly dependent upon the microenvironment around the cysteine residue in the native state of the protein, which eventually dictates the pK_a of the thiol.

Figure 1.2. Low molecular weight reduced thiols found in cells

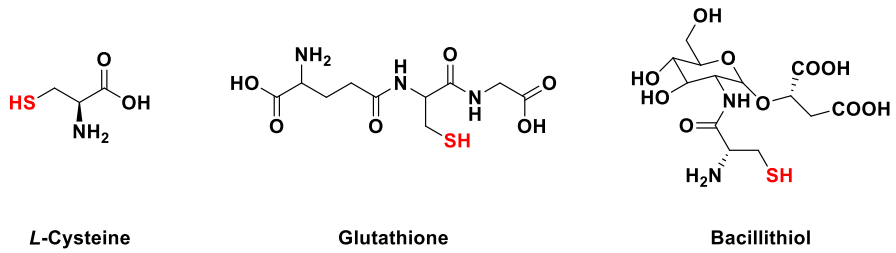

Thiols as primary antioxidants play an important part in maintaining cellular redox homeostasis.[8–13] The other important players of redox homeostasis, reactive species such as Reactive oxygen species (ROS),[14,15] Reactive nitrogen species (RNS)[14,15] and Reactive sulfur

species (RSS)[16] are an integral part of the cellular machinery and are important for a number of signalling processes. However, there may exist a state when the levels of these reactive species exceed a particular threshold; this can lead to damage in biomacromolecules such as DNA, lipids and proteins resulting into redox stress. This state can further lead to cell death. In order to protect the cell from the onslaught of these reactive species, Nature has an in-built protective mechanism using antioxidants such as thiols. For instance, the thiol of a cysteine residue on a protein can be oxidized to a sulfenic acid in the presence of hydrogen peroxide, a major ROS in the cell (Fig. 1.3).[3] Further, depending upon the levels of ROS inside the cell, the sulfenic acid can react with hydrogen peroxide to generate a sulfinic acid, and later, even a sulfonic acid, where sulfur is in its highest oxidation state (VI). These are irreversible modifications to the cysteine thiol and take place only when the levels of the reactive species are considerably high inside the cell. In a less oxidative condition, the sulfenic acid formed can react with another thiol, forming a disulfide bond. This thiol can be another cysteine residue on the same or different protein or even a low molecular weight thiol inside the cell, such as Glutathione. These disulfides are then further reduced to the free thiol by a number of reductases such as thioredoxin reductase,[17] glutathione reductase *etc.* This process can also be done using commercially available reagents such as dithiothreitol (DTT) and β-mercaptoethanol (BME). Thus, upon reduction of the disulfide, the free thiol is again available for countering ROS. Thus, this entire process helps in maintaining the redox balance of a cell. Interestingly, this entire process involves a number of important reversible as well as irreversible post-translational modifications of the protein involved *via* a cysteine residue.

Figure 1.3. Role of thiol in redox homeostasis

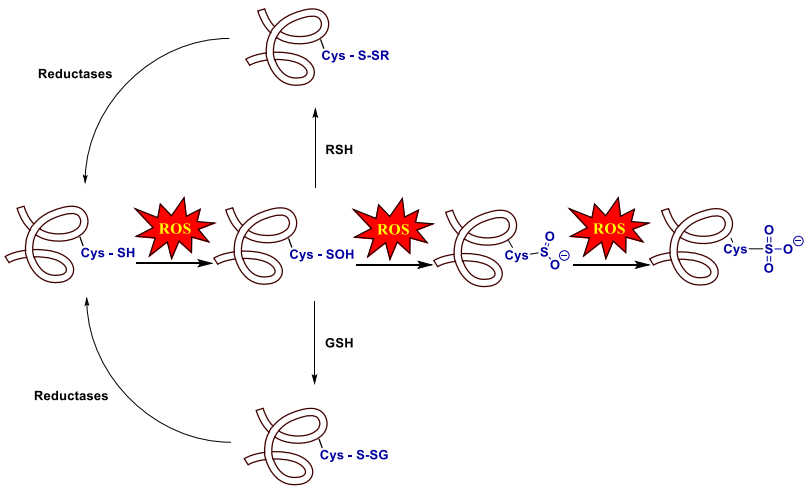

1.4. Cysteine-reactive scaffolds

Owing to the distinctive chemical properties that it displays, and the biological roles that it performs, cysteine has acquired a unique importance in medicinal chemistry and drug discovery.[18] Targeting important cysteine residues on key proteins has generated significant therapeutic interest that has resulted in inhibition of bacterial infections, cancers and other deadly diseases.[19–22] The focus of a majority of the studies is on covalently modifying a particular cysteine residue in a reversible or irreversible manner.[23] Due to the unique reactivity displayed by thiols, and the important role they play in number of cellular processes in various biological systems, thiol-reactive probes have always been in demand.[24–26] A number of fluorescence-based[27–31] and luminescence-based[32] probes and chemosensors have been designed, wherein a number of cysteine-reactive electrophiles have been incorporated, and chemical probes with novel chemistry[33,34] have also been developed. Targeted covalent inhibitors (TCI) is another category of inhibitors, which are extensively employed for therapeutic purposes.[35] TCIs selectively target cysteine residues on proteins using various *i.* electrophilic warheads such as Michael acceptors like maleimides, vinyl sulfonates, and *ii*. nucleophilic substitutions on epoxides, β-haloacetamides, arylsulfonamides and others. Amongst these warheads, *N*-ethylmaleimide (NEM), iodoacetamide (IAM), 5,5′-dithiobis-(2-nitrobenzoic acid) (DTNB), 1-Fluoro-2,4-dinitrobenzene (FDNB), monobromobimane[36] (mBBr) *etc*. are the most commonly used thiol-reactive probes, which are extensively used in thiol-detection and labelling assays or even as thiol-blocking agents. Some of these are summarized in Fig. 1.4.

Figure 1.4. Some selected thiol-reactive scaffolds

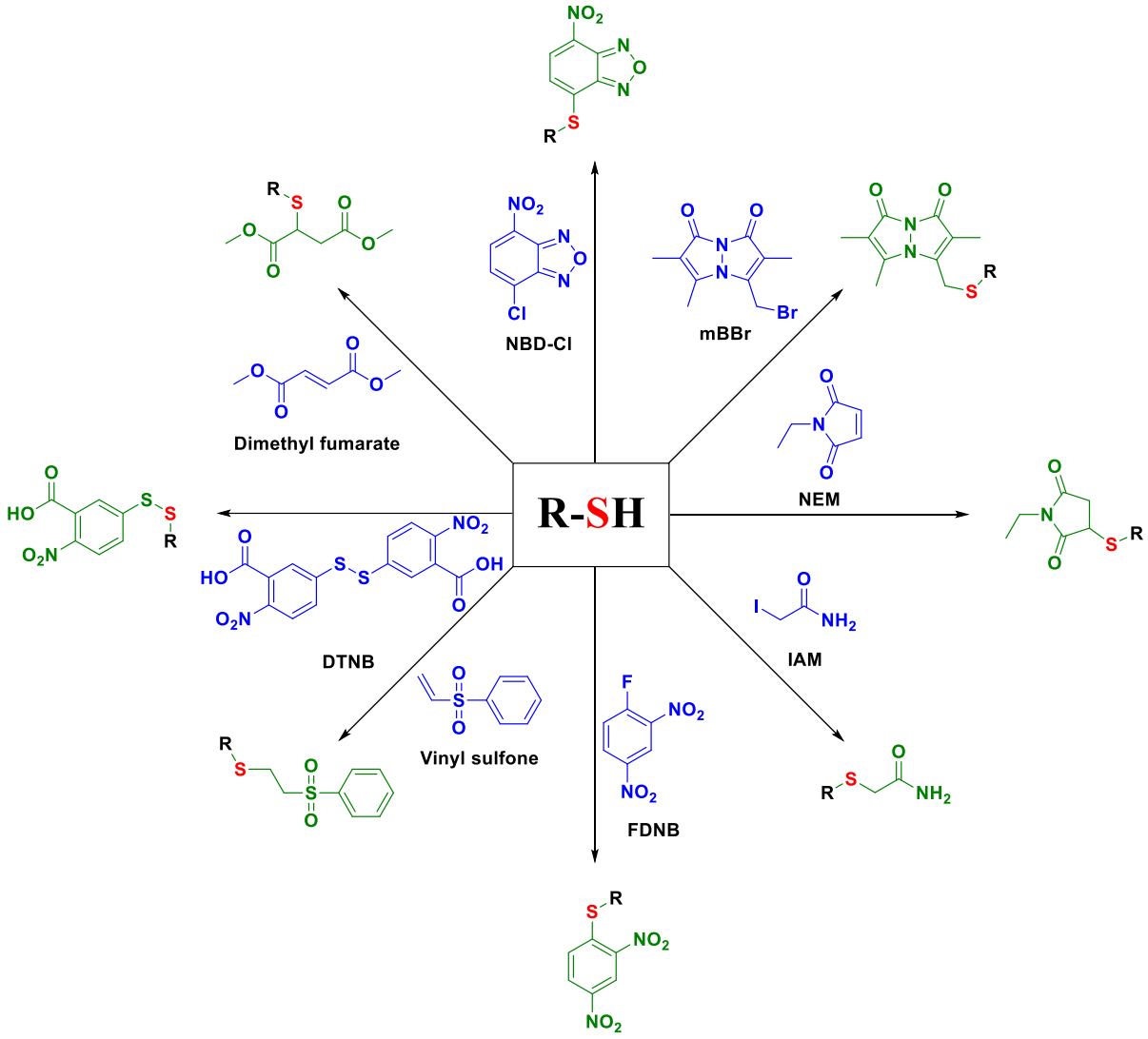

1.4.1. Cysteine-selective modification - new scaffolds added to the arsenal

Cysteine is one of the most distinguished amino acids on any protein that can be utilized for reversible as well as irreversible modification, firstly, due to its low abundance[37] that makes it a specific and selective target, and secondly, the deprotonation at physiological pH of its side-chain thiol, which enhances its reactivity as a nucleophile.[3] Cysteine residues on proteins play vital functional roles such as redox catalysis, metal binding, formation of structural disulfides, allosteric regulation and nucleophilic activity for various biochemical reactions.[4] Apart from these, cysteine residues are also involved in a number of post-translational Modifications (PTMs) including the oxPTMs (Fig. 1.2), *S*-sulfhydration, *S*-nitrosation, *S*-prenylation, *S*-palmitoylation, Lipid-derived electrophiles (LDE) adducts *etc*.[38] Thus, covalent irreversible

inhibitors targeting cysteine residues on protein have spurred a new revelation for drug development, and a number of drugs have hit the market for the treatment of various diseases including cancers, myeloma and Alzheimers.[18] Also, a number of cysteine-reactive scaffolds are well-established and utilized for chemical proteomics applications.[39] These include maleimides, haloacetamides, epoxides, α,β-unsaturated carbonyls, sulfonate esters, methylsulfonylbenzothiazoles *etc*. Thus, there always is a continuous demand for new and better thiol-reactive molecules and probes that can help in further investigation of cysteine residues that are still untracked or unexplored. Some of these reports are discussed below.

Pan and co-workers have used Michael acceptor groups and reported Ibrutinib-based irreversible Bruton's Tyrosine Kinase (BTK) inhibitors and studied a series of analogues by changing the Michael acceptor group on the pyrazole.[40] This study suggests the reactivity of cysteine residue on BTK is critical for the inhibition and can be tuned by the structural modifications on the Michael acceptor installed. Carroll and co-workers have reported an iododimedone scaffold that can selectively react with cysteine residues on proteins (Fig. 1.5. A).[41] Using isotope-coded dimedone and iododimedone and chemoproteomic techniques, they have differentiated between cysteine thiol and sulfenic acid. Taunton and co-workers have extensively studied the reversible targeting of non-catalytic cysteines on p90 ribosomal protein S6 kinase RSK2 and other similar kinases using acrylamide as a thiol reacting scaffold.[42] The reactivity could be tuned by installing an electron withdrawing functional group 'cyano' on the olefin (Fig. 1.5. B). The amide moiety was further varied for enhancing the selectivity for the target protein. Using chloroacetamide as the cysteine-reactive group, Weerapana and co-workers have proposed a novel strategy to identify zinc-binding cysteines.[43] Zinc ions (Zn^{2+}) play a vital role in regulatory functions of the cell and are generally linked to chelation with cysteines on the protein surface. In another study they present a strategy to identify functional cysteines in mitochondria following a mito-enrichment protocol and probing with an iodoacetamide alkyne.[44] Another study from Teck-Peng Loh and co-workers uses allenamides as orthogonal handles for cysteine modification in peptides and proteins (Fig. 1.5. C).[45] This method works very efficiently in aqueous medium with site selectivity and quantitative conversion, yielding a stable covalent modification. Virdee and co-workers report use of new probes- tosyl-substituted doubly activated ene (TDAE) for profiling transthiolation, a fundamental biochemical reaction involved in the conjugation of ubiquitin-like proteins (Fig. 1.5. D).[46] Zheng and co-workers have utilized the uricosuric agent Benzbromarone (BBR) and investigated the reasons for its hepatotoxicity.[47] BBR gets metabolized by P450 3A to an active

epoxide intermediate (Fig. 1.5. E) which reacts with cysteines on proteins and covalently modifies them possibly leading to hepatotoxicity. Chiba and co-workers have achieved dual functionalization of cysteine residues in peptides and proteins using 2-azidoacrylates (Fig. 1.5. F).[48] Here, the azidoacrylate can be installed with various functional groups such as a fluorescent dye. Azide-alkyne cycloaddition further allows for the installation of the second functional group, thus affording dual functionalization. Furdui and co-workers have presented a heteroaromatic sulfone MSTP, as a new class of thiol-selective reagent for use in biological applications (Fig. 1.5. G).[49] MSTP 4-(5-methanesulfonyl-[1,2,3,4]tetrazol-1-yl)-phenol, unlike certain other thiol-reactive reagents, was found to be highly selective and reactive in blocking protein thiols. In another study, Adams and co-workers have utilized 2-chloropropionamide as a steric-driven low reactivity electrophile that selectively acts as a PDI (Protein Disulfide Isomerase) inhibitor (Fig. 1.5. H).[50] 5-methylene pyrrolones have been employed for reversible bioconjugation of proteins *via* a Michael addition by Zhou and co-workers (Fig. 1.5. I).[51] This Michael adduct can undergo a thiol exchange at physiological pH or a retro-Michael reaction at alkaline pH. These properties of the scaffold can be utilized for the delivery of a drug or other molecules having biological significance. On similar lines, Yin and co-workers have reported 4-substituted cyclopentenone scaffold for reversible protein modification *via* a cysteine-specific reaction (Fig. 1.5. J).[52] The reaction takes place via a Michael addition tandem elimination process. The thiol-adduct formed can further be easily removed by a Michael addition donor without compromising on the enzymatic activity of the protein. Recently, Diness and co-workers have reported fluorobenzene-based probes for cysteine-selective modification (Fig. 1.5. K).[53] Here, they find that the presence of an electron withdrawing group around the reactive fluorine group increases the rate of reaction with cysteines while an electron-donating group reduces reactivity. This elegant design and structure activity relationship studies allow for tuneable reaction with protein thiols. Pentelute and co-workers have recently presented a cysteine-cyclooctyne conjugation using a DBCO (dibenzocyclooctyne, seven-residue peptide) tag that increases the rate of thiol-yne reaction by more than 200-fold, and is chemo and regio-selective in nature.[54] Bernardes and co-workers have recently reported the utility of vinyl/alkynyl pyridine quaternary salts in enabling an ultrafast cysteine-selective protein modification (Fig. 1.5. L).[55] These scaffolds also possibly play a role in charge modulation of the protein after adduct formation. A new electrophilic warhead was recently reported by Poulsen and co-workers, STEFs (semi-oxamide vinylogous thioesters), for the covalent modification of proteins (Fig. 1.5. M).[56] This scaffold can react with thiols as well as amines, however the selectivity and reactivity can be tuned by structural

modifications on the scaffold. Recently, Ojida and co-workers have reported reversible modification of kinase cysteines using chlorofluoroacetamides (Fig. 1.5. N) and have explored new warheads for TCI (Targeted Covalent Inhibition) by inhibiting EGFRs.[57]

Figure 1.5. New thiol-reactive scaffolds in the arsenal

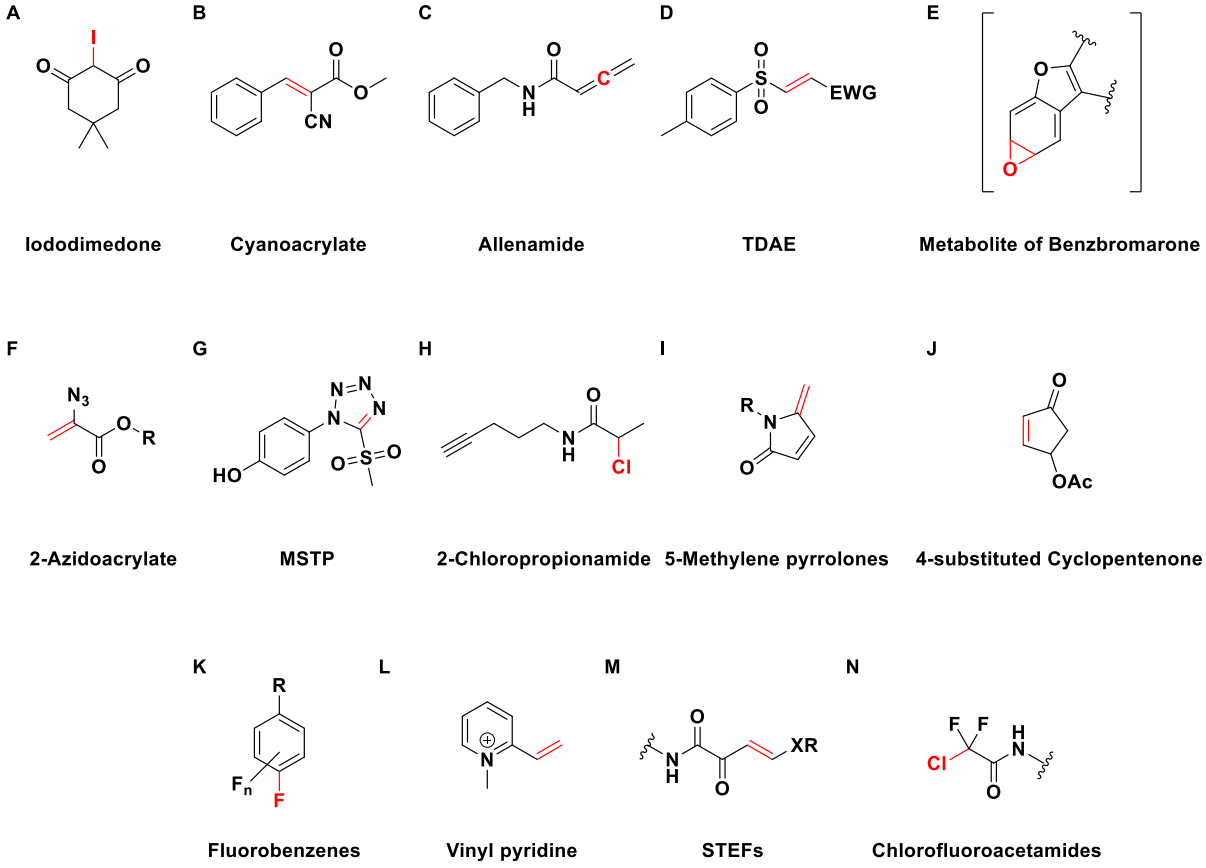

Finn and co-workers have reported a norbornadiene-based molecule that can react with thiols and undergo a retro Diels-Alder reaction to release the furan molecule along with the Michael -addition based thiol adduct.[58] However, lack of selectivity limits the usage of this scaffold in cellular experiments. Chakrapani and co-workers have described a thiol-selective phenacrylate scaffold embedded with a self-immolative linker.[59] This scaffold shows tunable reactivity with a thiol depending upon the electronic nature of the group installed on it, however cytotoxicity deters the usage of this molecule for any biological applications.

1.4.2. Epoxide as a constituent of electrophilic natural products in targeting cysteine residues of proteins for therapeutic activity

It is evident that the cysteine residues on proteins are attractive targets in biological systems, and a number of probes have been designed targeting them, particularly from the view point of diagnostic investigations and therapeutic applications. Amongst several scaffolds discussed earlier, the ones with 'epoxide' as the electrophilic warhead have been underutilized. E64 (*L*-trans-Epoxysuccinyl-leucylamido(4-guanidino)butane), a natural product bearing an epoxide ring, is a very well-known inhibitor of cysteine proteases, including cathepsin, and found to be selective towards reacting with a thiol.[60] Subsequent derivatives of E64 and other peptides synthesized, bearing the epoxide, have shown good inhibitory activity against other cysteine proteases.[61–64] Certain derivatives inhibited bacterial cysteine protease in *S. epidermis*[65] and *C. difficile*.[66] In another study, the epoxide warhead in E64 was utilized and the probe was developed for monitoring the activation of the lysosomal cysteine protease cathepsin B in endocytic compartments which were infected by the deadly Gram-negative pathogen *S. typhimurium*.[67]

Figure 1.6. Structure of E-64

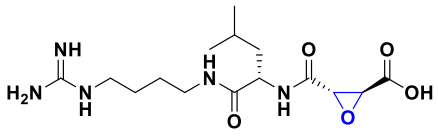

E64

Fosfomycin, a clinically used broad-spectrum antibiotic, derived from the *streptomyces* species, has an epoxide ring as its reactive component. Fosfomycin inhibits bacterial growth by targeting the cell wall biosynthetic enzyme UDP-*N*-acetylglycosamine-1-carboxyvinyltransferase (*MurA*).[68] It covalently binds to Cys115 of *MurA via* epoxide ring opening (Fig. 1.7).[69]

Figure 1.7. Mechanism of action of Fosfomycin

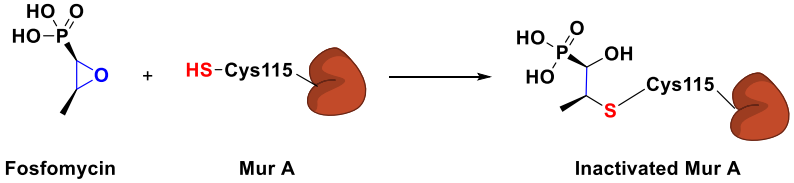

Fosfomycin **Mur A** **Inactivated Mur A**

1.4.3. 2,3-epoxy-1,4-naphthoquinones

2,3-epoxy-1,4-naphthoquinone functional group is found to be a constituent of a number of natural products with medicinal properties. Compounds such as 2,3-epoxysesamone,[70,71] Frenolicin[72] have antibacterial, antifungal properties respectively and Vitamin K3-Epoxide[73] is important in blood coagulation (Fig. 1.8). This scaffold has also been reported to be reactive with thiols *via* opening of the epoxide warhead.[74,75]

Figure 1.8. 2,3 epoxy-1,4-naphthoquinone scaffold with naturally occurring scaffolds

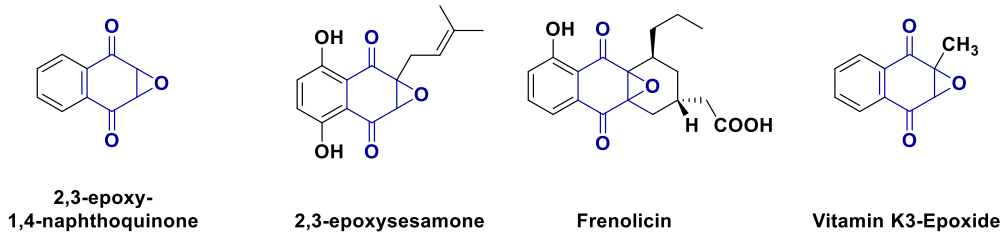

Terreic acid, a fungal metabolite, is an inhibitor of Bruton's tyrosine kinase (BTK) (Fig. 1.9).[76] Sieber and co-workers have reported the amino-2,3-epoxy-1,4-naphthoquinone (AEC-FM233, Fig. 1.9) scaffold to be reactive with cellular thiols, targeting certain redox-active proteins, and proving to be detrimental to the growth of Gram-negative *S. typhimurium*.[77] Recently, Miyoshi and co-workers have reported epoxycyclohexenedione-type compounds (ECHD-AMM-59, Fig. 1.9) as potent inhibitors of bovine mitochondrial ADP/ATP carrier.[78]

Figure 1.9. Reported examples with quinone-epoxide as reactive moiety

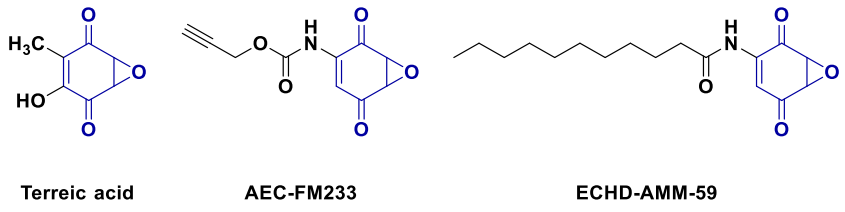

The aforementioned examples, the range of applications and properties displayed by the 2,3-epoxy-1,4-naphthoquinone based scaffolds suggest its potential in therapeutic applications. The compounds bearing this core structure inhibit key proteins which has a direct impact on biological processes. This inhibition takes place through the covalent modification of the cysteine residue on the protein *via* the opening of the epoxide, which is the reactive warhead in the electrophile. Inhibition of a protein by the covalent modification in an irreversible manner has greater effectivity as compared to non-covalent or covalent reversible modification, as it helps in achieving selectivity and is long-lasting in nature.[79] These inhibitors also work in

a time-dependent manner and are important from the standpoint of identifying the target protein, due to the covalent bond formation with other similar reactive residues as well.

Utilizing this information and inspired from the 2,3-epoxy-1,4-naphthoquinone scaffold, a rational design of an indole-based naphthoquinone epoxide (INDQE) for the tunable reactivity with thiol was developed. This is discussed in Chapter 2. The reactivity with thiol could well lead into inhibiting drug-resistant pathogenic bacteria, which may thus prove to be beneficial. This may open up a novel route in making inroads against one of the greatest challenge in world health care today, that of antimicrobial resistance.

1.5. Antimicrobial resistance (AMR)

Tackling infectious diseases has been a taxing challenge for the past century. Two possible lines of confronting this problem have been proposed, first, the isolation of numerous natural products that may have potent antibiotic activity, and second, the synthesis of improved antibacterial agents by medicinal chemists.[80] These possible routes are however, stalled by the ever increasing antimicrobial resistance (AMR). In the 21st century, AMR has become one of the leading causes of deaths across the globe as documented by the World Health Organisation (WHO) in the 2014 global report on surveillance on antimicrobial resistance.[81] Community-acquired bacterial infections are on the rise constantly and resistance developed against the clinically used antibiotics makes it difficult to propose appropriate treatment strategies to combat these infections. Due to extreme levels of resistance, in the near future, it would be difficult to treat even routine bacterial infections using clinically used antibiotics.

Apart from TB, which is one of the leading causes of deaths by infectious diseases, nosocomial infections caused by ESKAPE pathogens (*E. coli*, *S. aureus*, *K. pneumonia*, *A. baumannii*, *P. aeruginosa*, *E. faecalis*, *E. faecium*) have also led to heavy casualty in the past few decades. These infections are extremely difficult to treat as most of them are multidrug resistant isolates. Mechanisms of resistance include drug inactivation, formation of biofilms, alteration to binding sites, reduced permeability or activated efflux pumps.[82] Thus, the issue underlines the ever-increasing demand for better antibacterial agents with novel mechanism of action.

Amongst the ESKAPE pathogens, Gram-positive *Staphylococcus aureus* (*S. aureus*) is a deadly pathogen causing numerous nosocomial infections, sepsis, infective endocarditis, osteoarticular and skin and soft tissue infections and others.[83] The pathogen, mostly associated with hospital and other health care settings, is known to develop resistance to antibiotics.[84] *S.*

aureus infections were initially treated with penicillin, which, following development of resistance were clinically treated with methicillin and other drugs of the penicillin family. However, emergence of MRSA (Methicillin-resistant *S. aureus*) strains in a short span of time, and the emergence of CA-MRSA (Community-associated MRSA) has increased the overall burden on global health. Later, in 1972, vancomycin was introduced for the treatment of MRSA infections. VISA (Vancomycin-intermediate *S. aureus*) and VRSA (Vancomycin-resistant *S. aureus*) infections were reported by the end of the 20th century, posing a tougher challenge in front of the global health care systems.[85,86] Cross-resistance observed for VRSA to Daptomycin,[87] the antibiotic of last resort to treat multidrug-resistant *S. aureus* infections, has clearly put forth the grim reality of the rapidly narrowing race between antibiotics and AMR. Thus, there is a desperate need for development of new effective strategies to combat AMR. One plausible route is development of new antibacterial agents with novel mechanism of action. The impact would be greater if resistance developing strategies of pathogenic bacteria are targeted, which would possibly help in controlling drug-resistant infections in the future.

As discussed earlier, the designed indole-based naphthoquinone epoxide scaffold can be screened against pathogenic bacteria. The structure-activity relationship studies can further propagate the identification of a lead compound that could potently inhibit drug-resistant bacteria like MRSA and VRSA. These studies will be discussed in detail in Chapter 2. The mechanism of action is hypothesized to be *via* the covalent modification of cysteine residues on key proteins in *S. aureus*. Target identification and validation can be done by Activity-based protein profiling (ABPP) technique.

1.6. Activity-based protein profiling (ABPP)

Activity-based protein profiling (ABPP) is a technique established about two decades ago,[88] to study the complex proteomes in various biological systems especially cancer cells[89] and pathogenic bacteria.[90] The aim of the study is either from a diagnostic or therapeutic point-of-view, where reactivity of certain important protein residues is utilized to interrogate diverse biological processes. A typical ABPP experiment involves a probe called Activity-based probe (ABP). Generally, an ABP comprises of three parts. First, a reactive or a binding group where the protein residue will react, second, an analytical handle comprising of an alkyne, an azide or a biotin tag which can guide in obtaining a readout, and thirdly, a linker that connects the binding group to the analytical handle (Fig. 1.10).[91]

Figure 1.10. Design of Activity Based Probe (ABP)

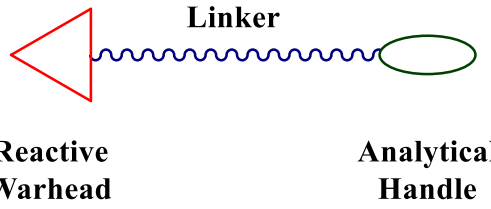

Amongst many, the extensively studied residues on the protein surfaces are serine,[92,93] cysteine[35,39] and lysine[94] due to their unique reactivity and nucleophilicity that can be utilized by electrophilic warheads, and also due to the important role they play in various biochemical processes. For example, a number of reports have been published by Cravatt and co-workers,[89,91,95] Bogyo and co-workers,[90,96,97] on a series of serine hydrolase inhibitors and cysteine-based ABPP strategies. Similarly, Weerapana and co-workers[38,44,98] have demonstrated the use of ABPP for profiling of cysteine residues in complex proteomes. Adibekian and co-workers have reported ethynyl benziodoxolones which are hypervalent iodine compounds that can selectively label thiol proteome better than that done by Iodoacetamide Alkyne (IAA).[99]

Thus, chemoproteomics has been extensively used in the process of drug discovery and development.[95] A few examples of the applications and utilization of the ABPP technique for addressing AMR are discussed. Fan, Cravatt and co-workers have been successful in inhibiting *Chlamydia trachomatis* by targeting its peptide deformylase, which is a metalloprotease enzyme.[100] They have used two metalloprotease inhibitors GM6001 and TAPI-0 and designed an alkyne-tagged probe AspR1, which was employed in the ABPP experiment to identify the target. Sieber and co-workers have developed a series of probes to target AMR and interrogate virulence factors of pathogenic bacteria.[101] Synthetic β-lactam-based probes tagged with an alkyne were designed for the selective *in vivo* labelling of enzymes involved in cell wall biosynthesis, antibiotic resistance and virulence.[102] These probes selectively attenuate the production of extracellular virulence factors in *S. aureus* by inhibiting caseinolytic protein protease (ClpP), a serine protease responsible for the virulence of the bacterium (MRSA).[103] The expanded compound library was further found to be inhibiting various enzymes from pathogenic bacteria like *Pseudomonas putida*, *Listeria welshimeri*, *Bacillus licheniformis*, *Bacillus subtilis*, and *Escherichia coli*,[104] including virulence factors[105] and also decrease the intracellular virulence of *Listeria monocytogenes* in macrophages.[106] Sieber and co-workers have further developed derivatives of α-methylene-γ-butyrolactones as inhibitors of drug-

resistant *S. aureus*.[107] These compounds decreased the expression of α-hemolysin (Hla), the most prominent virulence factor in *S. aureus* and also decreased the invasion frequency of the bacterium. Sieber and co-workers have then targeted certain redox-active proteins to inhibit Gram-negative *S. typhimurium* using scaffolds inspired from the natural product aminoepoxybenzoquinone.[77] Huston and co-workers have reported the finding of the first essential protease for *Chlamydia trachomatis* CtHtrA using inhibitor JO146 and ABPP techniques.[108] JO146 is a serine protease inhibitor and affects the cell morphology of the bacterium due to the reduction of the inclusion vacuole. Waldor, Weerapana and co-workers have used fluorophosphonate-based ABPs namely FP-TAMRA and FP-Biotin to profile the host and pathogen serine hydrolase enzymes in cholera and display the crosstalk between these enzymes during infection.[93] Pires and co-workers have developed a synthetic cell-wall analogue tagged with an alkyne, which helps in understanding the response of the drug-resistant cells (VRSA) to antibiotics.[109] This is the first *in vivo VanX* reporter that can facilitate the understanding of mechanisms related to antibiotic resistance. Bogyo and co-workers have identified a serine hydrolase FphB in *S. aureus* that is an important virulence factor.[110] Using chemoproteomics, they have identified small molecule inhibitors of this serine hydrolase that can potently reduce *in vivo* infection. All the aforementioned examples present strong evidence in using chemoproteomics approach for drug development and target identification to target AMR.

As discussed earlier, an epoxide warhead with the designed indole-based naphthoquinone epoxide scaffold can be extensively used as a cysteine-reactive group. For ABPP studies, in order to fish out targets of the active compounds, an alkyne can be used as an analytical handle and CuAAC (Copper-catalyzed Azide-Alkyne Cycloaddition)[111] chemistry can be employed to tag the active probe. A competitive-ABPP experiment can be conducted using an active probe that acts as a chaser to the lead compound identified in the study (Fig. 1.11).

Figure 1.11. Schematic for competitive ABPP

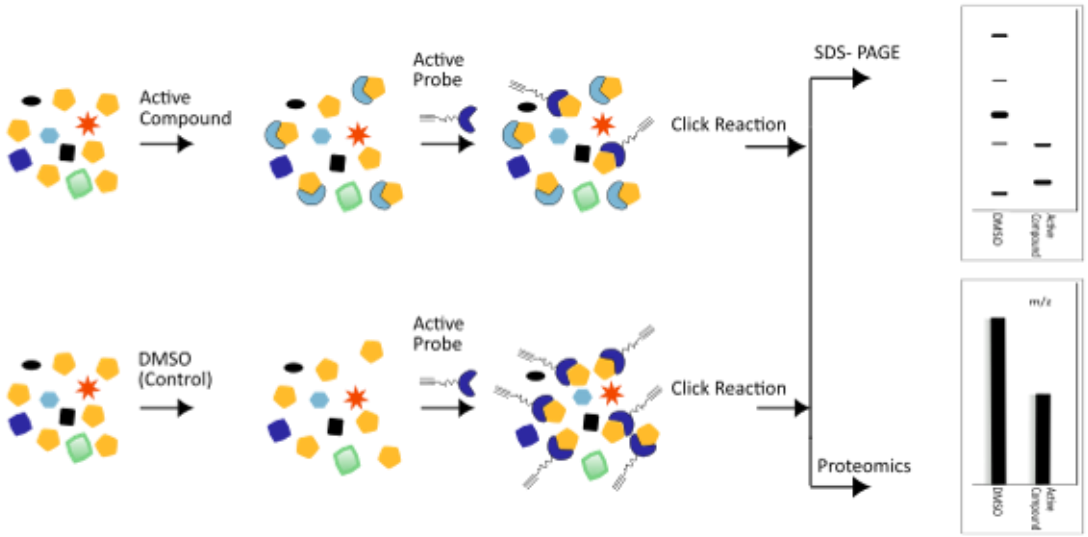

Courtesy: Shraddha Bhurkunde

Here, an active lead compound identified from the study is first reacted with the proteome of interest, where it can covalently react with the target proteins. This active compound, which is not tagged with any alkyne handle, will then be chased by an active probe which is pre-loaded with an alkyne handle. Now, this probe can only react with the remaining proteins that are not labelled by the active compound. Thus, using SDS-PAGE analysis, only those proteins could be visualized that are labelled by the active probe. On the other hand, a control experiment conducted should label the entire set of proteins modified by the active probe. Using LC-MS/MS based proteomics, the target proteins of the active compound could then be identified.

Using two alkyne probes of the INDQE scaffold, the thiol proteome of *S. aureus* was profiled and probable targets were pulled down using mass spectrometry techniques, discussed in Chapter 3. The most promising of these targets were cloned, purified and validated using ABPP techniques. The cysteine point mutants of these probable targets were generated which further supported the claim that these proteins are inhibited by covalent modification of a cysteine residue. This will be discussed in Chapter 4.

1.7. Aims

Taking all the aforementioned points into perspective, a unique scaffold with the following characteristics needs to be designed:

1) **Tunability in reactivity with thiol:** Based on the preliminary data from our lab (discussed in Chapter 2), the 2,3-epoxy-1,4-benzoquinone moiety was chosen as a thiol-reactive scaffold. The design required certain systematic modifications that would facilitate tunability in reactivity with a thiol. This could be achieved by introducing different substituents around the epoxide, the reactive moiety in the said design, which would possibly dictate the reaction dynamics with a thiol (Fig. 1.12). The reactivity can be modulated by sterics or the electronics introduced by the substituents.

Figure 1.12. Substitutions around the epoxide

2) **Cell permeability in bacteria:** The designed scaffold should be cell permeable. Indole, a known privileged scaffold[112] can be incorporated in the design which can enhance the permeability in bacterial cells (Fig. 1.13). Indole is also known to improve the pharmacological activity of the pharmacophore attached to it.

Figure 1.13. Indole - as a privileged scaffold

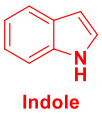

3) **Selectively targeting cysteine residues on proteins:** The structure-activity relationship study will enable identification of certain analogues which can target cysteine residues on bacterial proteins in an irreversible manner. This covalent modification to certain key proteins may result in inhibition of bacteria.

4) **Inhibition of bacteria at low concentrations (MIC):** Lead compounds need to be identified that can target cysteine residues on the bacterial proteome resulting in inhibition at low concentrations. These leads can then be taken for subsequent biological studies.

5) **No significant cytotoxicity:** The lead compounds with potent antibacterial activity should not show any significant cytotoxicity in mammalian cells. Thus, a high selectivity index would be beneficial.

6) **Novel drug targets in order to tackle antimicrobial resistance:** In order to identify the targets of the lead compounds, ABPP technique can be utilised. Activity-based probes based on the designed scaffold can be synthesized to profile the bacterial thiol proteome. Using chemoproteomic approaches, these probes can then be employed to identify and validate the targets. From a therapeutic standpoint, it would be desirable to identify novel protein targets which are important for the survival of bacteria. This would also provide an impetus in tackling the problem of AMR.

All these aims and corresponding challenges would be discussed in this thesis. The thesis will discuss the approach of designing a novel thiol-reactive scaffold as a potent antibacterial agent, targeting novel proteins *via* covalent cysteine modification.

1.8. References

(1) Tajc, S. G.; Tolbert, B. S.; Basavappa, R.; Miller, B. L. Direct Determination of Thiol p K a by Isothermal Titration Microcalorimetry. *J. Am. Chem. Soc.* **2004**, *126* (34), 10508–10509.

(2) Yin, C.; Huo, F.; Zhang, J.; Martínez-Máñez, R.; Yang, Y.; Lv, H.; Li, S. Thiol-Addition Reactions and Their Applications in Thiol Recognition. *Chem. Soc. Rev.* **2013**, *42* (14), 6032.

(3) Paulsen, C. E.; Carroll, K. S. Cysteine-Mediated Redox Signaling: Chemistry, Biology, and Tools for Discovery. *Chem. Rev.* **2013**, *113* (7), 4633–4679.

(4) Pace, N. J.; Weerapana, E. Diverse Functional Roles of Reactive Cysteines. *ACS Chem. Biol.* **2013**, *8* (2), 283–296.

(5) Loi, V. Van; Busche, T.; Preuß, T.; Kalinowski, J.; Bernhardt, J.; Antelmann, H. The AGXX® Antimicrobial Coating Causes a Thiol-Specific Oxidative Stress Response and Protein S-Bacillithiolation in Staphylococcus Aureus. *Front. Microbiol.* **2018**, *9*, 3037.

(6) Imber, M.; Huyen, N. T. T.; Pietrzyk-Brzezinska, A. J.; Loi, V. Van; Hillion, M.; Bernhardt, J.; Thärichen, L.; Kolšek, K.; Saleh, M.; Hamilton, C. J.; et al. Protein S - Bacillithiolation Functions in Thiol Protection and Redox Regulation of the Glyceraldehyde-3-Phosphate Dehydrogenase Gap in Staphylococcus Aureus Under Hypochlorite Stress. *Antioxid. Redox Signal.* **2018**, *28* (6), 410–430.

(7) Sun, F.; Ding, Y.; Ji, Q.; Liang, Z.; Deng, X.; Wong, C. C. L.; Yi, C.; Zhang, L.; Xie, S.; Alvarez, S.; et al. Protein Cysteine Phosphorylation of SarA/MgrA Family Transcriptional Regulators Mediates Bacterial Virulence and Antibiotic Resistance. *Proc. Natl Acad. Sci. U S A* **2012**, *109* (38), 15461–15466.

(8) Newton, G. L.; Rawat, M.; La Clair, J. J.; Jothivasan, V. K.; Budiarto, T.; Hamilton, C. J.; Claiborne, A.; Helmann, J. D.; Fahey, R. C. Bacillithiol Is an Antioxidant Thiol Produced in Bacilli. *Nat. Chem. Biol.* **2009**, *5* (9), 625–627.

(9) Newton, G. L.; Fahey, R. C.; Rawat, M. Detoxification of Toxins by Bacillithiol in Staphylococcus Aureus. *Microbiol.* **2012**, *158* (Pt 4), 1117–1126.

(10) Deneke, S. M. Thiol-Based Antioxidants. *Curr. Top. Cell. Regul.* **2000**, *36*, 151–180.

(11) Balcerczyk, A.; Bartosz, G. Thiols Are Main Determinants of Total Antioxidant

Capacity of Cellular Homogenates. *Free Radic. Res.* **2003**, *37* (5), 537–541.

(12) Gout, I. Coenzyme A: A Protective Thiol in Bacterial Antioxidant Defence. *Biochem. Soc.Trans.* **2019**, *47* (1), 469–476.

(13) Norambuena, J.; Flores, R.; Cárdenas, J. P.; Quatrini, R.; Chávez, R.; Levicán, G. Thiol/Disulfide System Plays a Crucial Role in Redox Protection in the Acidophilic Iron-Oxidizing Bacterium Leptospirillum Ferriphilum. *PLoS One* **2012**, *7* (9), e44576.

(14) Fang, F. C. Antimicrobial Reactive Oxygen and Nitrogen Species: Concepts and Controversies. *Nat. Rev. Micro.* **2004**, *2* (10), 820–832.

(15) Kalyanaraman, B. Teaching the Basics of Redox Biology to Medical and Graduate Students: Oxidants, Antioxidants and Disease Mechanisms. *Redox Biol.* **2013**, *1* (1), 244–257.

(16) Giles, G. I.; Tasker, K. M.; Jacob, C. Hypothesis: The Role of Reactive Sulfur Species in Oxidative Stress. *Free Radic. Biol. Med.* **2001**, *31* (10), 1279–1283.

(17) Mustacich, D.; Powis, G. Thioredoxin Reductase. *Biochem. J.* **2000**, *346 Pt 1* (Pt 1), 1–8.

(18) Long, M. J. C.; Aye, Y. Privileged Electrophile Sensors: A Resource for Covalent Drug Development. *Cell Chem. Biol.* **2017**, *24* (7), 787–800.

(19) Casini, A.; Scozzafava, A.; Supuran, C. T. Cysteine-Modifying Agents: A Possible Approach for Effective Anticancer and Antiviral Drugs. *Environ. Heal. Perspect.* **2002**, *110 Suppl* (Suppl 5), 801–806.

(20) Visscher, M.; Arkin, M. R.; Dansen, T. B. Covalent Targeting of Acquired Cysteines in Cancer. *Curr. Opin. Chem. Biol.* **2016**, *30*, 61–67.

(21) Hallenbeck, K. K.; Turner, D. M.; Renslo, A. R.; Arkin, M. R. Targeting Non-Catalytic Cysteine Residues Through Structure-Guided Drug Discovery. *Curr. Top. Med. Chem.* **2017**, *17* (1), 4–15.

(22) Belete, T. M. Novel Targets to Develop New Antibacterial Agents and Novel Alternatives to Antibacterial Agents. *Hum. Microbiome J.* **2019**, *11*, 100052.

(23) Kathman, S. G.; Statsyuk, A. V. Covalent Tethering of Fragments for Covalent Probe Discovery. *Medchemcomm* **2016**, *7* (4), 576–585.

(24) Chen, X.; Zhou, Y.; Peng, X.; Yoon, J. Fluorescent and Colorimetric Probes for Detection of Thiols. *Chem. Soc. Rev.* **2010**, *39* (6), 2120–2135.

(25) Peng, H.; Chen, W.; Cheng, Y.; Hakuna, L.; Strongin, R.; Wang, B. Thiol Reactive Probes and Chemosensors. *Sensors (Basel).* **2012**, *12* (11), 15907–15946.

(26) Wang, K.; Peng, H.; Wang, B. Recent Advances in Thiol and Sulfide Reactive Probes. *J. Cell. Biochem.* **2014**, *115* (6), 1007–1022.

(27) Huang, R.; Wang, B.-B.; Si-Tu, X.-M.; Gao, T.; Wang, F.-F.; He, H.; Fan, X.-Y.; Jiang, F.-L.; Liu, Y. A Lysosome-Targeted Fluorescent Sensor for the Detection of Glutathione in Cells with an Extremely Fast Response. *Chem. Commun.* **2016**, *52* (77), 11579–11582.

(28) Zhou, P.; Yao, J.; Hu, G.; Fang, J. Naphthalimide Scaffold Provides Versatile Platform for Selective Thiol Sensing and Protein Labeling. *ACS Chem. Biol.* **2016**, *11* (4), 1098–1105.

(29) Liu, Y.; Xiang, K.; Tian, B.; Zhang, J. A Fluorescein-Based Fluorescence Probe for the Fast Detection of Thiol. *Tetrahedron Lett.* **2016**, *57* (23), 2478–2483.

(30) Liu, Z.; Zhou, X.; Miao, Y.; Hu, Y.; Kwon, N.; Wu, X.; Yoon, J. A Reversible Fluorescent Probe for Real-Time Quantitative Monitoring of Cellular Glutathione. *Angew. Chem. Int. Ed.* **2017**, *56* (21), 5812–5816.

(31) Umezawa, K.; Yoshida, M.; Kamiya, M.; Yamasoba, T.; Urano, Y. Rational Design of Reversible Fluorescent Probes for Live-Cell Imaging and Quantification of Fast Glutathione Dynamics. *Nat. Chem.* **2017**, *9* (3), 279–286.

(32) Yuan, M.; Ma, X.; Jiang, T.; Zhang, C.; Chen, H.; Gao, Y.; Yang, X.; Du, L.; Li, M. A Novel Coelenterate Luciferin-Based Luminescent Probe for Selective and Sensitive Detection of Thiophenols. *Org. Biomol. Chem.* **2016**, *14* (43), 10267–10274.

(33) Malwal, S. R.; Labade, A.; Andhalkar, A. S.; Sengupta, K.; Chakrapani, H. A Highly Selective Sulfinate Ester Probe for Thiol Bioimaging. *Chem. Commun.* **2014**, *50* (78), 11533–11535.

(34) Hemmi, M.; Ikeda, Y.; Shindo, Y.; Nakajima, T.; Nishiyama, S.; Oka, K.; Sato, M.; Hiruta, Y.; Citterio, D.; Suzuki, K. Highly Sensitive Bioluminescent Probe for Thiol Detection in Living Cells. *Chem. Asian J.* **2018**, *13* (6), 648–655.

(35) Ábrányi-Balogh, P.; Petri, L.; Imre, T.; Szijj, P.; Scarpino, A.; Hrast, M.; Mitrović, A.; Fonovič, U. P.; Németh, K.; Barreteau, H.; et al. A Road Map for Prioritizing Warheads for Cysteine Targeting Covalent Inhibitors. *Eur. J. Med. Chem.* **2018**, *160*, 94–107.

(36) Kosower, N. S.; Kosower, E. M. Thiol Labeling with Bromobimanes. *Methods Enzym.* **1987**, *143*, 76–84.

(37) Marino, S. M.; Gladyshev, V. N. Cysteine Function Governs Its Conservation and Degeneration and Restricts Its Utilization on Protein Surfaces. *J. Mol. Biol.* **2010**, *404* (5), 902–916.

(38) Couvertier, S. M.; Zhou, Y.; Weerapana, E. Chemical-Proteomic Strategies to Investigate Cysteine Posttranslational Modifications. *Biochim. Biophys. Acta* **2014**, *1844* (12), 2315–2330.

(39) Hoch, D. G.; Abegg, D.; Adibekian, A. Cysteine-Reactive Probes and Their Use in Chemical Proteomics. *Chem. Commun.* **2018**, *54* (36), 4501–4512.

(40) Pan, Z.; Scheerens, H.; Li, S.-J.; Schultz, B. E.; Sprengeler, P. A.; Burrill, L. C.; Mendonca, R. V.; Sweeney, M. D.; Scott, K. C. K.; Grothaus, P. G.; et al. Discovery of Selective Irreversible Inhibitors for Bruton's Tyrosine Kinase. *ChemMedChem* **2007**, *2* (1), 58–61.

(41) Seo, Y. H.; Carroll, K. S. Quantification of Protein Sulfenic Acid Modifications Using Isotope-Coded Dimedone and Iododimedone. *Angew. Chem. Int. Ed.* **2011**, *50* (6), 1342–1345.

(42) Serafimova, I. M.; Pufall, M. A.; Krishnan, S.; Duda, K.; Cohen, M. S.; Maglathlin, R. L.; McFarland, J. M.; Miller, R. M.; Frödin, M.; Taunton, J. Reversible Targeting of Noncatalytic Cysteines with Chemically Tuned Electrophiles. *Nat. Chem. Biol.* **2012**, *8* (5), 471–476.

(43) Pace, N. J.; Weerapana, E. A Competitive Chemical-Proteomic Platform To Identify Zinc-Binding Cysteines. *ACS Chem. Biol.* **2014**, *9* (1), 258–265.

(44) Bak, D. W.; Pizzagalli, M. D.; Weerapana, E. Identifying Functional Cysteine Residues in the Mitochondria. *ACS Chem. Biol.* **2017**, *12* (4), 947–957.

(45) Abbas, A.; Xing, B.; Loh, T.-P. Allenamides as Orthogonal Handles for Selective Modification of Cysteine in Peptides and Proteins. *Angew. Chem. Int. Ed.* **2014**, *53* (29),

7491–7494.

(46) Stanley, M.; Han, C.; Knebel, A.; Murphy, P.; Shpiro, N.; Virdee, S. Orthogonal Thiol Functionalization at a Single Atomic Center for Profiling Transthiolation Activity of E1 Activating Enzymes. *ACS Chem. Biol.* **2015**, *10* (6), 1542–1554.

(47) Wang, H.; Feng, Y.; Wang, Q.; Guo, X.; Huang, W.; Peng, Y.; Zheng, J. Cysteine-Based Protein Adduction by Epoxide-Derived Metabolite(s) of Benzbromarone. *Chem. Res. Toxicol.* **2016**, *29* (12), 2145–2152.

(48) Ariyasu, S.; Hayashi, H.; Xing, B.; Chiba, S. Site-Specific Dual Functionalization of Cysteine Residue in Peptides and Proteins with 2-Azidoacrylates. *Bioconjugate Chem.* **2017**, *28* (4), 897–902.

(49) Chen, X.; Wu, H.; Park, C.-M.; Poole, T. H.; Keceli, G.; Devarie-Baez, N. O.; Tsang, A. W.; Lowther, W. T.; Poole, L. B.; King, S. B.; et al. Discovery of Heteroaromatic Sulfones As a New Class of Biologically Compatible Thiol-Selective Reagents. *ACS Chem. Biol.* **2017**, *12* (8), 2201–2208.

(50) Allimuthu, D.; Adams, D. J. 2-Chloropropionamide As a Low-Reactivity Electrophile for Irreversible Small-Molecule Probe Identification. *ACS Chem. Biol.* **2017**, *12* (8), 2124–2131.

(51) Zhang, Y.; Zhou, X.; Xie, Y.; Greenberg, M. M.; Xi, Z.; Zhou, C. Thiol Specific and Tracelessly Removable Bioconjugation via Michael Addition to 5-Methylene Pyrrolones. *J. Am. Chem. Soc.* **2017**, *139* (17), 6146–6151.

(52) Yu, J.; Yang, X.; Sun, Y.; Yin, Z. Highly Reactive and Tracelessly Cleavable Cysteine-Specific Modification of Proteins via 4-Substituted Cyclopentenone. *Angew. Chem. Int. Ed.* **2018**, *57* (36), 11598–11602.

(53) Embaby, A. M.; Schoffelen, S.; Kofoed, C.; Meldal, M.; Diness, F. Rational Tuning of Fluorobenzene Probes for Cysteine-Selective Protein Modification. *Angew. Chem. Int. Ed.* **2018**, *57* (27), 8022–8026.

(54) Zhang, C.; Dai, P.; Vinogradov, A. A.; Gates, Z. P.; Pentelute, B. L. Site-Selective Cysteine-Cyclooctyne Conjugation. *Angew. Chem. Int. Ed.* **2018**, *57* (22), 6459–6463.

(55) Matos, M. J.; Navo, C. D.; Hakala, T.; Ferhati, X.; Guerreiro, A.; Hartmann, D.; Bernardim, B.; Saar, K. L.; Compañón, I.; Corzana, F.; et al. Quaternization of

Vinyl/Alkynyl Pyridine Enables Ultrafast Cysteine-Selective Protein Modification and Charge Modulation. *Angew. Chem. Int. Ed.* **2019**, *58* (20), 6640–6644.

(56) Hansen, B. K.; Loveridge, C. J.; Thyssen, S.; Wørmer, G. J.; Nielsen, A. D.; Palmfeldt, J.; Johannsen, M.; Poulsen, T. B. STEFs: Activated Vinylogous Protein-Reactive Electrophiles. *Angew. Chem. Int. Ed.* **2019**, *58* (11), 3533–3537.

(57) Shindo, N.; Fuchida, H.; Sato, M.; Watari, K.; Shibata, T.; Kuwata, K.; Miura, C.; Okamoto, K.; Hatsuyama, Y.; Tokunaga, K.; et al. Selective and Reversible Modification of Kinase Cysteines with Chlorofluoroacetamides. *Nat. Chem. Biol.* **2019**, *15* (3), 250–258.

(58) Kislukhin, A. A.; Higginson, C. J.; Hong, V. P.; Finn, M. G. Degradable Conjugates from Oxanorbornadiene Reagents. *J. Am. Chem. Soc.* **2012**, *134* (14), 6491–6497.

(59) Sankar, R. K.; Kumbhare, R. S.; Dharmaraja, A. T.; Chakrapani, H. A Phenacrylate Scaffold for Tunable Thiol Activation and Release. *Chem. Commun.* **2014**, *50* (97), 15323–15326.

(60) Barrett, A. J.; Kembhavi, A. A.; Brown, M. A.; Kirschke, H.; Knight, C. G.; Tamai, M.; Hanada, K. L-Trans-Epoxysuccinyl-Leucylamido(4-Guanidino)Butane (E-64) and Its Analogues as Inhibitors of Cysteine Proteinases Including Cathepsins B, H and L. *Biochem. J.* **1982**, *201* (1), 189–198.

(61) Murata, M.; Miyashita, S.; Yokoo, C.; Tamai, M.; Hanada, K.; Hatayama, K.; Towatari, T.; Nikawa, T.; Katunuma, N. Novel Epoxysuccinyl Peptides Selective Inhibitors of Cathepsin B, in Vitro. *FEBS Lett.* **1991**, *280* (2), 307–310.

(62) Bogyo, M.; Verhelst, S.; Bellingard-Dubouchaud, V.; Toba, S.; Greenbaum, D. Selective Targeting of Lysosomal Cysteine Proteases with Radiolabeled Electrophilic Substrate Analogs. *Chem. Biol.* **2000**, *7* (1), 27–38.

(63) Sadaghiani, A. M.; Verhelst, S. H. L.; Gocheva, V.; Hill, K.; Majerova, E.; Stinson, S.; Joyce, J. A.; Bogyo, M. Design, Synthesis, and Evaluation of In Vivo Potency and Selectivity of Epoxysuccinyl-Based Inhibitors of Papain-Family Cysteine Proteases. *Chem. Biol.* **2007**, *14* (5), 499–511.

(64) Kisselev, A. F.; van der Linden, W. A.; Overkleeft, H. S. Proteasome Inhibitors: An Expanding Army Attacking a Unique Target. *Chem. Biol.* **2012**, *19* (1), 99–115.

(65) Oleksy, A.; Golonka, E.; Bańbula, A.; Szmyd, G.; Moon, J.; Kubica, M.; Greenbaum, D.; Bogyo, M.; Foster, T. J.; Travis, J.; et al. Growth Phase-Dependent Production of a Cell Wall-Associated Elastinolytic Cysteine Proteinase by Staphylococcus Epidermidis. *Biol. Chem.* **2004**, *385* (6), 525–535.

(66) Dang, T. H. T.; Riva, L. de la; Fagan, R. P.; Storck, E. M.; Heal, W. P.; Janoir, C.; Fairweather, N. F.; Tate, E. W. Chemical Probes of Surface Layer Biogenesis in Clostridium Difficile. *ACS Chem. Biol.* **2010**, *5* (3), 279–285.

(67) Hang, H. C.; Loureiro, J.; Spooner, E.; van der Velden, A. W. M.; Kim, Y.-M.; Pollington, A. M.; Maehr, R.; Starnbach, M. N.; Ploegh, H. L. Mechanism-Based Probe for the Analysis of Cathepsin Cysteine Proteases in Living Cells. *ACS Chem. Biol.* **2006**, *1* (11), 713–723.

(68) Kahan, F. M.; Kahan, J. S.; Cassidy, P. J.; Kropp, H. The Mechanism of Action of Fosfomycin (Phosphonomycin). *Ann. N. Y. Acad. Sci.* **1974**, *235* (1), 364–386.

(69) Marquardt, J. L.; Brown, E. D.; Lane, W. S.; Haley, T. M.; Ichikawa, Y.; Wong, C.-H.; Walsh, C. T. Kinetics, Stoichiometry, and Identification of the Reactive Thiolate in the Inactivation of UDP-GlcNAc Enolpyruvoyl Transferase by the Antibiotic Fosfomycin. *Biochemistry* **1994**, *33* (35), 10646–10651.

(70) Feroj Hasan, A. F. M.; Furumoto, T.; Begum, S.; Fukui, H. Hydroxysesamone and 2,3-Epoxysesamone from Roots of Sesamum Indicum. *Phytochemistry* **2001**, *58*, 1225–1228.

(71) Furumoto, T. Biosynthetic Origin of 2,3-Epoxysesamone in a Sesamum Indicum Hairy Root Culture. *Biosci., Biotechnol., Biochem.* **2009**, *73*, 2535–2537.

(72) Ellestad, G. A.; Whaley, H. A.; Patterson, E. L. The Structure of Frenolicin. *J. Am. Chem. Soc.* **1966**, *88*, 4109–4110.

(73) Westhofen, P.; Watzka, M.; Marinova, M.; Hass, M.; Kirfel, G.; Müller, J.; Bevans, C. G.; Müller, C. R.; Oldenburg, J. Human Vitamin K 2,3-Epoxide Reductase Complex Subunit 1-like 1 (VKORC1L1) Mediates Vitamin K-Dependent Intracellular Antioxidant Function. *J. Biol. Chem.* **2011**, *286* (17), 15085–15094.

(74) Brunmark, A.; Cadenas, E. 1,4-Reductive Addition of Glutathione to Quinone Epoxides. Mechanistic Studies with h.p.l.c. with Electrochemical Detection under Anaerobic and

Aerobic Conditions. Evaluation of Chemical Reactivity in Terms of Autoxidation Reactions. *Free Radic. Bio. Med.* **1989**, *6* (2), 149–165.

(75) Dharmaraja, A. T.; Dash, T. K.; Konkimalla, V. B.; Chakrapani, H. Synthesis, Thiol-Mediated Reactive Oxygen Species Generation Profiles and Anti-Proliferative Activities of 2,3-Epoxy-1,4-Naphthoquinones. *Med. Chem. Commun.* **2012**, *3* (2), 219–224.

(76) Kawakami, Y.; Hartman, S. E.; Kinoshita, E.; Suzuki, H.; Kitaura, J.; Yao, L.; Inagaki, N.; Franco, A.; Hata, D.; Maeda-Yamamoto, M.; et al. Terreic Acid, a Quinone Epoxide Inhibitor of Bruton's Tyrosine Kinase. *Proc. Natl Acad. Sci. U S A* **1999**, *96* (5), 2227–2232.

(77) Mandl, F. A.; Kirsch, V. C.; Ugur, I.; Kunold, E.; Vomacka, J.; Fetzer, C.; Schneider, S.; Richter, K.; Fuchs, T. M.; Antes, I.; et al. Natural-Product-Inspired Aminoepoxybenzoquinones Kill Members of the Gram-Negative Pathogen Salmonella by Attenuating Cellular Stress Response. *Angew. Chem. Int. Ed.* **2016**, *55* (47), 14852–14857.

(78) Aoyama, A.; Murai, M.; Ichimaru, N.; Aburaya, S.; Aoki, W.; Miyoshi, H. Epoxycyclohexenedione-Type Compounds Make Up a New Class of Inhibitors of the Bovine Mitochondrial ADP/ATP Carrier. *Biochemistry* **2018**, *57* (6), 1031–1044.

(79) Tuley, A.; Fast, W. The Taxonomy of Covalent Inhibitors. *Biochemistry* **2018**, *57* (24), 3326–3337.

(80) Walsh, C.; Wright, G. Introduction: Antibiotic Resistance. *Chem. Rev.* **2005**.

(81) *ANTIMICROBIAL RESISTANCE Global Report on Surveillance*.

(82) Santajit, S.; Indrawattana, N. Mechanisms of Antimicrobial Resistance in ESKAPE Pathogens. *BioMed Res. Int.* **2016**, *2016*, 1–8.

(83) Tong, S. Y. C.; Davis, J. S.; Eichenberger, E.; Holland, T. L.; Fowler, V. G. Staphylococcus Aureus Infections: Epidemiology, Pathophysiology, Clinical Manifestations, and Management. *Clin. Microbiol. Rev.* **2015**, *28* (3), 603–661.

(84) Chambers, H. F.; DeLeo, F. R. Waves of Resistance: Staphylococcus Aureus in the Antibiotic Era. *Nat. Rev. Microbiol.* **2009**, *7* (9), 629–641.

(85) Hiramatsu, K.; Aritaka, N.; Hanaki, H.; Kawasaki, S.; Hosoda, Y.; Hori, S.; Fukuchi, Y.; Kobayashi, I. Dissemination in Japanese Hospitals of Strains of Staphylococcus Aureus Heterogeneously Resistant to Vancomycin. *Lancet* **1997**, *350* (9092), 1670–1673.

(86) Kobayashi, S. D.; Musser, J. M.; DeLeo, F. R. Genomic Analysis of the Emergence of Vancomycin-Resistant Staphylococcus Aureus. *MBio* **2012**, *3* (4).

(87) Sass, P.; Berscheid, A.; Jansen, A.; Oedenkoven, M.; Szekat, C.; Strittmatter, A.; Gottschalk, G.; Bierbaum, G. Genome Sequence of Staphylococcus Aureus VC40, a Vancomycin- and Daptomycin-Resistant Strain, To Study the Genetics of Development of Resistance to Currently Applied Last-Resort Antibiotics. *J. Bacteriol.* **2012**, *194* (8), 2107–2108.

(88) Liu, Y.; Patricelli, M. P.; Cravatt, B. F. Activity-Based Protein Profiling: The Serine Hydrolases. *Proc. Natl Acad. Sci. U S A* **1999**, *96* (26), 14694–14699.

(89) Speers, A. E.; Cravatt, B. F. Chemical Strategies for Activity-Based Proteomics. *ChemBioChem* **2004**, *5* (1), 41–47.

(90) Puri, A. W.; Bogyo, M. Using Small Molecules To Dissect Mechanisms of Microbial Pathogenesis. *ACS Chem. Biol.* **2009**, *4* (8), 603–616.

(91) Evans, M. J.; Cravatt, B. F. Mechanism-Based Profiling of Enzyme Families. *Chem. Rev.* **2006**, *106* (8), 3279–3301.

(92) Liu, Y.; Patricelli, M. P.; Cravatt, B. F. Activity-Based Protein Profiling: The Serine Hydrolases. *Proc. Natl Acad. Sci. U S A* **1999**, *96* (26), 14694–14699.

(93) Hatzios, S. K.; Abel, S.; Martell, J.; Hubbard, T.; Sasabe, J.; Munera, D.; Clark, L.; Bachovchin, D. A.; Qadri, F.; Ryan, E. T.; et al. Chemoproteomic Profiling of Host and Pathogen Enzymes Active in Cholera. *Nat. Chem. Biol.* **2016**, *12*, 268.

(94) Hacker, S. M.; Backus, K. M.; Lazear, M. R.; Forli, S.; Correia, B. E.; Cravatt, B. F. Global Profiling of Lysine Reactivity and Ligandability in the Human Proteome. *Nat. Chem.* **2017**, *9* (12), 1181–1190.

(95) Moellering, R. E.; Cravatt, B. F. How Chemoproteomics Can Enable Drug Discovery and Development. *Chem. Biol.* **2012**, *19* (1), 11–22.

(96) Paulick, M. G.; Bogyo, M. Application of Activity-Based Probes to the Study of Enzymes Involved in Cancer Progression. *Curr. Opin. Genet. Dev.* **2008**, *18* (1), 97–106.

(97) Puri, A. W.; Bogyo, M. Applications of Small Molecule Probes in Dissecting Mechanisms of Bacterial Virulence and Host Responses. *Biochemistry* **2013**, *52* (35), 5985–5996.

(98) Weerapana, E.; Wang, C.; Simon, G. M.; Richter, F.; Khare, S.; Dillon, M. B. D.; Bachovchin, D. A.; Mowen, K.; Baker, D.; Cravatt, B. F. Quantitative Reactivity Profiling Predicts Functional Cysteines in Proteomes. *Nature* **2010**, *468* (7325), 790–795.

(99) Abegg, D.; Frei, R.; Cerato, L.; Prasad Hari, D.; Wang, C.; Waser, J.; Adibekian, A. Proteome-Wide Profiling of Targets of Cysteine Reactive Small Molecules by Using Ethynyl Benziodoxolone Reagents. *Angew. Chem. Int. Ed.* **2015**, *54* (37), 10852–10857.

(100) Balakrishnan, A.; Patel, B.; Sieber, S. A.; Chen, D.; Pachikara, N.; Zhong, G.; Cravatt, B. F.; Fan, H. Metalloprotease Inhibitors GM6001 and TAPI-0 Inhibit the Obligate Intracellular Human Pathogen Chlamydia Trachomatis by Targeting Peptide Deformylase of the Bacterium. *J. Biol. Chem.* **2006**, *281* (24), 16691–16699.

(101) Gersch, M.; Kreuzer, J.; Sieber, S. A. Electrophilic Natural Products and Their Biological Targets. *Nat. Prod. Rep.* **2012**, *29* (6), 659–682.

(102) Staub, I.; Sieber, S. A. β-Lactams as Selective Chemical Probes for the in Vivo Labeling of Bacterial Enzymes Involved in Cell Wall Biosynthesis, Antibiotic Resistance, and Virulence. *J. Am. Chem. Soc.* **2008**, *130* (40), 13400–13409.

(103) Böttcher, T.; Sieber, S. A. β-Lactones as Specific Inhibitors of ClpP Attenuate the Production of Extracellular Virulence Factors of Staphylococcus Aureus. *J. Am. Chem. Soc.* **2008**, *130* (44), 14400–14401.

(104) Böttcher, T.; Sieber, S. A. β-Lactones as Privileged Structures for the Active-Site Labeling of Versatile Bacterial Enzyme Classes. *Angew. Chem. Int. Ed.* **2008**, *47* (24), 4600–4603.

(105) Böttcher, T.; Sieber, S. A. Structurally Refined β-Lactones as Potent Inhibitors of Devastating Bacterial Virulence Factors. *ChemBioChem* **2009**, *10* (4), 663–666.

(106) Böttcher, T.; Sieber, S. A. β-Lactones Decrease the Intracellular Virulence of *Listeria Monocytogenes* in Macrophages. *ChemMedChem* **2009**, *4* (8), 1260–1263.

(107) Kunzmann, M. H.; Bach, N. C.; Bauer, B.; Sieber, S. A. α-Methylene-γ-Butyrolactones Attenuate Staphylococcus Aureus Virulence by Inhibition of Transcriptional Regulation. *Chem. Sci.* **2014**, *5* (3), 1158.

(108) Gloeckl, S.; Ong, V. A.; Patel, P.; Tyndall, J. D. A.; Timms, P.; Beagley, K. W.; Allan, J. A.; Armitage, C. W.; Turnbull, L.; Whitchurch, C. B.; et al. Identification of a Serine Protease Inhibitor Which Causes Inclusion Vacuole Reduction and Is Lethal to Chlamydia Trachomatis. *Mol. Microbiol.* **2013**, *89* (4), 676–689.

(109) Pidgeon, S. E.; Pires, M. M. Vancomycin-Dependent Response in Live Drug-Resistant Bacteria by Metabolic Labeling. *Angew. Chem. Int. Ed.* **2017**, *56* (30), 8839–8843.

(110) Lentz, C. S.; Sheldon, J. R.; Crawford, L. A.; Cooper, R.; Garland, M.; Amieva, M. R.; Weerapana, E.; Skaar, E. P.; Bogyo, M. Identification of a S. Aureus Virulence Factor by Activity-Based Protein Profiling (ABPP). *Nat. Chem. Biol.* **2018**, *14* (6), 609–617.

(111) Anna E. Speers; Gregory C. Adam, A.; Cravatt, B. F. Activity-Based Protein Profiling in Vivo Using a Copper(I)-Catalyzed Azide-Alkyne [3 + 2] Cycloaddition. *J. Am. Chem. Soc.* **2003**, *125* (16), 4686–4687.

(112) Welsch, M. E.; Snyder, S. A.; Stockwell, B. R. Privileged Scaffolds for Library Design and Drug Discovery. *Curr. Opin. Chem. Bio.* **2010**, *14* (3), 347–361.

CHAPTER 2. Design, synthesis and evaluation of INDQE compounds as thiol targeting probes with potent antibacterial activity

2.1. Introduction

In Chapter 1, 2,3-epoxy-1,4-naphthoquinone epoxides were discussed as scaffolds with potent medicinal properties.[1–4] A number of other literature reports suggest the potential of using small molecules wherein this scaffold is incorporated, for various therapeutic purposes. For example, Kawakami and co-workers have reported Terreic acid (Fig. 2.1.A), which is a fungal metabolite produced by the fungus *Aspergillus Terreus*, as an inhibitor of Bruton's tyrosine kinase (BTK).[5] BTK plays a very important role in the activation of mast cell and development of B cells. Terreic acid was thus found to be a very useful probe for understanding the functions of BTK in mast cells and other immune systems. Olesen and co-workers have shown that Terreic acid can inhibit bacterial growth and suggest that it is bacteriostatic in nature.[6] Another study by Sieber and co-workers has utilized a natural-product inspired aminoepoxybenzoquinone scaffold as a potent antibacterial.[7] A lead compound, amino-2,3-epoxy-1,4-naphthoquinone (**AEC-FM233**) (Fig. 2.1.B) was reported to react with cellular thiols, targeting certain redox-active proteins such as glutaredoxin 2 (GrxB), thioredoxin-1 (TrxA), and thus proved to be detrimental to the growth of Gram-negative *S. typhimurium*. One of the most interesting targets, was the sigma cross-reacting protein 27A (SCRP-27A), which is a protein of unknown function, belonging to the DJ-1 protein superfamily. However, certain biochemical assays showed that the binding of **AEC-FM233** to SCRP-27A was not important for the antibacterial mechanism of action. This study was followed up by another, where the same group reported a similar scaffold to monitor Parkinsonism-associated protein DJ-1 (PARK7) in live cells.[8] The molecule could effectively label the cysteine residue on this protein in its reduced state *via* the epoxide warhead. However, the active inhibitor, **AEC-FM247** (Fig. 2.1.C), had an epoxide flanked between a carbonyl group on one side and a hydroxyl group on the other, and thus was not a quinone-epoxide. Recently, Miyoshi and co-workers reported epoxycyclohexenedione-type compounds (**ECHD-AMM-59**, Fig. 2.1.D) to be potent inhibitors of bovine mitochondrial ADP/ATP carrier (AAC).[9] Biochemical characterization suggested that **ECHD-AMM-59** inhibits the function of AAC by covalently binding to cysteine residues, leading to their aggregation.

Chakrapani and co-workers had earlier reported Naphthoquinone epoxides (NQEs, Fig. 2.1.E) as potent inhibitors of human leukemia (THP1) cell proliferation.[10] These compounds were potent Reactive Oxygen Species (ROS) generators, activated by their reaction with a cellular thiol. Structure-Activity Relationship (SAR) studies were conducted by changing the groups on the aryl ring on the epoxide and analyzing the amount of ROS generated. Compounds capable of generating higher amounts of ROS were found to be better at inhibiting human leukemia.

Figure 2.1. Reported examples with quinone-epoxide as reactive moiety

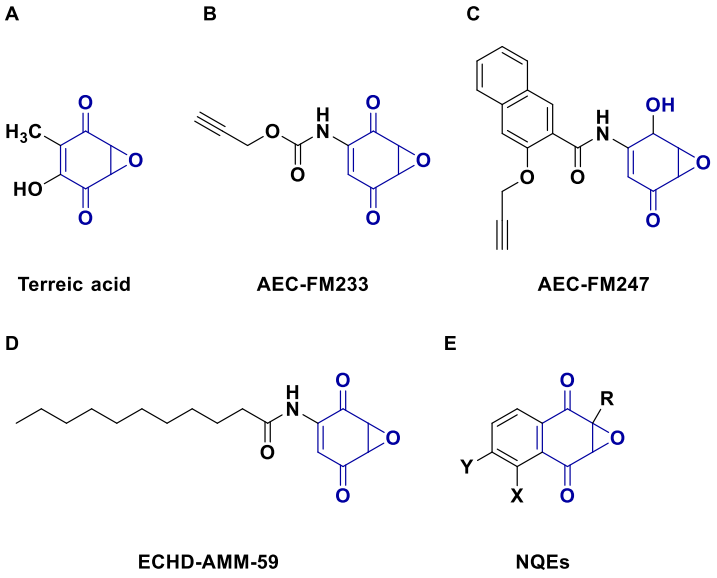

Thus, the aforementioned examples strongly suggest that the 2,3-epoxy-1,4-naphthoquinone scaffold is of significant therapeutic importance. Also, this scaffold can react with cellular thiols and inhibits key proteins in cancer cells as well as pathogenic bacteria. Thus, incorporation of this scaffold can open new paradigms in the fight against antimicrobial resistance. Structure activity relationship (SAR) studies would enable identifying lead compounds that could potently inhibit bacterial growth.

The timeline of AMR for *S. aureus* (Fig. 2.2) was discussed in Chapter 1. As the resistance to clinically used antibiotics increases, it makes it difficult to propose proper treatment strategies to combat these infections. Thus, new antibacterial agents with a novel mechanism of action are in demand.

Figure 2.2. AMR Timeline for *Staphylococcus aureus*

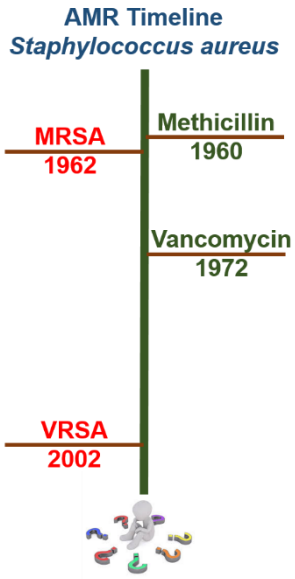

2.1.1. Prolog

Earlier, 2,3-epoxy-1,4-naphthoquinones were reported as thiol-reactive molecules showing antiproliferative properties.[10] When tested against drug-resistant Gram-positive bacteria, such as *S. aureus*, they were found to be good inhibitors (Fig. 2.3), inhibiting the resistant strain MRSA with MIC values of 16 μg/mL.[11]

Figure 2.3. NQEs as potent inhibitors of MRSA

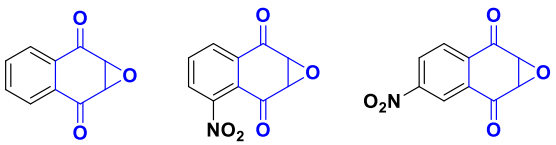

However, permeability and tunability of reactivity with thiols could not be further improved within the said design of the scaffold. Hence, in order to improve the potency of these compounds, this design was further modified. For this restructuring of the scaffold, indole was considered and added to the scaffold. An indole-based 1,4-naphthoquinone epoxide scaffold was thus designed (Fig. 2.4). Indole is a constituent of the core scaffold structure of a number of natural products and drugs, is known to improve the pharmacological properties of the drug, and is thus considered as a privileged scaffold.[12]

Figure 2.4. Revised design - From NQEs to INDQEs

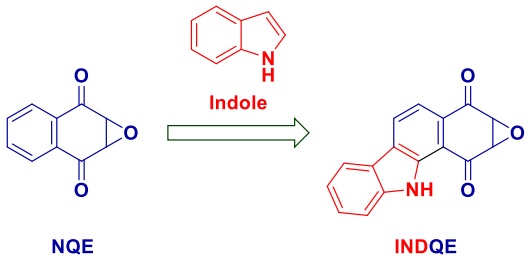

With this revised design, a series of analogues were synthesized following the general synthetic Scheme 2.1.

Scheme 2.1. Synthesis of INDQE scaffold

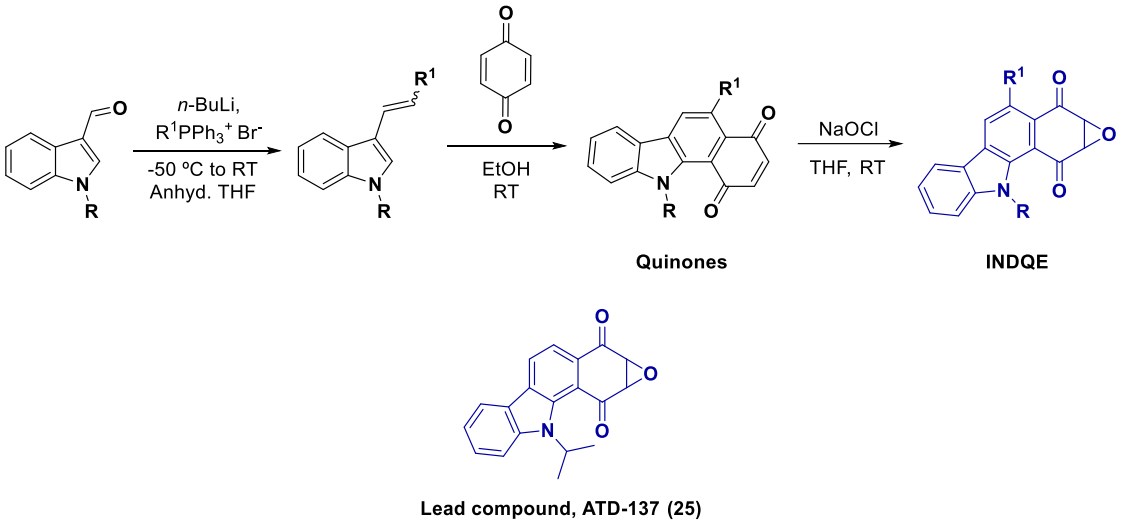

These compounds were screened for their antibacterial activity and a lead compound, **ATD-137 (25)**, was identified, showing potent inhibitory activity against MRSA.[11] The MIC of this compound (Table 2.1) was better than the clinically used antibiotic, vancomycin. Using mBBr assay, the lead compound was also found to deplete thiols intracellularly in *S. aureus*. A Structure-Activity Relationship (SAR) study also highlighted that compounds with R^1 = Me show diminished reactivity with thiols as compared to their R^1 = H counterparts (Table 2.1). The SAR study underlined that higher reactivity with thiols correlated with lower MIC values and thus potent antibacterial activity.

Table 2.1. Structure Activity Relationship studies as a prologue, suggesting correlation between reactivity with a thiol and antibacterial potency (representative compounds listed)

R	R^1 = H			R^1 = Me		
	Cpd	% Remaining[a]	MIC[b] (μg/mL)	Cpd	% Remaining[a]	MIC[b] (μg/mL)
H	**ATD-135**	33	4	**ATD-140**	86	4
Et	**ATD-136**	33	2	**ATD-141**	93	>16
^{i}Pr	**ATD-137 (25)**[c]	34	0.125	**ATD-142**	84	4

[a]HPLC studies, reaction with 1 eq. *L*-Cysteine; [b]MIC against *S. aureus* ATCC 25912; [c]Lead compound from background study, present code for this study

This study explored the role of substituents in deciding thiol-reactivity for the designed INDQE scaffold. It also underlined that reactivity with thiols was directly correlated to antibacterial activity for these compounds. Further studies could investigate the effects of substitution on the epoxide of this scaffold and how that correlates with reactivity toward thiols and antibacterial activity. Substitutions on the epoxide is expected to help modulate thiol reactivity through sterics and electronics. This will, in turn, provide data for a better understanding of the nature of reactivity of the epoxide with the thiol, and further help in elucidating the mechanism of action of the antibacterial activity of these compounds.

2.2. Results and Discussion

2.2.1. Synthesis

In order to further understand the role of increasing sterics at R^1 on reactivity with thiol, compound **26** was synthesized following Scheme 2.2, with R^1=Et, as an analogue of the lead compound **25**. First, *N*-alkylation of indole-3-carboxaldehyde was done using isopropyl bromide. This product was then subjected to a Wittig olefination reaction using propyltriphenylphosphonium bromide in presence of *n*-butyl lithium. The Wittig adduct was found to be unstable and was not isolated, and directly reacted with 1,4 benzoquinone. Aerobic oxidation in ethanol gave quinone **2** in 17% yield. This quinone was then epoxidized to the final INDQE compound **26** using sodium hypochlorite, and was obtained in 76% yield.

Scheme 2.2. Synthetic scheme for compound 26

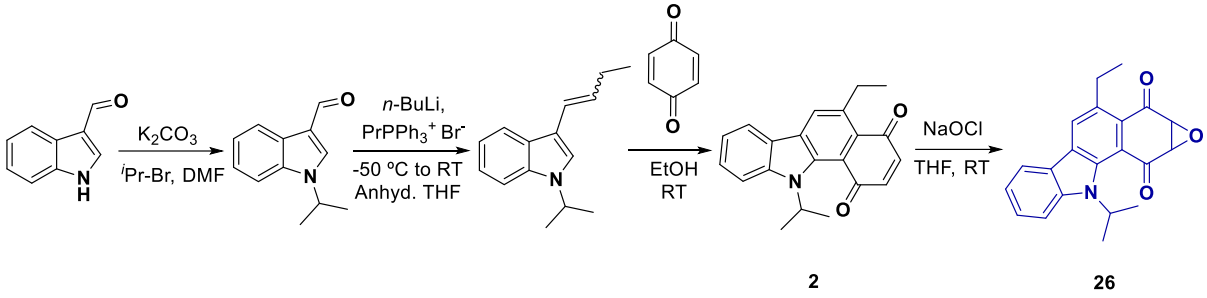

Table 2.2. Synthesis of compounds 25 and 26

Entry	Quinone	% Yield[a]	Epoxide	R	R^1	% Yield[a]
1	**1**	23	**25**	^{i}Pr	H	96
2	**2**	17	**26**	^{i}Pr	Et	76

[a]Crude yield reported

Synthesis of derivatives with a bulkier group at R^1 was attempted. However, the Diels-Alder reaction did not yield the expected product in these cases, possibly due to the steric hindrance. Hence, the synthesis of these derivatives was unsuccessful.

Crystalline compound **25** was obtained and X-ray diffraction analysis suggested a boat-shaped quinone-epoxide (Fig. 2.5 A). Further analysis of the crystal structure suggested an overlap of Van der Waals radii[13] between the carbonyl oxygens of the quinone and neighbouring groups (Fig. 2.5 B). Now, when a thiol attacks on the carbon(s) bearing the epoxide, the epoxide ring opens up and the quinone flap is pushed into the plane. Depending upon the extent of overlap of the carbonyl oxygen with the neighbouring groups, the hindrance for attack at carbons '1' or '10' could be estimated. A significant overlap between carbonyl oxygen next to the carbon at '10' position and the substituent group on the indole nitrogen (carbon) was observed. Although, earlier studies with compounds **ATD 135-137**, had shown that this overlap is not affecting the reactivity with thiol or the antibacterial activity substantially. (Table 2.1). The overlap between carbonyl oxygen next to the carbon at '1' position and substituent at the '3' position also contributed to the reactivity with thiol and antibacterial potency as observed in the case of the compounds **ATD 140-142** (Table 2.1). Here, when the substituent is R^1 = Me (compound **ATD-142**), the extent of overlap is expected to be greater as compared with compound **25**, where R^1 = H. This suggests that there is an increase in the steric strain when the quinone tries to attain planarity after the thiol attack on the epoxide. As was observed, the

compound had low reactivity with thiol and 16-fold less potency (MIC = 4 μg/mL) as compared to its R^1 = H counterpart, compound **25**. This was also observed for the other similar pairs of compounds (Table 2.1). All in all, this data suggested that the position '1' was more favoured for attack by a nucleophile (thiol) as compared to position '10'.

Figure 2.5. ORTEP diagrams of compound 25, A) Boat-shape of the quinone-epoxide; B) Van der Waals overlap between carbonyl oxygens and neighbouring groups

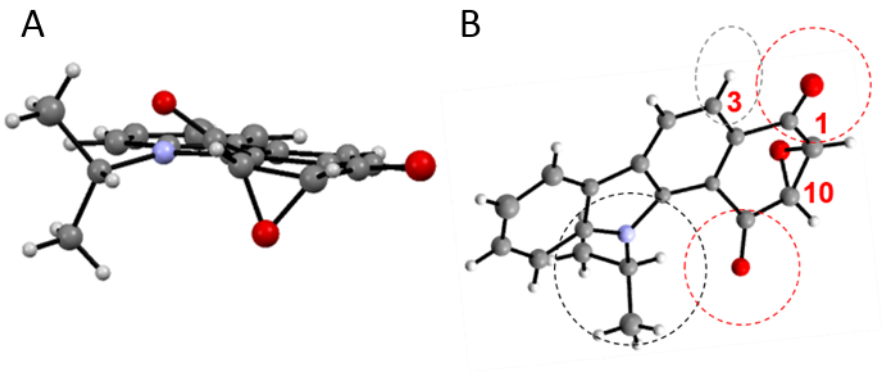

Next, compounds with substitution on the epoxide were synthesized. As the epoxide is the reactive site in the scaffold, these substitutions would testify the tunability in reactivity towards thiols. For this, substituted benzoquinones were first synthesized using Scheme 2.3.

Scheme 2.3. Arylation of benzoquinone; two schemes followed

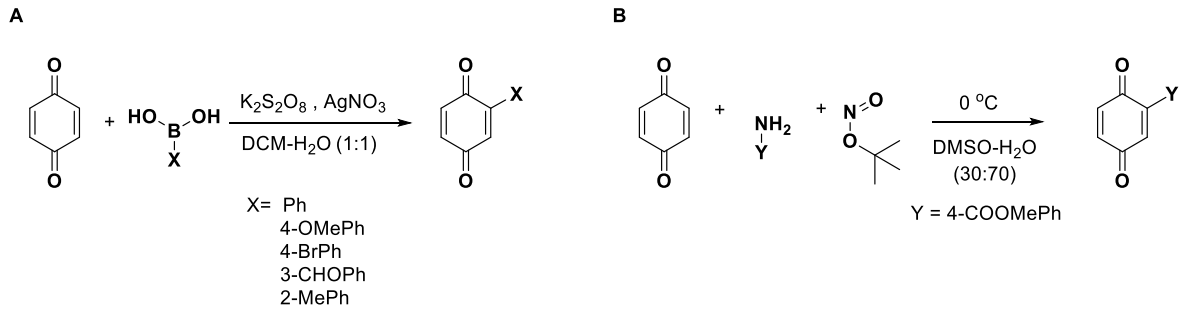

These substituted benzoquinones were further incorporated in the synthetic scheme employed to synthesize the analogues with substitution at the epoxide (Scheme 2.4. A, Scheme 2.5 as general scheme). Majority of the analogues were synthesized with the isopropyl group at the indole nitrogen, as earlier SAR studies suggested the importance of this group for the compound's antibacterial potency, as also seen with the lead compound **25**.

Scheme 2.4. A) Synthesis of INDQE compounds with substitution at the epoxide (compounds 27 and 28); B) Two possible orientations of the dienophile in the Diels-Alder reaction

(reproduced with permission from *J. Med. Chem.* <https://pubs.acs.org/doi/10.1021/acs.jmedchem.9b00774>)

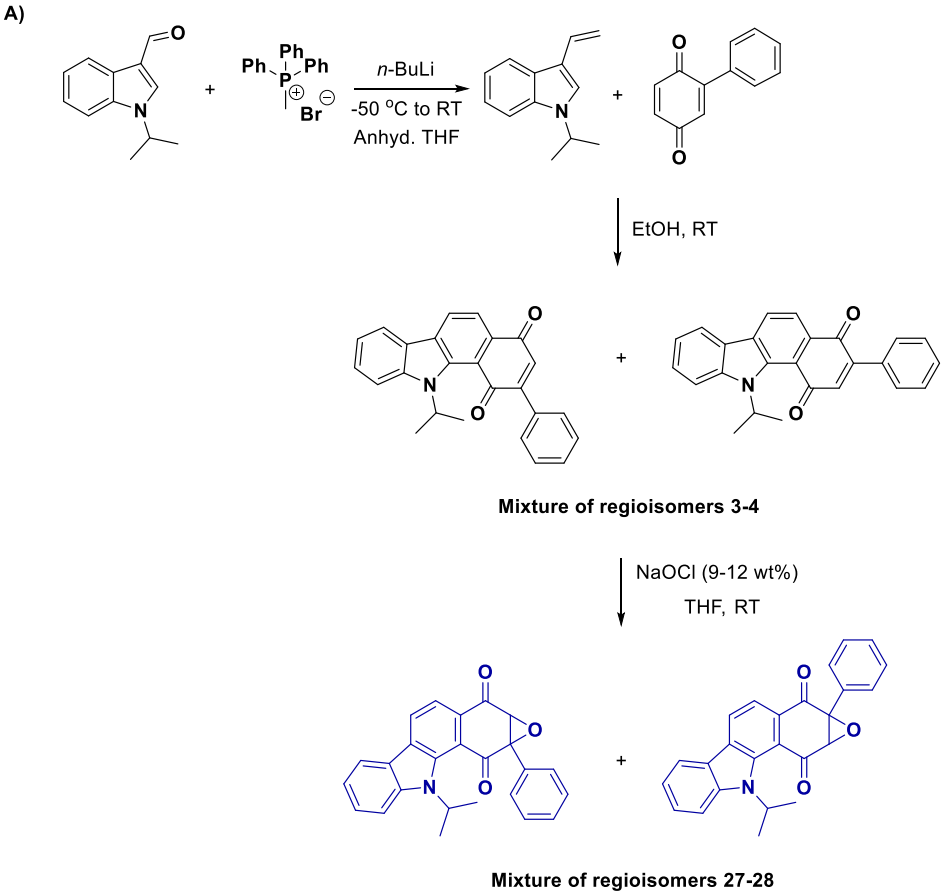

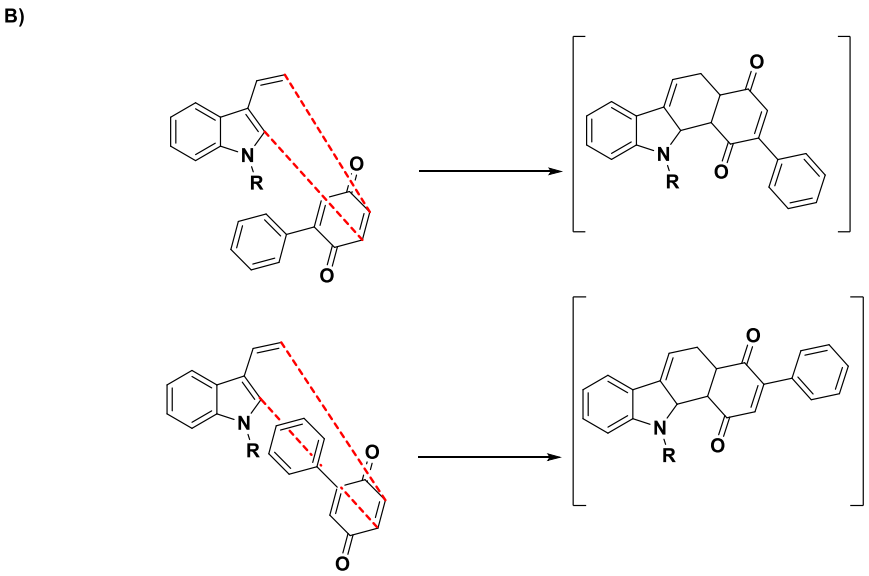

Again, Wittig olefination resulted in an unstable compound and the product, not isolated, was subjected to Diels-Alder cycloaddition reaction. In this step, the dienophile, benzoquinone, is substituted, and hence unsymmetric. Thus, it can approach the diene in two possible ways for the attack, possibly resulting in a set of regioisomers (Scheme 2.4. B). Aerobic oxidation gave the compounds **3-24** (Scheme 2.5). The obtained pair of regioisomers were inseparable using silica-gel column chromatography purification techniques. The mixture of regioisomers were used as such for the last step i.e. epoxidation. The resulting epoxides were again obtained as a mixture of regioisomers, compounds **27-46**. These mixtures of two compounds could not be further separated using silica-gel column chromatography methods.

Scheme 2.5. General synthesis scheme for INDQE compounds with substitution at the epoxide

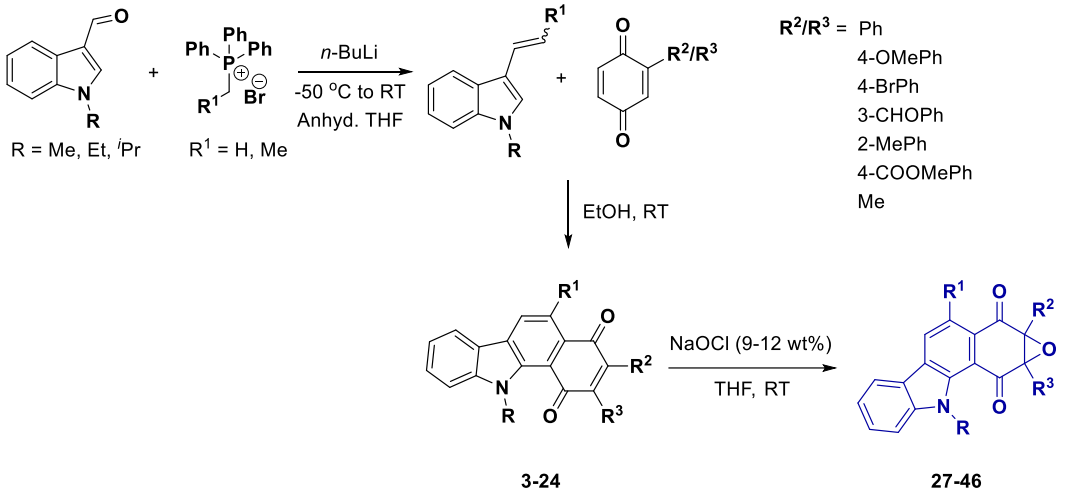

In order to separate these mixtures of regioisomers into their individual two components, the mixtures were subjected to a reversed-phase HPLC based purification protocol. The first set of compounds with a phenyl substituent on the epoxide (**27**, **28**) was successfully separated and individual compounds were thoroughly analysed. Using techniques such as ^{1}H, ^{13}C, ^{1}H-^{1}H NOESY, ^{1}H-^{13}C HSQC NMR, IR, HRMS and crystallography, the first set of compounds was analysed and the regiochemistry of the two isomers distinctly established, isomer having the substituent at R^2 position, termed as '1' isomer, and isomer having the substituent at R^3 position termed as '10' isomer, the positions numbered in accordance with their IUPAC nomenclature (Fig. 2.6).

Figure 2.6. General structures of regioisomers

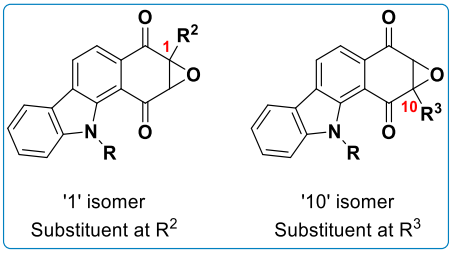

X-ray diffraction analysis was conducted for these isomers and the crystal structures of both these compounds suggested a boat-like conformation of the quinone-epoxide (Fig. 2.7). Both the crystal structures were analysed for various bond-lengths, bond angles and variations in the plane of the six-membered quinone ring containing the epoxide.

Figure 2.7. X-ray diffraction analysis- ORTEP diagram for A) 27, B) 28, C) Schematic showing deviation of the boat from the plane of the ring for both the isomers

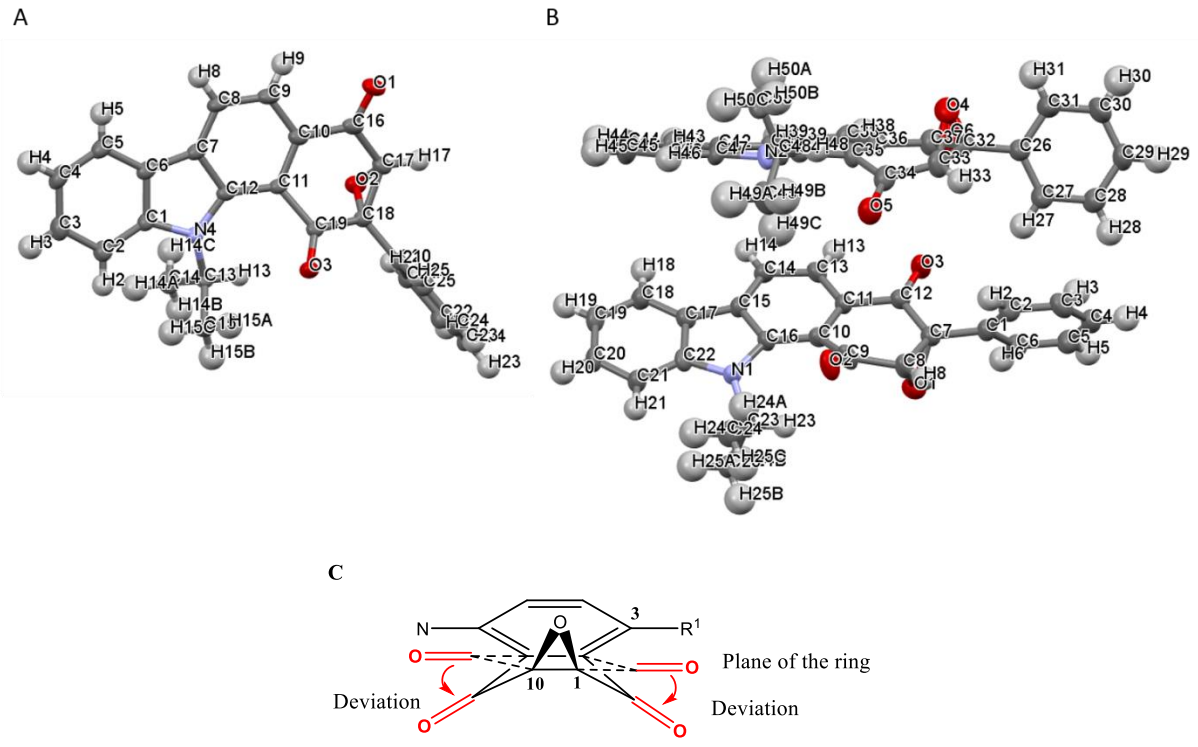

Table 2.3. Analysis of crystal structures of regioisomers 27-28

Side of the boat	Angle of deviation (degrees)[a]	
	Compound **27**	Compound **28**
αC_1	16.0	11.3
αC_{10}	29.0	25.1

[a]Calculated using Mercury 4.0.0

When the deviation of the boat formed by the quinone-epoxide from the plane of the quinone ring (expected) was analysed, it was found that in both the compounds, the deviation of the carbonyl group α to the '10' Carbon (αC_{10}) is away from the plane of the ring more than the carbonyl group α to the '1' carbon (αC_1). Also, the boat of the '10' isomer (**27**) was found to be more deviated than that of '1' isomer (**28**), suggesting more steric strain on the '10' isomer.

Next, in order to study the steric and electronic effects at the epoxide, different analogues of compounds **27** and **28** were synthesized. The regioisomers obtained were separated using reversed-phase HPLC methods (compounds **29-34**) (Table 2.4). To assign the regiochemistry between the isomers, again, a number of analytical methods were used, such as ^{1}H, ^{13}C, ^{1}H-^{1}H NOESY, ^{1}H-^{13}C HSQC NMR, IR, HRMS and crystallography. The crystal structure could only be obtained for compound **32** (Fig. 2.8). Also, NOESY and HSQC NMR (recorded for compounds **29** and **30**) did not provide conclusive information for distinguishing between the isomers. Hence, preliminary ^{1}H NMR data of these compounds was used and characteristic chemical shifts were analysed, and their regiochemistry was assigned keeping compounds **27** and **28** as reference.

Figure 2.8. X-ray diffraction analysis- ORTEP diagram for 32

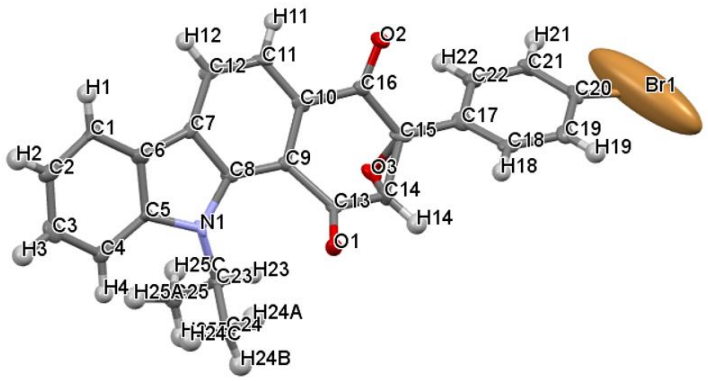

Table 2.4. Compounds synthesized in this study with substitutions on the epoxide (27-34)

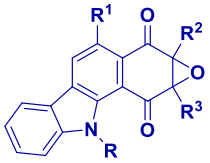

Entry	Quinone mixture	% Yield[a]	Epoxide	R	R^1	R^2	R^3	% Yield[a]
1	**3, 4**	31	**27**	^{i}Pr	H	H	Ph	58
2			**28**		H	Ph	H	58
3	**5, 6**	52	**29**	^{i}Pr	H	H	4-OMe-Ph	50
4			**30**		H	4-OMe-Ph	H	50
5	**7, 8**	68	**31**	^{i}Pr	H	H	4-Br-Ph	93
6			**32**		H	4-Br-Ph	H	93
7	**9, 10**	25	**33**	^{i}Pr	H	H	4-COOMe-Ph	58
8			**34**		H	4-COOMe-Ph	H	58

[a]Crude yield reported

For some regioisomers, the differences in polarity were not substantial. Hence, some mixtures of regioisomers (compounds **35-38**) (Table 2.5) could not be separated into their individual components. These were used as mixtures for further studies. Next, for understanding the combined effect of substitution on the epoxide and that at R^1, compounds **39** and **40** (Table 2.5) were synthesized. This set of regioisomers could not be separated into individual components as well.

Table 2.5. Compounds synthesized in this study with substitutions on the epoxide (35-40)

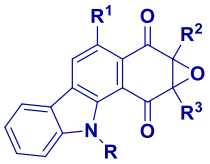

Entry	Quinone mixture	% Yield[a]	Epoxide	R	R^1	R^2 / R^3	% Yield[a]
1	**11, 12**	38	**35, 36**	^{i}Pr	H	3-CHO Ph	40
2	**13, 14**	-	**37, 38**	^{i}Pr	H	2-Me Ph	63
3	**15, 16**	39	**39, 40**	^{i}Pr	Me	Ph	49

[a]Crude yield reported

To further understand the combined effect of substitutions at the indole nitrogen as well as at the epoxide, two compounds with varying 'R' groups, namely methyl and ethyl groups, were synthesized with phenyl group on the epoxide. Interestingly, the quinones in these cases could not be isolated as pure compounds and were taken further as crude compounds for the next reaction, epoxidation. Upon purification, strangely, in both the cases, it yielded a single compound, as opposed to a mixture of regioisomers in the earlier cases (compounds **41** and **42,** Table 2.6). After analysis, referring to the parent compounds **27** and **28**, we hypothesized that both the obtained compounds are '1' isomers. We also investigated in the NOESY NMR for compound **28**, but no conclusive evidence regarding the regiochemistry could be obtained.

Finally, alkyl substituents such as the methyl group was incorporated into the scaffold on the epoxide. Different 'R' groups such as Et and ^{i}Pr were utilized for making these analogues. Again, these regioisomers obtained were inseparable and were used as mixtures for further studies. We next tried to synthesize an analogue with methyl groups on both the sides of the epoxide. This compound was expected to hinder the thiol attack completely which would serve as a perfect negative control compound to test the hypothesis of reactivity with thiol. But, due to certain synthetic difficulties, the compound could not be synthesized.

Table 2.6. Compounds synthesized in this study with substitutions on the epoxide (41-46)

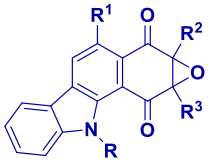

Entry	Quinone	% Yield[a]	Epoxide	R	R^1	R^2	R^3	% Yield[a]
1	**17[b], 18[b]**	-	**41[c]**	Et	H	Ph	H	85
2	**19[b], 20[b]**	-	**42[c]**	Me	H	Ph	H	59
3	**21, 22**	41	**43, 44**	^{i}Pr	H	Me		90
4	**23, 24**	68	**45, 46**	Et	H	Me		87

[a]Crude yield reported; [b]not isolated, crude; [c]Single isomer obtained

2.2.2. Reactivity with thiol

Having synthesized these analogues of lead compound **25**, next, their reactivity with thiol was evaluated. Reversed-phase analytical HPLC was employed for these studies. First, the stability of these compounds in phosphate buffer was checked. All the compounds were found to be stable in buffer. Next, for evaluating the reactivity with thiol, the compound and thiol were co-incubated at 37 °C and the reaction mixture was analysed for remaining unreacted compound after 1 h. Compound **26**, with R^1 = Et showed diminished reactivity with thiol when compared with **25** (Table 2.7). This was an anticipated result, as earlier studies with R^1 = Me had shown similar trends.

Table 2.7. Reactivity with thiol for compound 26

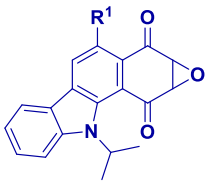

Entry	Compound	R^1	% Remaining[a]
1	**25**	H	34
2	**26**	Et	88

[a]HPLC analysis: compound treated with 1 eq. *L*-Cysteine for 1 h

Next, analogues with substituents on the epoxide were reacted with *L*-cysteine (1 eq.). In theory and as suggested by earlier reports,[10,14] a substituent on the epoxide should sterically hinder (in some cases, electronically as well) and further lower down the reactivity with a thiol when compared with the lead compound **25**, having no substitution at the epoxide. Surprisingly, when tested, both the regioisomers showed variable reactivity with a thiol. The regioisomer with a phenyl substituent at the R^3 position, compound **27**, showed reactivity comparable to that of compound **25**. Whereas, the regioisomer with a phenyl substituent at the R^2 position, compound **28**, was found completely unreactive towards a thiol (Table 2.8).

Table 2.8. Reactivity with thiol for compounds with substitution on the epoxide (27-28)

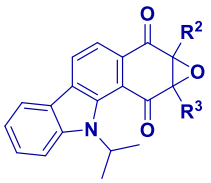

Entry	Compound	R^2	R^3	% Remaining[a]
1	**25**	H	H	34
2	**27**	H	Ph	33
3	**28**	Ph	H	100

[a]HPLC analysis: compound treated with 1 eq. *L*-Cysteine for 1 h

To understand this contrasting behaviour of the isomers, these two compounds were next independently reacted with increasing equivalents of thiol for a time period of 15 min. Compound **27** was found to react in a dose-dependent manner with increasing equivalents of thiol, whereas compound **28** was found to be unreactive with a lower dose of thiol and showed moderate reactivity with a higher dose (Fig. 2.9).

Figure 2.9. Reactivity difference between 27 and 28 with thiol

(reproduced with permission from *J. Med. Chem.* <https://pubs.acs.org/doi/10.1021/acs.jmedchem.9b00774>)

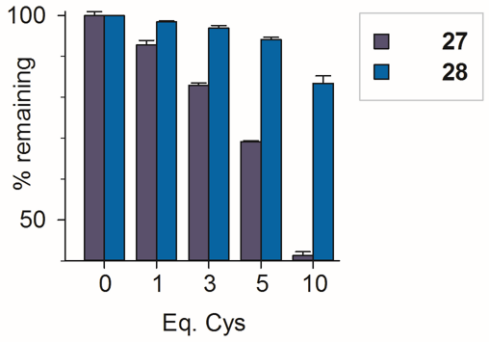

Thus, these regioisomers were further reacted with 10 eq. of *L*-cysteine for 1 h. Similar results were obtained, where compound **27**, reacted extensively within 1 h (19% remaining), and compound **28** was 62% remaining after 1 h (Fig. 2.10, Table 2.9. entries 1-2). Considering, the effect a substituent on the epoxide should have on reactivity with a thiol, and the surprising result obtained, excess of thiol (10 equiv.) was used for the next studies.

Figure 2.10. HPLC traces for compounds A) 27 and B) 28 (*after reaction with *L*-cysteine for 1 h)

(reproduced with permission from *J. Med. Chem.* <https://pubs.acs.org/doi/10.1021/acs.jmedchem.9b00774>)

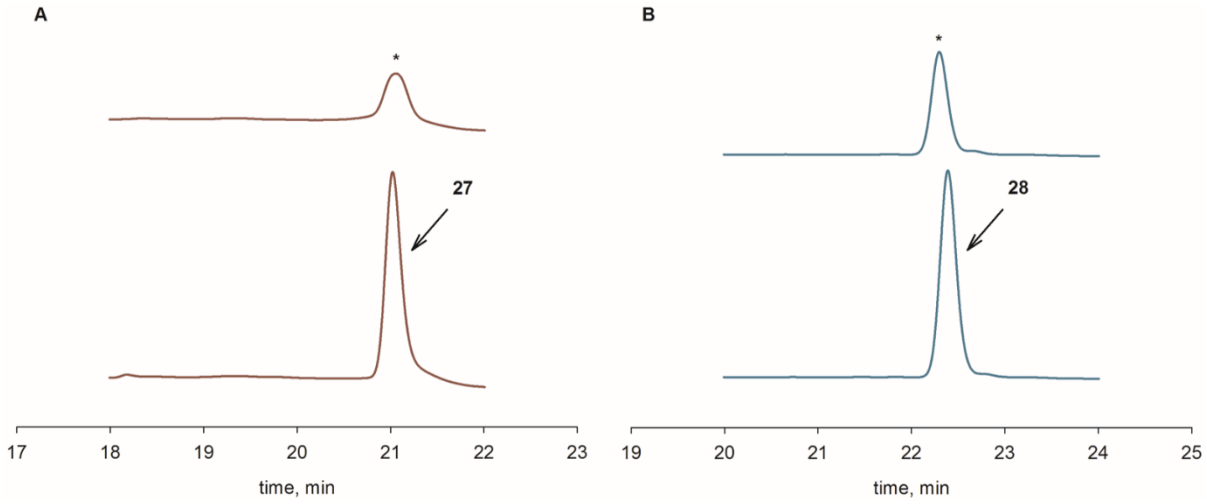

The next set of regioisomers of the analogues were tested for their reactivity with thiol. Compounds **29** and **30** with 4-methoxy substitution on the phenyl ring showed similar trends as the parent phenyl compounds. Compound **29** was found to be better at reacting with thiol (61% remaining after 1 h) when compared with compound **30** (75% remaining after 1 h, Table 2.9. entries 3-4). The other sets of compounds with 4-bromo-phenyl and 4-COOMe-phenyl

substitution also showed similar results, with the '10' isomer being more reactive with thiol than the '1' isomer (Table 2.9. entries 5-8). Thus, the hypothesis about the variable reactivity of these two isomers w.r.t. the '1' and '10' positions of substituents as suggested from the analysis of the crystal structures of compounds **27** and **28** proved to be correct. The deviation of the boat from the plane of the quinone was indeed playing a major role in deciding the reactivity of this scaffold with a thiol.

Table 2.9. Reactivity with thiol for compounds with substitution on the epoxide (27-34)

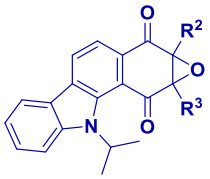

Entry	Epoxide	R^2	R^3	% Remaining[a]
1	**27**	H	Ph	19
2	**28**	Ph	H	62
3	**29**	H	4-OMe-Ph	61
4	**30**	4-OMe-Ph	H	75
5	**31**	H	4-Br-Ph	35
6	**32**	4-Br-Ph	H	74
7	**33**	H	4-COOMe-Ph	43
8	**34**	4-COOMe-Ph	H	90

[a]HPLC analysis: compound treated with 10 eq. *L*-Cysteine for 1 h

Next the mixture of regioisomers were tested for their reactivity with thiol. It was suspected that the presence of regioisomers in the mixture would hamper the trend in reactivity and give an average readout. Surprisingly, this was not observed at all. The compounds with 3-CHO-phenyl (mixture **35-36**) and 2-methyl-phenyl (mixture **37-38**) substitution were first tested. Interestingly, the 3-CHO-phenyl substituted mixture was found to be efficient in reaction with a thiol (31% remaining after 1 h, Table 2.10. entry 1), whereas, the 2-methyl-phenyl substituted mixture was extremely unreactive towards a thiol (92% remaining after 1 h, Table 2.10. entry 2). The 3-CHO group, being an electron withdrawing group would facilitate the nucleophilic attack of the thiol at the epoxide carbon. On the contrary, the group 2-MePh would sterically hinder the attack, and hence was found to be less reactive with the thiol. Further, compound with R^1 = Me and having a phenyl substituent on the epoxide (mixture **39-40**) was tested. As found earlier, appending a methyl substituent at the R^1 position does make the compound less

reactive with a thiol. To add to this, a phenyl substituent on the epoxide should further lower down the reactivity with the thiol. When tested, indeed mixture **39-40** was found to have diminished reactivity (Table 2.10. entry 3).

Next, compounds **41** and **42** were tested. Compound **41** with R = Et, showed good reactivity with thiol (Table 2.10. entry 4), whereas, compound **42** was found to be less reactive when reacted with a thiol (Table 2.10. entry 5).

Finally, mixtures **43-44** and **45-46** with methyl substituents on the epoxide, were reacted with a thiol. Both these mixtures were found to be highly reactive with thiol suggesting steric control on reactivity (Table 2.10. entries 6-7).

Thus, the rationale behind the synthesis of the analogues of lead compound **25**, was well complemented and supported by the results of the study of reactivity with thiol.

Table 2.10. Reactivity with thiol for compounds with substitution on the epoxide (35-46)

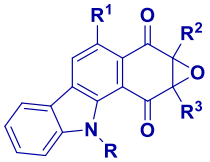

Entry	Epoxide[a]	R	R^1	R^2	R^3	% Remaining[b]
1	**35, 36**	^{i}Pr	H	3-CHO Ph		31
2	**37, 38**	^{i}Pr	H	2-Me Ph		92
3	**39, 40**	^{i}Pr	Me	Ph		82
4	**41**[c]	Et	H	Ph	H	28
5	**42**[c]	Me	H	Ph	H	75
6	**43, 44**	^{i}Pr	H	Me		3
7	**45, 46**	Et	H	Me		11

[a]Mixtures of regioisomers; [b]HPLC analysis: compound treated with 10 eq. *L*-Cysteine for 1 h; [c]Single isomer

2.2.3. Antibacterial studies

The INDQE scaffold was earlier assessed for antibacterial activity against Gram-positive *S. aureus*. A number of positive hits were obtained and lead compound **25** was identified. Thus, after establishing the trend in reactivity with a thiol for the analogues synthesized in this study,

these compounds were assessed for their antibacterial potency and the MIC values obtained were compared with that of lead compound **25**. The analogues synthesized earlier had shown good correlation between thiol reactivity and antibacterial activity. Thus, it was hypothesized that the analogues synthesized in this study will follow a trend in antibacterial activity similar to that of their reactivity with thiols.

Compound **26**, with R^1 = Et, was first assessed. It was found to be a very poor inhibitor of *S. aureus* (Table 2.11. entry 2). This was in accordance with the low reactivity of **26** with thiol. Also, similar results were obtained earlier when analogues with R^1 = Me were analysed and were found to be poorer inhibitors of *S. aureus*. Thus, increasing sterics at the R^1 position was hampering reactivity with the thiol as well as the antibacterial potency, thus reiterating the higher probability of thiol attack at the '1' position.

Table 2.11. Antibacterial activity of INDQE analogues 25-26

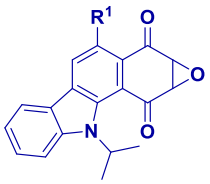

Entry	Compound	R^1	% Remaining[a]	MIC[b]
1	**25**	H	34	0.125
2	**26**	Et	88	>64

[a]HPLC analysis: compound treated with 1 eq. *L*-Cysteine for 1 h; [b]MIC in μg/mL against MSSA 29213

(Data courtesy: Dr. Sidharth Chopra Lab, CDRI Lucknow)

Further, compounds with the substituents on the epoxide were assessed for their antibacterial activity. The two regioisomers **27** and **28** with phenyl substituent at the epoxide were first tested. As hypothesized, the MIC values were in good correlation to the reactivity with thiol. Compound **27**, showing higher reactivity with a thiol, also showed a highly potent MIC value of 0.0625 μg/mL (Table 2.12. entry 1), better than that of the lead compound **25**, whereas compound **28**, which was unreactive towards a thiol, was found to be inactive (MIC > 64 μg/mL, Table 2.12. entry 2). Thus, the '10' isomer was found to be active inhibitor of *S. aureus*, whereas the '1' isomer was found to be inactive. Further, the analogues in the series also showed a similar trend. Compound **29**, the '10' isomer with 4-methoxy phenyl substituent was found to inhibit the bacteria (MIC 0.5 μg/mL, Table 2.12. entry 3), whereas its regioisomer '1', compound **30**, was found to be completely inactive (MIC > 64 μg/mL, Table 2.12. entry 4).

Similarly, compound **31** (‘10’ isomer) with 4-bromo phenyl substituent was found to be active inhibitor (MIC 1 μg/mL, Table 2.12. entry 5) whereas its regioisomer compound **32** (‘1’ isomer) was found to be inactive (MIC > 64 μg/mL, Table 2.12. entry 6). With 4-COOMe phenyl group, both the regioisomers obtained had diminished solubility, thus generating higher MIC values (Table 2.12. entries 7-8).

Table 2.12. Antibacterial activity of INDQE analogues

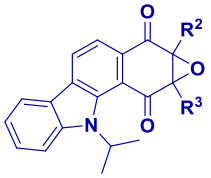

Entry	Epoxide	R^2	R^3	% Remaining[a]	MIC[b]
1	**27**	H	Ph	0	0.0625
2	**28**	Ph	H	56	>64
3	**29**	H	4-OMe-Ph	61	0.5
4	**30**	4-OMe-Ph	H	75	>64
5	**31**	H	4-Br-Ph	35	1
6	**32**	4-Br-Ph	H	74	>64
7	**33**	H	4-COOMe-Ph	43	32
8	**34**	4-COOMe-Ph	H	90	>64

[a]HPLC analysis: compound treated with 10 eq. *L*-Cysteine for 1 h; [b]MIC in μg/mL against MSSA 29213

(Data courtesy: Dr. Sidharth Chopra Lab, CDRI Lucknow)

Next, the mixtures of regioisomers were tested for their antibacterial activity. Mixture **35-36**, which was reactive with a thiol showed a potent MIC value of 0.5 μg/mL (Table 2.13. entry 1), whereas, mixtures **37-38** and **39-40**, which show diminished reactivity with a thiol were found to be inactive against *S. aureus* (Table 2.13. entries 2-3).

The single isomers obtained, compounds **41** and **42** were found to be inactive (Table 2.13. entries 4-5), suggesting that they were possibly the ‘1’ isomers, although no other evidence could be obtained for this.

Both the mixtures **43-44** and **45-46** with methyl substituents on the epoxide had excellent MIC of 1 μg/mL (Table 2.13. entries 6-7) consistent with their higher reactivity with thiol.

Table 2.13. Antibacterial activity of INDQE analogues 35-46

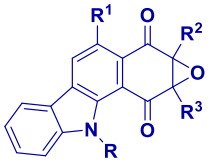

Entry	Epoxide	R	R^1	R^2	R^3	% Remaining[a]	MIC[b]
1	**35, 36**	^{i}Pr	H	3-CHO Ph		31	0.5
2	**37, 38**	^{i}Pr	H	2-Me Ph		92	>64
3	**39, 40**	^{i}Pr	Me	Ph		82	>64
4	**41**	Et	H	Ph	H	28	>64
5	**42**	Me	H	Ph	H	75	>64
6	**43, 44**	^{i}Pr	H	Me		3	1
7	**45, 46**	Et	H	Me		11	1

[a]HPLC analysis: compound treated with 10 eq. *L*-Cysteine for 1 h; [b]MIC in µg/mL against MSSA 29213

(Data courtesy: Dr. Sidharth Chopra Lab, CDRI Lucknow)

Undoubtedly, both the reactivity with thiol and the antibacterial activity was found to be in good correlation and supported the hypothesis that targeting thiols inside bacteria was a viable route to generating better antibacterial agents. The reactivity with thiol and corresponding antibacterial activity may result from kinetic control over reactivity, as well as targeting key cysteine residues on important proteins of the bacteria. Detailed investigation will be required for identifying the targets of the lead compounds.

From the present study, the active compounds **25** and **27** were chosen for further studies. These were tested against a panel of ESKAPE (*E. coli*, *S. aureus*, *K. pneumonia*, *A. baumannii*, *P. aeruginosa*, *E. faecalis*, *E. faecium*) pathogens (Table 2.14). Unexpectedly, both the compounds were unable to inhibit any other bacteria than *S. aureus*. These compounds may not be permeable across the membrane of the Gram-negative pathogens, although further studies would be required to justify the obtained result. The compounds **26** and **28** were also tested (Table 2.14), and as expected, these compounds were found to be poor inhibitors of the ESKAPE pathogens. Thus, this data suggested that the potent INDQE compounds are extremely selective towards inhibiting *S. aureus.*

Table 2.14. MIC against ESKAPE pathogens

	MIC[a] (μg/mL)						
Epoxide	*E. coli*	*S. aureus*	*K. pneumoniae*	*A. baumannii*	*P. aeruginosa*	*E. faecalis*	*E. faecium*
25	64	0.125	64	64	64	64	64
26	64	64	64	64	64	64	64
27	64	0.0625	64	64	64	64	64
28	64	64	64	64	64	64	64

E. coli ATCC 25922, *S. aureus* ATCC 29213, *K. pneumoniae* BAA 1705, *A. baumannii* BAA 1605, *P. aeruginosa* ATCC 27853, *E. faecalis* Strain B3119, *E. faecium* Strain Patient #1-1, [a]MIC against ESKAPE pathogens (Data courtesy: Dr. Sidharth Chopra Lab, CDRI Lucknow)

Having got this data, compound **25** was chosen for further studies as the lead compound as compound **27** which had potency comparable to **25**, was synthetically more challenging.

Compound **25** was then tested against a series of drug-resistant clinical isolates of *S. aureus* such as VISA (Vancomycin-intermediate *S. aureus*) and VRSA (Vancomycin-resistant *S. aureus*) and was found to be potent against all of these, even better than clinically used vancomycin (Table 2.15).

Table 2.15. Antibacterial activity of 25 against clinical drug-resistant isolates

Entry	Bacterium	Strain	MIC of **25**	MIC of Vancomycin
1	*S. aureus*	SA-HIP-14300	0.5	>64
2	*S. aureus*	SA-HIP-11983	0.5	32-64
3	*S. aureus*	AIS100050	0.5	32-64
4	*S. aureus*	SA-HIP-15178	0.5	32-64
5	*S. aureus*	SA-71080	0.5	32-64
6	*S. aureus*	HIP11714	0.5	>64
7	*S. aureus*	HIP14300	0.5	>64
8	*S. aureus*	1002434	0.5	>64

[a]MIC in μg/mL (Data courtesy: Dr. Sidharth Chopra Lab, CDRI Lucknow)

2.2.4. Covalent thiol-adduct formation for lead compound 25

A covalent modification of a thiol was proposed as the underlying rationale and the driving force for the INDQE analogues to be potent antibacterial agents. Thus, the chemistry of the reaction between an INDQE analogue and a thiol was next explored. For this study, compound **25** was reacted with 4-nitrobenzyl thiol. This reaction was analysed using an analytical reversed-phase HPLC setup. At time points of 30 min and 60 min, the reaction mixture showed diminishing intensities of **25** (R_t = 15.7 min) and simultaneous formation of a product at R_t = 16.1 min. The expected product, **47**, was synthetically made from compound **1** (Scheme 2.6). The reaction mixture was then spiked with compound **47** (250 μM conc.), and the product peak formed (R_t = 16.1 min) showed an increase in its intensity, suggesting the covalent adduct formation of **25** with 4-nitro-benzyl thiol Fig. 2.11 C).

Figure 2.11. Covalent thiol-adduct formation for lead compound 25; HPLC traces for compound A) 25; B) 47; C) For the reaction: 0 min (red); 30 min (green); *spiking experiment at 60 min (blue)

(reproduced with permission from *J. Med. Chem.* <https://pubs.acs.org/doi/10.1021/acs.jmedchem.9b00774>)

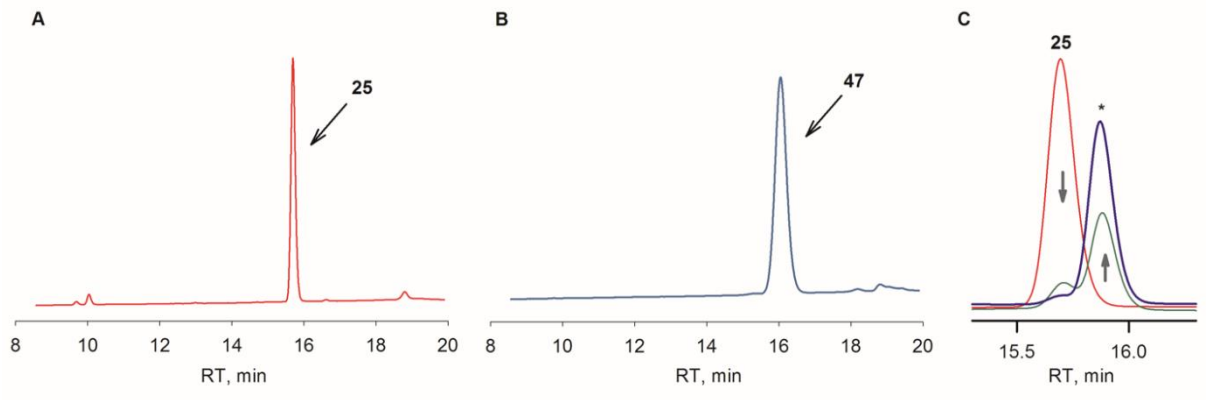

Scheme 2.6. Synthesis of thiol-adduct of compound 25

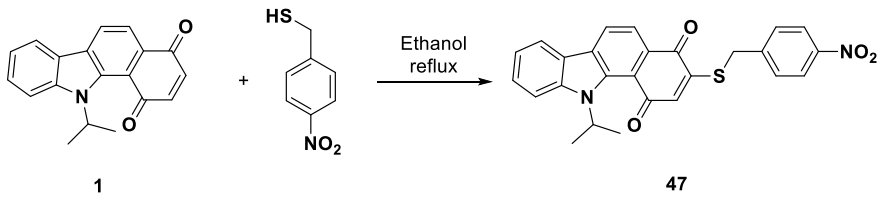

1 47

2.2.5. Kinetics of reaction with thiol

It was established that the INDQE scaffold reacts with a thiol via a covalent adduct formation and this is in direct correlation with its antibacterial activity. Having a large variation across the analogues in terms of reactivity with thiol, the kinetics of reaction for a subset of these analogues were next studied. For this study, along with compound **25**, compounds **26**, **27** and **28** were chosen. This offered a distinct subset of compounds, **25** and **27** were reactive with thiol and potent inhibitors of *S. aureus*, having a different substitution at R^3, and **26** and **28** were unreactive towards thiol, did not show any potent antibacterial activity, and had distinct substitutions at R^1 and R^2. This study was conducted using reversed-phase HPLC setup. The compound was reacted with 10 eq. of *L*-cysteine in phosphate buffer and aliquots were injected in the HPLC at time-points of every 10 min between 0-60 min. Area under the peak was recorded and corresponding values of % remaining of the compound was calculated at every time-point. These values were then plotted and curve-fitting to an exponential decay gave rate constants (Fig. 2.12).

Figure 2.12. Kinetics of reaction of INDQE compounds with thiol

(reproduced with permission from *J. Med. Chem.* <https://pubs.acs.org/doi/10.1021/acs.jmedchem.9b00774>)

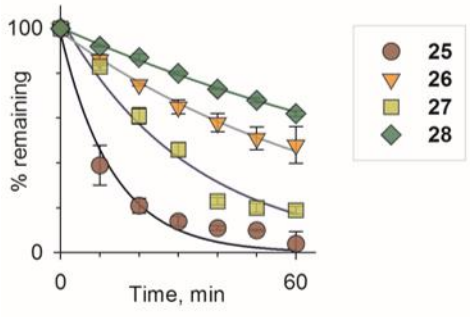

We found a 10-fold difference in rate constants of **25** and **28**, and about 6-fold difference between rate constants of **25** and **26** (Table 2.16). Using Eyring-Polanyi equation,[15,16] the Gibbs free energy ($\Delta G^{\ddagger}$) for all the 4 reactions was calculated. This magnitude of difference translated to about 1.4 kcal/mol and 1.1 kcal/mol difference in $\Delta G^{\ddagger}$ energy barrier respectively. Not surprisingly, **25** and **27**, the active inhibitors of *S. aureus*, had a mere 2.5-fold difference in rate constants, which also can be attributed to the fact that **27** has a phenyl substituent on the epoxide at '10' position, which possibly slows down the reaction with thiol as compared to unsubstituted **25**, affecting the kinetics of the reaction. This study, along with the results of the antibacterial activity study, strongly suggested that kinetic control over the reaction with a thiol is key to the antibacterial potency of INDQE compounds.

Table 2.16. Estimated $\Delta G^{\ddagger}$ values using Eyring-Polanyi equation for pseudo-first order kinetics experiment for different compounds with 10 eq. *L*-Cysteine

Epoxide	Rate constant k (x 10^{-2} min^{-1})	$\Delta G^{\ddagger}$ (kcal/mol) (estimated)[a]	R^2
25	7.54	19.76	0.9739
26	1.3	20.84	0.9932
27	3	20.33	0.9742
28	0.78	21.16	0.9970

[a]$\Delta G^{\ddagger} = RT \ln (kh/\kappa_B T)$

2.2.6. *In situ* reaction with a thiol - mBBr assay

Having shown that these compounds react with thiols *in vitro*, next, the studies of reactivity with thiol *in situ* were of greater significance. For this, mBBr assay was conducted. mBBr (monobromobimane) is a non-fluorescent molecule. On reaction with a thiol, the bromide gets displaced and generates a thiol adduct which is fluorescent in nature (Scheme 2.7). Thus, if a compound reacts with thiol, it will deplete the available thiol pool for the reaction with mBBr and will generate a lower readout value. mBBr and its other derivatives, bBBr and qBBr, have been shown to be selectively labelling thiols in complex biological systems.[17] Especially, mBBr was found to be very useful in fluorescently labelling proteins and also in alkylating thiols in biological systems.

Scheme 2.7. Reaction of mBBr with a thiol

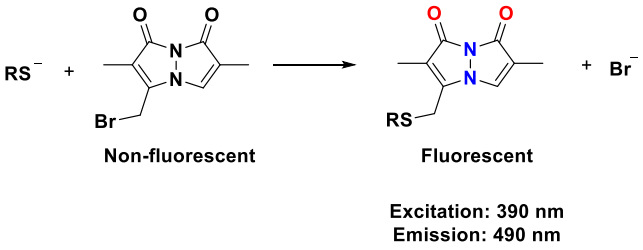

Earlier, using mBBr assay, intracellular thiol depletion was studied in *S. aureus*, and the thiol reactivity of lead compound **25** was found to be comparable to that of Fosfomycin and *N*-phenyl-maleimide. With this preliminary data, a similar mBBr assay was conducted with MRSA (Methicillin-resistant *S. aureus*) ATCC 33591 with the two most-active compounds **25** and **27** (Fig. 2.13). MRSA, being a resistant strain, is known to have better adaptation to oxidative stress as compared to *S. aureus*. Thus, evaluating the ability of the lead compounds

in reacting with cellular thiols in MRSA was of greater significance. For this assay, chloro-dinitrobenzene (CDNB), which is known to react with thiols, was used as a control compound (Fig. 2.14).

The bacterial culture was first incubated with the compound for 1 h. After this, excess compound was washed out from the bacterial pellet. This was then followed with a treatment of mBBr reagent for 30 min in the dark. Aliquots were then assessed, and their fluorescence intensities measured. Both the compounds **25** and **27** were found to deplete thiols *in situ* as compared with the untreated control.

Figure 2.13. *In situ* mBBr assay MRSA ATCC 33591

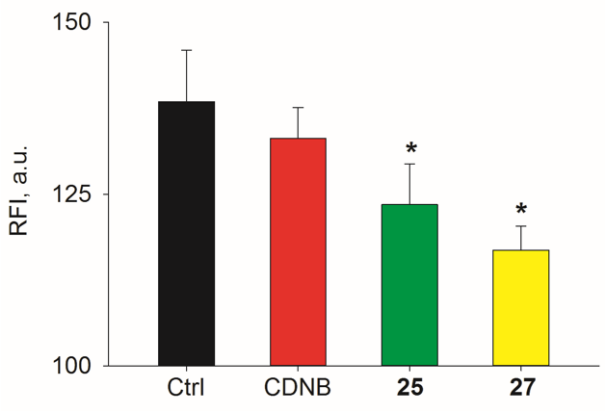

Figure 2.14. Structures of lead compounds 25 and 27 and control compound CDNB

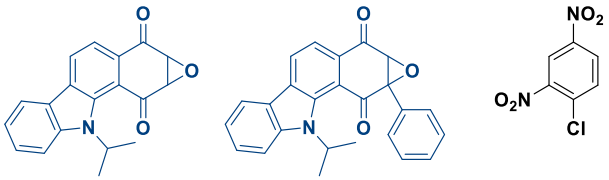

25 **27** **CDNB**

2.2.7. Cyclic voltammetry

To understand the redox nature and the reduction potential of INDQE compounds, cyclic voltagram of compound **25** was recorded (Fig. 2.15). The CV plot showed two trenches for two reduction potentials, suggesting the redox nature of this compound. This could directly be correlated to its ability to generate ROS.

25: First reduction potential: –1.44 mV, Second reduction potential: –1.56 mV

Figure 2.15. CV of 25

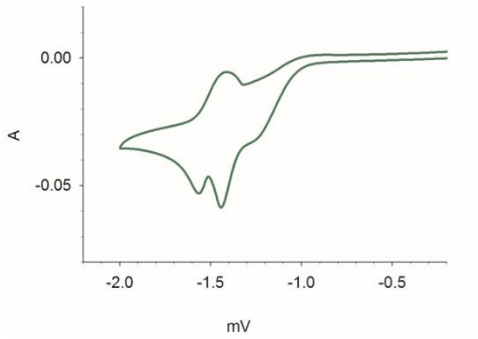

2.3. Summary

INDQE scaffold was earlier designed and reported to be a thiol-reactive molecule. The compounds were tested for their antibacterial activity, and some derivatives were obtained as highly potent inhibitors of Gram-positive pathogen *S. aureus*. A positive correlation between reactivity with thiol and antibacterial activity of these compounds was well established. However, the precise mechanism of action is yet to be deciphered.

In this chapter, we further studied the structure-activity relationship of this scaffold. The structural aspects of this design were explored and a series of analogues with substitutions at the reactive centre of the molecule, the epoxide, were generated. These substitutions gave rise to a mixture of regioisomers with respect to the position of the substituent on either side of the epoxide ring. Surprisingly, this structural variation brought in a disparity for the reactivity with a thiol for every set of regioisomers obtained. One regioisomer (‘10’ isomer) was found to be better at reacting with a thiol, whereas the other regioisomer (‘1’ isomer) was found to be comparatively unreactive. This variation in reactivity with a thiol was very well complemented by the antibacterial activity of these compounds. A potent compound **27** was identified from this study with MIC 0.0625 μg/mL against *S. aureus*. The crystal structures of potent compounds **25** and **27** and inactive compound **28** were analysed which could give an explanation for the directed thiol attack, preferably on carbon ‘1’, bearing the epoxide, although further experiments are required to better support this hypothesis. Compound **25**, being synthetically easily accessible, was chosen as the lead compound for further studies. The covalent nature of the bond in the thiol-adduct of compound **25** was next studied using HPLC. The kinetics of the reaction with a thiol for a subset of these compounds was next studied, that suggested kinetic control in reaction with thiol is directly responsible for the antibacterial

activity of these compounds. Compound **25** was also found to be a potent inhibitor of a number of drug-resistant clinical isolates including VISA and VRSA. The *in situ* reactivity with thiol for potent compounds **25** and **27** was also studied, and these were found to react with intracellular thiols. When tested against other Gram-negative pathogens, both compounds were found to be inactive, suggesting high level of selectivity towards *S. aureus*, and also pointed out potential issues with permeability of this scaffold in Gram-negative bacteria. Further work would focus on identification of the biological targets of the lead compound in *S. aureus* and to understand the mechanism of action. This would be extensively discussed in Chapter 3 and Chapter 4. A systematic modification to the scaffold needs to be done to improve the permeability, in order to target Gram-negative pathogens. This would be addressed in the future studies with this scaffold.

2.4. Experimental and characterization data

2.4.1. General procedure for synthesis of *N*-substituted indole-3-carboxaldehydes[18]

To an ice-cold solution of indole-3-carboxaldehyde (1 g, 1 eq.) in dry DMF (10 mL), NaH (60% dispersion in mineral oil, 199 mg, 1.2 eq.) was added in portions and the solution was stirred for 30 min. The alkyl halide (1.2 eq.) was then added with stirring which was continued in melting ice bath for 2h. Upon complete consumption of the starting material (TLC analysis), the reaction mixture was diluted with ice-cold water (20 mL). The aqueous layer was extracted with multiple fractions of ethyl acetate (3 × 10 mL), the combined organic phase was washed with brine (10 mL), dried over anhydrous Na_2SO_4 (5g), filtered and the filtrate was evaporated under reduced pressure to obtain the crude product. This was purified by silica gel (60-120 mesh) chromatography using ethyl acetate and hexane mixture as an eluent.

2.4.2. Procedure for synthesis of N-isopropyl indole-3-carboxaldehyde

2-bromopropane (3.56 mL, 1.1 eq.) was added dropwise to the stirring mixture of indole-3-carboxaldehyde (5 g, 1 eq.) and K_2CO_3 (5.24 g, 1.1 eq.) in dry DMF (40 mL) in a 100 mL RB flask. Reaction was then setup for reflux at 155 ^oC under nitrogen atmosphere and monitored by TLC analysis. Reaction was then quenched at completion (8 h) by adding water (60 mL). The organic mixture was then extracted in ethyl acetate and washed with water (3 × 50 mL), dried over Na_2SO_4 before affording the crude mixture under reduced pressure. Crude was purified by silica gel (60-120 mesh) chromatography using ethyl acetate and hexane (1:4, v/v) as an eluent.

2.4.3. General procedure for Wittig olefination[19]

A turbid solution of Wittig salt, alkyltriphenylphosphonium bromide (1.5 eq.) in anhydrous THF was cooled to -50 ^oC. To this, *n*-BuLi (2.5 M in hexane, 1.1 eq.) was added drop wise, and stirred for 60 min at -50 ^oC. A solution of indole-3-carboxaldehyde (1 eq.) in anhydrous THF was added drop wise to the above solution and stirred at -50 ^oC for 4 h. Then the reaction mixture was quenched with cold water (0 – 4 ^oC, 20 mL), and extracted using ethyl acetate (5 × 10 mL). The combined organic layer was washed with brine (10 mL), dried over anhydrous Na_2SO_4 (5 g), filtered and the filtrate evaporated to dryness under reduced pressure. The crude material was purified by silica gel column chromatography eluting with ethyl acetate and hexane mixture (1:4, v/v). Note: During purification compound decomposes on silica column,

needs to be eluted out within 15-20 min from the silica column. These olefins are unstable and are used for the next reaction immediately.

2.4.4. General procedure for Diels-Alder Cycloaddition[19]

To a solution of the 3-alkenylindole (1 eq.) in ethanol (10 mL), *p*-benzoquinone OR 2-substituted *p*-benzoquinone (2.5 eq.) was added portion-wise at room temperature, and stirring was continued at RT until complete consumption of the starting material was observed (TLC analysis). The volatiles were removed under reduced pressure to obtain the crude product and this was purified by silica gel column chromatography using ethyl acetate and hexane mixture as an eluent.

11-isopropyl-1H-benzo[a]carbazole-1,4(11H)-dione (1).

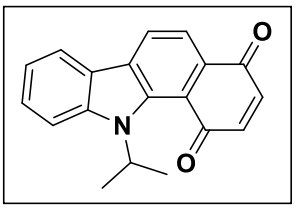

Starting from *N*-isopropyl-3-vinylindole (765 mg, 4.13 mmol), **1** was isolated as dark red-brown solid (280 mg, 23%): mp 138 – 140 °C; FT-IR (ν_{max}, cm^{-1}): 1740, 1643, 1512, 1443, 1375, 1038; ^{1}H NMR (400 MHz, $CDCl_3$): δ 8.32 (d, *J* = 7.8 Hz, 1H), 8.05 (d, *J* = 7.7 Hz, 1H), 7.96 (d, *J* = 7.8 Hz, 1H), 7.71 (d, *J* = 8.4 Hz, 1H), 7.44-7.48 (m, 1H), 7.25 (t, *J* = 7.4 Hz, 1H), 6.92 (d, 2H), 4.85-4.96 (m, 1H), 1.71 (d, *J* = 6.9 Hz, 6H); ^{13}C NMR (100 MHz, $CDCl_3$): δ 186.3, 185.8, 142.9, 140.0, 139.7, 136.8, 136.6, 131.5, 131.4, 127.6, 124.9, 123.7, 121.2, 120.8, 118.8, 118.4, 114.4, 52.3, 21.2; HRMS (ESI) for $C_{19}H_{15}NO_2$ $[M+H]^+$: Calculated: 290.1181, Found: 290.1184.

5-ethyl-11-isopropyl-1H-benzo[a]carbazole-1,4(11H)-dione (2).

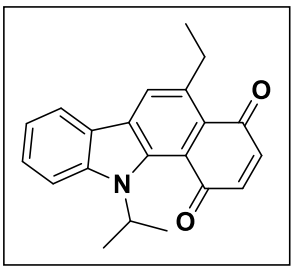

Starting from *N*-isopropyl-3-(but-1-en-1-yl)-indole (1.02 g, 4.8 mmol), compound **2**, was isolated as dark red-brown solid (261 mg, 13%). FT-IR(ν_{max}, cm^{-1}): 1741, 1693, 1651, 1617, 1589, 1534, 1463, 1428, 1391, 1368, 1308, 1282, 1233, 1199, 1156, 1105, 1062; ^{1}H NMR (400 MHz, $CDCl_3$): δ 8.10 (s, 1H), 8.10 (d, *J* = 7.6 Hz, 1H), 7.74 (d, *J* = 8.6 Hz, 1H), 7.5 (td, *J* = 7.2 Hz, 1.2 Hz, 1H), 7.28 (td, *J* = 7.8 Hz, 0.7 Hz, 1H), 6.87 (dd, *J* = 17.4 Hz, 10.1Hz, 2H), 4.74 (h, *J* = 7 Hz, 1H), 3.26 (q, *J* = 7.4 Hz, 2H), 1.67 (d, *J* = 6.9 Hz, 6H), 1.35 (t, *J*=7.4 Hz, 3H); ^{13}C NMR (100 MHz, $CDCl_3$): δ 188.1, 186.9, 143.7,

139.8, 139.2, 138.8, 137.7, 131.2, 129.1, 127.8, 127.5, 123.6, 121.2, 120.7, 120.1, 114.4, 52.5, 28.9, 21.1, 15.7; HRMS (ESI) for $C_{21}H_{19}O_2N$ $[M+H]^+$: Calculated: 318.1494, Found: 318.1501.

11-isopropyl-2-phenyl-1H-benzo[a]carbazole-1,4(11H)-dione + 11-isopropyl-3-phenyl-1H-benzo[a]carbazole-1,4(11H)-dione (3, 4).

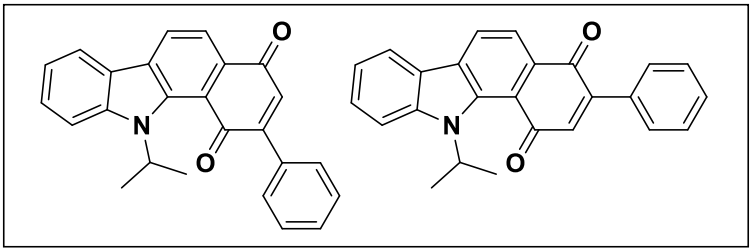

Starting from 3-vinyl, *N*-isopropyl-indole (250 mg, 1.35 mmol), mixture of **3, 4** was isolated as dark red-brown solid (100 mg, 20 %); FT-IR (ν_{max}, cm^{-1}): 1643, 1590, 1469, 1418, 1294, 1180, 1139, 1099, 1044; ^1H NMR (400 MHz, $CDCl_3$): δ 8.34 (d, *J* = 7.9 Hz, 1H), 8.13 (dd, *J* = 7.9, 2.8 Hz, 2H), 7.79 (d, *J* = 8.3 Hz, 1H), 7.63 (dd, *J* = 6.6, 2.9 Hz, 2H), 7.60 - 7.43 (m, 5H), 7.32 (t, *J* = 7.5 Hz, 1H), 7.07 (s, 1H), 5.09 (h, *J* = 7.0 Hz, 1H), 1.73 (d, *J* = 7.0 Hz, 6H); ^{13}C NMR (100 MHz, $CDCl_3$): δ 187.8, 186.8, 146.1, 137.2, 136.4, 132.8, 130.3, 129.5, 129.4, 128.7, 124.8, 121.2, 120.8, 118.3, 114.3, 64.3, 52.4, 21.2; HRMS (ESI) for $C_{25}H_{19}O_2N$ $[M+H]^+$ - Calculated: 366.1494, Found: 366.1493.

11-isopropyl-2-(4-methoxyphenyl)-1H-benzo[a]carbazole-1,4(11H)-dione + 11-isopropyl-3-(4-methoxyphenyl)-1H-benzo[a]carbazole-1,4(11H)-dione (5, 6).

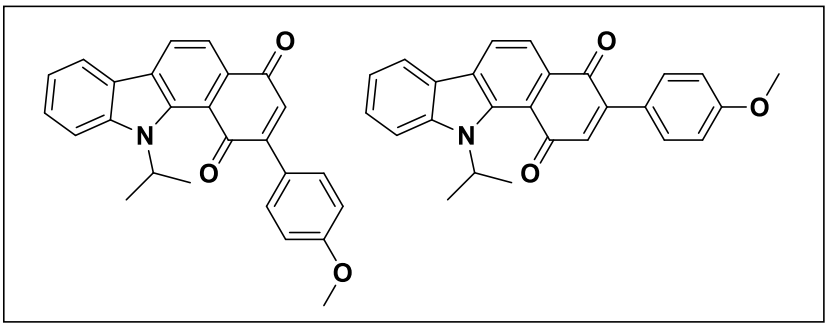

Starting from 3-vinyl, *N*-isopropyl-indole (190.2 mg, 1.03 mmol), mixture of **5, 6** was isolated as dark red-brown solid (210.2 mg, 52%); FT-IR (ν_{max}, cm^{-1}): 1648, 1602, 1556, 1511, 1462, 1417, 1366, 1298, 1230, 1178, 1134, 1086, 1031; ^1H NMR (400 MHz, $CDCl_3$): δ 8.33 (d, *J* = 7.9 Hz, 1H), 8.13-8.04 (m, 2H), 7.88 (d, *J* = 8.4 Hz, 1H), 7.63 (d, *J* = 6.9 Hz, 2H), 7.52 (t, *J* = 7.4 Hz, 1H), 7.30 (t, *J* = 7.4 Hz, 1H), 7.05-7.00 (m, 3H), 5.0 (h, *J* = 7.0 Hz, 1H), 3.88 (s, 3H), 1.74 (d, *J* = 7 Hz, 6H) (Regioisomer ratio 4:1); ^{13}C NMR (100

MHz, $CDCl_3$): δ 186.3, 185.4, 161.2, 145.6, 143.0, 139.4, 134.9, 132.3, 131.2, 131.0, 127.6, 125.8, 124.7, 123.8, 121.2, 120.8, 119.4, 118.7, 114.4, 114.3, 114.1, 55.5, 52.3, 21.3; MALDI-TOF for $C_{26}H_{21}O_3N$: Expected Mass: 395.4498, Found: 395.0778.

2-(4-bromophenyl)-11-isopropyl-1H-benzo[a]carbazole-1,4(11H)-dione + 3-(4-bromophenyl)-11-isopropyl-1H-benzo[a]carbazole-1,4(11H)-dione (7, 8).

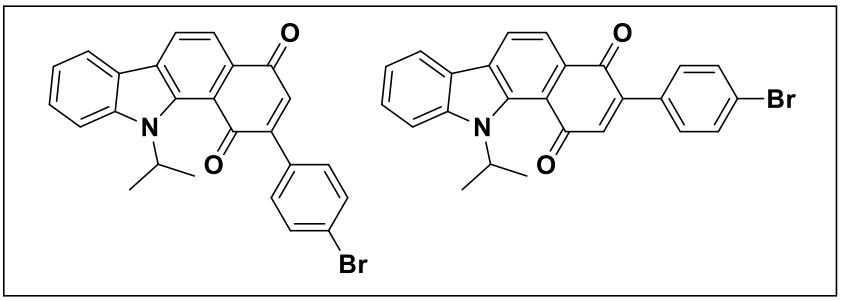

Starting from 3-vinyl, *N*-isopropyl-indole (400 mg, 2.16 mmol), mixture of **7, 8** was isolated as dark red-brown solid (653.1 mg, 68%); FT-IR (ν_{max}, cm^{-1}): 1741, 1725, 1707, 1694, 1678, 1646, 1615, 1547, 1532, 1516, 1485, 1463, 1425, 1396, 1366, 1340, 1311, 1227, 1134; ^1H NMR (400 MHz, $CDCl_3$): δ 8.33 (d, *J* = 7.9 Hz, 1H), 8.14-8.04 (m, 2H), 7.88 (d, *J* = 3.6Hz, 1H), 7.66-7.61 (m, 2H), 7.55-7.50 (m, 3H), 7.32 (t, *J* = 7.5 Hz, 1H), 7.04 (d, *J* = 9.0 Hz, 1H), 5.08 (h, *J* = 7.0 Hz, 1H), 1.73 (s, 6H) (Regioisomer ratio: 1.22:1); ^{13}C NMR (100 MHz, $CDCl_3$): δ 186.0, 185.9, 185.7, 184.7, 148.2, 145.1, 143.0, 142.8, 139.8, 139.4, 136.4, 133.3, 133.0, 132.4, 132.0, 131.8, 131.6, 131.5, 131.1, 131.0, 127.7, 125.0, 124.8, 124.6, 123.8, 121.3, 120.9, 119.5, 119.4, 118.6, 118.4, 114.4, 114.4, 52.4, 52.3, 21.3, 21.2; HRMS (ESI) for $C_{25}H_{18}O_2NBr$ $[M+H]^+$ - Calculated: 444.0599, Found: 444.0600.

methyl 4-(11-isopropyl-1,4-dioxo-4,11-dihydro-1H-benzo[a]carbazol-2-yl)benzoate + methyl 4-(11-isopropyl-1,4-dioxo-4,11-dihydro-1H-benzo[a]carbazol-3-yl)benzoate (9, 10).

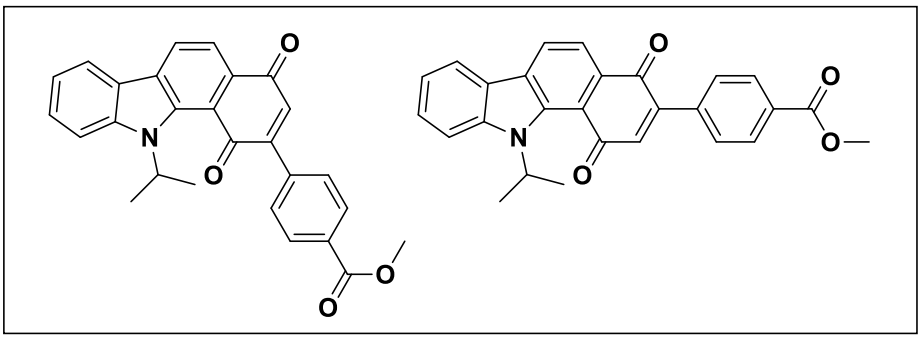

Starting from 3-vinyl, *N*-isopropyl-indole (255 mg, 1.38 mmol), mixture of **9, 10** was isolated as dark red-brown solid

(231 mg, 40%); FT-IR (ν_{max}, cm^{-1}): 1715, 1649, 1604, 1553, 1453, 1285, 1228, 1181, 1104, 1018.; ^1H NMR (400 MHz, $CDCl_3$): δ 8.35 (d, *J* = 8.0 Hz, 1H), 8.19 – 8.05 (m, 4H), 7.79 (dd, *J* = 8.4, 3.6 Hz, 1H), 7.70 (d, *J* = 8.2 Hz, 2H), 7.56 – 7.52 (m, 1H), 7.33 (t, *J* = 7.5 Hz, 1H), 7.10 (s, 1H), 5.11 – 4.86 (m, 1H), 3.96 (s, 3H), 1.74 (s, 6H); ^{13}C NMR (100 MHz, $CDCl_3$): δ 185.9, 183.7, 166.8, 146.0, 143.0, 138.0, 137.2, 135.5, 131.2, 129.7, 129.5, 127.8, 126.9, 125.1, 123.8, 121.3, 121.0, 119.5, 114.5, 52.5, 52.4, 21.3; HRMS (ESI) for $C_{27}H_{21}O_4N$ $[M+H]^+$- Calculated: 424.1549, Found: 424.1546.

3-(11-isopropyl-1,4-dioxo-4,11-dihydro-1H-benzo[a]carbazol-2-yl)benzaldehyde + 3-(11-isopropyl-1,4-dioxo-4,11-dihydro-1H-benzo[a]carbazol-3-yl)benzaldehyde (11, 12).

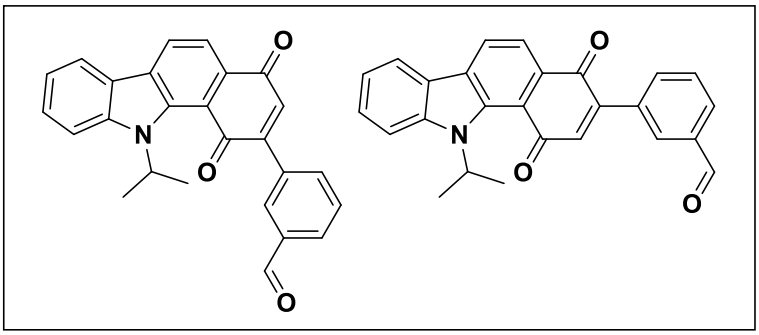

Starting from 3-vinyl, *N*-isopropyl-indole (147.4 mg, 0.8 mmol), mixture of **11, 12** was isolated as dark red-brown solid (120 mg, 38%); FT-IR (ν_{max}, cm^{-1}): 1696, 1649, 1610, 1585, 1551, 1516, 1461, 1416, 1366, 1301, 1231, 1195, 1165, 1133,1105, 1053, 1018; ^1H NMR (400 MHz, $CDCl_3$): δ 10.10 (s, 1H), 8.36 (d, *J* = 7.8 Hz, 1H), 8.15 – 8.00 (m, 4H), 7.90 (d, *J* = 7.9 Hz, 1H), 7.80 (d, *J* = 8.3 Hz, 1H), 7.70 – 7.65 (m, 1H), 7.56 – 7.52 (m, 1H), 7.33 (t, *J* = 7.5 Hz, 1H), 7.12 (s, 1H), 5.12 - 4.87 (m, 1H), 1.75 (s, 6H) (regioisomer ratio: 1.8:1); ^{13}C NMR (100 MHz, $CDCl_3$): δ 191.9, 185.8, 184.7, 144.9, 143.1, 137.1, 136.7, 135.2, 134.6, 131.9, 131.6, 131.1, 130.5, 129.4, 127.8, 125.1, 123.8, 121.3, 121.0, 119.5, 114.5, 52.4, 21.3; HRMS (ESI) for $C_{26}H_{19}O_3N$ $[M+H]^+$ - Calculated: 394.1443, Found:394.1439.

11-isopropyl-2-(o-tolyl)-1H-benzo[a]carbazole-1,4(11H)-dione + 11-isopropyl-3-(o-tolyl)-1H-benzo[a]carbazole-1,4(11H)-dione (13, 14).

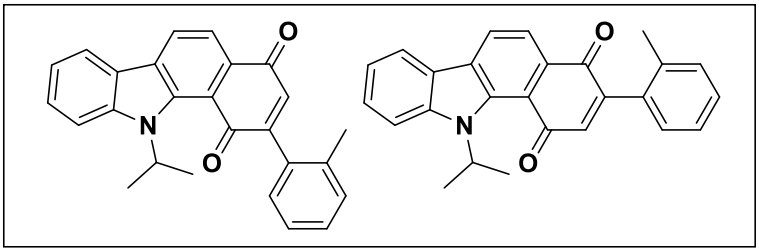

Starting from 3-vinyl, *N*-isopropyl-indole (186 mg, 1.01 mmol), mixture of **13, 14** was isolated as dark red-brown solid; FT-IR (ν_{max}, cm^{-1}): 1650, 1616,

1583, 1552, 1460, 1418, 1368, 1303, 1231, 1193, 1132, 1083, 1027, 737; ^{1}H NMR (500 MHz, $CDCl_3$): δ 8.34 (d, *J* = 7.8 Hz, 1H), 8.14 (d, *J* = 7.8 Hz, 1H), 8.09 (d, *J* = 7.9 Hz, 1H), 7.79 (d, *J* = 8.4 Hz, 1H), 7.54 (t, *J* = 7.7 Hz, 1H), 7.40-7.27 (m, 5H), 6.92 (s, 1H), 5.14 - 5.05 (m, 1H), 2.29 (s, 3H), 1.74 (d, *J* = 6.9 Hz, 6H); ^{13}C NMR (125 MHz, $CDCl_3$): δ 186.3, 184.7, 148.6, 143.0, 139.6, 138.1, 136.5, 134.0, 132.0, 131.4, 130.5, 129.7, 129.4, 129.3, 127.7, 126.3, 125.9, 124.9, 123.8, 121.2, 120.9, 119.5, 118.6, 114.4, 52.3, 21.3, 21.1, 20.7; HRMS (ESI) for $C_{26}H_{21}O_2N$ $[M+H]^+$ - Calculated: 380.1650, Found: 380.1650.

11-isopropyl-5-methyl-2-phenyl-1H-benzo[a]carbazole-1,4(11H)-dione + 11-isopropyl-5-methyl-3-phenyl-1H-benzo[a]carbazole-1,4(11H)-dione (15, 16).

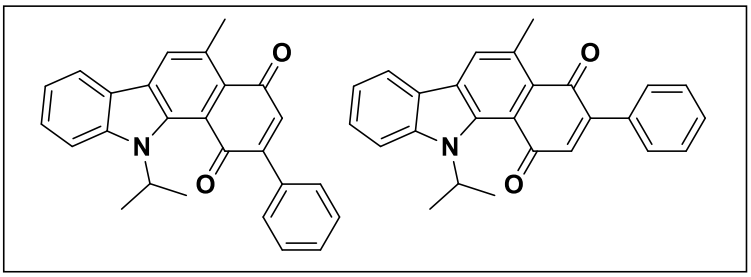

Starting from 3-allyl, *N*-isopropyl-indole (428.8 mg, 2.15 mmol), mixture of **15, 16** was isolated as dark red-brown solid (321.2 mg, 39%); FT-IR (ν_{max}, cm^{-1}): 1741, 1725, 1707, 1694, 1677, 1645, 1616, 1563, 1546, 1532, 1516, 1485, 1463, 1426, 1396, 1366, 1341, 1310, 1222, 1145; ^{1}H NMR (400 MHz, $CDCl_3$): δ 8.12 (d, *J* = 5.6 Hz, 4H), 7.70 (dd, *J* = 8.4, 5.4 Hz, 2H), 7.59- 7.57 (m, 2H), 7.53-7.51 (m, 2H), 7.44-7.40 (m, 10H), 7.01 (s, 2H), 4.81 (h, *J* = 6.9 Hz, 2H), 2.88 (s, 6H), 1.70 (d, *J* = 4.9 Hz, 12H) (Regioisomer ratio: 1:1); ^{13}C NMR (100 MHz, $CDCl_3$): δ 187.9, 187.5, 187.3, 186.6, 147.6, 147.2, 143.7, 143.4, 139.7, 139.5, 134.7, 134.6, 134.0, 133.8, 133.1, 132.7, 132.4, 130.8, 130.7, 130.3, 130.2, 130.0, 129.8, 129.5, 129.4, 129.1, 128.8, 128.7, 128.6, 128.5, 127.7, 127.6, 123.6, 121.2, 120.7, 120.6, 120.0, 114.4, 114.3, 109.7, 52.5, 29.8, 28.6, 24.0, 23.7, 22.8, 21.2, 21.0; HRMS (ESI) for $C_{26}H_{21}O_2N$ $[M+H]^+$ - Calculated: 380.1650, Found: 380.1649.

11-isopropyl-2-methyl-1H-benzo[a]carbazole-1,4(11H)-dione + 11-isopropyl-3-methyl-1H-benzo[a]carbazole-1,4(11H)-dione (21, 22).

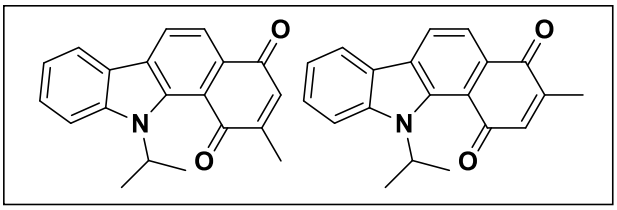

Starting from 3-vinyl, *N*-isopropyl-indole (mg, mmol), mixture of **21, 22** was isolated as dark red-brown solid (200 mg, 66%); FT-IR (ν_{max}, cm^{-1}): 1647, 1581, 1549, 1459, 1409, 1368, 1295, 1246, 1195, 1135, 1103, 1018; ^{1}H NMR (500 MHz, $CDCl_3$): δ 8.29 (t, *J* = 1.8 Hz, 1H), 8.11 (s, 1H), 8.04 (dd, *J* = 9.9, 1.6 Hz, 1H), 7.77 (d, *J* = 3 Hz, 1H), 7.53 – 7.49 (m, 1H), 7.30 (t, *J* = 7.5 Hz, 1H), 6.80 – 6.79 (m, 1H), 5.07 – 4.97 (m, 1H), 2.25 (d, *J* = 2.05 Hz, 3H), 1.70 (d, *J* = 7 Hz, 6H); ^{13}C NMR (100 MHz, $CDCl_3$): δ 187.1, 186.4, 186.3, 185.9, 149.2, 146.0, 143.0, 136.9, 134.0, 132.0, 131.2, 127.5, 124.6, 121.2, 120.8, 119.0, 118.5, 114.4, 52.2, 21.3, 17.2, 16.2; HRMS (ESI) for $C_{20}H_{17}O_2N$ $[M+H]^+$ - Calculated: 304.1337, Found: 304.1342.

11-ethyl-2-methyl-1H-benzo[a]carbazole-1,4(11H)-dione + 11-ethyl-3-methyl-1H-benzo[a]carbazole-1,4(11H)-dione (23, 24).

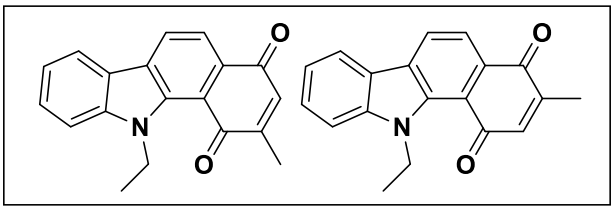

Starting from 3-vinyl, *N*-ethyl-indole (400 mg, 2.34 mmol), mixture of **23, 24** was isolated as dark red-brown solid (461 mg, 68%); FT-IR (ν_{max}, cm^{-1}): 1647, 1582, 1549, 1459, 1416, 1375, 1326, 1292, 1250, 1196, 1128, 1043. ^{1}H NMR (500 MHz, $CDCl_3$): δ 8.35 (s, 1H), 8.10 (d, *J* = 9.8 Hz, 1H), 8.06 (d, *J* = 10.0 Hz, 1H), 7.60 - 7.54 (m, 2H), 7.34 – 7.30 (m, 1H), 6.82 (q, *J* = 1.9 Hz, 1H), 4.72 – 4.61 (m, 2H), 2.25 (d, *J* = 2.1Hz, 3H), 1.40 (t, *J* = 8.9 Hz, 3H); ^{13}C NMR (125 MHz, $CDCl_3$): δ 186.9, 186.1, 185.7, 149.5, 146.2, 144.3, 137.1, 134.2, 131.8, 131.4, 128.3, 128.3, 125.0, 124.9, 122.4, 121.0, 118.9, 118.3, 110.9, 42.4, 17.2, 16.1, 14.4; HRMS (ESI) for $C_{19}H_{15}O_2N$ $[M+H]^+$ - Calculated: 290.1181, Found: 290.1187.

2.4.5. General procedure for epoxidation[10]

To a solution of the Diels-Alder cycloaddition adduct in THF, sodium hypochlorite (9-12 wt.% in water, excess) was added and the reaction mixture was stirred at RT in an open container. Upon complete consumption of the starting material (TLC analysis), the reaction mixture was diluted with water (10 mL), and extracted with multiple portions of ethyl acetate (5 × 5 mL). The combined organic phase was washed with brine (10 mL), dried over anhydrous Na_2SO_4 (5

g), filtered and the filtrate was evaporated to dryness to get the crude product. Silica gel chromatography of the crude using a mixture of ethyl acetate and hexane as an eluent gave pure product.

9-isopropyl-1a,10a-dihydro-2H-oxireno[2′,3′:4,5]benzo[1,2-a]carbazole-2,10(9H)-dione (25).

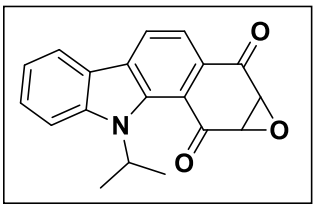

Starting from **1** (70 mg, 0.242 mmol), **25** (74 mg, 96%) was isolated as a bright yellow crystalline solid: mp 204 – 206 °C; FT-IR (ν_{max}, cm^{-1}): 2968, 1683, 1622, 1569, 1416, 1373, 1200, 1116, 1026; ^{1}H NMR (400 MHz, $CDCl_3$): δ 8.24 (d, *J* = 8.0 Hz, 1H), 8.06 (d, *J* = 7.8 Hz, 1H), 7.83 (d, *J* = 7.8 Hz, 1H), 7.72 (d, *J* = 8.5 Hz, 1H), 7.50 (td, *J* = 8.2, 1.0 Hz, 1H), 7.26 (dd, *J* = 14.1, 7.6 Hz, 1H), 4.64-4.74 (m, 1H), 4.10 (s, 2H), 1.96 (d, *J* = 6.8 Hz, 3H), 1.39 (d, *J* = 6.9 Hz, 3H); ^{13}C NMR (100 MHz, $CDCl_3$): δ 193.3, 191.1, 142.1, 138.6, 131.0, 130.1, 127.8, 125.0, 123.4, 121.2, 120.7, 118.4, 117.8, 113.9, 56.5, 54.6, 51.3, 20.7, 20.5; HRMS (ESI) for $C_{19}H_{15}NO_3$ $[M+H]^+$: Calculated: 306.1125, Found: 306.1126.

3-ethyl-9-isopropyl-1a,10a-dihydro-2H-oxireno[2′,3′:4,5]benzo[1,2-a]carbazole-2,10(9H)-dione (26).

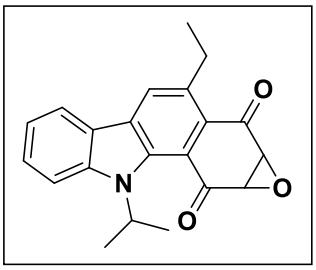

Starting from **2** (250 mg, 0.79 mmol), **26** (200 mg, 76%) was isolated as a yellow solid. FT-IR (ν_{max}, cm^{-1}): 1741, 1725, 1706, 1679, 1647, 1626, 1547, 1532, 1516, 1478, 1464, 1426, 1395, 1367, 1310, 1200; ^{1}H NMR (400 MHz, $CDCl_3$): δ 8.18 (s, 1H), 8.11 (d, *J* = 7.8 Hz, 1H), 7.71 (d, *J* = 8.4 Hz, 1H), 7.51 (t, *J* = 7.6 Hz, 1H), 7.28 (t, *J* = 7.6 Hz, 1H), 4.63 (h, *J* = 6.9 Hz, 1H), 4.16 (d, *J* = 4.6 Hz, 1H), 4.15 (d, *J* = 4 Hz, 1H), 3.21-3.03 (m, 2H), 1.94 (d, *J* = 6.9 Hz, 3H), 1.42 (d, *J* = 7 Hz, 3H), 1.34 (t, *J* = 7.4 Hz, 3H); ^{13}C NMR (100 MHz, $CDCl_3$): δ 195.1, 193.0, 142.5, 137.5, 137.2, 130.0, 127.7, 126.7, 123.2, 121.2, 120.4, 118.7, 113.8, 56.5, 54.4, 51.1, 27.5, 20.7, 20.3, 16.4; HRMS (ESI) for $C_{21}H_{19}O_3N$ $[M+H]^+$: Calculated: 334.1443, Found: 334.1445.

9-isopropyl-10a-phenyl-1a,10a-dihydro-2H-oxireno[2′,3′:4,5]benzo[1,2-a]carbazole-2,10(9H)-dione (27).

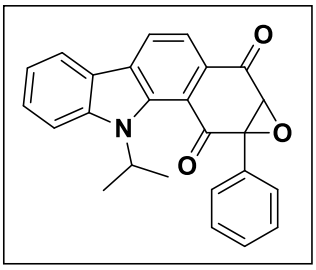

Starting from the mixture of **3, 4** (40 mg, 0.105 mmol), the mixture of regioisomers was isolated as a yellow solid (30 mg, 73%). Using reversed-phase semi-preparative HPLC, compound **27** was isolated as an orange-yellow solid: FT-IR (ν_{max}, cm^{-1}): 1679, 1617, 1553, 1455, 1416, 1376, 1323, 1286, 1221, 1167, 1128, 1078, 1021; ^{1}H NMR (400 MHz, $CDCl_3$): δ 8.36 (d, *J* = 8.0 Hz, 1H), 8.15 (d, *J*= 8.0 Hz, 1H), 7.92 (d, *J* = 7.9 Hz, 1H), 7.74 (d, *J* = 8.3 Hz, 1H), 7.63 – 7.59 (m, 2H), 7.55 – 7.47 (m, 4H), 7.34 – 7.29 (m, 1H), 4.61 (h, *J* = 7.0 Hz, 1H), 4.06 (s, 1H), 1.90 (d, *J* = 4 Hz, 3H), 1.40 (d, *J* = 4 Hz, 3H); ^{13}C NMR (100 MHz, $CDCl_3$): δ 192.7, 191.4, 142.2, 139.0, 131.1, 129.9, 129.4, 128.7, 128.6, 128.3, 128.2, 127.7, 124.8, 123.5, 121.3, 120.7, 119.0, 118.0, 114.0, 63.9, 63.4, 51.4, 20.8, 20.6; HRMS (ESI) for $C_{25}H_{19}O_3N$ $[M+H]^+$ - Calculated: 382.1443, Found: 382.1443.

9-isopropyl-1a-phenyl-1a,10a-dihydro-2H-oxireno[2′,3′:4,5]benzo[1,2-a]carbazole-2,10(9H)-dione (28).

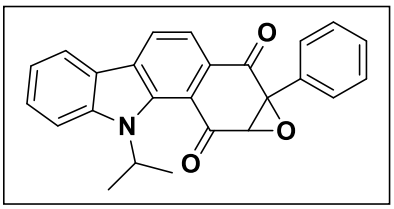

Starting from the mixture of **3, 4** (40 mg, 0.105 mmol), the mixture of regioisomers was isolated as a yellow solid (30 mg, 73%). Using reversed-phase semi-preparative HPLC, compound **28** was isolated as a yellow solid: FT-IR (ν_{max}, cm^{-1}): 1676, 1559, 1455, 1423, 1297, 1257, 1213, 1131, 1102, 1064, 1028; ^{1}H NMR (400 MHz, $CDCl_3$): δ 8.34 (d, *J* = 8 Hz, 1H), 8.14 (d, *J* = 8 Hz, 1H), 8.00 (d, *J* = 8.0 Hz, 1H), 7.77 (d, *J* = 8 Hz, 1H), 7.58 – 7.52 (m, 3H), 7.49 - 7.45 (m, 3H), 7.33 (t, *J* = 7.5 Hz, 1H), 4.81 (h, *J* = 6.9 Hz, 1H), 4.09 (s, 1H), 2.00 (d, *J* = 6.9 Hz, 3H), 1.46 (d, *J* = 7.0 Hz, 3H). ^{13}C NMR (100 MHz, $CDCl_3$): δ 193.2, 190.7, 142.2, 138.4, 131.3, 130.9, 130.8, 129.4, 128.6, 127.9, 127.7, 125.0, 123.4, 121.3, 120.7, 119.1, 118.2, 113.9, 65.8, 62.3, 51.3, 20.8, 20.6; HRMS (ESI) for $C_{25}H_{19}O_3N$ $[M+H]^+$ - Calculated: 382.1443, Found: 382.1443.

9-isopropyl-10a-(4-methoxyphenyl)-1a,10a-dihydro-2H-oxireno[2′,3′:4,5]benzo[1,2-a]carbazole-2,10(9H)-dione (29).

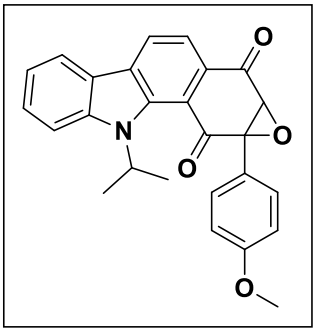

Starting from the mixture of **5, 6** (244 mg, 0.592 mmol), the mixture of regioisomers was isolated as a yellow solid (91 mg, 36%). Using reversed-phase semi-preparative HPLC, compound **29** was isolated as a yellow solid: FT-IR (ν_{max}, cm^{-1}): 1687, 1601, 1514, 1456, 1424, 1385, 1332, 1292, 1245, 1168, 1134, 1024; ^{1}H NMR (400 MHz, $CDCl_3$): δ 8.35 (d, *J* = 7.9 Hz, 1H), 8.14 (d, *J* = 7.7 Hz, 1H), 7.91 (d, *J* = 8.1Hz, 1H), 7.74 (d, *J* = 8.5 Hz, 1H), 7.56 – 7.50 (m, 3H), 7.31 (t, *J* = 7.6 Hz, 1H), 7.04 – 7.00 (m, 2H), 4.61 (h, *J* = 6.9 Hz, 1H), 4.05 (s, 1H), 3.87 (s, 3H), 1.91 (d, *J* = 6.9 Hz, 3H), 1.42 – 1.39 (m, 3H); ^{13}C NMR (100 MHz, $CDCl_3$): δ 193.2, 191.7, 160.4, 142.2, 139.0, 131.1, 129.9, 129.6, 127.7, 124.8, 123.5, 122.9, 121.3, 120.6, 118.0, 114.1, 114.0, 64.0, 55.5, 51.4, 20.8, 20.6; HRMS (ESI) for $C_{26}H_{21}O_4N$ $[M+H]^+$ - Calculated: 412.1549, Found: 412.1546.

9-isopropyl-1a-(4-methoxyphenyl)-1a,10a-dihydro-2H-oxireno[2′,3′:4,5]benzo[1,2-a]carbazole-2,10(9H)-dione (30).

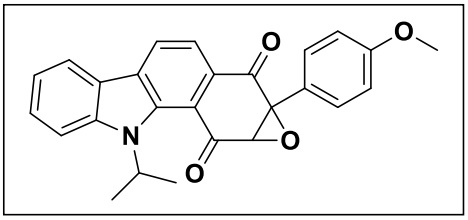

Starting from the mixture of **5, 6** (244 mg, 0.592 mmol), the mixture of regioisomers was isolated as a yellow solid (91 mg, 36%). Using reversed-phase semi-preparative HPLC, compound **30** was isolated as a yellow solid: FT-IR (ν_{max}, cm^{-1}): 1682, 1606, 1513, 1454, 1425, 1379, 1293, 1245, 1169, 1026; ^{1}H-NMR (400 MHz, $CDCl_3$): δ 8.34 (d, *J* = 7.9 Hz, 1H), 8.14 (d, *J* = 7.8 Hz, 1H), 8.00 (d, *J* = 8.1Hz, 1H), 7.77 (d, *J* = 8.3 Hz, 1H), 7.54 (ddd, *J* = 8.5, 7.3, 1.3 Hz, 1H), 7.50 – 7.47 (m, 2H), 7.35 – 7.30 (m, 1H), 7.02 – 6.98 (m, 2H), 4.80 (h, *J* = 6.9 Hz, 1H), 4.09 (s, 1H), 3.86 (s, 3H), 2.00 (d, *J* = 6.9 Hz, 3H), 1.46 (d, *J* = 7.0 Hz, 3H); ^{13}C NMR (100 MHz, $CDCl_3$): δ 199.0, 198.6, 198.0, 194.1, 189.2, 173.1, 159.4, 140.8, 137.1, 130.2, 128.3, 128.1, 127.8, 126.2, 123.7, 121.4, 121.3, 121.2, 120.9, 118.8, 114.7, 114.6, 114.3, 114.1, 113.9, 113.7, 84.6, 60.1, 55.4, 55.4, 51.4, 51.2, 29.9, 21.5, 20.9, 20.5; HRMS (ESI) for $C_{26}H_{21}O_4N$ $[M+H]^+$ - Calculated: 412.1549, Found: 412.1546.

10a-(4-bromophenyl)-9-isopropyl-1a,10a-dihydro-2H-oxireno[2′,3′:4,5]benzo[1,2-a]carbazole-2,10(9H)-dione (31).

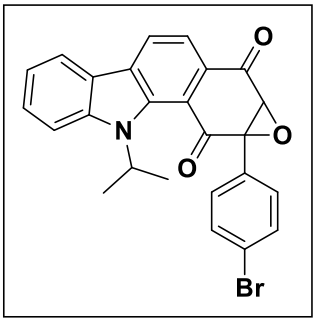

Starting from the mixture of **7, 8** (627.2 mg, 1.41 mmol), the mixture of regioisomers was isolated as a yellow solid (604.5 mg, 93%). Using reversed-phase semi-preparative HPLC, compound **31** was isolated as a yellow solid: FT-IR (ν_{max}, cm^{-1}): 1741, 1725, 1678, 1648, 1616, 1549, 1516, 1498, 1463, 1422, 1396, 1366, 1299, 1223, 1167, 1133, 1107; ^{1}H NMR (400 MHz, $CDCl_3$): δ 8.35 (d, *J* = 8.1Hz, 1H), 8.14 (d, *J* = 7.8 Hz, 1H), 7.91 (d, *J* = 7.8 Hz, 1H), 7.74 (d, *J* = 8.3 Hz, 1H), 7.65 – 7.61 (m, 2H), 7.57 – 7.46 (m, 3H), 7.35 – 7.29 (m, 1H), 4.57 (h, *J* = 7.0 Hz, 1H), 4.01 (s, 1H), 1.90 (d, *J* = 6.9 Hz, 3H), 1.40 (d, *J* = 7.0 Hz, 3H); ^{13}C NMR (100 MHz, $CDCl_3$): δ 192.1, 190.1, 142.2, 139.1, 131.8, 131.0, 131.3, 130.0, 129.8, 127.8, 125.0, 123.7, 123.4, 121.3, 120.7, 118.6, 118.1, 114.0, 64.0, 62.9, 51.5, 20.8, 20.6; HRMS (ESI) for $C_{25}H_{18}O_3NBr$ $[M+H]^+$ - Calculated: 460.0548, Found:460.0548.

1a-(4-bromophenyl)-9-isopropyl-1a,10a-dihydro-2H-oxireno[2′,3′:4,5]benzo[1,2-a]carbazole-2,10(9H)-dione (32).

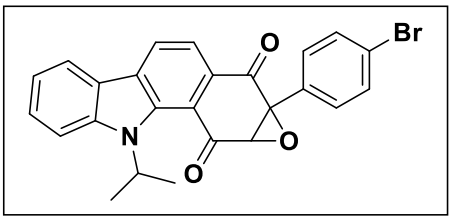

Starting from the mixture of **7, 8** (627.2 mg, 1.41 mmol), the mixture of regioisomers was isolated as a yellow solid (604.5 mg, 93%). Using reversed-phase semi-preparative HPLC, compound **32** was isolated as a yellow solid: FT-IR (ν_{max}, cm^{-1}): 1680, 1556, 1460, 1417, 1367, 1311, 1219, 1136, 1106, 1064, 1011; ^{1}H NMR (400 MHz, $CDCl_3$): δ 8.33 (d, *J* = 7.9 Hz, 1H), 8.14 (d, *J* = 7.8 Hz, 1H), 7.99 (d, *J* = 8.1Hz, 1H), 7.77 (d, *J* = 8.5 Hz, 1H), 7.63 – 7.59 (m, 2H), 7.55 (ddd, *J* = 8.4, 7.4, 1.2 Hz, 1H), 7.46 – 7.41 (m, 2H), 7.33 (t, *J* = 7.6 Hz, 1H), 4.78 (h, *J* = 6.9 Hz, 1H), 4.05 (s, 1H), 2.00 (d, *J* = 6.9 Hz, 3H), 1.45 (d, *J* = 7.0 Hz, 3H); ^{13}C NMR (100 MHz, $CDCl_3$): δ 192.7, 190.3, 142.2, 138.5, 131.8, 130.9, 130.6, 130.4, 129.6, 127.8, 125.1, 123.8, 123.4, 121.3, 120.8, 119.2, 118.0, 114.0, 65.3, 62.3, 51.3, 20.8, 20.6; HRMS (ESI) for $C_{25}H_{18}O_3NBr$ $[M+H]^+$ - Calculated: 460.0548, Found:460.0548.

methyl 4-(9-isopropyl-2,10-dioxo-1a,2,9,10-tetrahydro-10aH-oxireno[2′,3′:4,5]benzo[1,2-a]carbazol-10a-yl)benzoate (33).

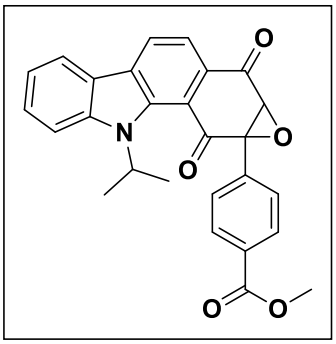

Starting from the mixture of **9, 10** (174 mg), the mixture of regioisomers was isolated as a yellow solid (104 mg, 58%). Using reversed-phase semi-preparative HPLC, compound **33** was isolated as a yellow solid: FT-IR (ν_{max}, cm^{-1}): 1724, 1682, 1617, 1560, 1456, 1421, 1282, 1174, 1102, 1020; ^{1}H NMR (400 MHz, $CDCl_3$) : δ 8.37 (d, *J* = 8.0 Hz, 1H), 8.18 – 8.14 (m, 3H), 7.93 (d, *J* = 8.0 Hz, 1H), 7.74 (d, *J* = 8.4 Hz, 1H), 7.69 (dd, *J* = 6.7, 1.9 Hz, 2H), 7.56 – 7.51 (m, 1H), 7.32 (t, *J* = 7.2 Hz, 1H), 4.61 – 4.54 (m, 1H), 4.03 (s, 1H), 3.96 (s, 3H), 1.90 (d, *J* = 6.9 Hz, 3H), 1.40 (d, *J* = 7.0 Hz, 3H); ^{13}C NMR (100 MHz, $CDCl_3$) : δ 191.9, 190.9, 166.7, 142.3, 139.1, 135.9, 131.3, 131.0, 129.8, 128.2, 127.9, 125.1, 123.5, 121.3, 120.8, 118.1, 114.0, 64.0, 63.0, 52.5, 51.5, 20.8, 20.6; HRMS (ESI) for $C_{27}H_{21}O_5N$ $[M+H]^+$ - Calculated: 440.1498, Found: 440.1493.

methyl 4-(9-isopropyl-2,10-dioxo-2,9,10,10a-tetrahydro-1aH-oxireno[2′,3′:4,5]benzo[1,2-a]carbazol-1a-yl)benzoate (34).

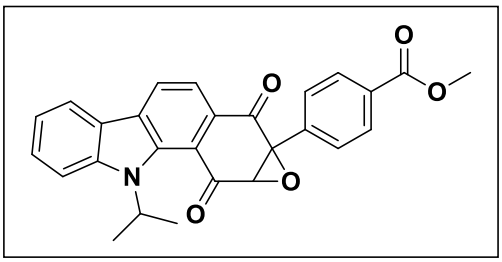

Starting from the mixture of **9, 10** (174 mg), the mixture of regioisomers was isolated as a yellow solid (104 mg, 58%). Using reversed-phase semi-preparative HPLC, compound **34** was isolated as a yellow solid: FT-IR (ν_{max}, cm^{-1}): 1718, 1674, 1616, 1555, 1516, 1438, 1281, 1211, 1107, 1021; ^{1}H NMR (400 MHz, $CDCl_3$) : δ 8.34 (d, *J* = 8.0 Hz, 1H), 8.14 (dd, *J* = 6.7, 1.7 Hz, 3H), 8.00 (d, *J* = 8.0 Hz, 1H), 7.77 (d, *J* = 8.4 Hz, 1H), 7.64 (dd, *J* = 6.7, 1.7 Hz, 2H), 7.57 – 7.53 (m, 1H), 7.33 (t, *J* = 7.5 Hz, 1H), 4.79 (m, 1H), 4.06 (s, 1H), 3.96 (s, 3H), 2.00 (d, *J* = 6.9 Hz, 3H), 1.46 (d, *J* = 7.0 Hz, 3H); ^{13}C NMR (100 MHz, $CDCl_3$) : δ 192.6, 190.2, 166.7, 142.2, 138.5, 136.2, 131.1, 130.7, 129.8, 127.9, 127.9, 125.1, 123.4, 121.3, 120.8, 119.2, 118.0, 114.0, 65.3, 62.3, 52.5, 51.4, 20.8, 20.6; HRMS (ESI) for $C_{27}H_{21}O_5N$ $[M+H]^+$ - Calculated: 440.1498, Found: 440.1493.

3-(9-isopropyl-2,10-dioxo-1a,2,9,10-tetrahydro-10aH-oxireno[2′,3′:4,5]benzo[1,2-a]carbazol-10a-yl)benzaldehyde + 3-(9-isopropyl-2,10-dioxo-2,9,10,10a-tetrahydro-1aH-oxireno[2′,3′:4,5]benzo[1,2-a]carbazol-1a-yl)benzaldehyde (35, 36).

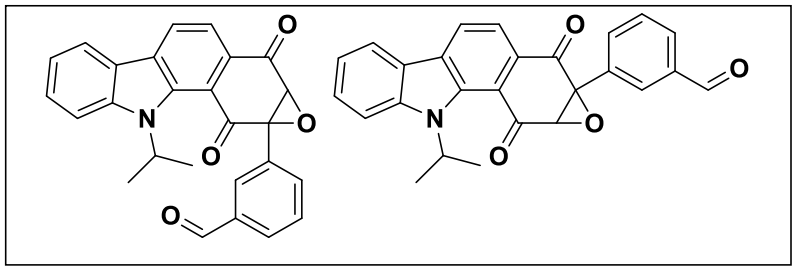

Starting from the mixture of **11, 12** (120 mg), the mixture of regioisomers **35, 36** was isolated as a yellow solid: FT-IR (ν_{max}, cm^{-1}): 1741, 1724, 1692, 1648, 1626, 1616, 1547, 1532, 1516, 1485, 1463, 1425, 1395, 1366, 1331, 1298; ^{1}H NMR (400 MHz, $CDCl_3$): δ 10.08 (s, 1H), 8.32 – 8.27 (m, 1H), 8.14 – 8.08 (m, 2H), 8.00-7.82 (m, 3H), 7.75 (dd, *J* = 12.6 Hz, 8.6 Hz, 1H), 7.66 (q, *J* = 7.8 Hz, 1H), 7.57 – 7.51 (m, 1H), 7.32 (td, *J* = 7.5 Hz, 3.2 Hz, 1H), 4.83 – 4.72 (m, 1H), 4.09 (s, 1H), 1.99 (d, *J* = 6.9 Hz, 3H), 1.45 (d, *J* = 7.1Hz, 3H) (regioisomer ratio: 1.4:1); ^{13}C NMR (100 MHz, $CDCl_3$): δ 192.5, 191.9, 190.7, 142.2, 141.5, 138.5, 136.6, 134.2, 133.9, 130.4, 129.8, 129.3, 127.9, 125.1, 123.4, 121.3, 120.8, 119.1, 118.1, 114.0, 65.1, 63.9, 62.3, 51.5, 51.4, 20.8, 20.6; HRMS (ESI) for $C_{26}H_{19}O_4N$ $[M+H]^+$ - Calculated: 410.1392, Found: 410.1389.

9-isopropyl-10a-(o-tolyl)-1a,10a-dihydro-2H-oxireno[2′,3′:4,5]benzo[1,2-a]carbazole-2,10(9H)-dione + 9-isopropyl-1a-(o-tolyl)-1a,10a-dihydro-2H-oxireno[2′,3′:4,5]benzo[1,2-a]carbazole-2,10(9H)-dione (37, 38).

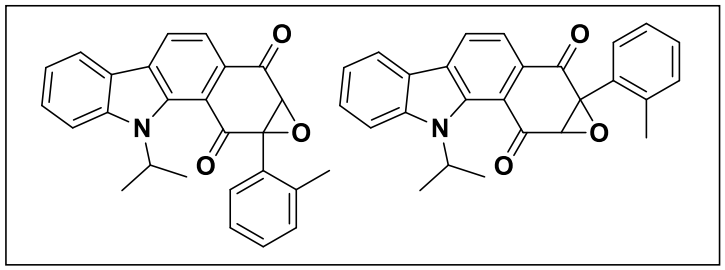

Starting from the mixture of **13, 14** the mixture of regioisomers **37, 38** was isolated as a yellow solid: FT-IR (ν_{max}, cm^{-1}): 1741, 1725, 1706, 1680, 1647, 1626, 1616, 1547, 1532, 1516, 1478, 1463, 1425, 1396, 1367, 1331, 1289, 1216, 1167, 1131. ^{1}H NMR (500 MHz, $CDCl_3$): δ 8.35 (d, *J* = 8.0 Hz, 1H), 8.15 (d, *J* = 7.7 Hz, 1H), 7.99 (d, *J* = 8.0 Hz, 1H), 7.77 (d, *J* = 8.4 Hz, 1H), 7.55 (t, *J* = 7.8 Hz, 1H), 7.45-7.28 (m, 5H), 4.86 – 4.78 (m, 1H), 4.15 (s, 1H), 2.31 (s, 3H), 2.01 (d, *J* = 6.8 Hz, 3H), 1.47 (d, *J* = 7.0 Hz, 3H); ^{13}C NMR (125 MHz, $CDCl_3$): δ 193.8, 190.7, 167.3, 142.1, 138.4, 135.7, 130.8, 130.7, 130.4, 129.7, 127.8, 126.1, 125.0, 124.7, 123.4, 123.3, 121.3, 120.7, 120.0, 119.2, 118.2, 115.6, 113.9, 85.2, 65.0, 61.3, 52.8, 51.3, 47.0, 20.8, 20.6, 19.6; HRMS (ESI) for $C_{26}H_{21}O_3N$ $[M+H]^+$ - Calculated: 396.1599, Found: 396.1606.

9-isopropyl-3-methyl-10a-phenyl-1a,10a-dihydro-2H-oxireno[2′,3′:4,5]benzo[1,2-a]carbazole-2,10(9H)-dione + 9-isopropyl-3-methyl-1a-phenyl-1a,10a-dihydro-2H-oxireno[2′,3′:4,5]benzo[1,2-a]carbazole-2,10(9H)-dione (39, 40).

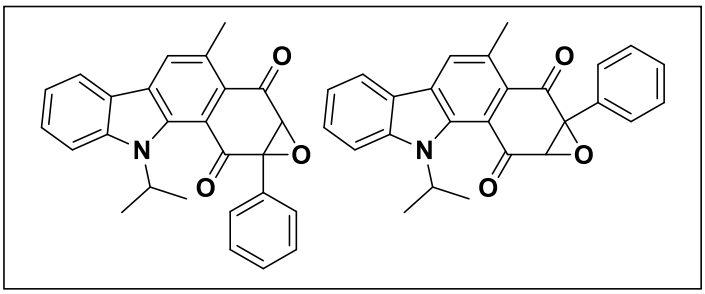

Starting from the mixture of **15, 16** (205 mg, 0.54 mmol), the mixture of regioisomers **39, 40** was isolated as an orange solid (105.2 mg, 49%): FT-IR (ν_{max}, cm^{-1}): 1742, 1707, 1693, 1677, 1647, 1627, 1547, 1532, 1516, 1485, 1463, 1426, 1395, 1366, 1340, 1316, 1197, 1145; ^{1}H NMR (400 MHz, $CDCl_3$): δ 8.13 (d, *J* = 3.0 Hz, 2H), 8.11 (d, *J* = 7.6 Hz, 2H), 7.64 (dd, *J* = 13.8 Hz, 8.3 Hz, 2H), 7.57-7.55(m, 2H), 7.51-7.46 (m, 2H), 7.45-7.39 (m, 8H), 7.24-7.20 (m, 2H), 4.71 (h, *J* = 7.0 Hz, 1H), 4.50 (h, *J* = 7.0 Hz, 1H), 4.04 (s, 1H), 4.00 (s, 1H), 2.75 (s, 3H), 2.6 (s, 3H), 1.96 (d, *J* = 6.9 Hz, 3H), 1.85 (d, *J* = 6.9 Hz, 3H), 1.43 (d, *J* = 7.0 Hz, 3H), 1.38 (d, *J* = 6.9 Hz, 3H); ^{13}C NMR (100 MHz, $CDCl_3$): δ 194.8, 194.4, 193.1, 192.7, 142.6, 137.9, 137.3, 131.5, 131.2, 130.8, 130.5, 130.0, 129.7, 129.4, 128.7, 128.5, 128.3, 128.2, 127.7, 127.3, 123.2, 121.2, 120.4, 120.3, 119.9, 118.9, 113.8, 65.8, 64.1, 63.5, 61.8, 51.2, 51.1, 22.6, 22.0, 20.7, 20.6, 20.4; HRMS (ESI) for $C_{26}H_{21}O_3N$ $[M+H]^+$ - Calculated: 396.1599, Found: 396.1596.

9-ethyl-1a-phenyl-1a,10a-dihydro-2H-oxireno[2′,3′:4,5]benzo[1,2-a]carbazole-2,10(9H)-dione (41).

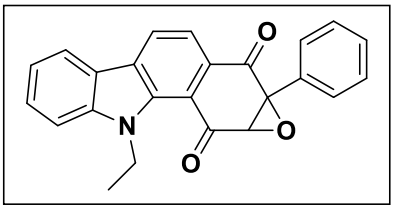

Starting from the crude Diels-Alder adduct (45 mg, 0.128 mmol), compound **41** was isolated as a yellow solid (40 mg, 85%); FT-IR (ν_{max}, cm^{-1}): 1686, 1513, 1473, 1424, 1386, 1302, 1213, 1132, 1038; ^{1}H NMR (400 MHz, $CDCl_3$): δ 8.41 – 8.38 (m, 1H), 8.14 (d, *J* = 7.8 Hz, 1H), 8.01 - 7.98 (m, 1H), 7.63 – 7.55 (m, 4H), 7.50 – 7.46 (m, 3H), 7.35 (t, *J* = 7.3 Hz, 1H), 4.62 – 4.45 (m, 2H), 4.11 (s, 1H), 1.34 (t, *J* = 7.1Hz, 3H); ^{13}C NMR (100 MHz, $CDCl_3$): δ 192.4, 191.1, 143.7, 136.6, 131.2, 131.0, 129.4, 128.6, 128.5, 127.9, 125.3, 122.1, 121.1, 121.0, 119.0, 117.9, 110.3, 65.4, 62.5, 40.7, 13.2; HRMS (ESI) for $C_{24}H_{17}O_3N$ $[M+H]^+$ - Calculated: 368.1286, Found: 368.1289.

9-methyl-1a-phenyl-1a,10a-dihydro-2H-oxireno[2′,3′:4,5]benzo[1,2-a]carbazole-2,10(9H)-dione (42).

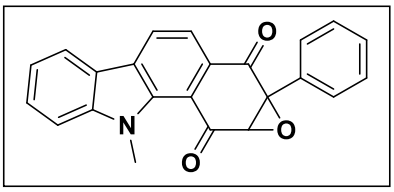

Starting from the crude Diels-Alder adduct compound **42** was isolated as a yellow solid (33 mg); FT-IR (ν_{max}, cm^{-1}): 1679, 1617, 1458, 1299, 1259, 1218, 1131, 1034; ^{1}H NMR (400 MHz, $CDCl_3$): δ 8.29 (d, *J* = 8.0 Hz, 1H), 8.10 (d, *J* = 7.7 Hz, 1H), 7.95 (d, *J* = 8.0 Hz, 1H), 7.63 – 7.56 (m, 3H), 7.52 – 7.46 (m, 4H), 7.36 – 7.32 (m, 1H), 4.09 (s, 1H), 3.84 (s, 3H); ^{13}C NMR (100 MHz, $CDCl_3$): δ 192.0, 190.9, 144.6, 138.3, 131.3, 130.7, 130.7, 129.4, 129.4, 128.6, 128.6, 128.5, 128.2, 128.0, 127.9, 125.1, 121.6, 121.0, 120.9, 120.9, 118.9, 117.5, 110.1, 65.6, 62.6, 34.5; HRMS (ESI) for $C_{23}H_{15}O_3N$ $[M+H]^+$ - Calculated: 354.113, Found: 354.1133.

9-isopropyl-10a-methyl-1a,10a-dihydro-2H-oxireno[2′,3′:4,5]benzo[1,2-a]carbazole-2,10(9H)-dione + 9-isopropyl-1a-methyl-1a,10a-dihydro-2H-oxireno[2′,3′:4,5]benzo[1,2-a]carbazole-2,10(9H)-dione (43, 44).

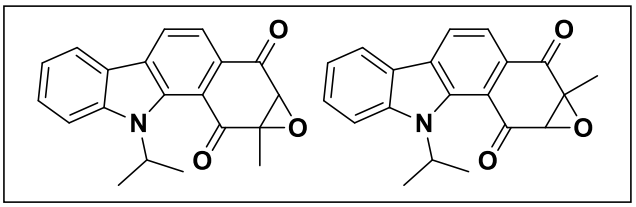

Starting from the mixture of **21, 22** (50 mg, 0.1637 mmol), the mixture of regioisomers **43, 44** was isolated as a yellow solid (47 mg, 90%); FT-IR (ν_{max}, cm^{-1}): 1681, 1620, 1555, 1460, 1419, 1327, 1293, 1221, 1163, 1134, 1081, 1018; ^{1}H NMR (400 MHz, $CDCl_3$): δ 8.28 (dd, *J* = 8.0, 2.1Hz, 1H), 8.10 (d, *J* = 7.8 Hz, 1H), 7.88 (dd, *J* = 28.3, 7.9 Hz, 1H), 7.74 (d, *J* = 8.6 Hz, 1H), 7.54 – 7.50 (m, 1H), 7.30 (t, *J* = 7.5 Hz, 1H), 4.80 – 4.69 (m, 1H), 3.96 (s, 1H), 2.00 (d, *J* = 4.1Hz, 3H), 1.84 (s, 3H), 1.43 (d, *J* = 5.2 Hz, 3H); ^{13}C NMR (100 MHz, $CDCl_3$): δ 194.2, 192.1, 149.7, 142.2, 137.1, 130.5, 127.7, 127.6, 124.9, 124.7, 121.2, 120.6, 118.7, 118.0, 113.9, 62.8, 62.5, 60.8, 60.4, 51.4, 51.2, 20.8, 20.6, 20.6, 15.2, 14.9; HRMS (ESI) for $C_{20}H_{17}O_3N$ $[M+H]^+$ - Calculated: 320.1286, Found: 320.1293.

9-ethyl-10a-methyl-1a,10a-dihydro-2H-oxireno[2′,3′:4,5]benzo[1,2-a]carbazole-2,10(9H)-dione + 9-ethyl-1a-methyl-1a,10a-dihydro-2H-oxireno[2′,3′:4,5]benzo[1,2-a]carbazole-2,10(9H)-dione (45, 46).

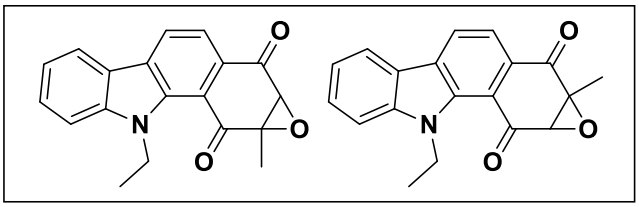

Starting from the mixture of **23, 24** (50 mg, 0.1728 mmol), the mixture of regioisomers **45, 46** was isolated as a yellow solid (45 mg, 87%); FT-IR (ν_{max}, cm^{-1}): 1679, 1555, 1517, 1464, 1423, 1379, 1295, 1216, 1168, 1136, 1082, 1051, 1017; ^{1}H NMR (400 MHz, $CDCl_3$): δ 8.36 – 8.32 (m, 1H), 8.11 (d, *J* = 7.6 Hz, 1H), 7.85 - 7.82 (m, 1H), 7.60 – 7.52 (m, 2H), 7.32 (t, *J* = 7.3 Hz, 1H), 4.55 – 4.41 (m, 2H), 3.96 (s, 1H), 1.84 (s, 3H), 1.32- 1.28 (m, 3H); ^{13}C NMR (100 MHz, $CDCl_3$): δ 192.8, 192.5, 143.7, 137.0, 131.6, 131.3, 130.2, 130.1, 129.8, 128.4, 125.2, 125.0, 122.1, 121.0, 120.9, 118.5, 117.8, 110.3, 62.3, 60.9, 60.6, 40.6, 15.1, 14.8, 13.2, 13.0; HRMS (ESI) for $C_{19}H_{15}O_3N$ $[M+H]^+$ - Calculated: 306.1130, Found: 306.1133.

2.4.6. Procedure for the synthesis of thiol-adduct 47[20]

1 and 4-nitrobenzyl thiol were dissolved in ethanol and the reaction was set under reflux conditions for 24 h. A precipitate was formed which was filtered using a glass funnel. The residue was washed with ethanol (2 × 5 mL) and then dried under high vacuum. The crude product was then purified on a Prep HPLC Column Kromasil C18 (21.5 mm x 250 mm 10 μm) with water and acetonitrile as the eluting solvents. The pure product was obtained at 92% ACN-water eluting system.

11-isopropyl-3-((4-nitrobenzyl)thio)-1H-benzo[a]carbazole-1,4(11H)-dione (47).

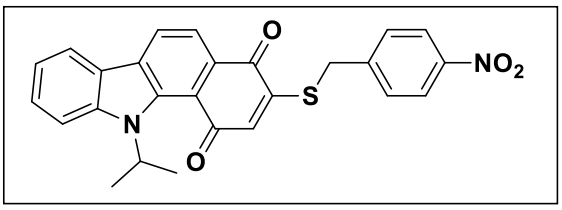

Starting from **1** (50 mg, 0.17 mmol), **47** (24 mg, 51%) was isolated as a reddish solid. FT-IR(ν_{max}, cm^{-1}): 1646, 1521, 1459, 1346, 1264, 1141; ^{1}H NMR (400 MHz, $CDCl_3$): δ 8.32 (d, *J* = 7.9 Hz, 1H), 8.27 – 8.23 (m, 2H), 8.11 (d, *J* = 7.8 Hz, 1H), 8.01 (d, *J* = 7.9 Hz, 1H), 7.76 (d, *J* = 8.4 Hz, 1H), 7.65 (d, *J* = 8.8 Hz, 2H), 7.54 - 7.50 (m, 1H), 7.34 - 7.30 (m, 1H), 6.59 (s, 1H), 4.91 (h, *J* = 8.0 Hz, 1H), 4.18 (s, 2H), 1.70 (d, *J* = 8.0 Hz, 6H); ^{13}C NMR (100 MHz, $CDCl_3$): δ 182.7, 182.4, 154.6, 147.8, 142.9, 142.1, 140.3, 131.3, 130.0, 127.8, 126.3, 125.6, 124.3, 123.8, 121.2, 121.1, 119.1, 117.7, 114.5, 52.5, 35.0, 21.3.; HRMS: (ESI) $C_{26}H_{20}O_4N_2S$ $[M+H]^+$ - Calculated: 457.524, Found: 457.03.

2.4.7. X-ray diffraction studies

25: Crystals of **25** were grown by slow evaporation from a solution of ethanol. A single crystal was mounted in a loop with a small amount of the mother liquor. The X-ray data was collected at 296 K temperature on a Bruker AXS SMART APEX CCD diffractometer using Mo Kα radiation (λ = 0.71073 Å), ω-scans (2θ= 52.52^o), for a total number of 2452 independent reflections. Space group *P-1*, *a* =10.734(4), *b* = 17.703(6), *c* = 24.368(9) Å, α= 75.860(9), β= 87.006(9), γ = 73.924(9), *V*= 4314(3) Å^3, monoclinic *P-1*, Z=2 for chemical formula $C_{19}H_{15}NO_3$. ρ calcd =1.411 g cm^{-3}, μ= 0.096 mm^{-1}, *F*(000)=1922.0, R_{int}= 0.1008. The structure was obtained by direct methods using SHELXS-97. All non-hydrogen atoms were refined anisotropically. The hydrogen atoms were fixed geometrically in the idealized position and refined in the final cycle of refinement as riding over the atoms to which they are bonded. The final *R* value was 0.1008 (*wR2*= 0.3824) for 21687, *S* = 0.901. (CCDC 1848949)

27: Crystals of **27** were grown by slow evaporation from a solution of Ethyl acetate/chloroform (1:1 v/v). A single crystal was mounted in a loop with a small amount of the mother liquor. The X-ray data was collected at 296 K temperature on a Bruker AXS SMART APEX CCD diffractometer using Mo Kα radiation (λ = 0.71073 Å), ω-scans (2θ= 52.52^o), for a total number of 3071 independent reflections. Space group *P - 1*, *a* = 8.699(1), *b* = 10.0745(13), *c* = 11.5324(15) Å, α= 95.001(3), β= 109.201(3), γ = 102.904(3), *V*= 916.1(2) Å^3, monoclinic *P - 1*, Z=2 for chemical formula $C_{25}H_{19}NO_3$. ρ calcd =1.383 g cm^{-3}, μ= 0.091 mm^{-1}, *F*(000)=400.0, R_{int}= 0.0443. The structure was obtained by direct methods using SHELXS-97. All non-hydrogen atoms were refined anisotropically. The hydrogen atoms were fixed geometrically in the idealized position and refined in the final cycle of refinement as riding over the atoms to which they are bonded. The final *R* value was 0.0443 (*wR2*= 0.1273) for 4531, *S* = 0.679. (CCDC 1848953)

28: Crystals of **28** were grown by slow evaporation from a solution of Ethyl acetate/chloroform (1:1 v/v). A single crystal was mounted in a loop with a small amount of the mother liquor. The X-ray data was collected at 296 K temperature on a Bruker AXS SMART APEX CCD diffractometer using Mo Kα radiation (λ = 0.71073 Å), ω-scans (2θ= 52.52^o), for a total number of 3403 independent reflections. Space group *P21/c*, *a* = 16.894(16), *b* = 15.704(14), *c* =

15.365(14) Å, α= 90, β= 113.270(17), γ = 90, V= 916.1(2) Å^3, monoclinic *P21/c*, Z=2 for chemical formula $C_{25}H_{19}NO_3$.ρ calcd =1.353 g cm^{-3}, μ= 0.089 mm^{-1}, F(000)=1600.0, R_{int}=0.1377. The structure was obtained by direct methods using SHELXS-97. All non-hydrogen atoms were refined anisotropically. The hydrogen atoms were fixed geometrically in the idealized position and refined in the final cycle of refinement as riding over the atoms to which they are bonded. The final R value was 0.1377 (*wR2*= 0.4169) for 9250, S = 1.049. (CCDC 1848952)

32: Crystals of **32** were grown by slow evaporation from a solution of Chloroform. A single crystal was mounted in a loop with a small amount of the mother liquor. The X-ray data was collected at 296 K temperature on a Bruker AXS SMART APEX CCD diffractometer using Cu Kα radiation (λ = 1.54178 Å), ω-scans (2θ= 52.52^o), for a total number of 3472 independent reflections. Space group *P21/c*, a = 13.2670(7), b = 8.6870(5), c = 17.6073(10) Å, α = 90, β = 105.100(4), γ = 90, V= 1959.18(19) Å^3, monoclinic *P21/c*, Z=4 for chemical formula $C_{25}H_{18}BrNO_3$. ρ calcd =1.561 g cm^{-3}, μ= 3.092 mm^{-1}, F(000)=936.0, R_{int} =0.2224. The structure was obtained by direct methods using SHELXS-97. All non-hydrogen atoms were refined anisotropically. The hydrogen atoms were fixed geometrically in the idealized position and refined in the final cycle of refinement as riding over the atoms to which they are bonded. The final R value was 0.2224 (*wR2*= 0.5927) for 3472, S = 2.758. (CCDC 1894426)

2.4.8. Reaction of the epoxide with thiols

2.4.8.1. For compounds 25-28

Compound (100 µM) was reacted with *L*-cysteine (100 µM, 1 eq.) in pH 7.4 phosphate buffer (100 mM): ACN (1:1 v/v) at 37 ºC for 1 h. The reaction mixture was filtered (0.22 µm filter) and injected (25 µL) in an Agilent high performance liquid chromatography (HPLC) attached with a diode-array detector (detection wavelength was 250 nm) and a Zorbax SB C-18 reversed phase column (250 mm × 4.6 mm, 5 µm). The following method with a mobile phase of water: acetonitrile was used with a run time of 25 min: multistep gradient with a flow rate of 1 mL/min – starting with 50:50 % → 0 – 5 min, 40:60 → 5 – 10 min, 30:70 → 10 – 15 min, 20:80 → 15 – 20 min, 50:50 → 20 – 23 min, 50:50 → 23 – 25 min.

2.4.8.2. For compounds 27-46

Compound (100 µM) was reacted with *L*-cysteine (1 mM, 10 eq.) in pH 7.4 phosphate buffer (100 mM): ACN (1:1 v/v) at 37 ºC for 1 h. The reaction mixture was filtered (0.22 µm filter) and injected (25 µL) in an Agilent high performance liquid chromatography (HPLC) attached with a diode-array detector (detection wavelength was 250 nm) and a Zorbax SB C-18 reversed phase column (250 mm × 4.6 mm, 5µm). The following method with a mobile phase of water:acetonitrile was used with a run time of 25 min: multistep gradient with a flow rate of 1 mL/min – starting with 50:50 % → 0 – 5 min, 40:60 → 5 – 10 min, 30:70 → 10 – 15 min, 20:80 → 15 – 20 min, 50:50 → 20 – 23 min, 50:50 → 23 – 25 min.

2.4.9. Minimum Inhibitory Concentration Determination[21]

Antibiotic susceptibility testing was done by calculating the Minimum Inhibitory Concentration (MIC) according to standard CLSI guidelines. MIC is defined as the minimum concentration of compound at which bacterial growth is inhibited and it can be detected visibly. Bacterial cultures were grown in Mueller Hinton II Broth (MHB). Optical density (OD_{600}) of the cultures was measured, followed by dilution for ~10^{5-6} CFU/ml. This inoculum is added into a series of test wells in a microtiter plate that contain various concentrations of compound under test. The concentration of compounds used were ranged from 0.03 µg/mL to 64 µg/mL. Plates were incubated at 37 ºC for 16-18 h. Minimum inhibitory concentration (MIC) was determined as the concentration at which no visible growth was seen. For each compound, MIC determinations were carried independently 3 times using duplicate samples each time.

2.4.10. HPLC studies: Covalent thiol adduct for 25

Compound **25** (25 µM) was reacted with 4-nitrobenzyl thiol (250 µM, 10 eq.) in pH 7.4 phosphate buffer (100 mM): ACN (1:1 v/v) at 37 ºC for two time-points of 30 min and 1 h. For the spiking experiment, the authentic product **47**, was added to the reaction mixture after 1 h. The reaction mixture was filtered (0.22 µm filter) and injected (25 µL) in an Agilent high performance liquid chromatography (HPLC) attached with a diode-array detector (detection wavelength was 250 nm) and a Zorbax SB C-18 reversed phase column (250 mm × 4.6 mm, 5µm). The following method with a mobile phase of water: acetonitrile was used with a run time of 25 min: multistep gradient with a flow rate of 1 mL/min – starting with 50:50 % → 0 – 5 min, 40:60 → 5 – 10 min, 30:70 → 10 – 15 min, 20:80 → 15 – 20 min, 50:50 → 20 – 23 min, 50:50 → 23 – 25 min.

2.4.11. Kinetics of reaction of IND-QE analogues with cysteine, used for compounds 25-28

Compound (100 µM) was reacted with *L*-cysteine (1 mM, 10 eq.) in pH 7.4 phosphate buffer (100 mM): ACN (1:1 v/v) at 37 ºC for different time points (0 to 60 min, with 10 min intervals). The reaction mixture was filtered (0.22 µm filter) and injected (25 µL) in an Agilent high performance liquid chromatograph (HPLC) attached with a diode-array detector (detection wavelength was 250 nm) and a Zorbax SB C-18 reversed phase column (250 mm × 4.6 mm, 5µm). The following method with a mobile phase of water:acetonitrile was used with a run time of 25 min: multistep gradient with a flow rate of 1 mL/min – starting with 50:50 % → 0 – 5 min, 40:60 → 5 – 10 min, 30:70 → 10 – 15 min, 20:80 → 15 – 20 min, 50:50 → 20 – 23 min, 50:50 → 23 – 25 min. Each assay was conducted in duplicate and an average is reported.

2.4.12. Intracellular thiol depletion (mBBr assay)

Methicillin-resistant *Staphylococcus aureus* (MRSA - ATCC 33591) was cultured in 5 mL of cation adjusted Mueller Hinton broth (CA-MHB) at 37 ºC for 2 h and re-suspended with fresh medium to an O.D of 1.0. A stock solution of the compound in DMSO was added so that the final concentration was 50 µM and incubated for 60 min at 37 ºC. Next, centrifugation of the bacterial suspension followed by removal of extracellular media to remove any excess compound was carried out. The collected bacterial pellet was re-suspended with pH 7.4 phosphate buffer. A solution of *mono*-Bromobimane (mBBr, final concentration 50 µM, 1:1 ratio) was added. 200 µL of this mixture was then added to each well of sterile flat bottom 96-well microtiter plate and then incubated. The fluorescence (excitation at 390 nm; emission at 490 nm) was measured at time points of 15 min and 30 min using a microtiter plate reader.

2.4.13. Cyclic Voltammetry

2.5 mL of a stock solution of **25** (10 mM in ACN) was added to a 25 mL volumetric flask and was diluted to 25 mL with electrolyte solution. Electrolyte used was tetra-butyl ammonium hexafluorophosphate (0.1 M solution in ACN). The solution was purged with argon for 2 minutes. The applied voltage range was 0 to -2 mV for determining the reduction potential. Glassy carbon was used as the working electrode and the counter electrode used was Platinum foil. Ag/Ag^{+} was used as the reference electrode.

2.5. Spectral charts

^{1}H NMR of **1**

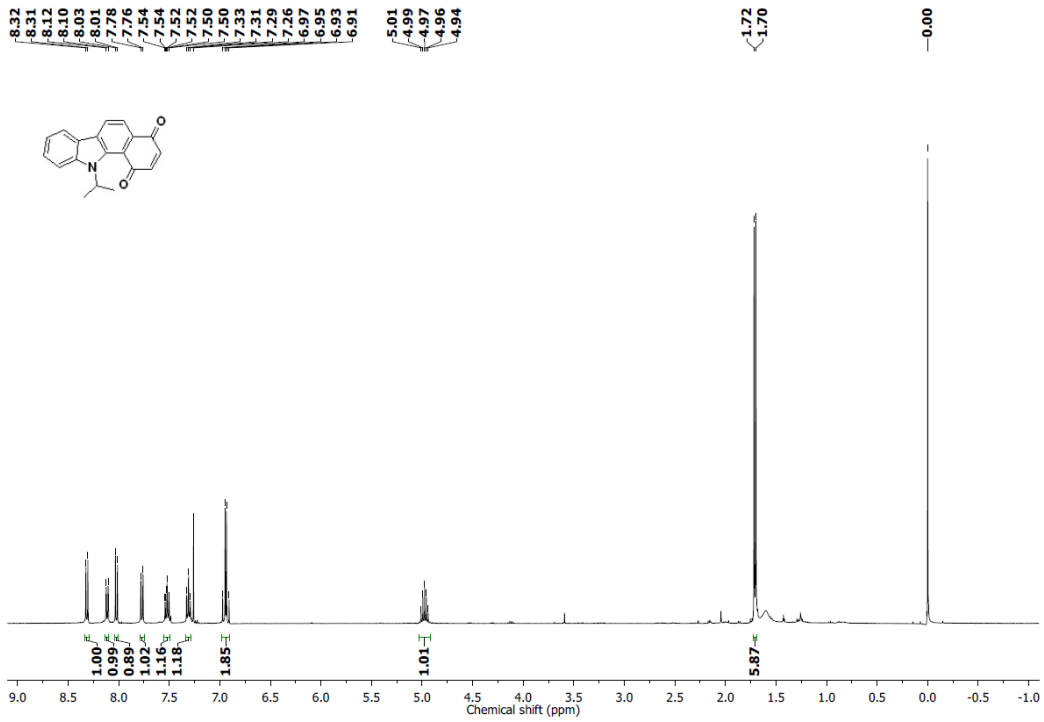

^{13}C NMR of **1**

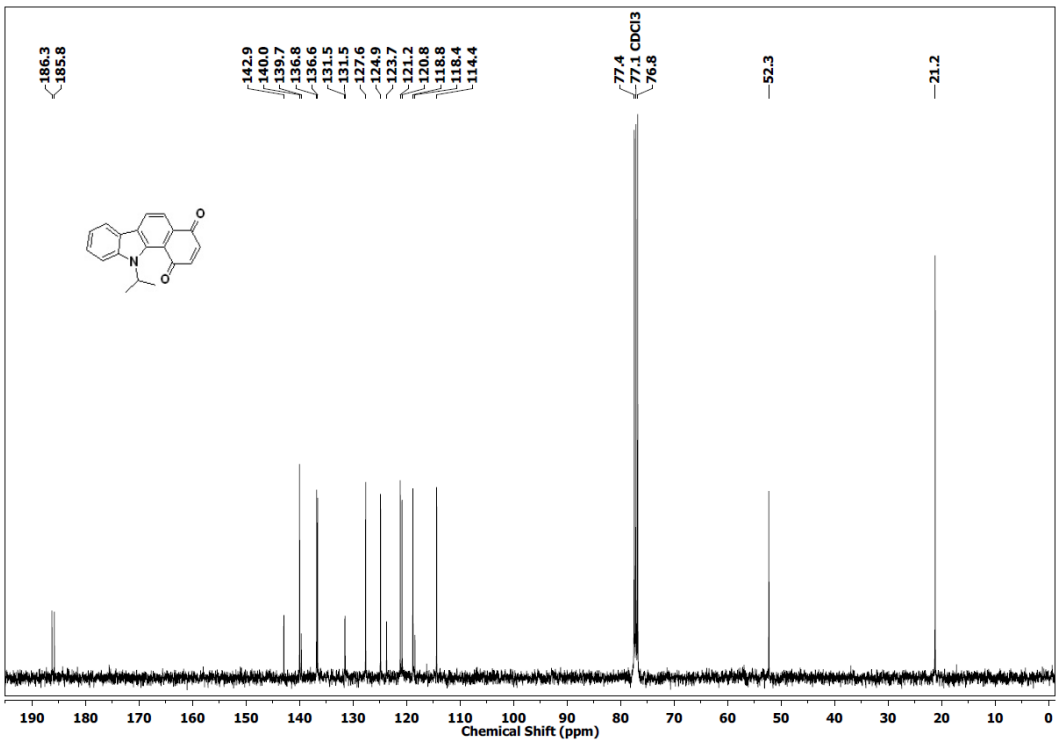

^{1}H NMR of **2**

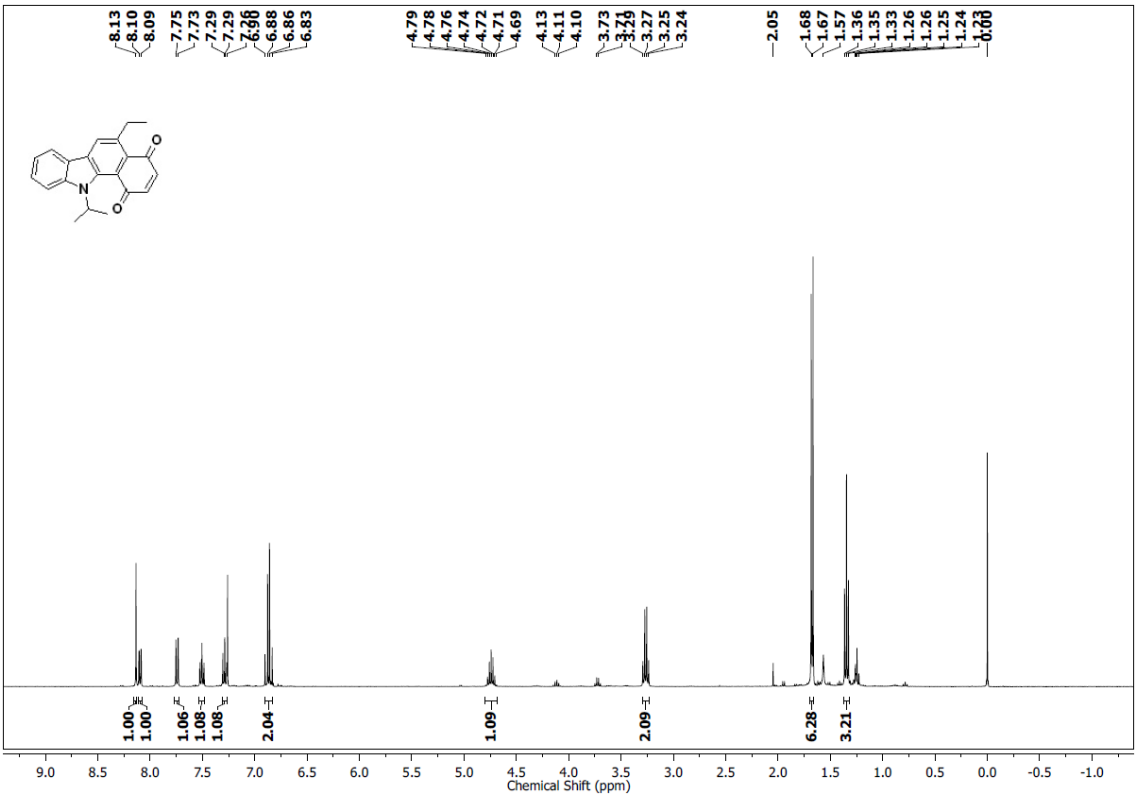

^{13}C NMR of **2**

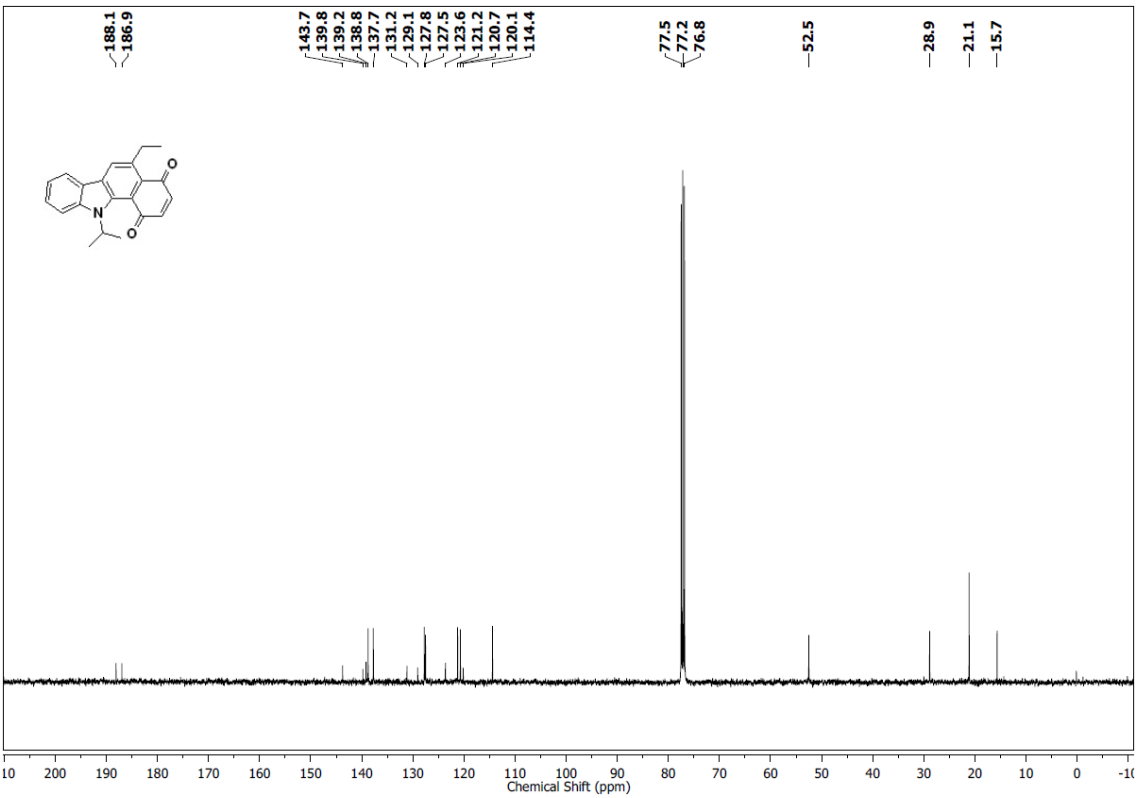

^{1}H NMR of **3, 4**

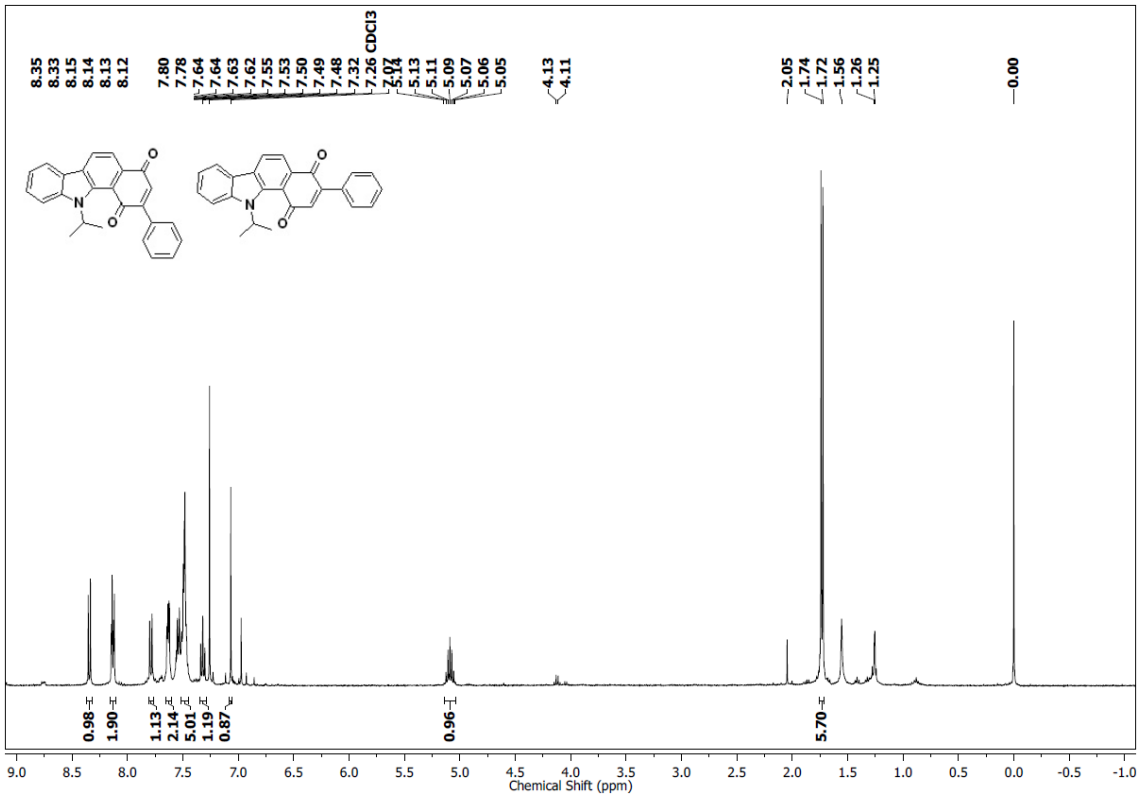

^{13}C NMR of **3, 4**

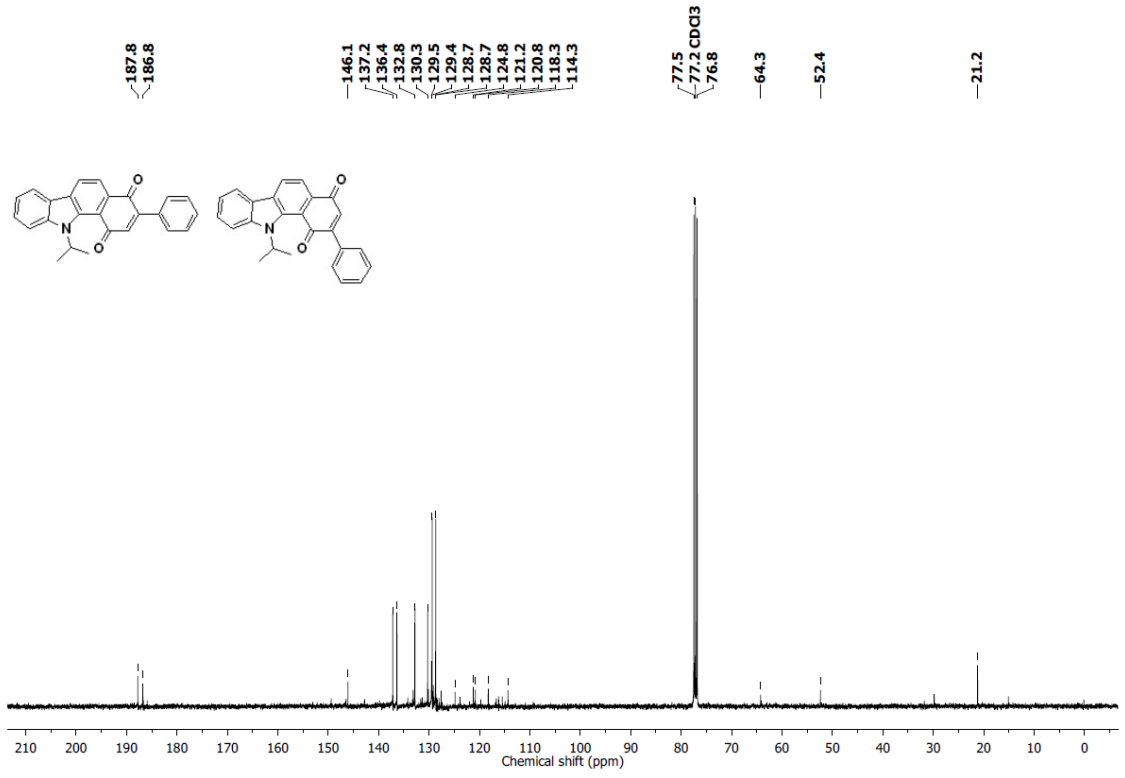

^{1}H NMR of **5, 6**

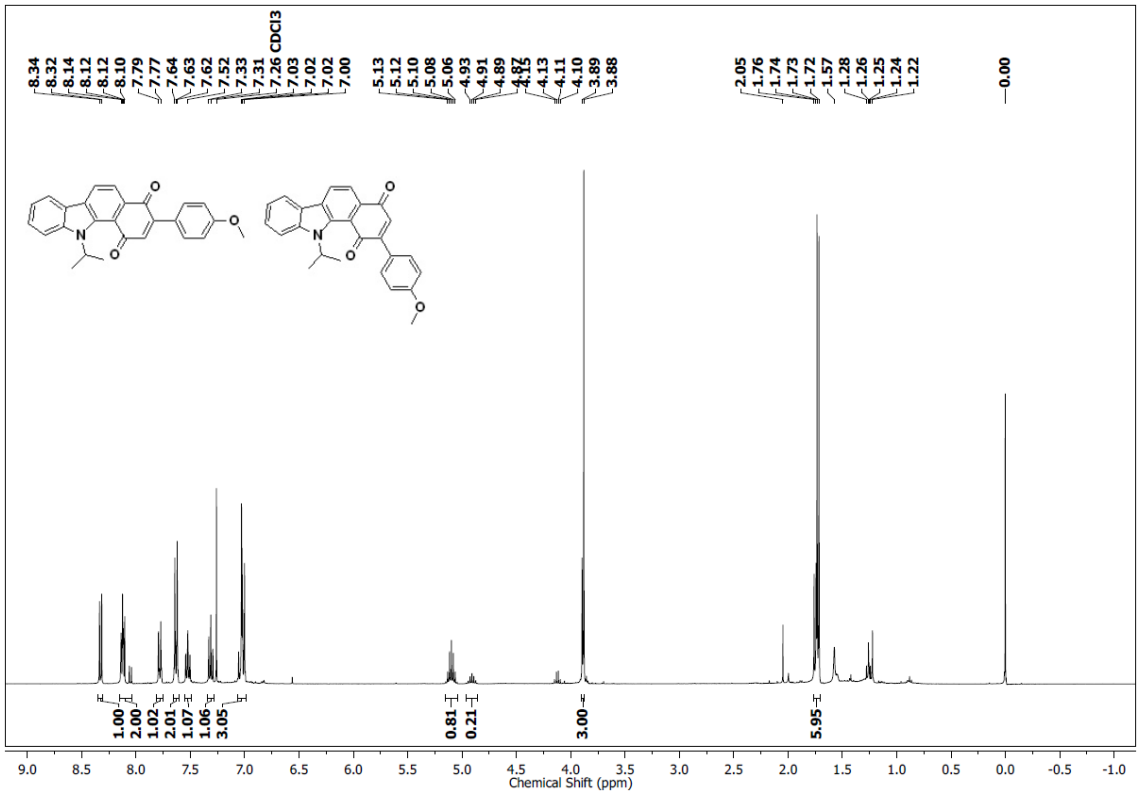

^{13}C NMR of **5, 6**

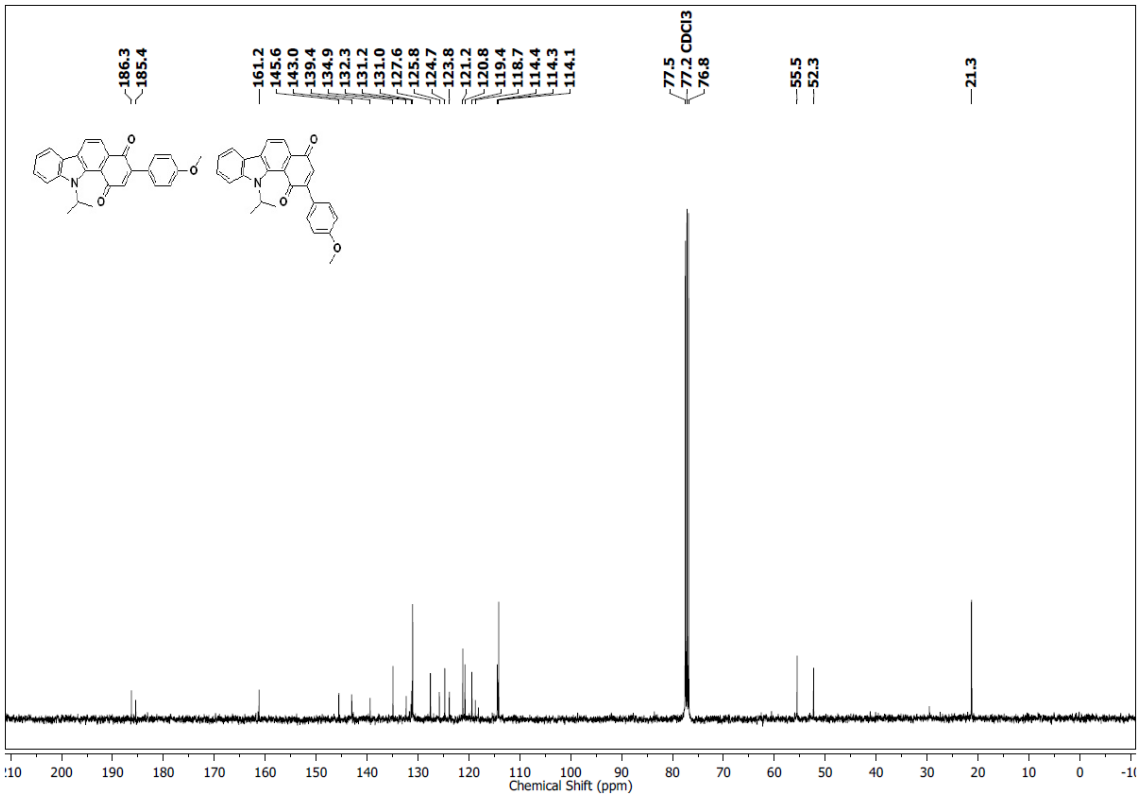

^{1}H NMR of **7, 8**

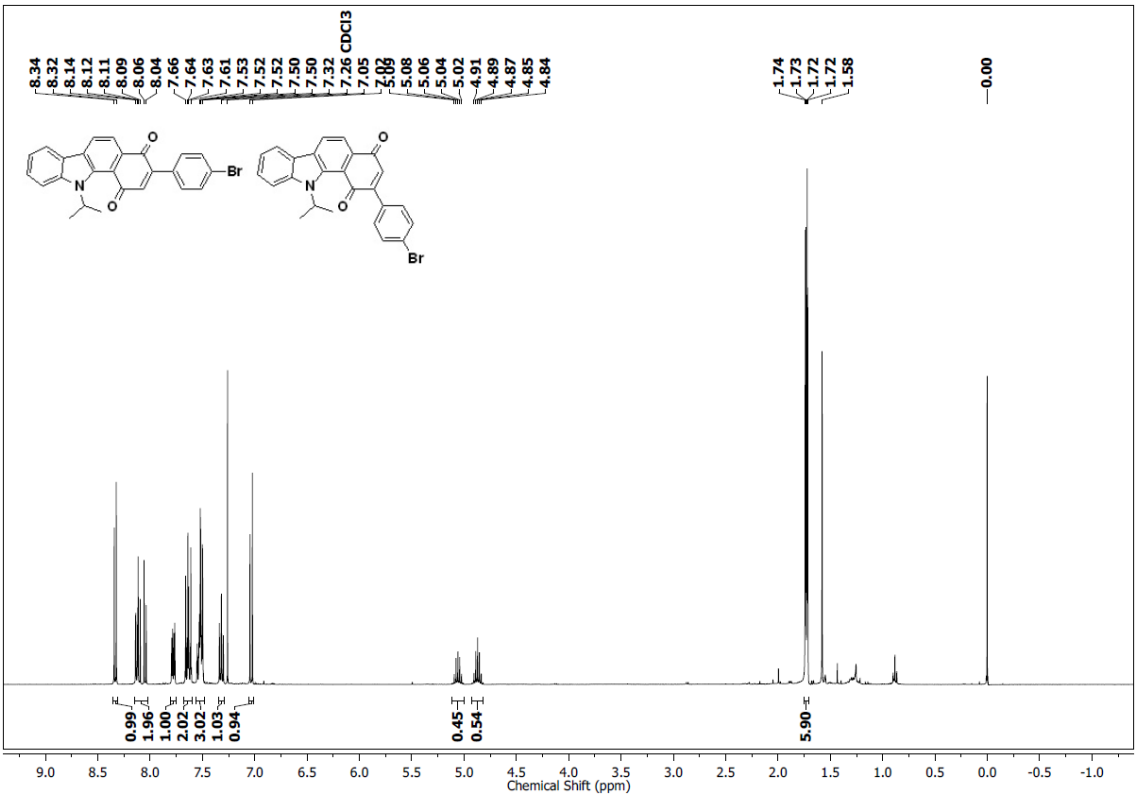

^{13}C NMR of **7, 8**

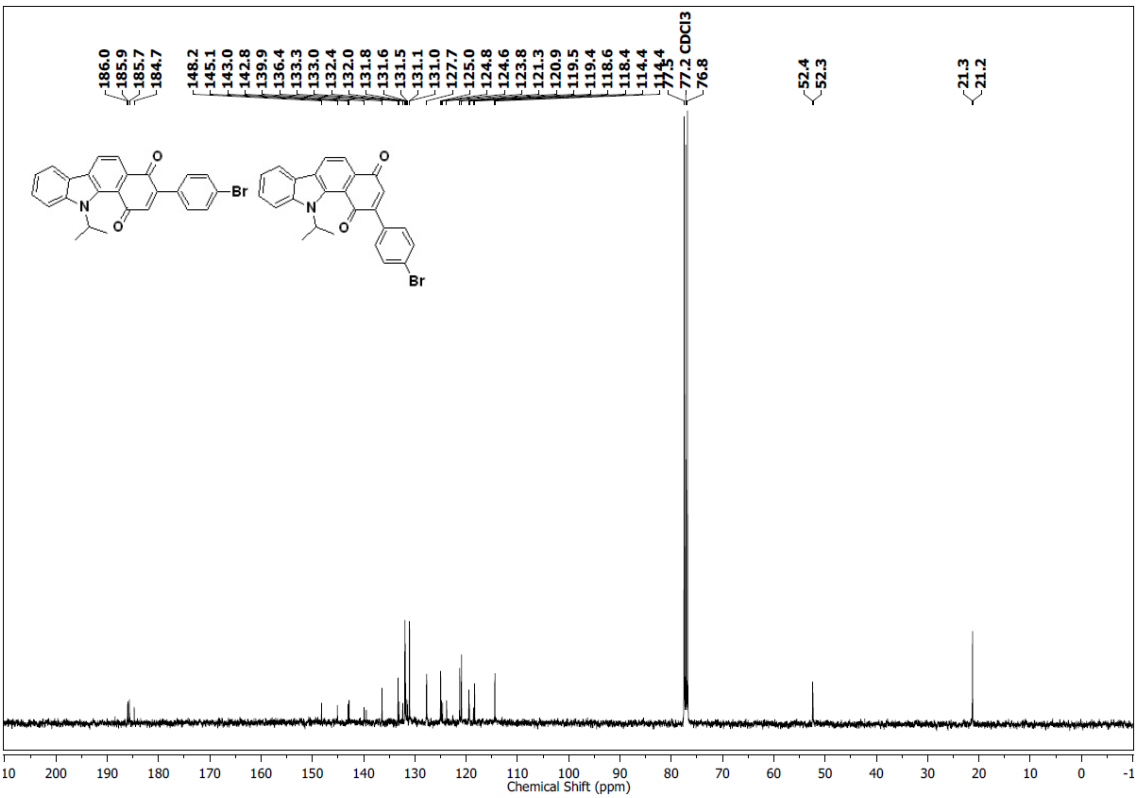

^{1}H NMR of **9, 10**

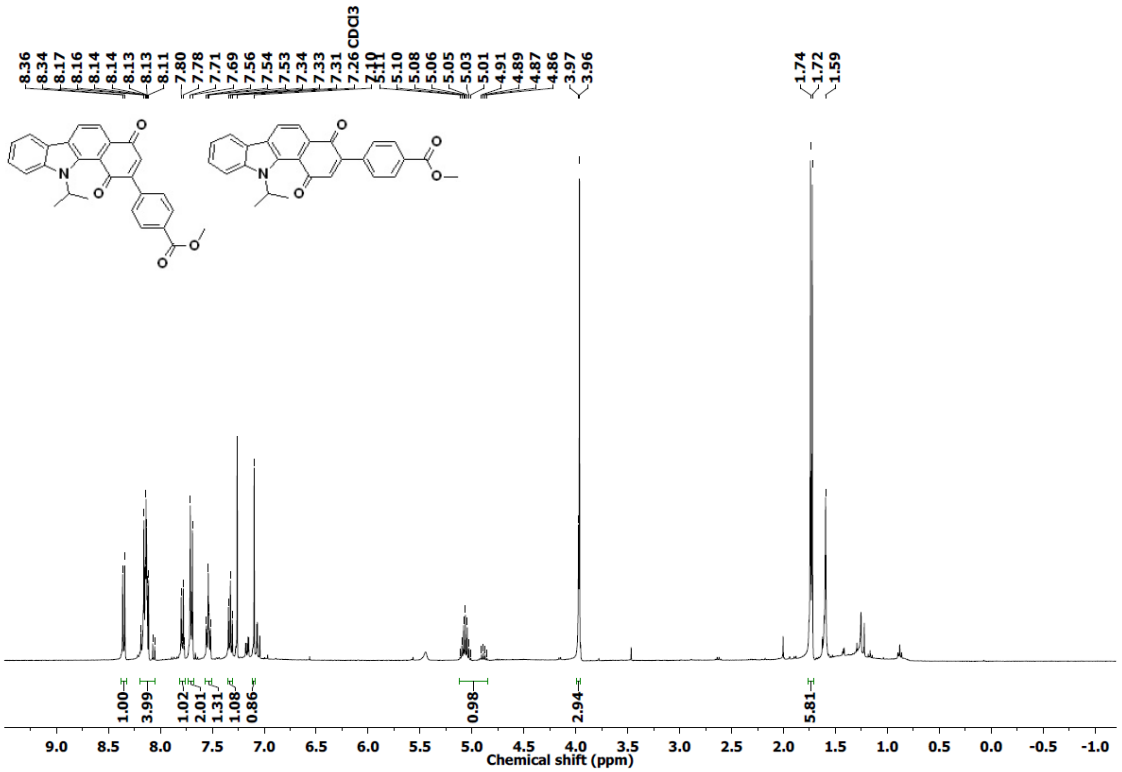

^{13}C NMR of **9, 10**

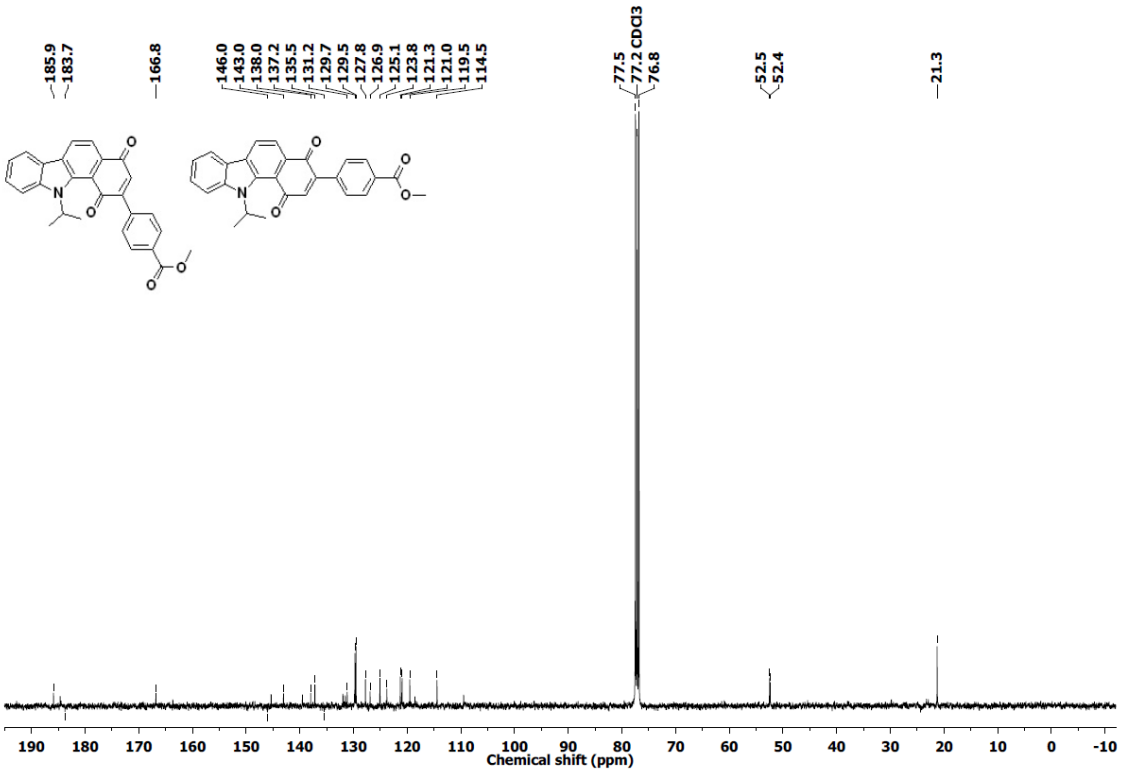

^{1}H NMR of **11, 12**

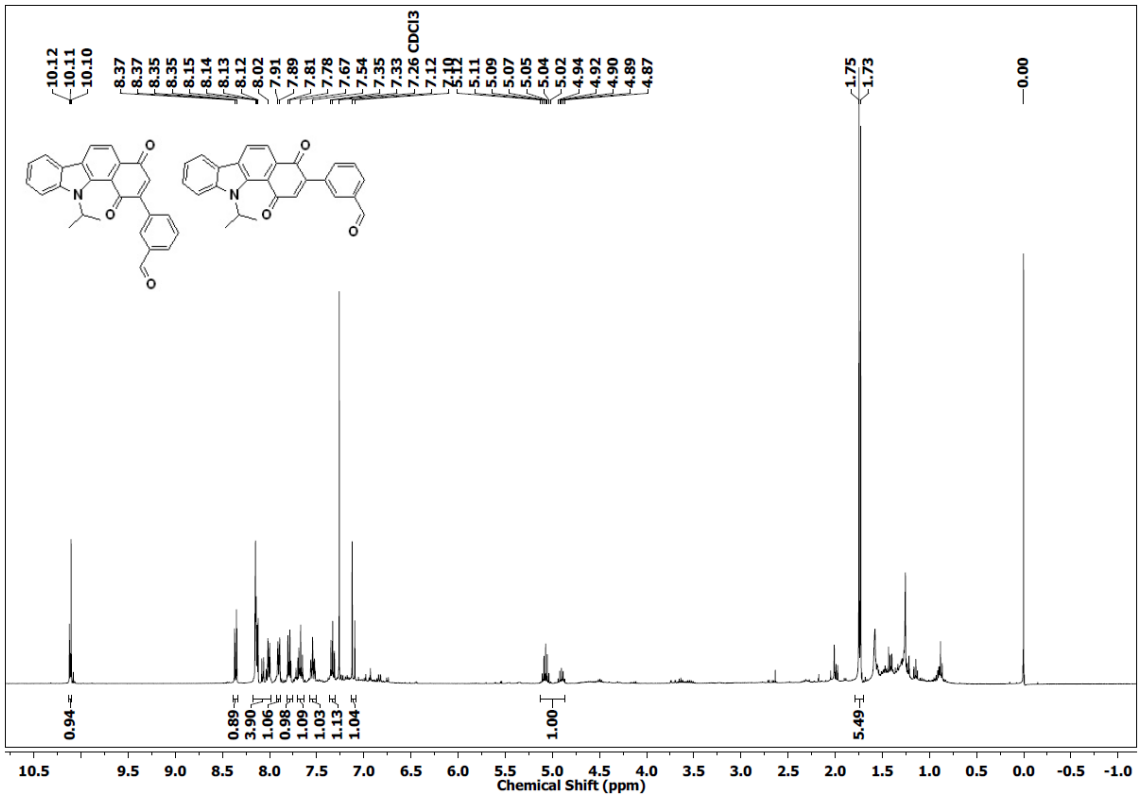

^{13}C NMR of **11, 12**

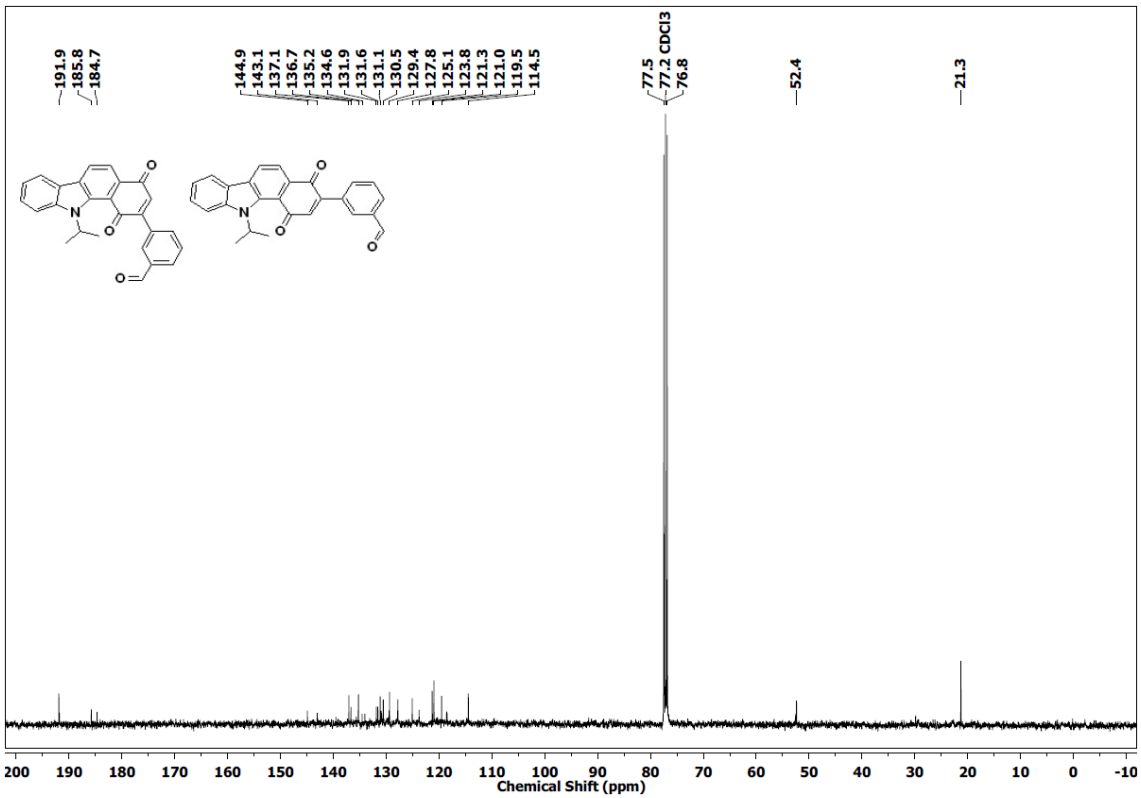

^{1}H NMR of **13, 14**

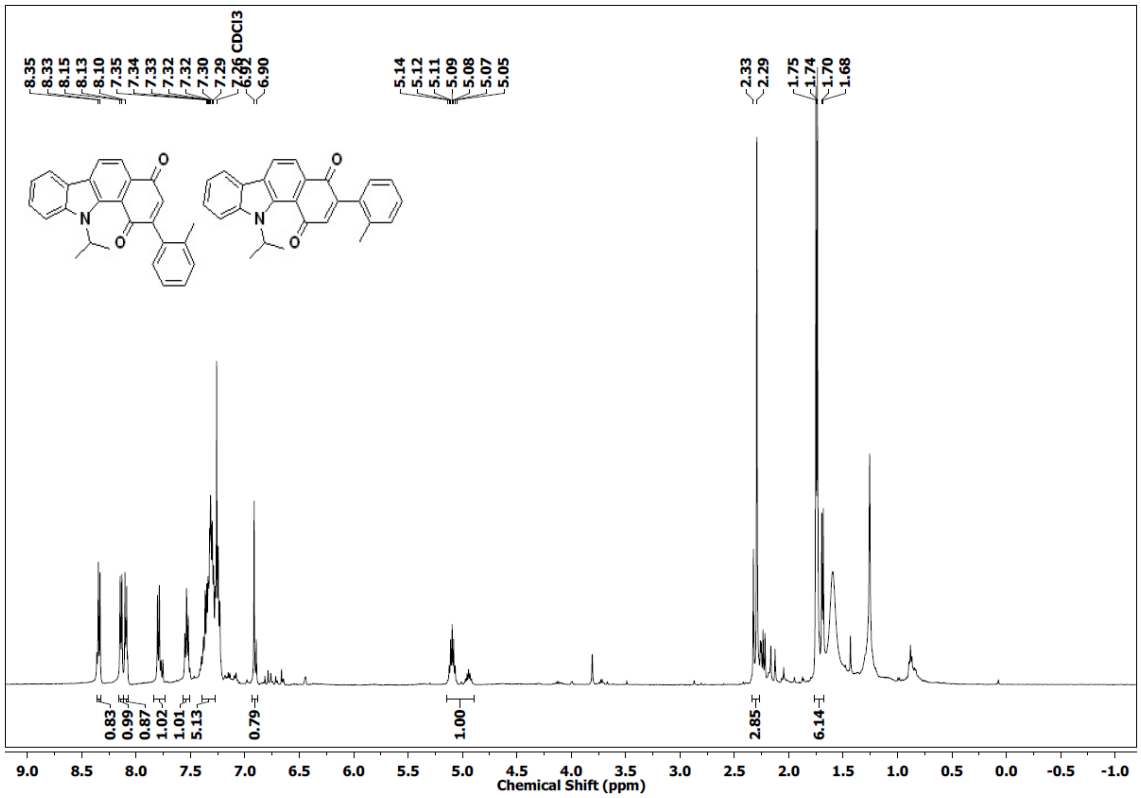

^{13}C NMR of **13, 14**

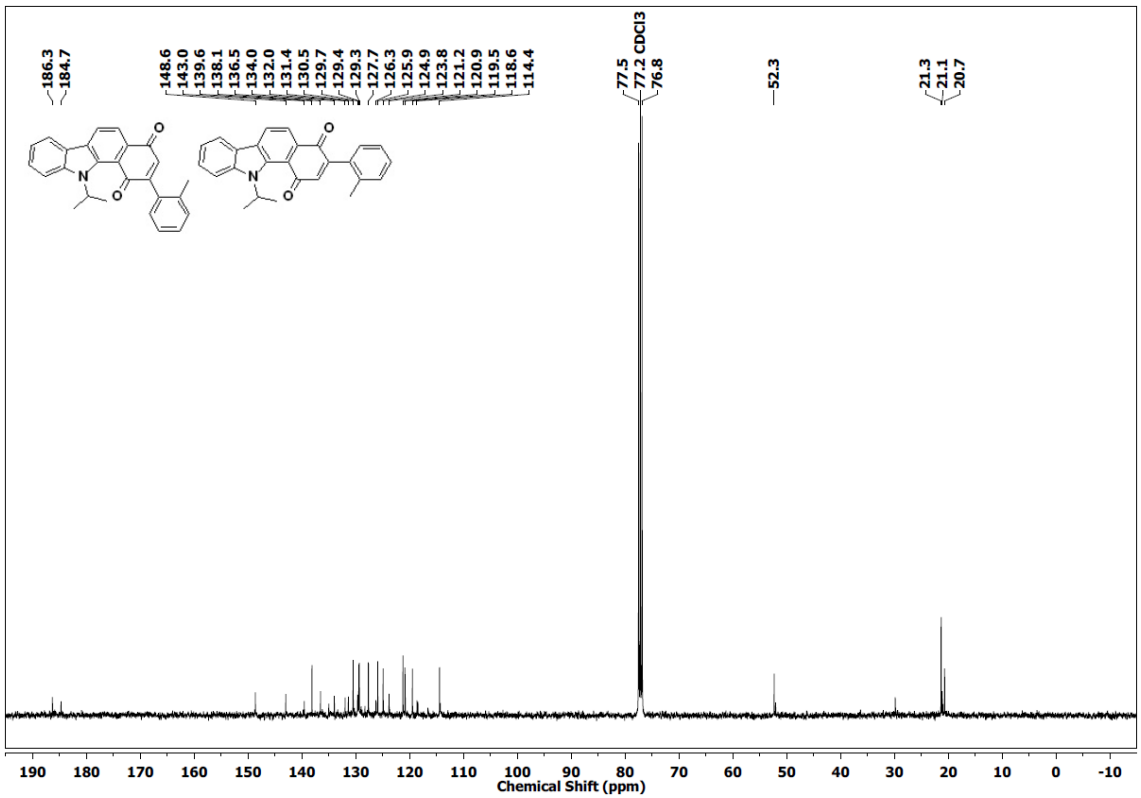

^{1}H NMR of **15, 16**

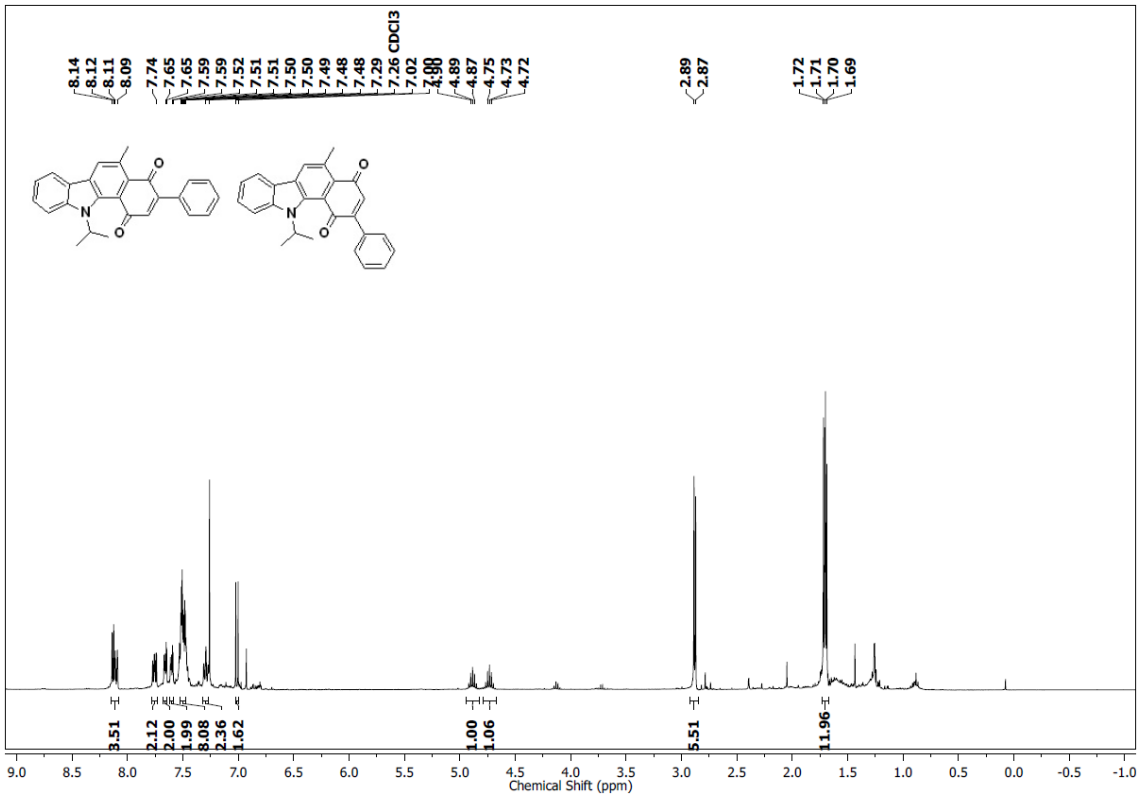

^{13}C NMR of **15, 16**

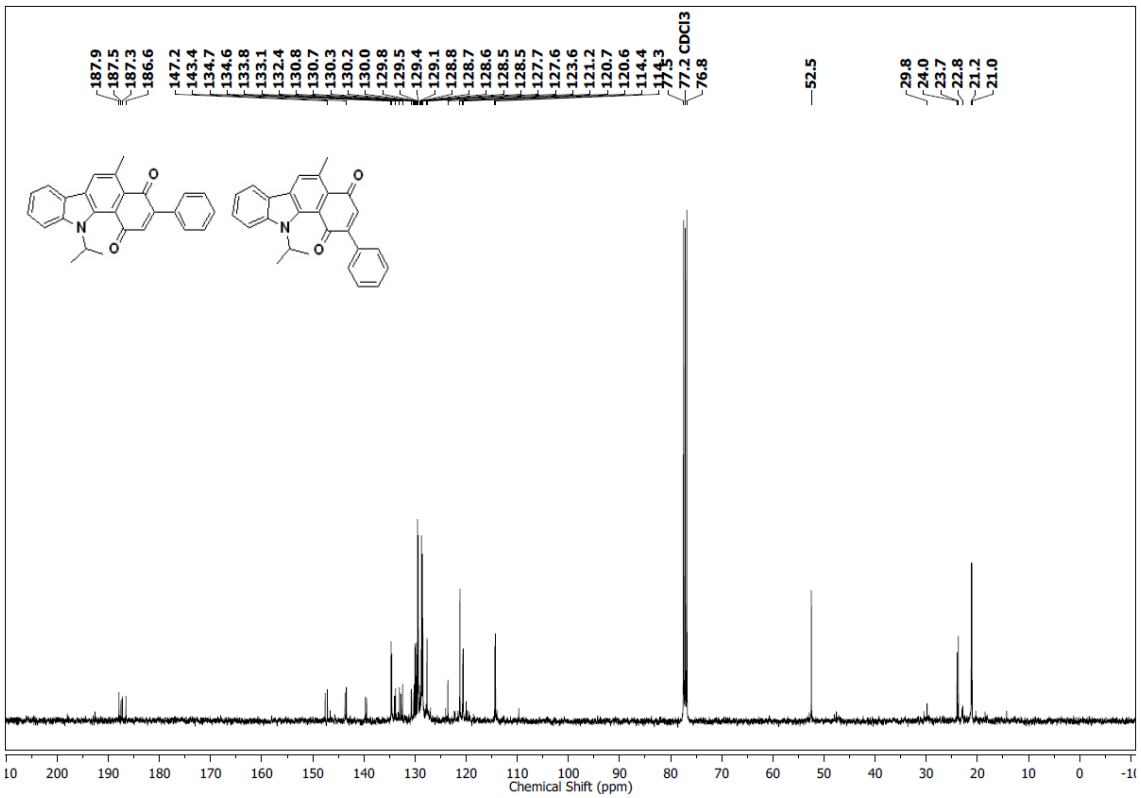

^{1}H NMR of **21, 22**

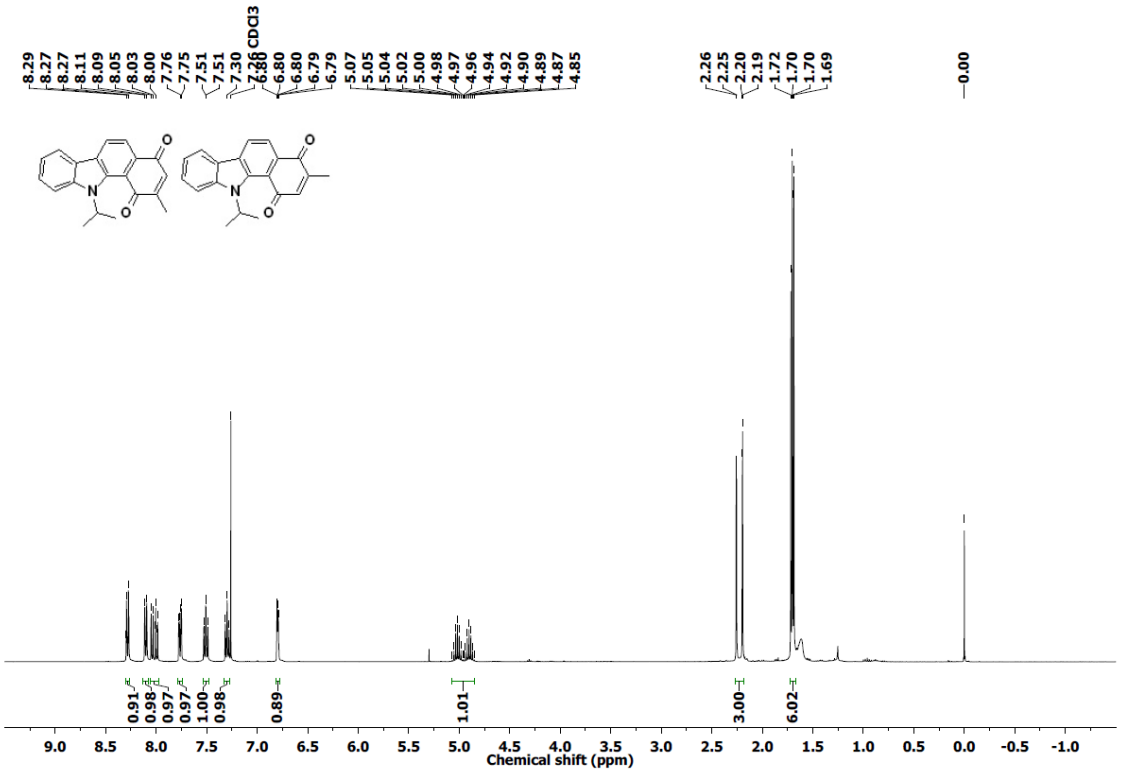

^{13}C NMR of **21, 22**

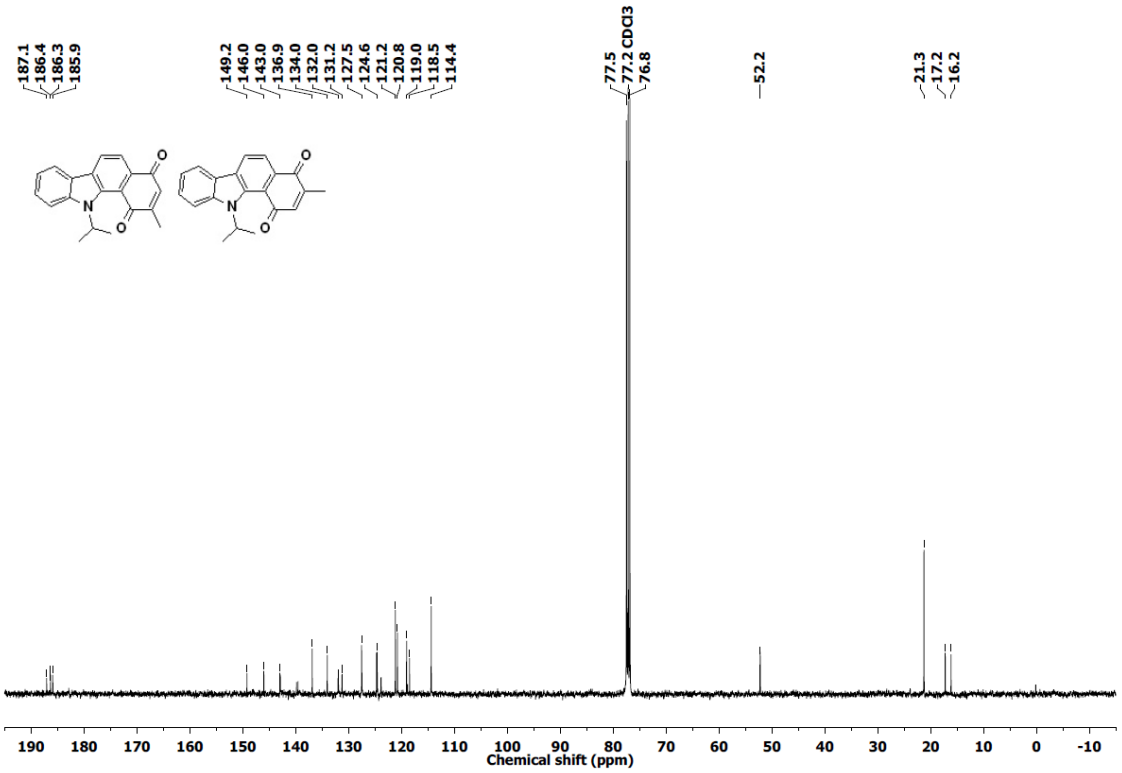

^{1}H NMR of **23, 24**

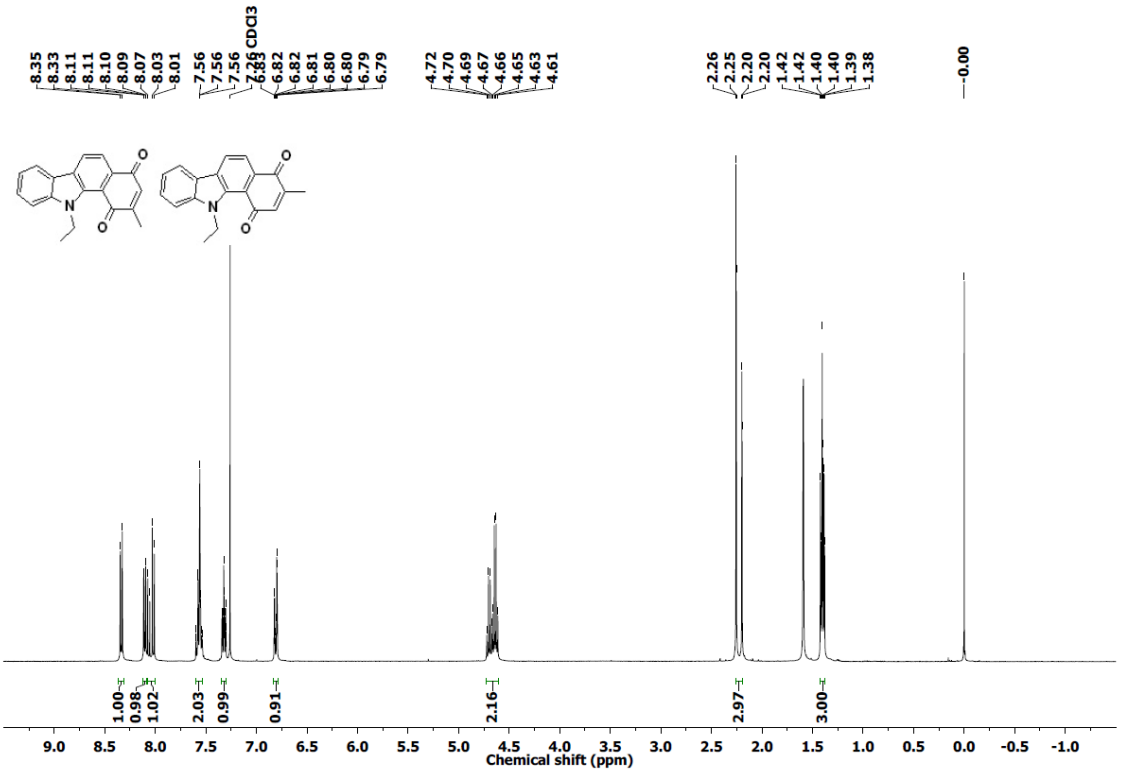

^{13}C NMR of **23, 24**

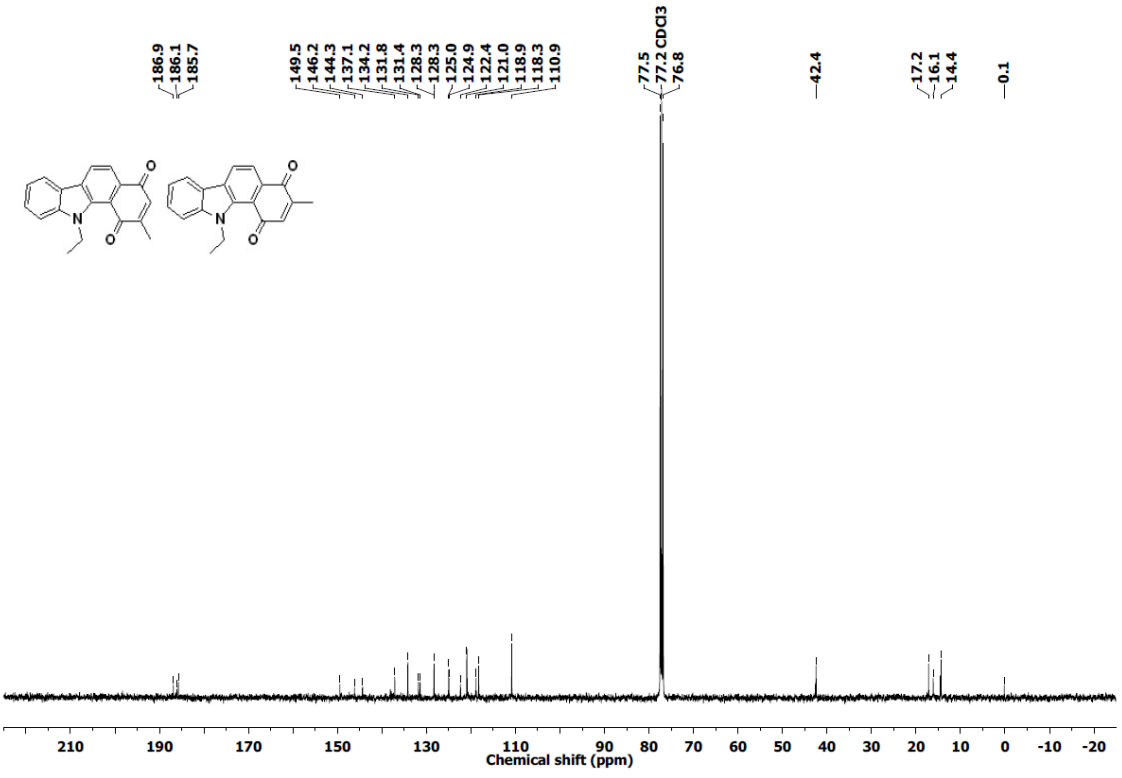

^{1}H NMR of **25**

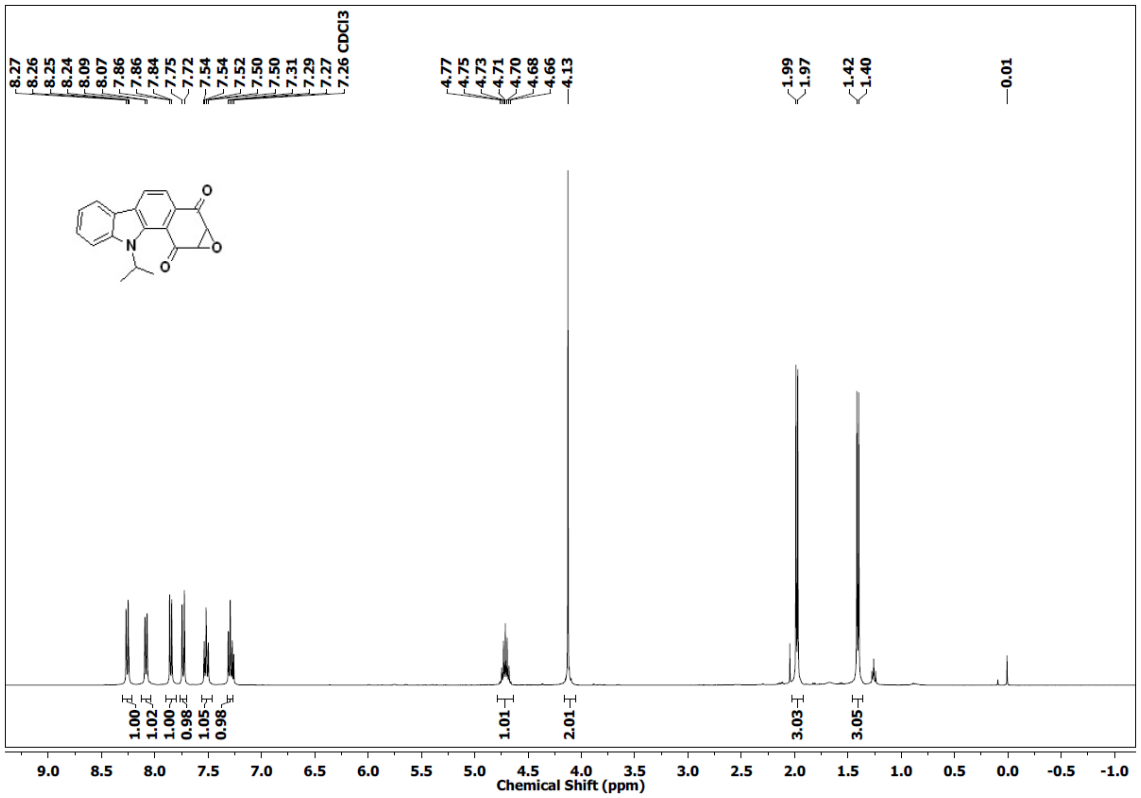

^{13}C NMR of **25**

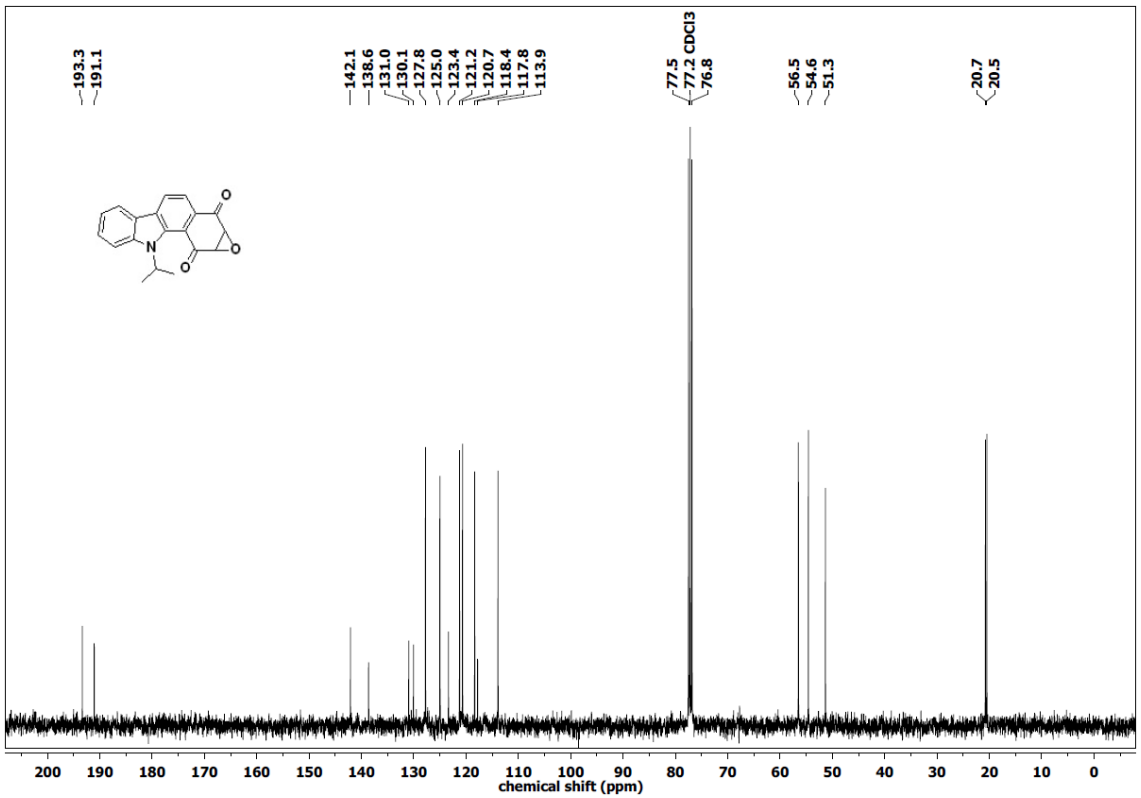

^{1}H NMR of **26**

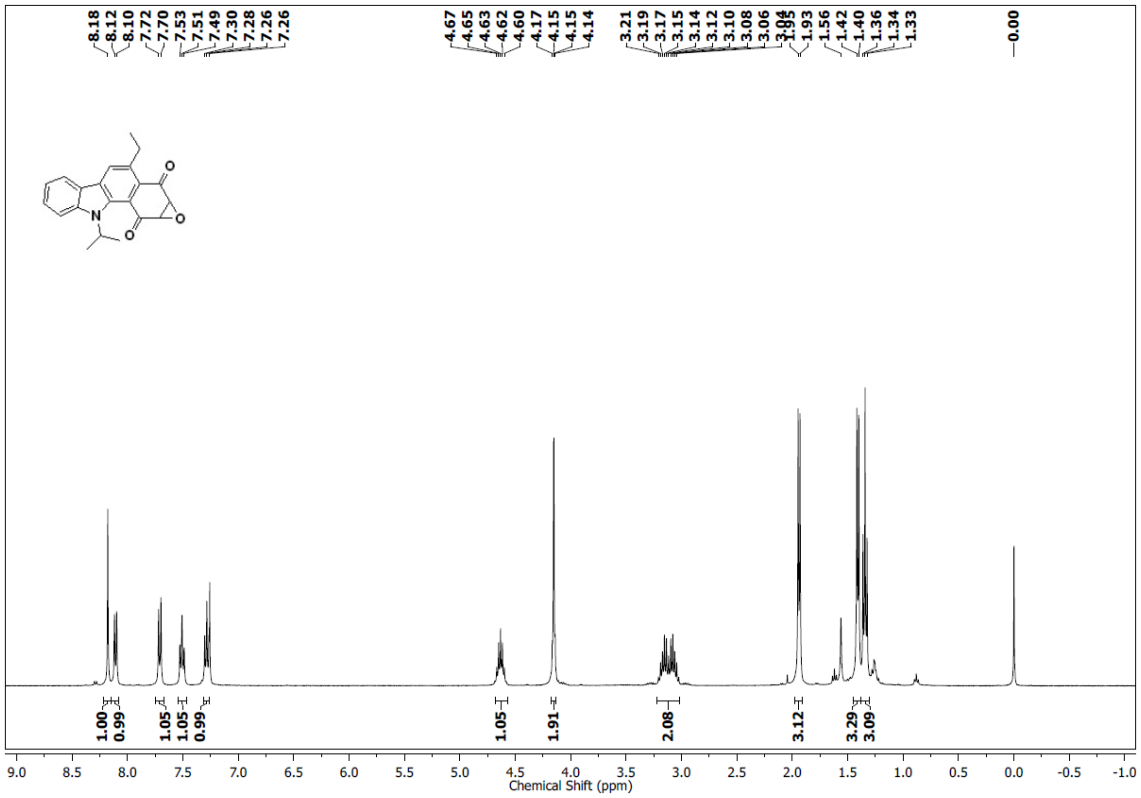

^{13}C NMR of **26**

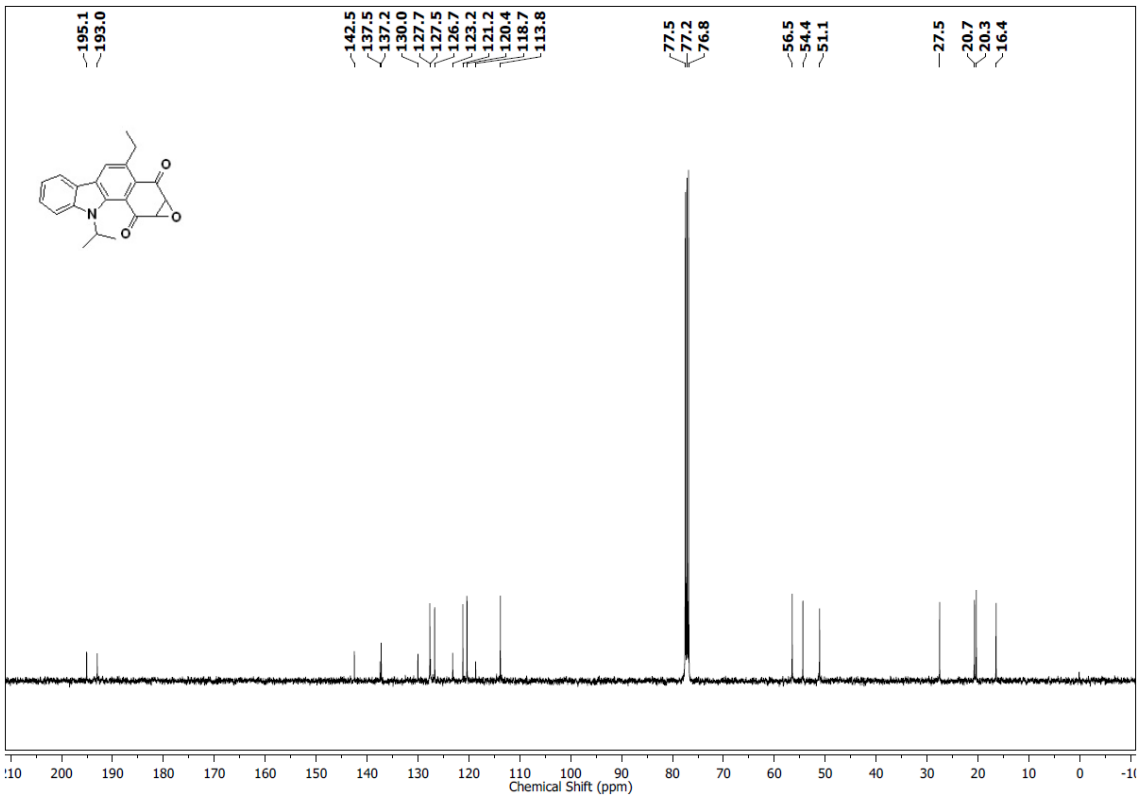

^{1}H NMR of **27**

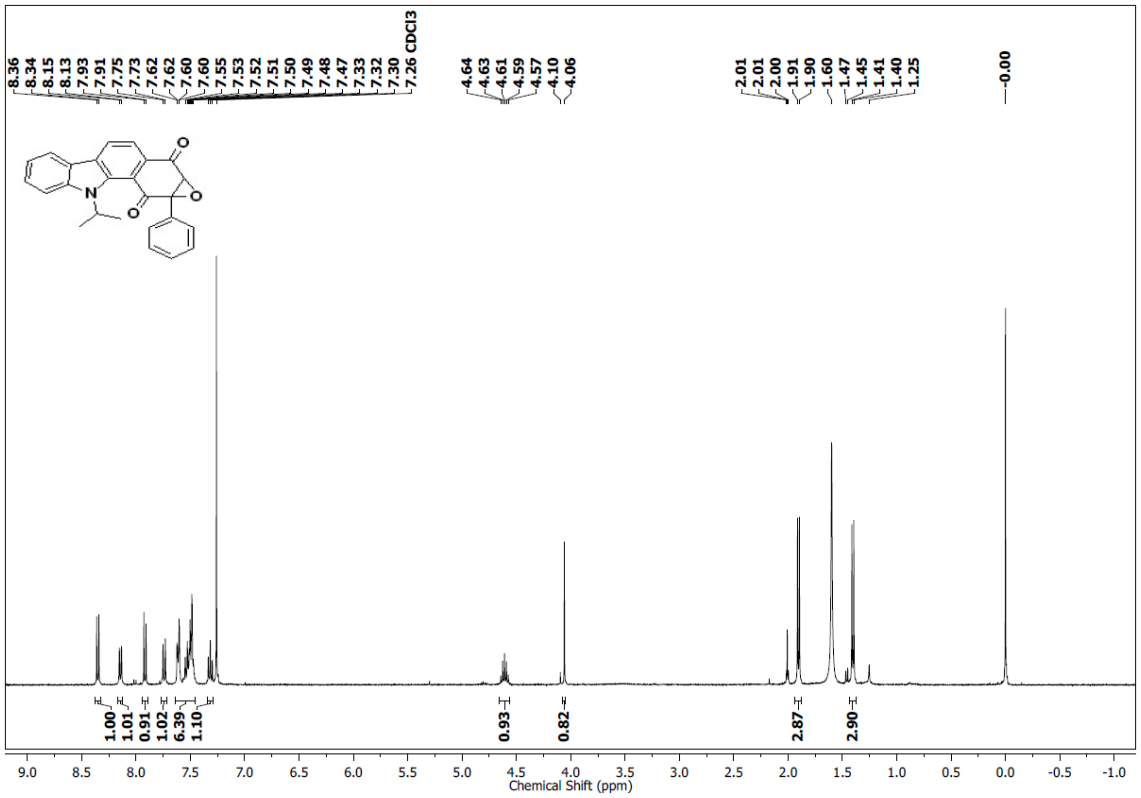

^{13}C NMR of **27**

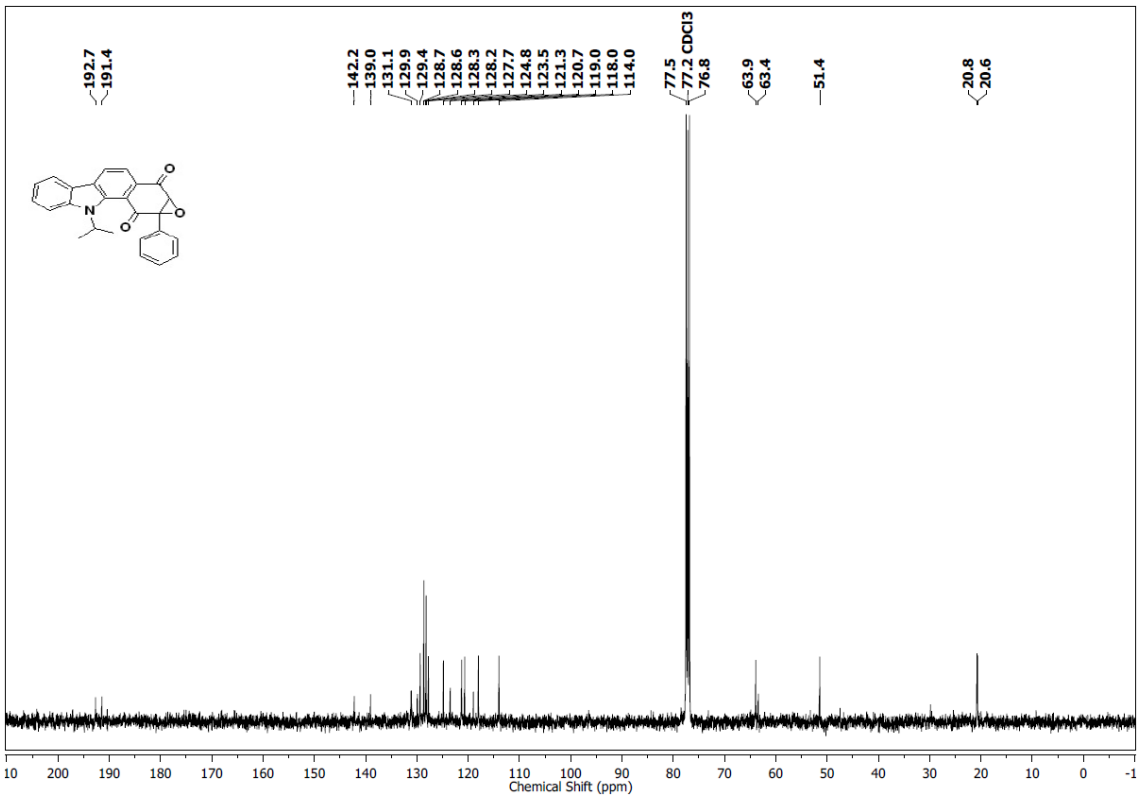

2D ^{1}H-^{1}H NOESY NMR of **27**

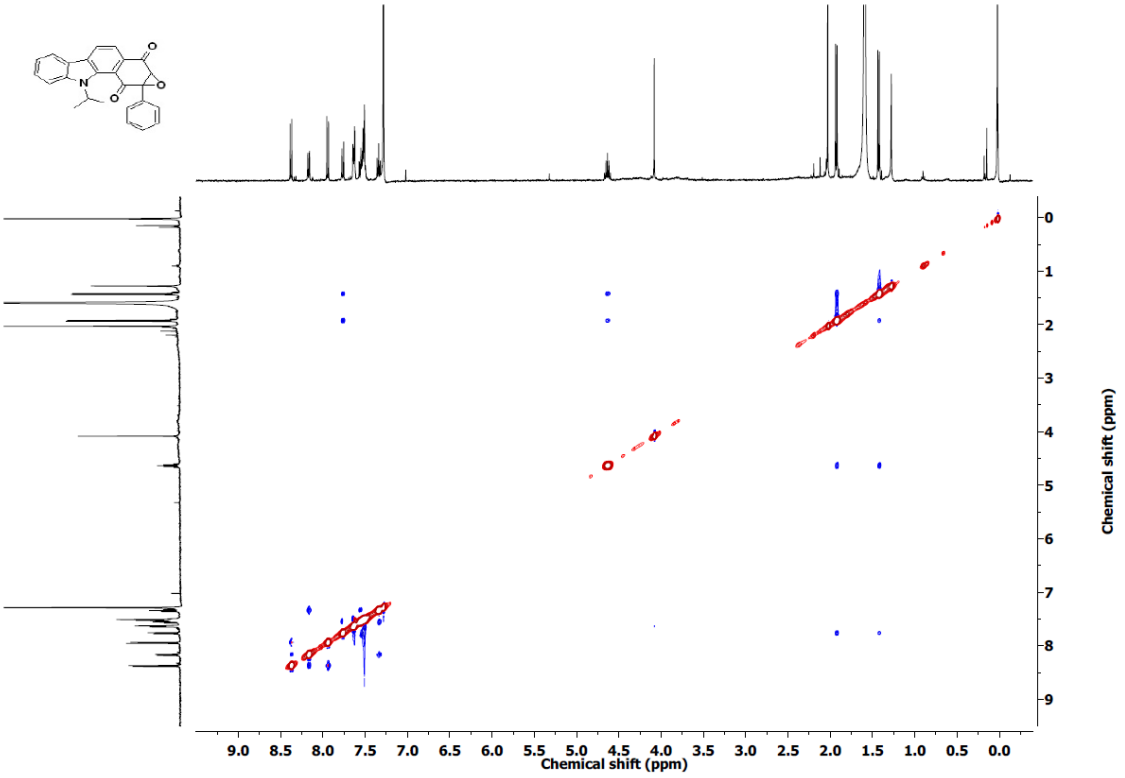

2D ^{1}H-^{13}C HSQC NMR of **27**

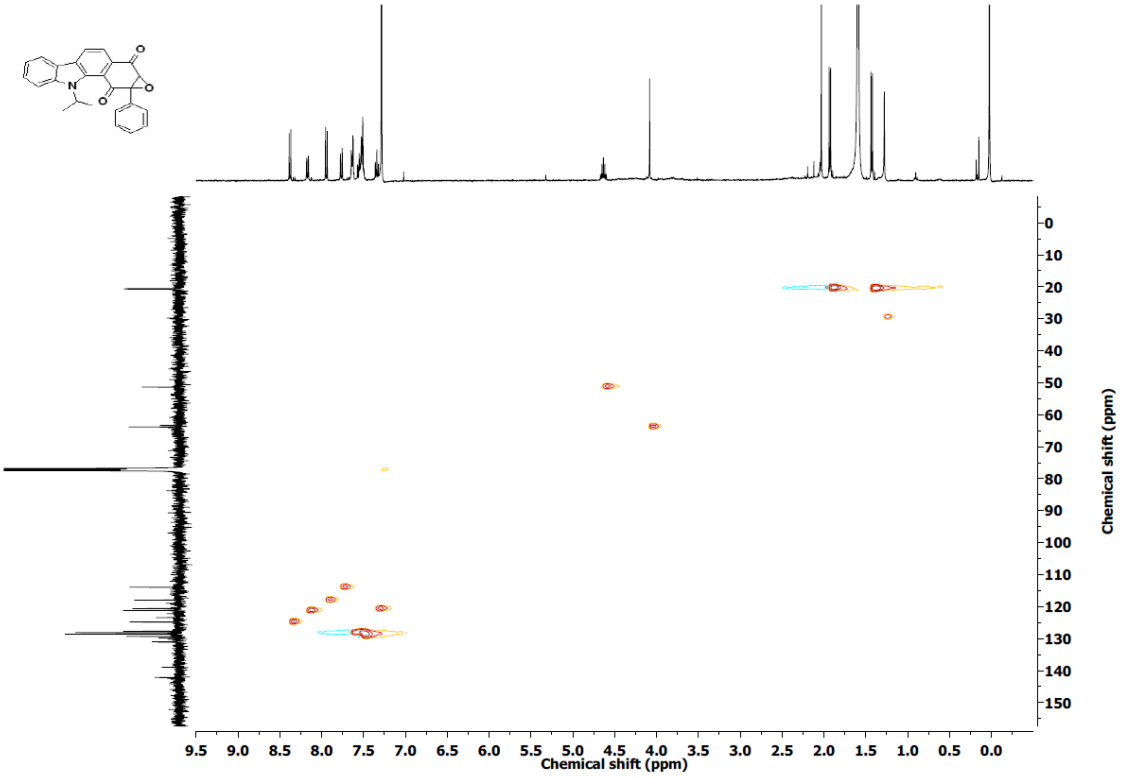

^{1}H NMR of **28**

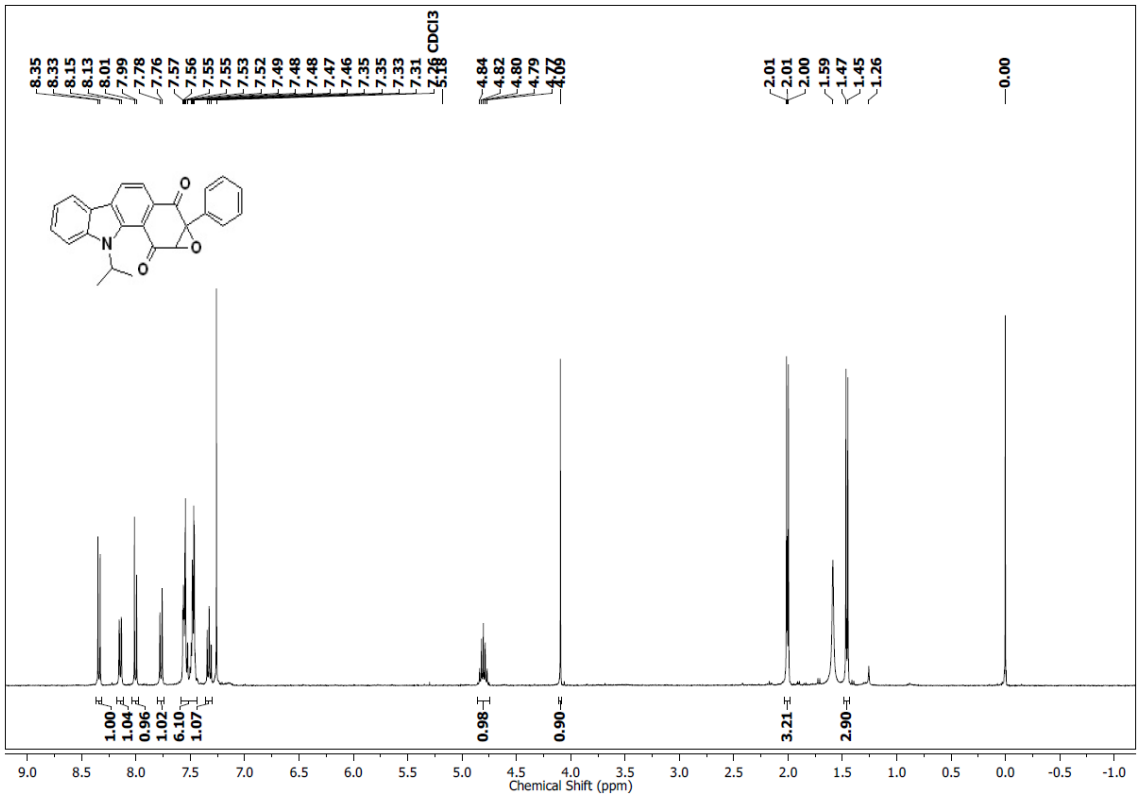

^{13}C NMR of **28**

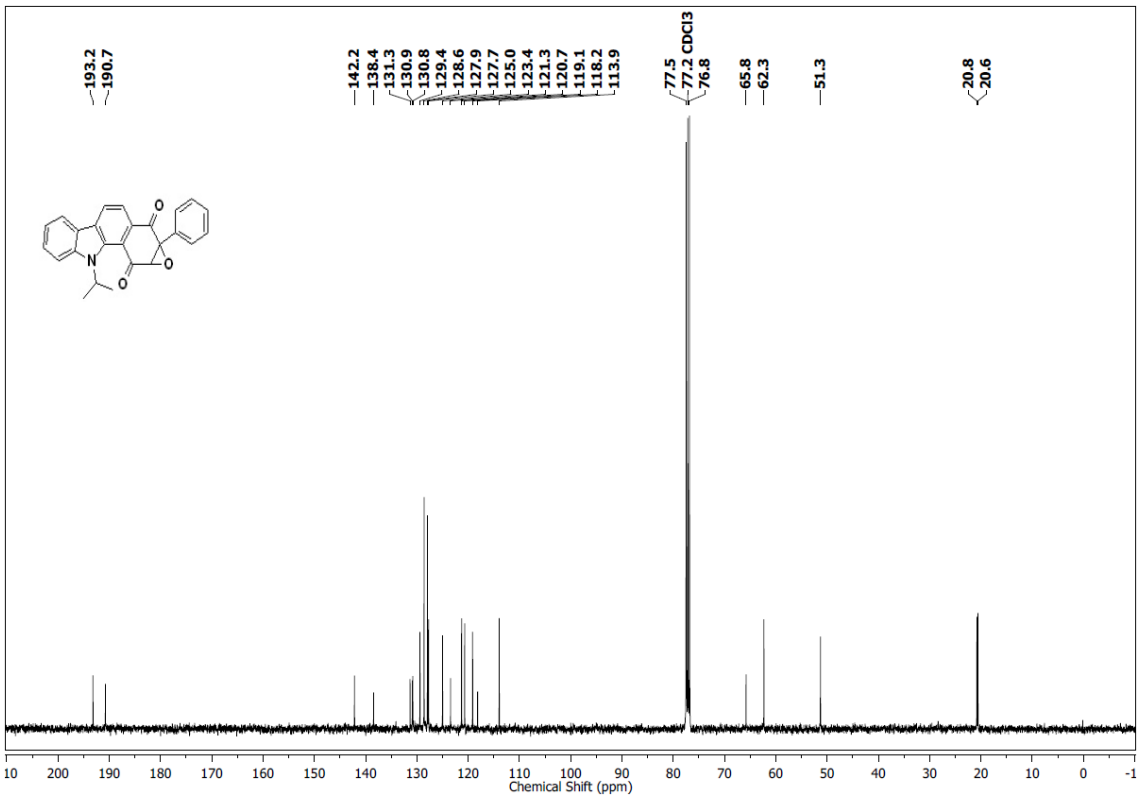

2D ^{1}H-^{1}H NOESY NMR of **28**

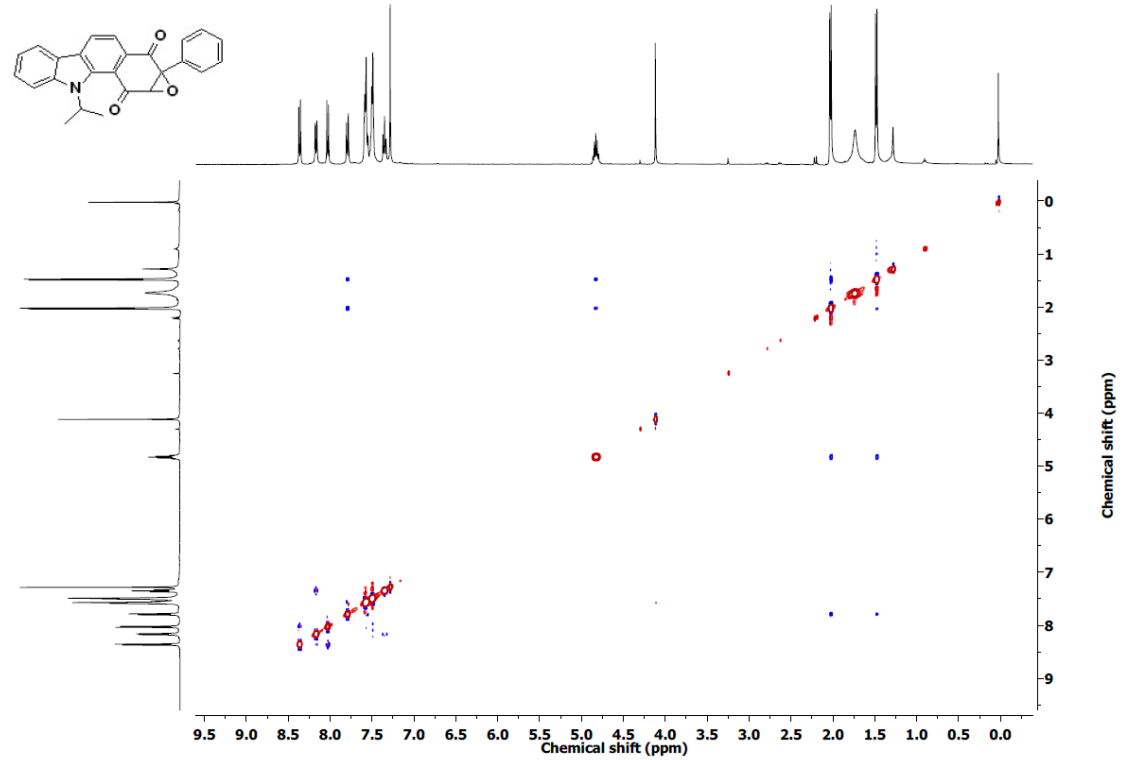

2D ^{1}H-^{13}C HSQC NMR of **28**

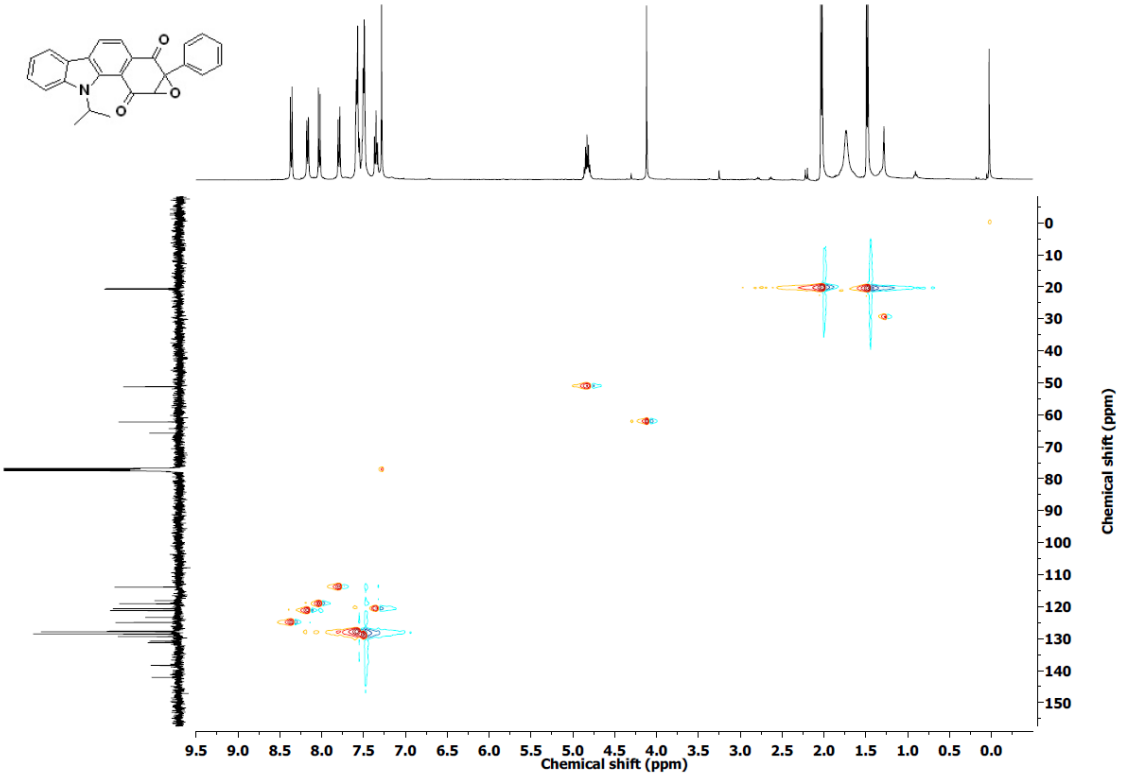

^{1}H NMR of **29**

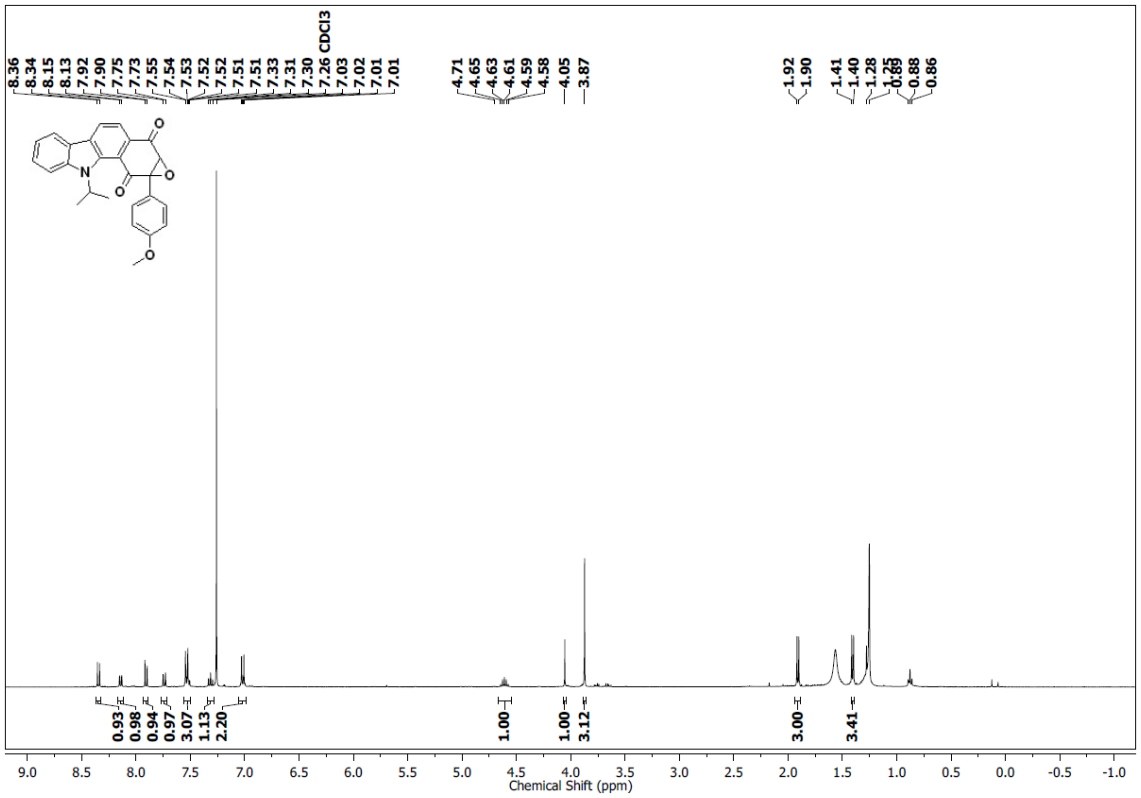

^{13}C NMR of **29**

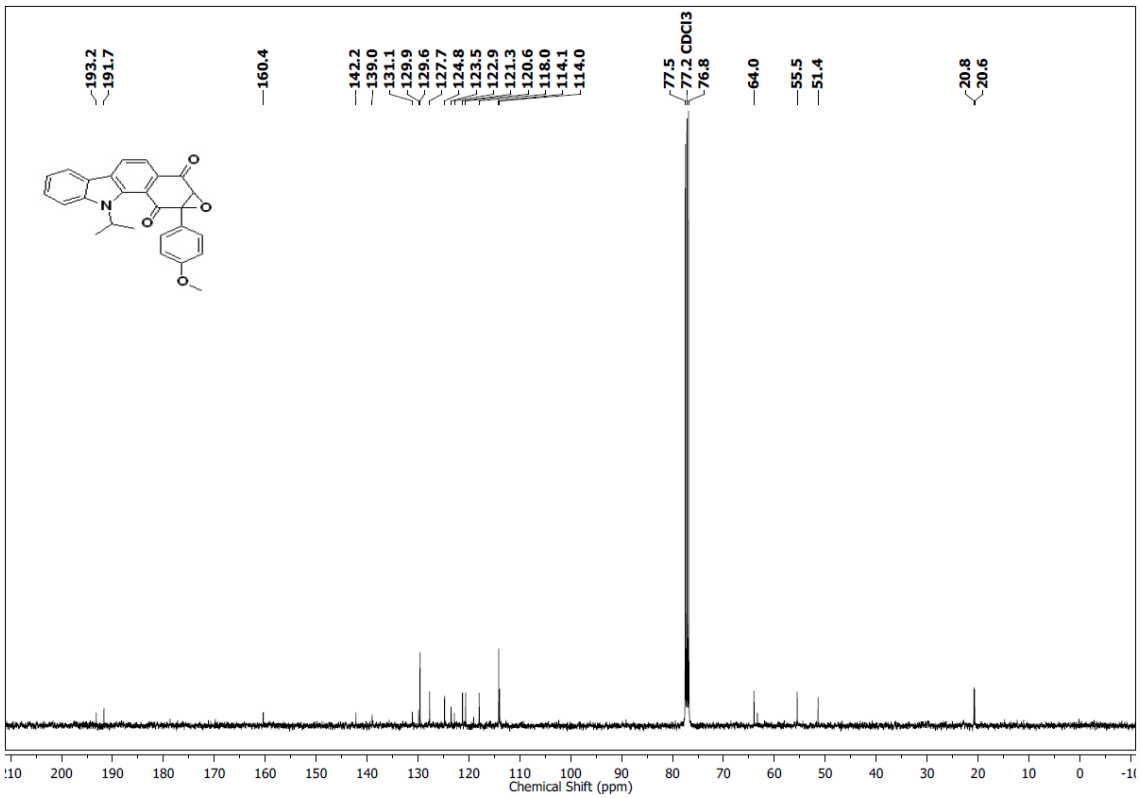

2D ^{1}H-^{1}H NOESY NMR of **29**

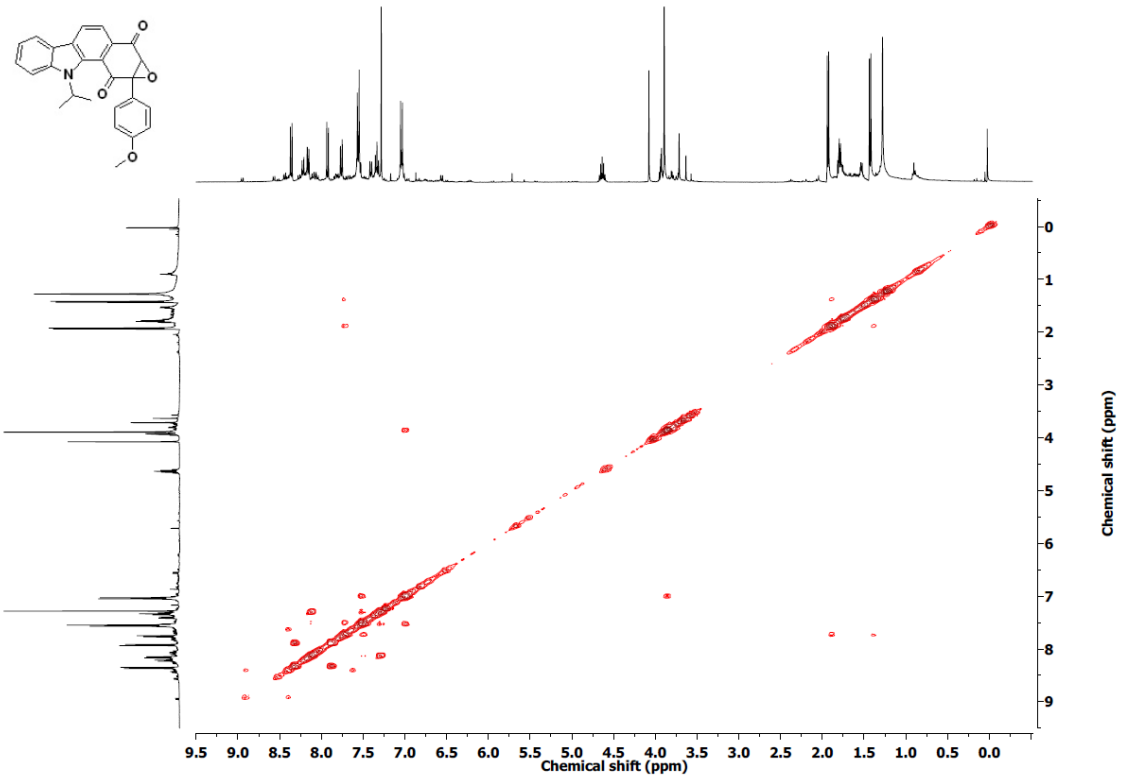

2D ^{1}H-^{13}C HSQC NMR of **29**

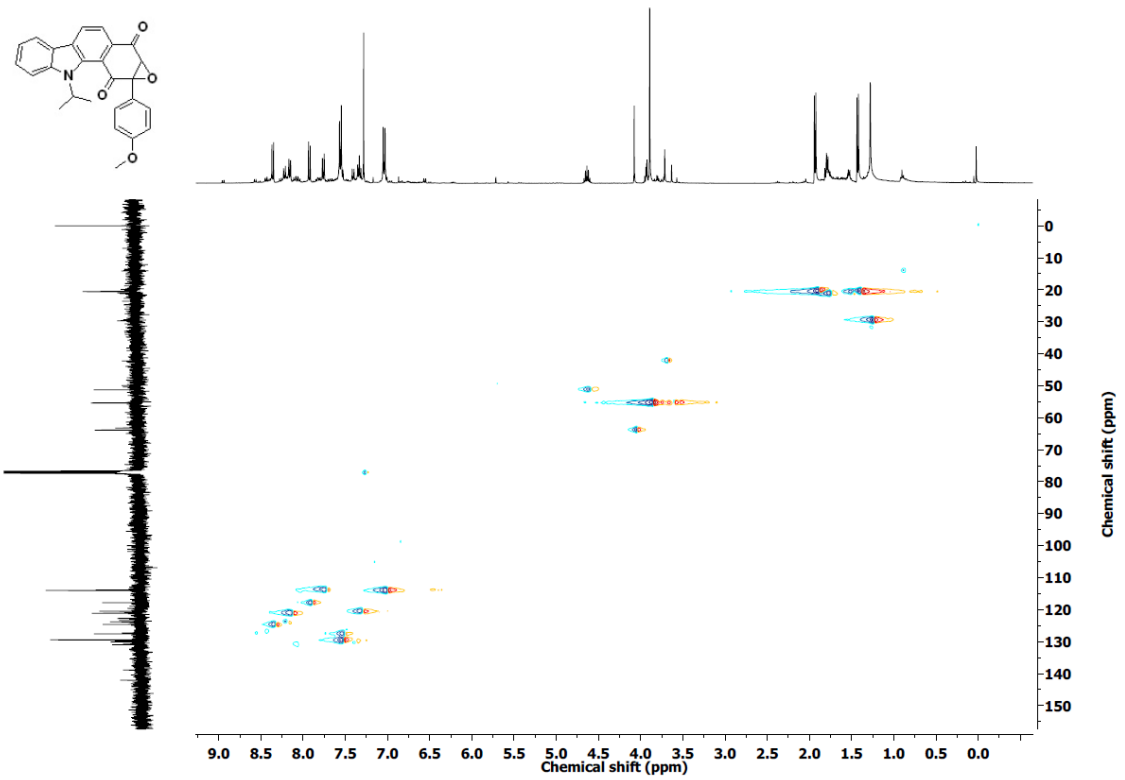

^{1}H NMR of **30**

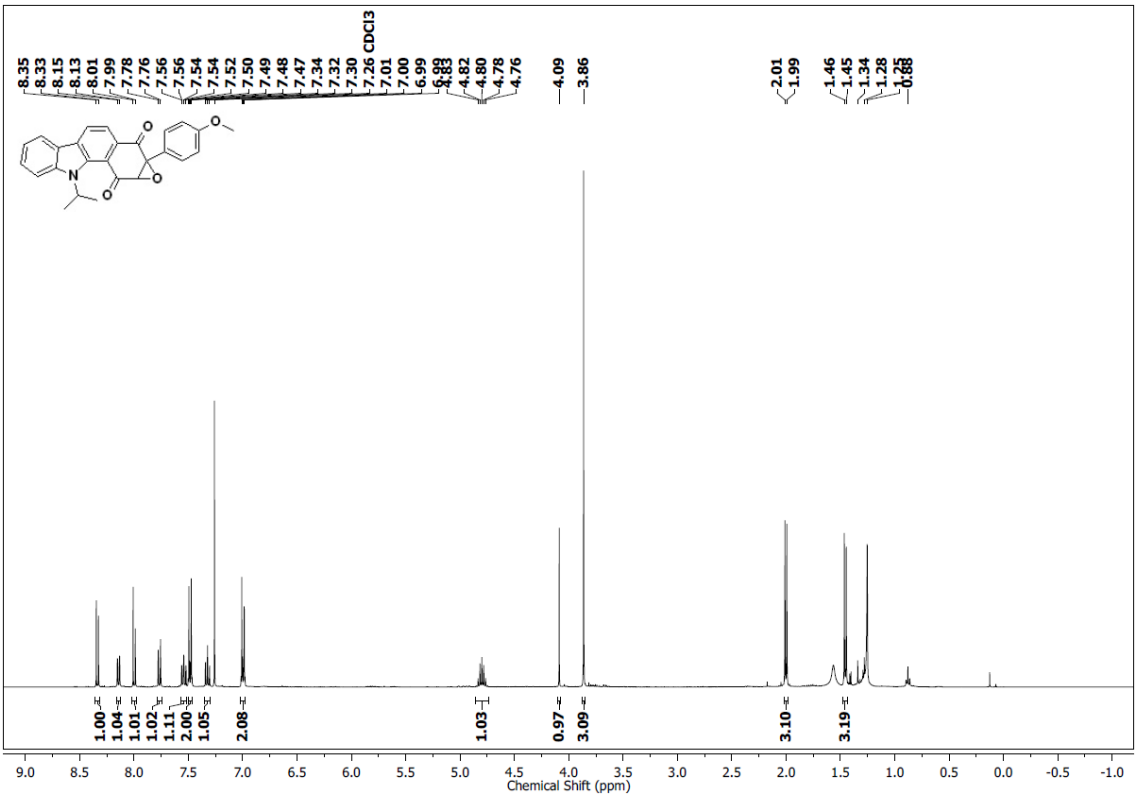

^{13}C NMR of **30**

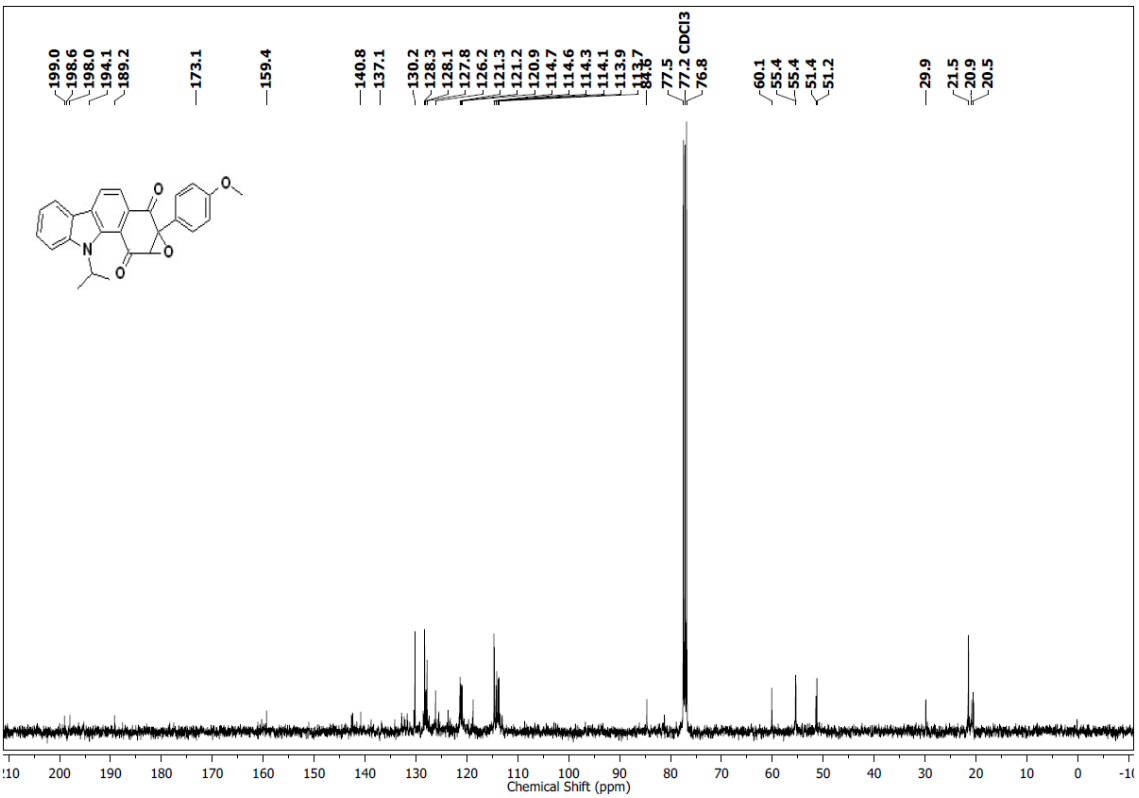

2D ^{1}H-^{1}H NOESY NMR of **30**

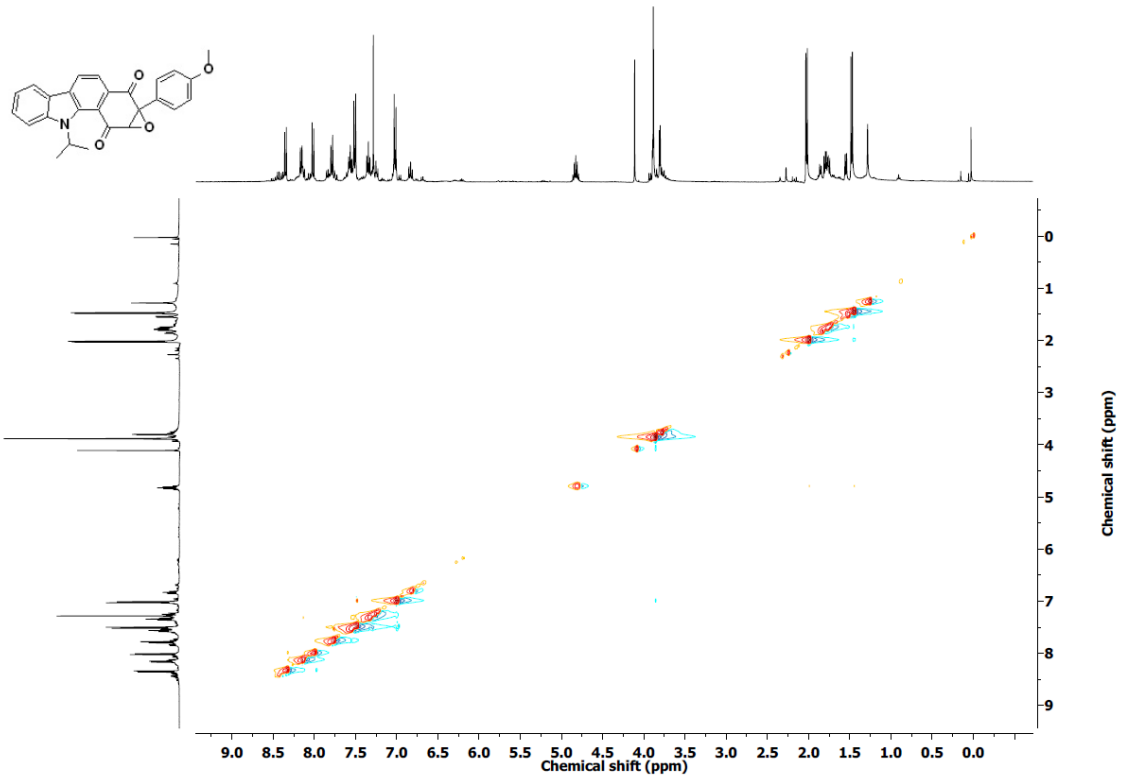

2D ^{1}H-^{13}C HSQC NMR of **30**

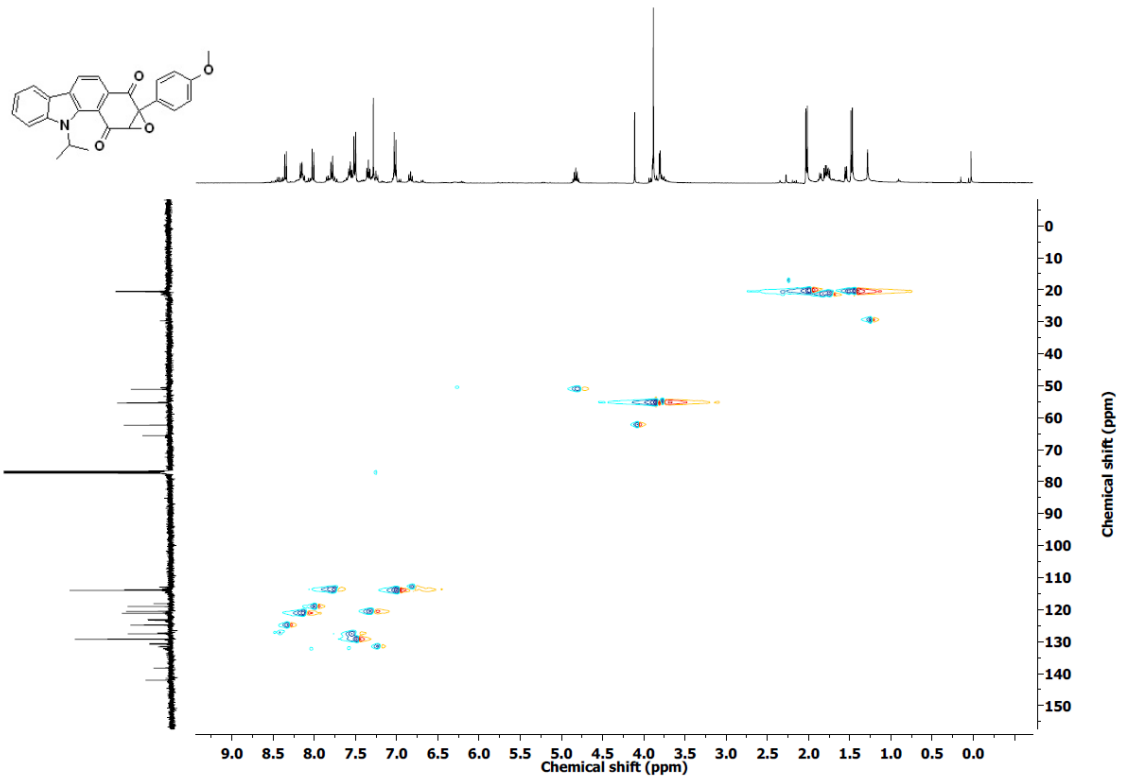

^{1}H NMR of **31**

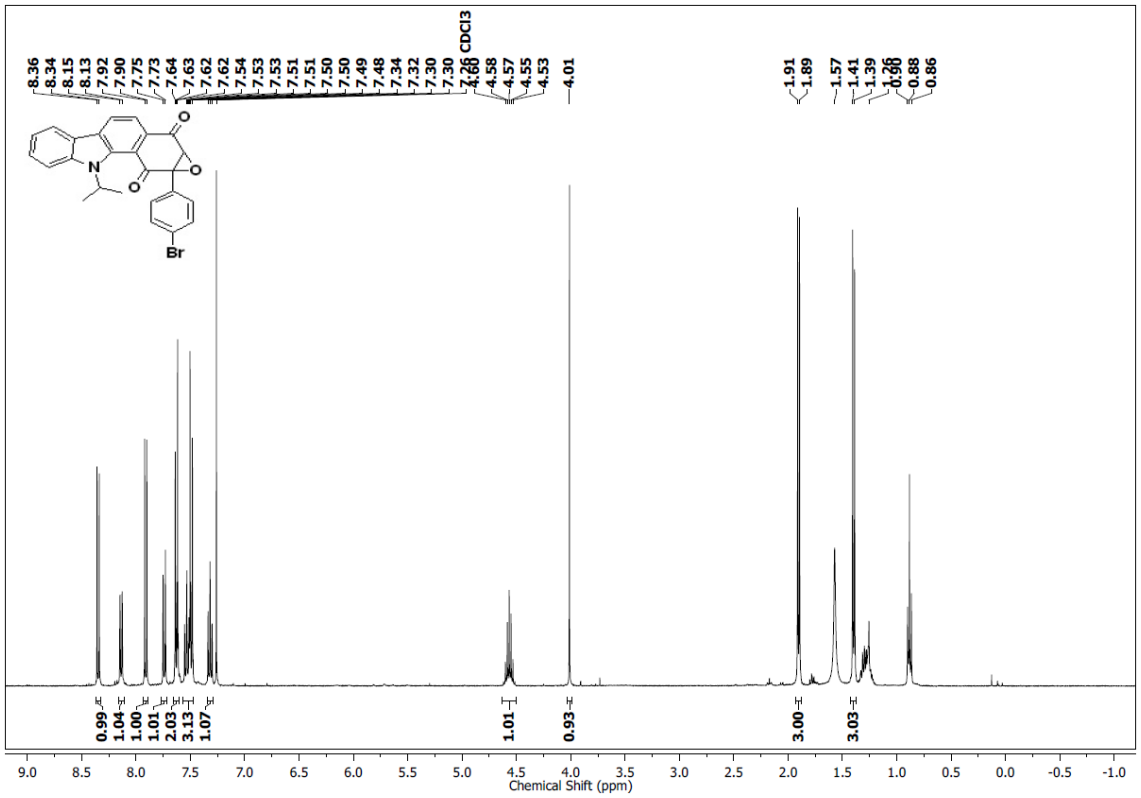

^{13}C NMR of **31**

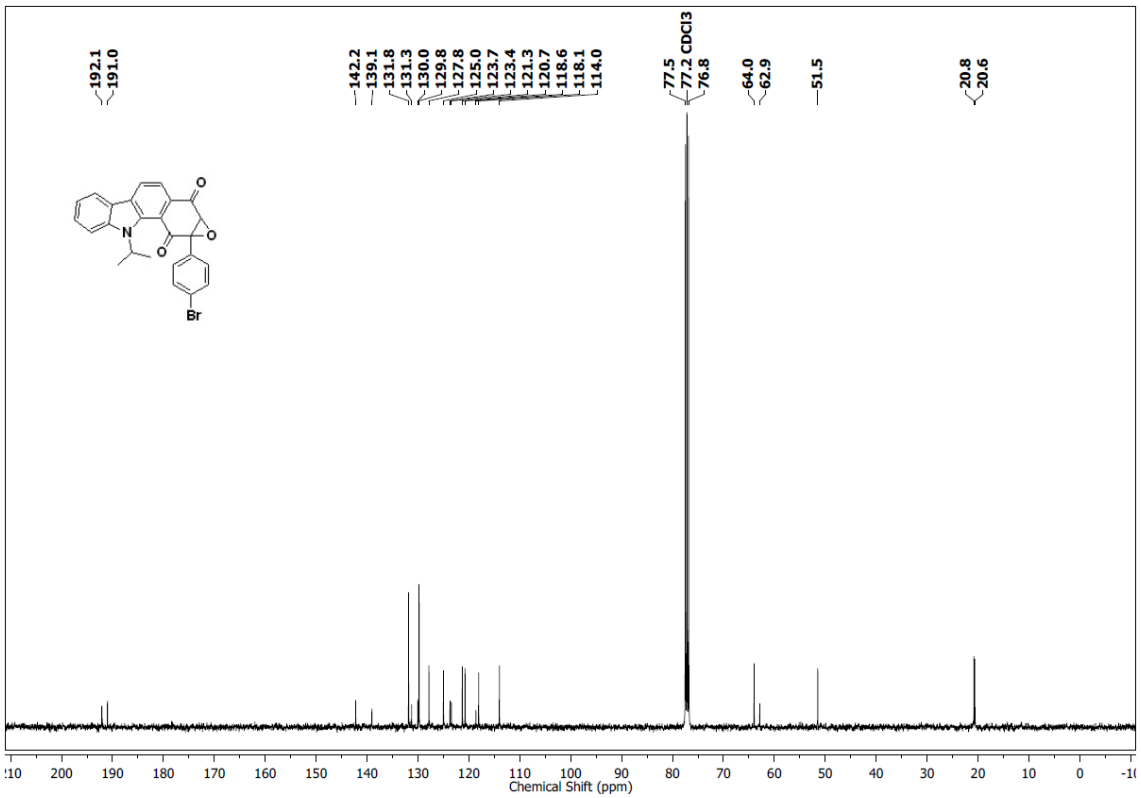

^{1}H NMR of **32**

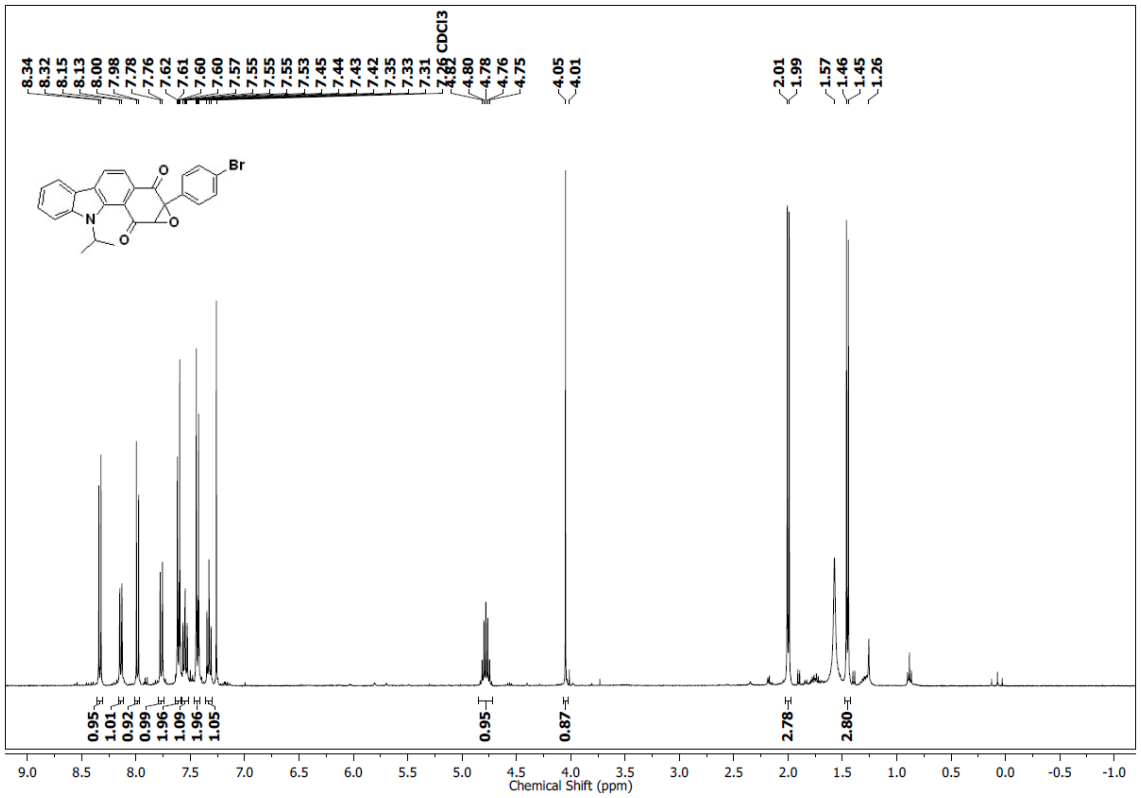

^{13}C NMR of **32**

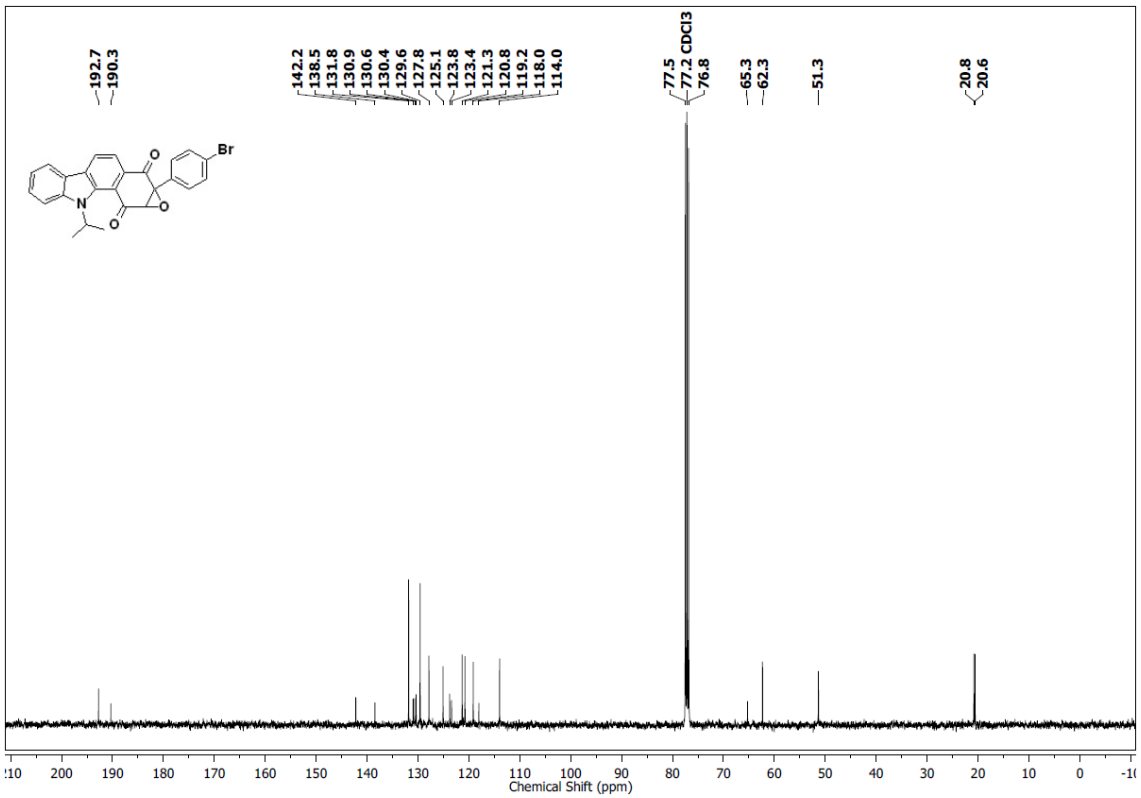

^{1}H NMR of **33**

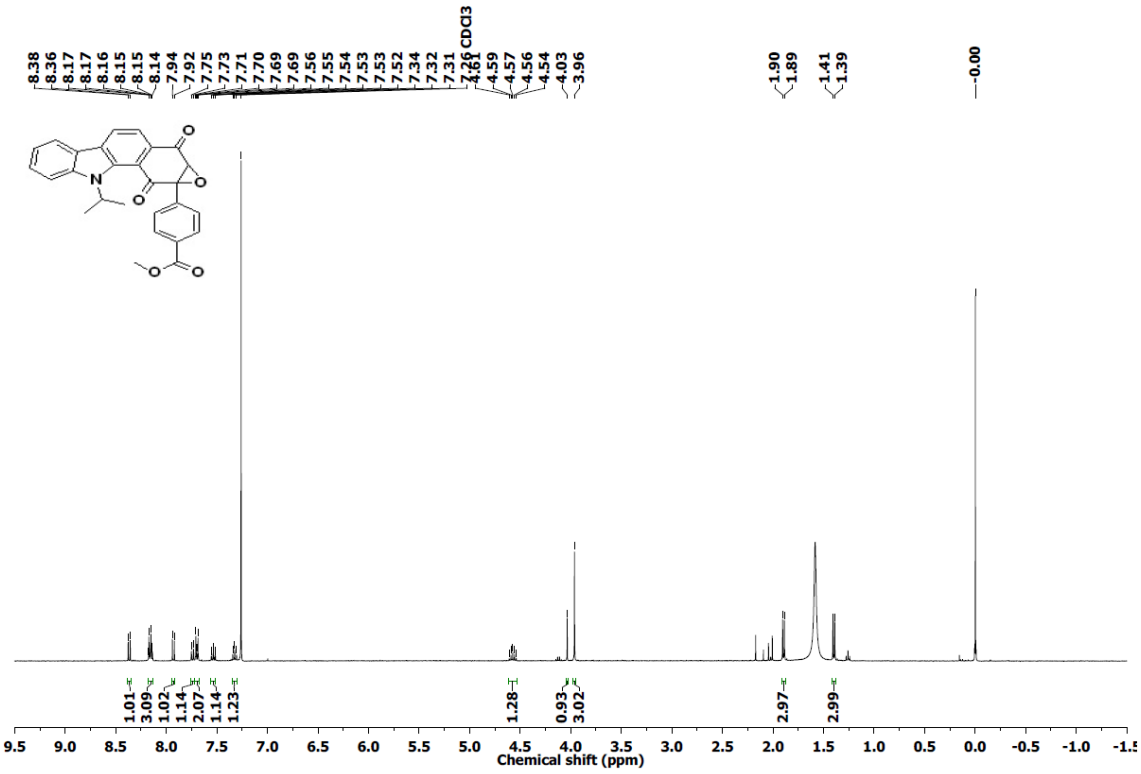

^{13}C NMR of **33**

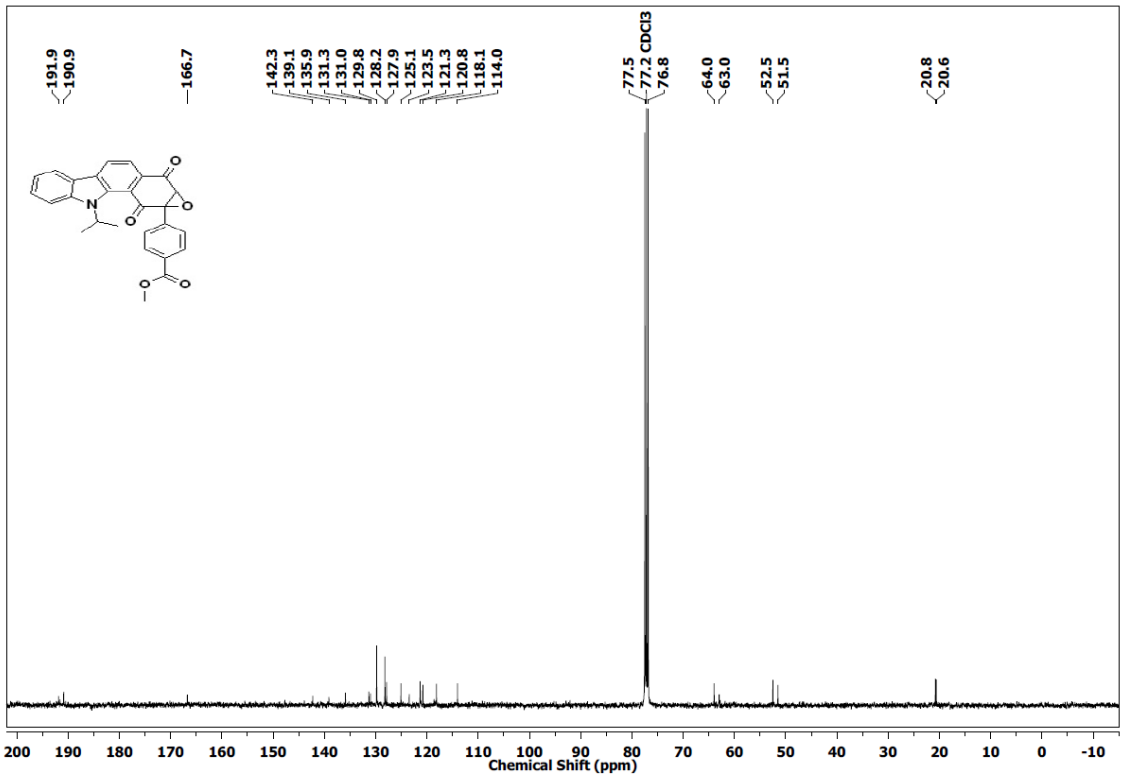

^{1}H NMR of **34**

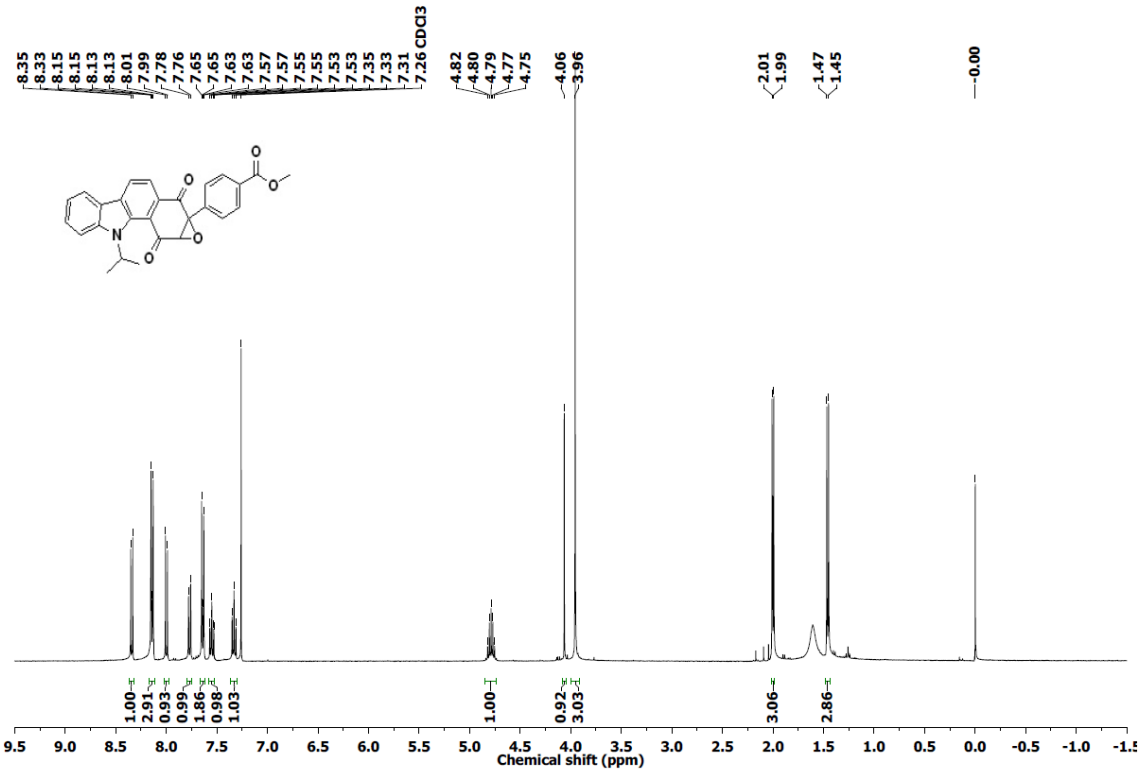

^{13}C NMR of **34**

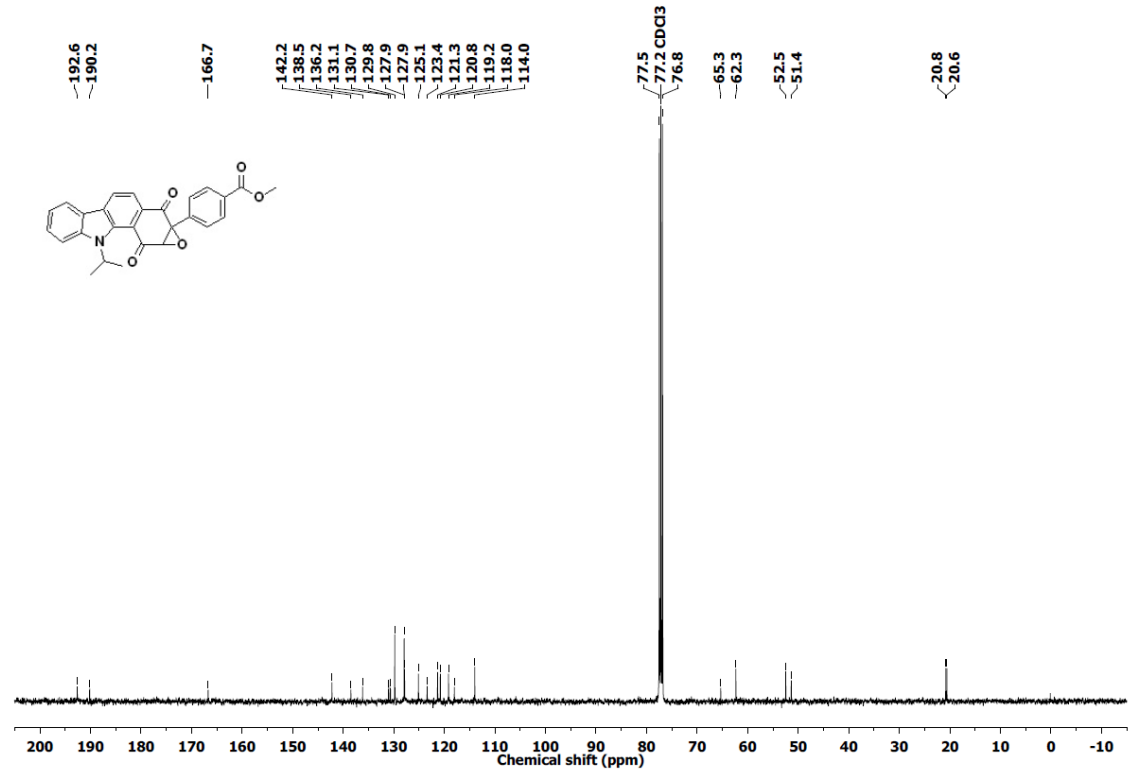

^{1}H NMR of **35, 36**

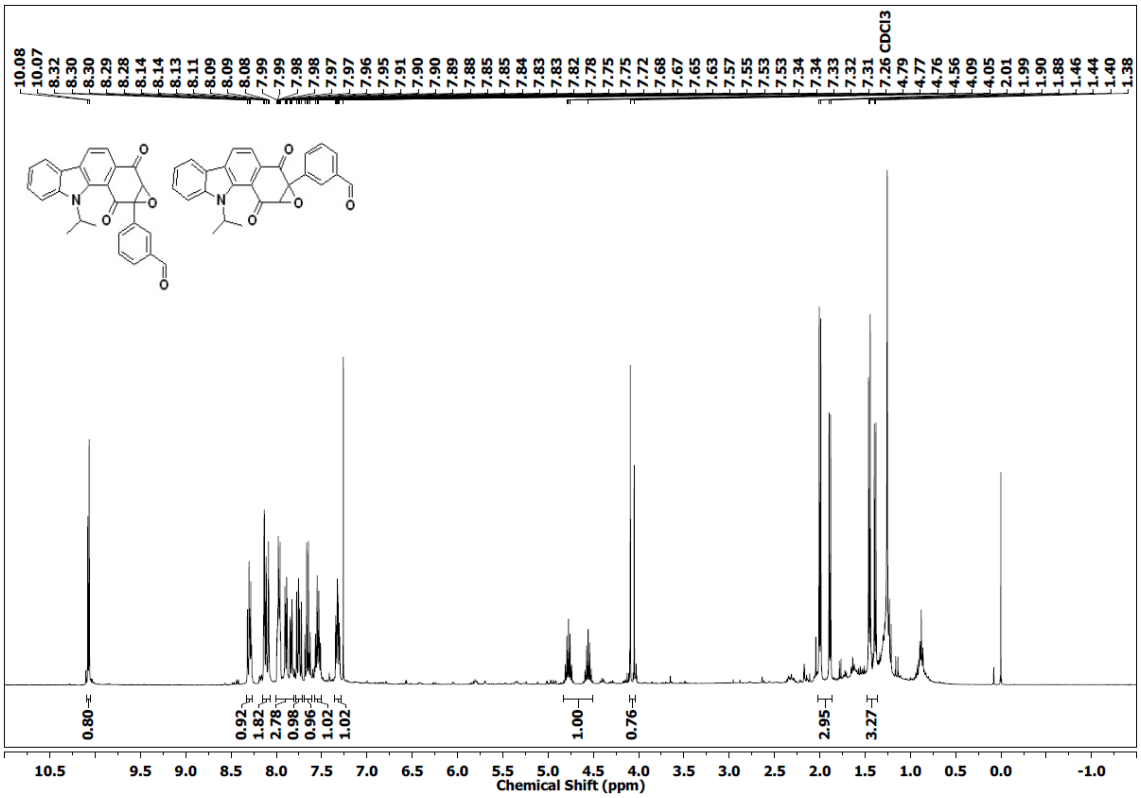

^{13}C NMR of **35, 36**

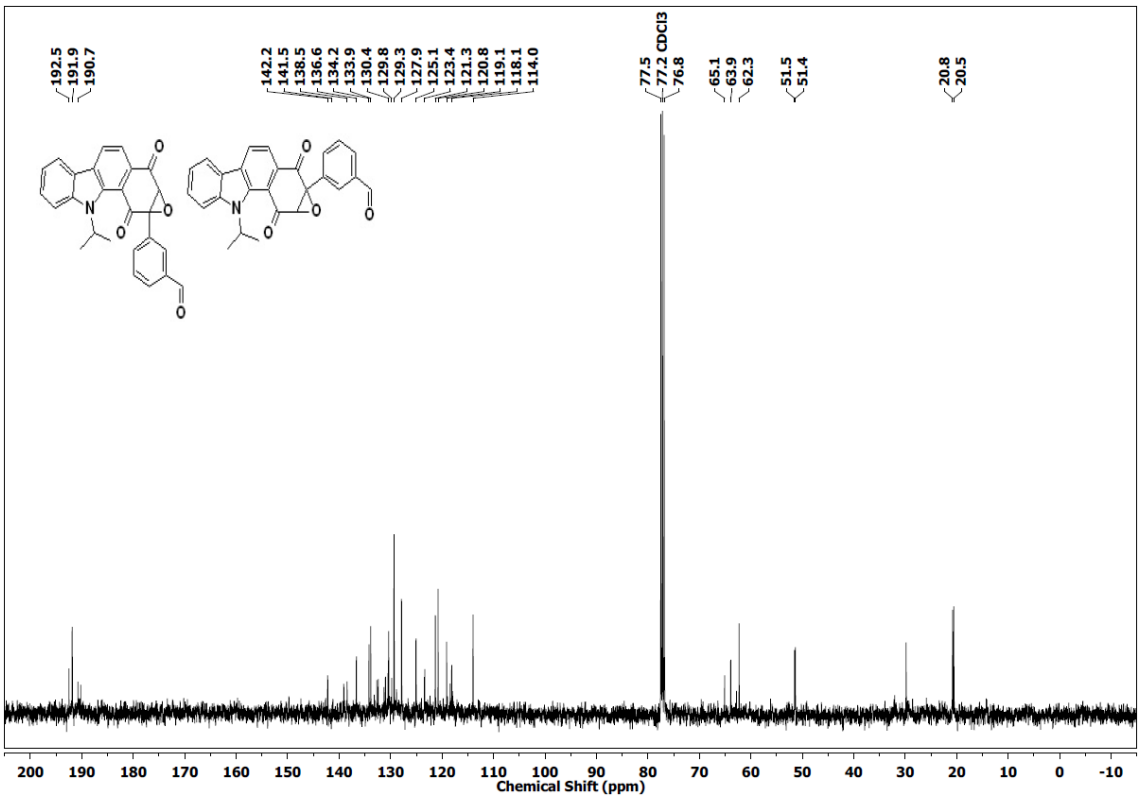

^{1}H NMR of **37, 38**

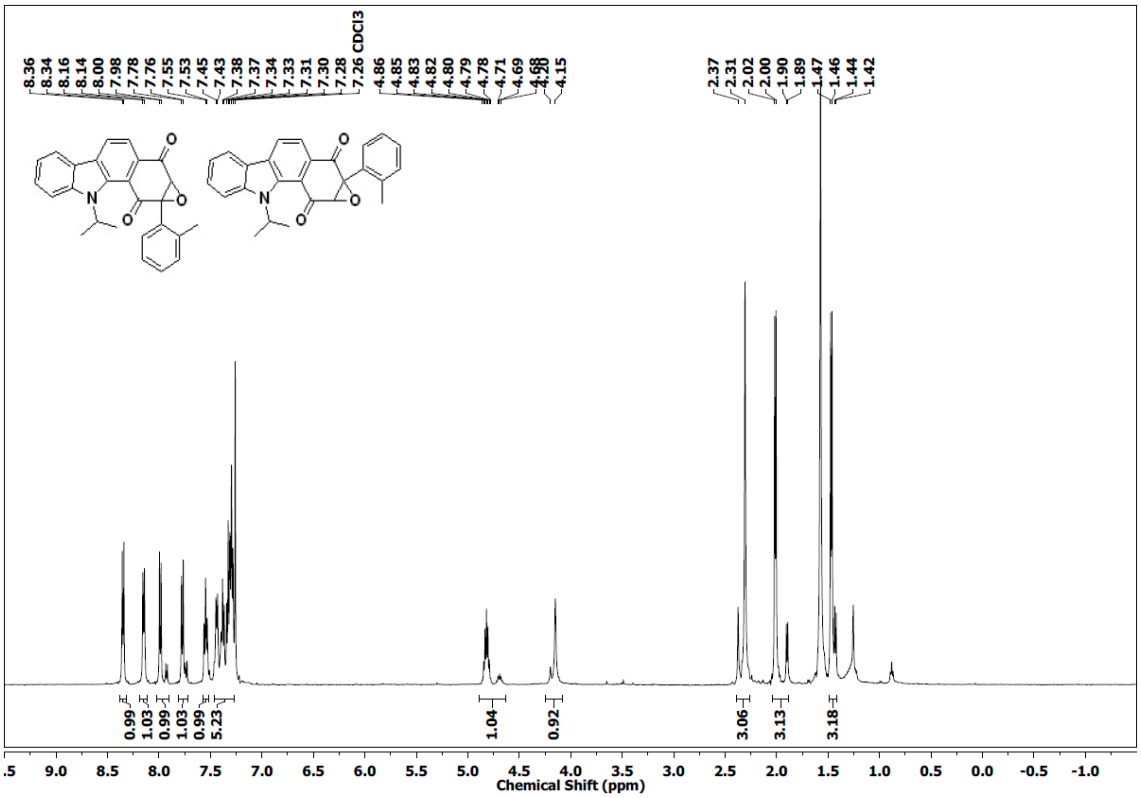

^{13}C NMR of **37, 38**

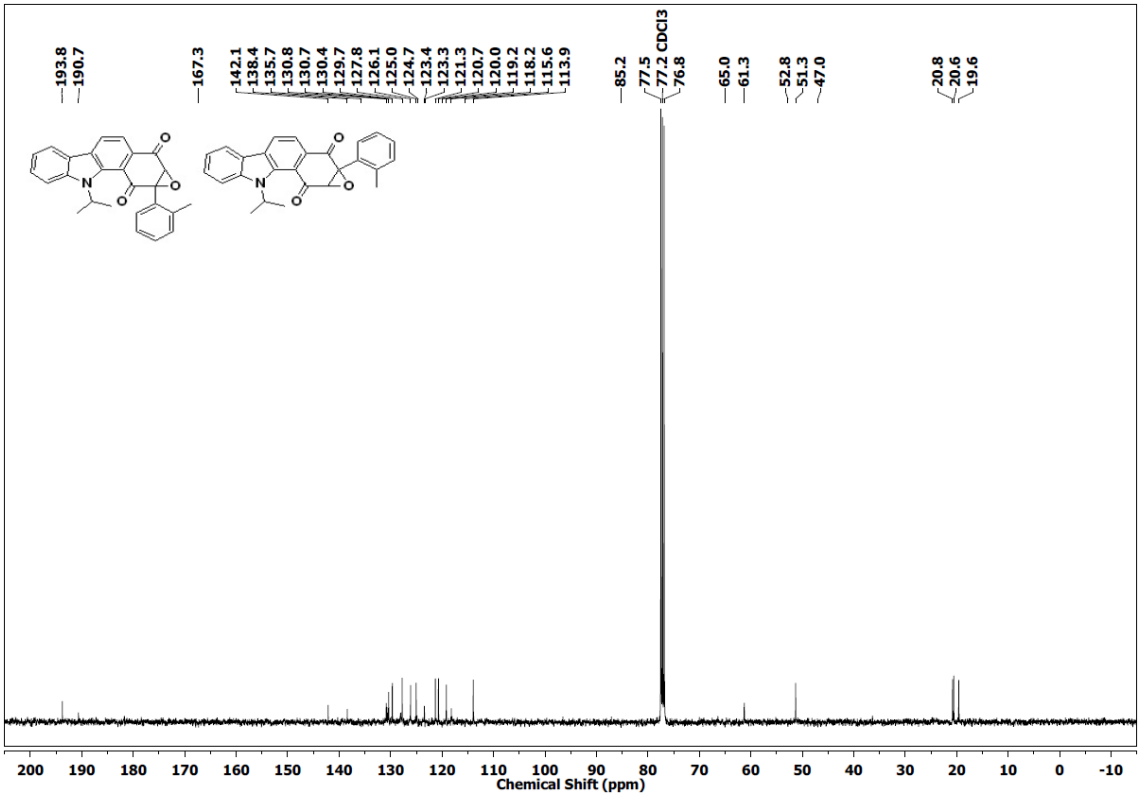

^{1}H NMR of **39, 40**

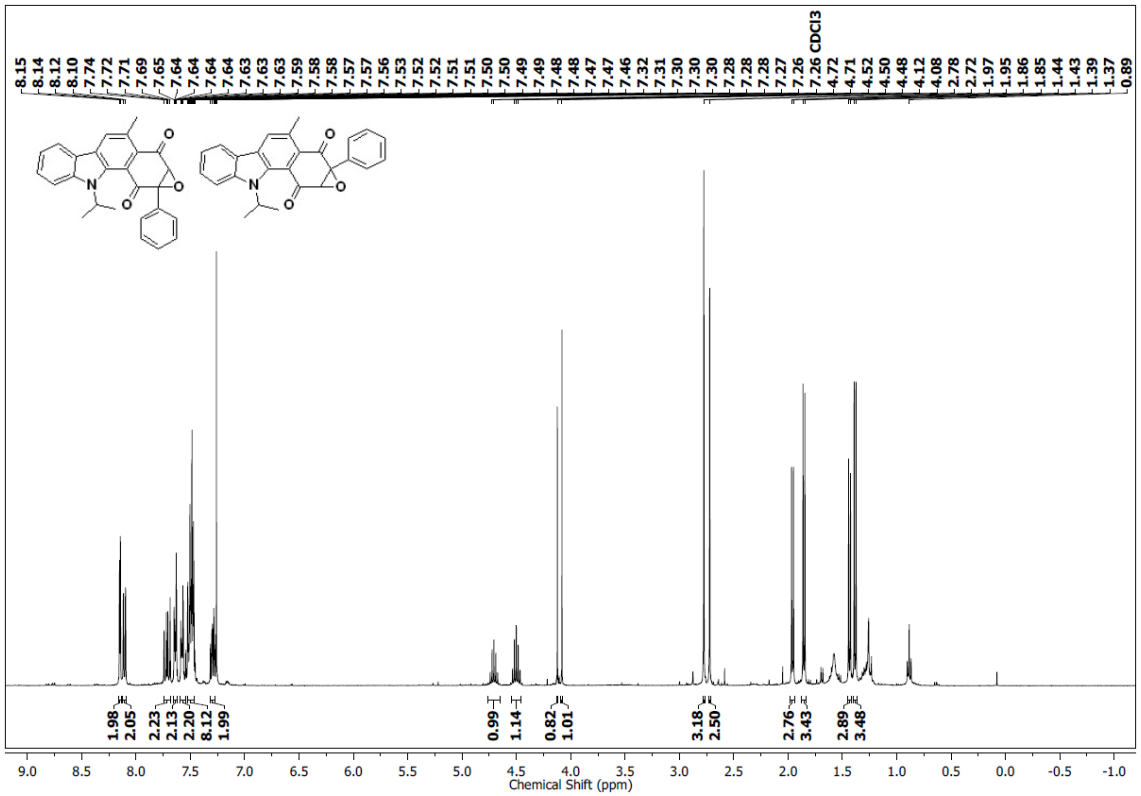

^{13}C NMR of **39, 40**

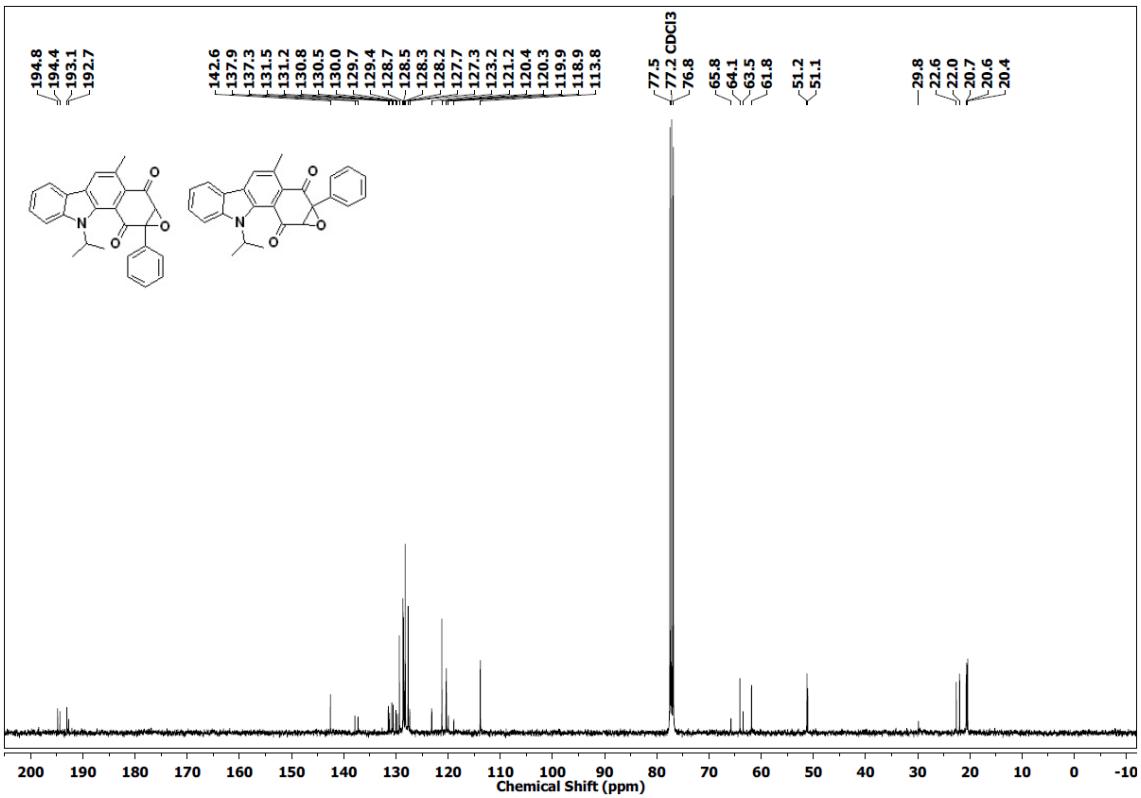

^{1}H NMR of **41**

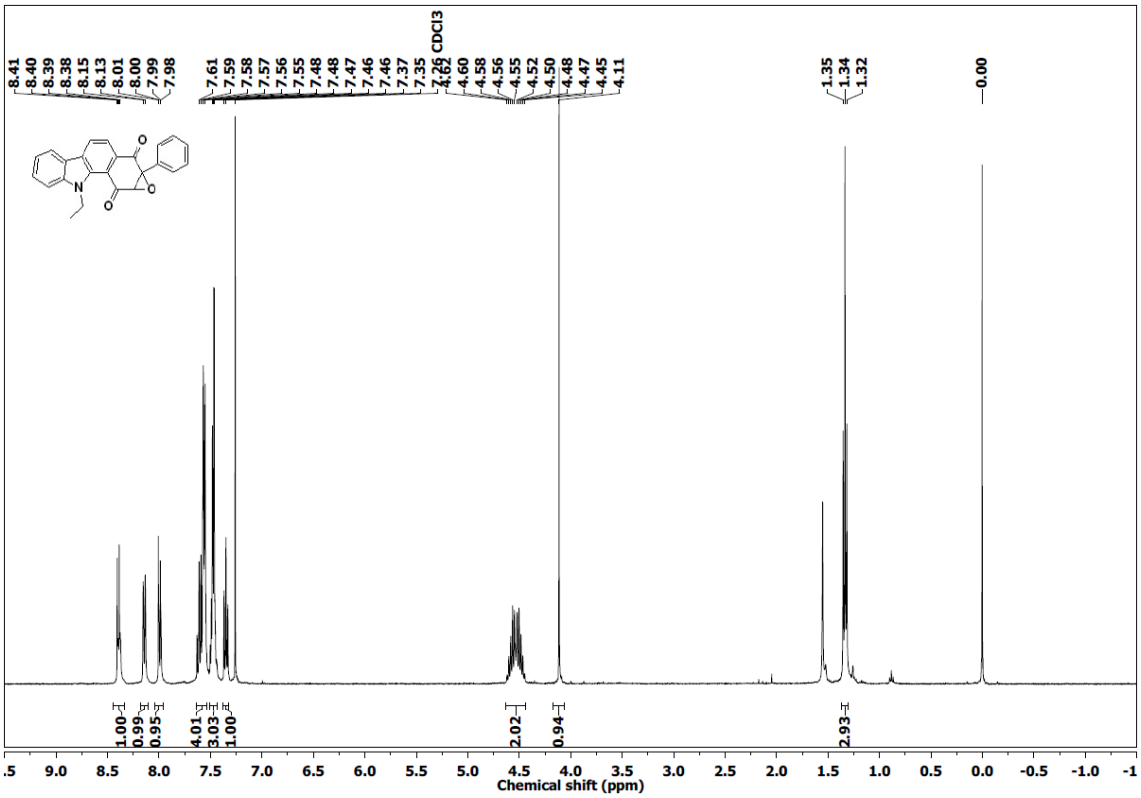

^{13}C NMR of **41**

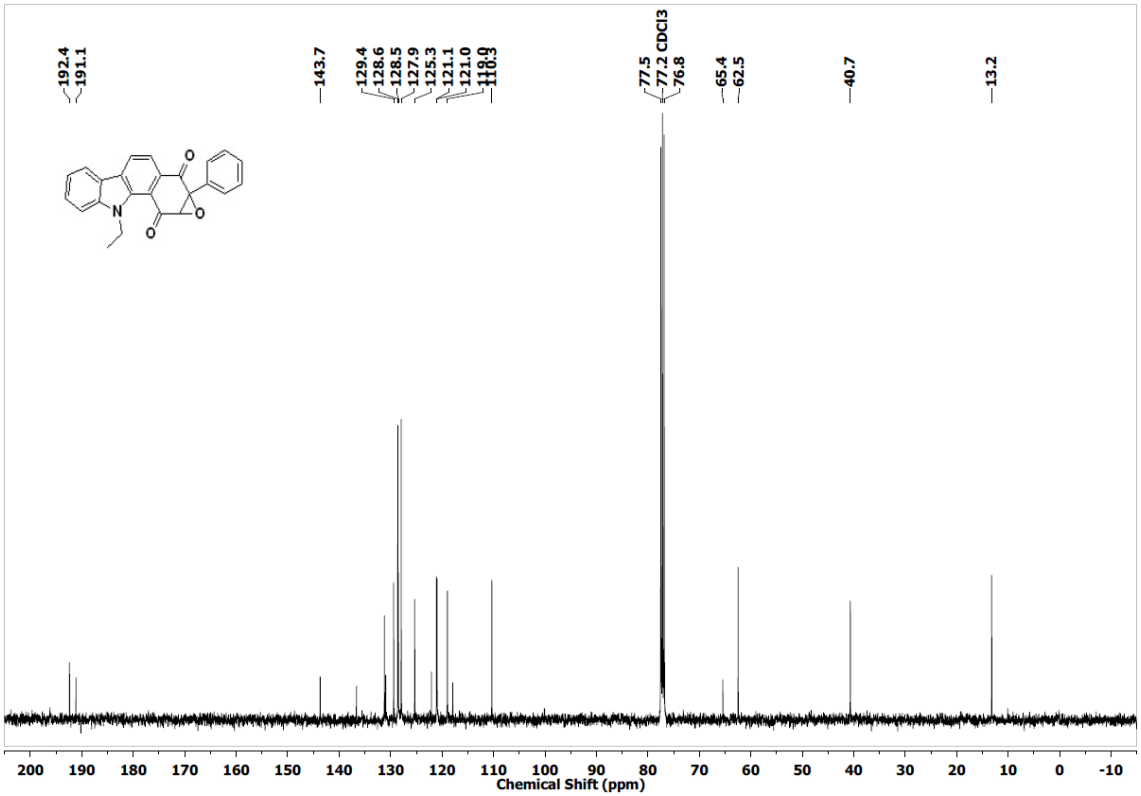

^{1}H NMR of **42**

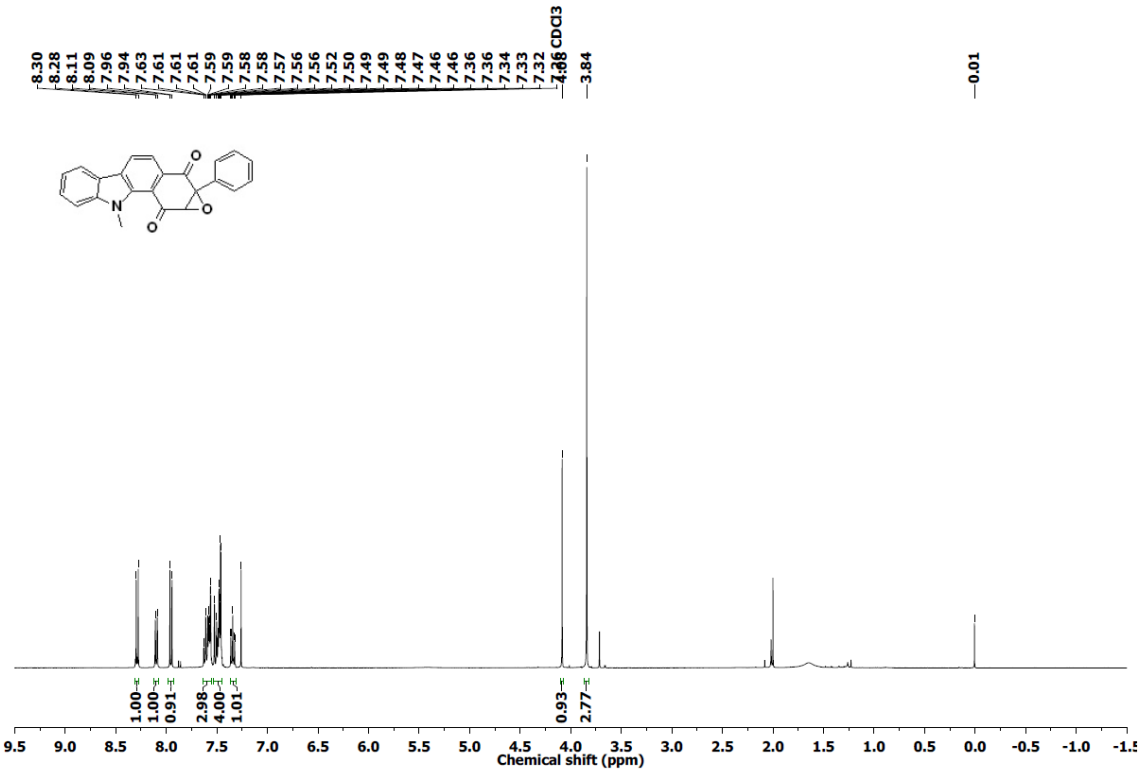

^{13}C NMR of **42**

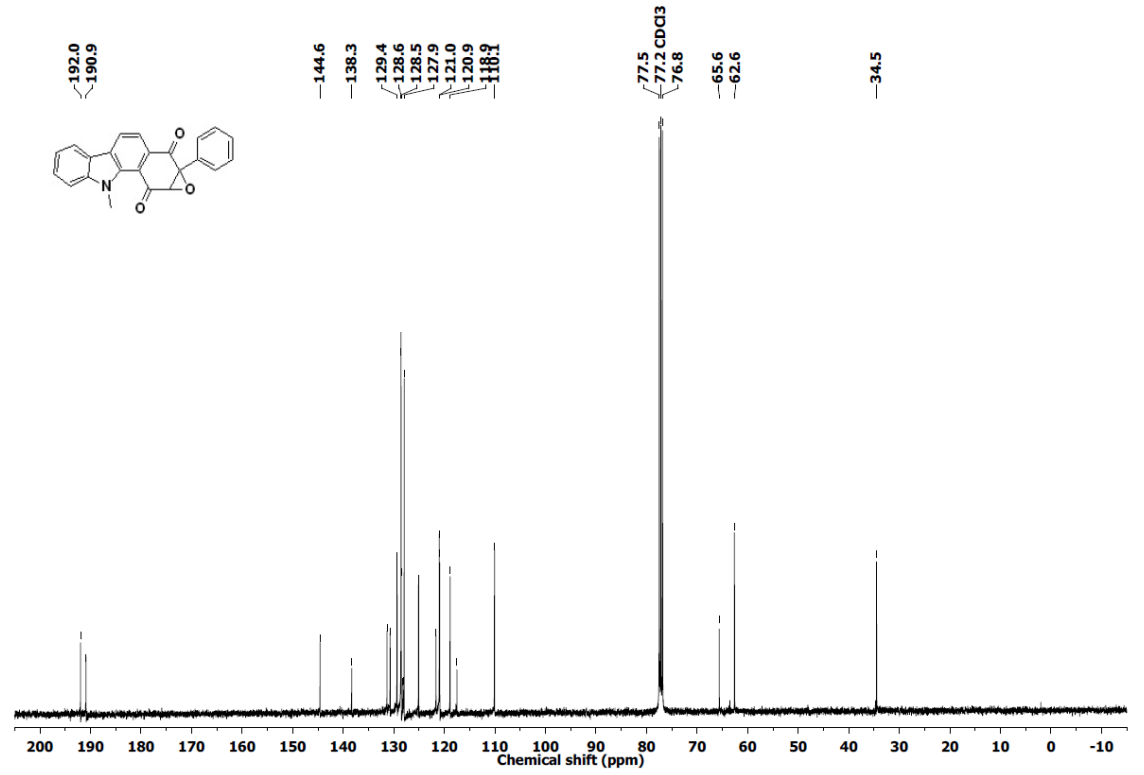

2D ^{1}H-^{1}H NOESY NMR of **42**

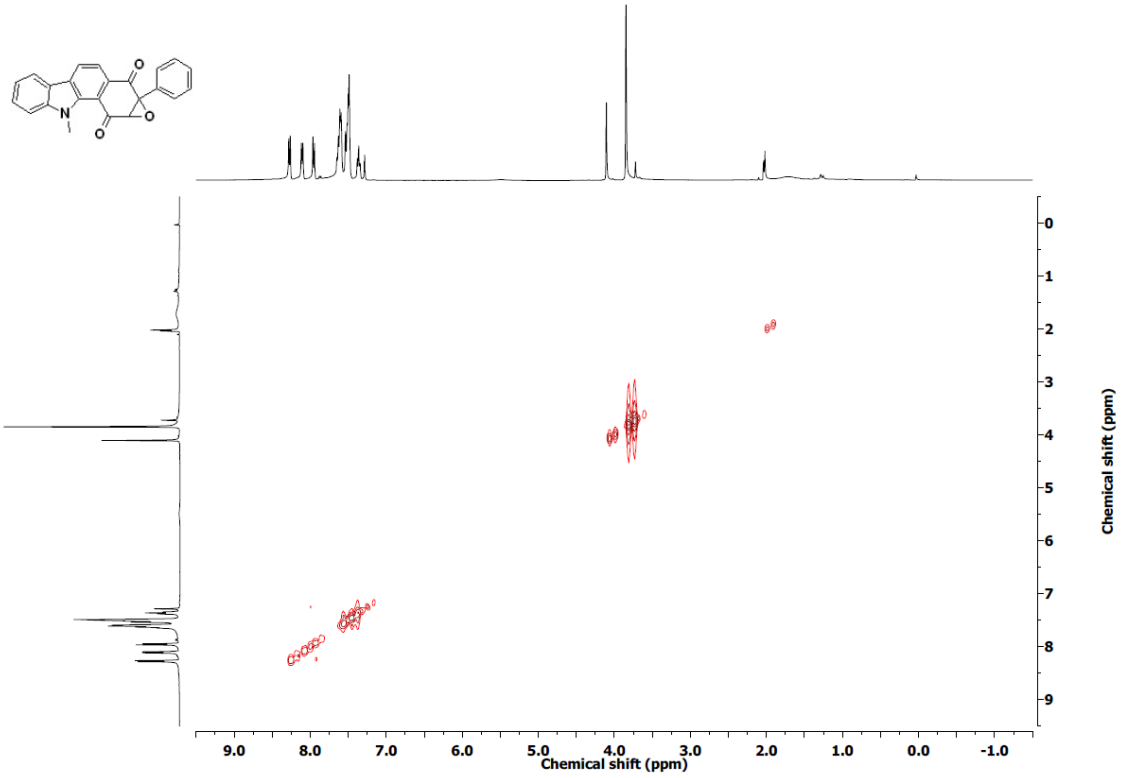

^{1}H NMR of **43, 44**

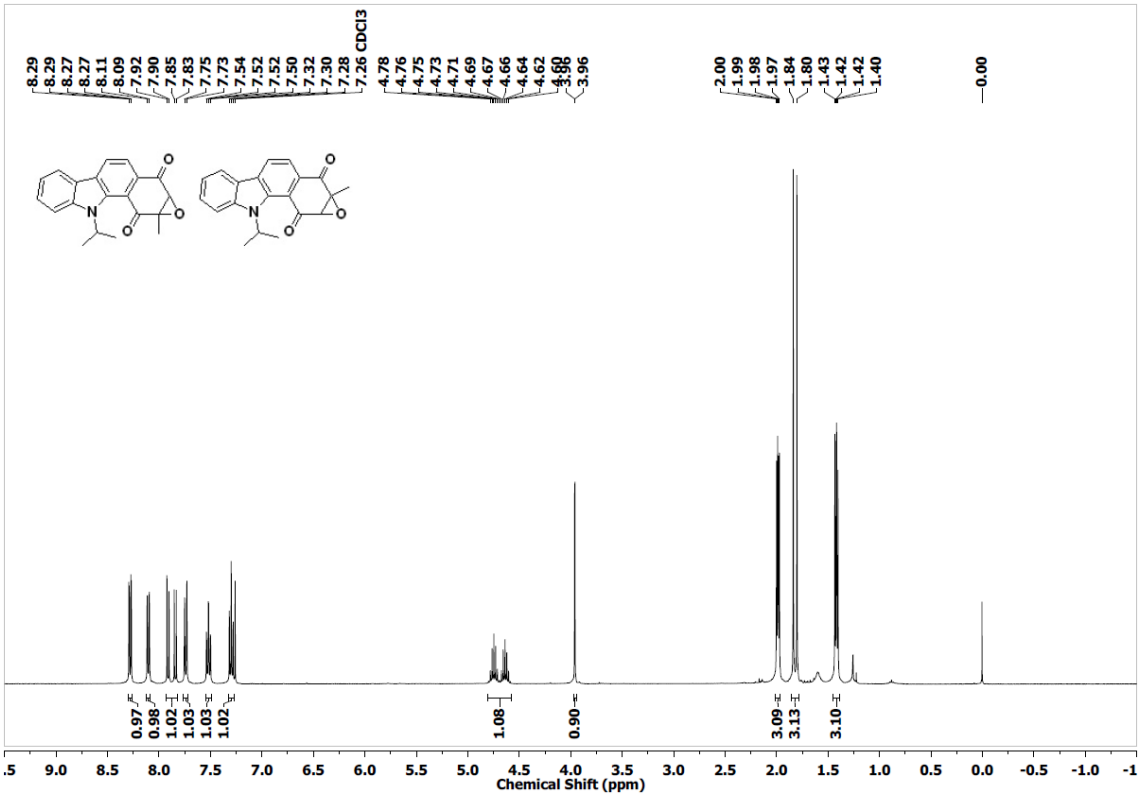

^{13}C NMR of **43, 44**

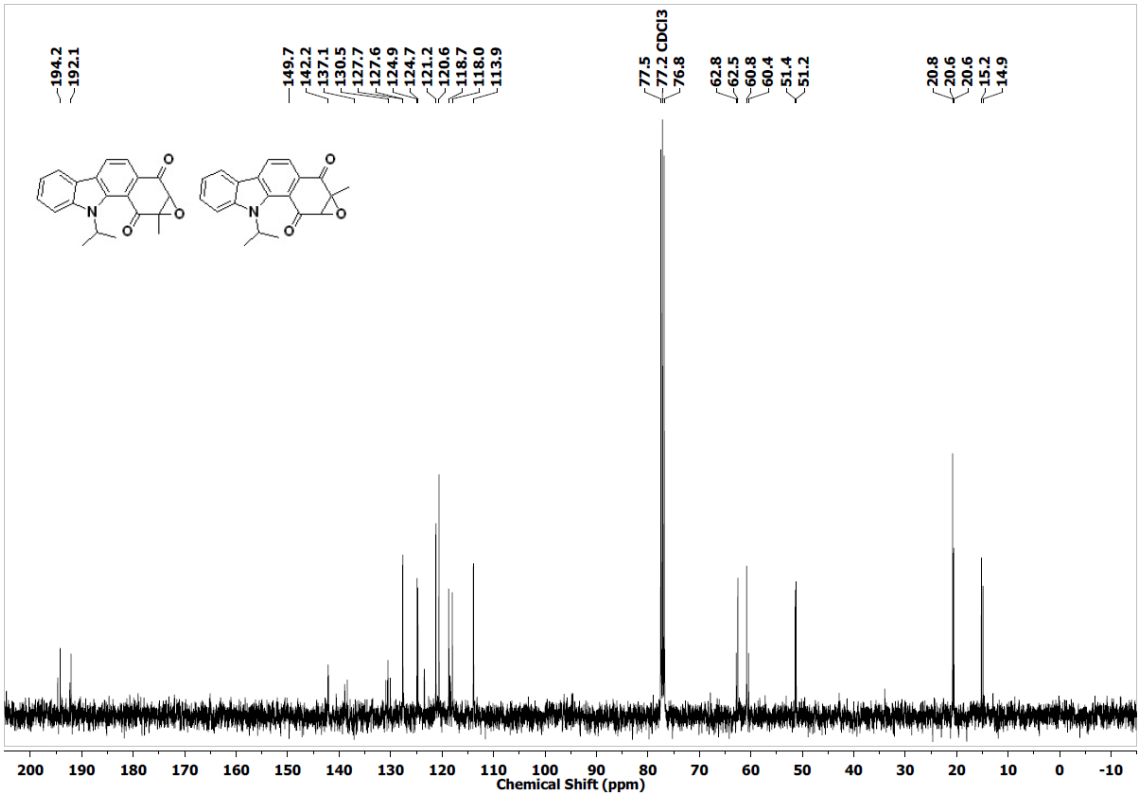

^{1}H NMR of **45, 46**

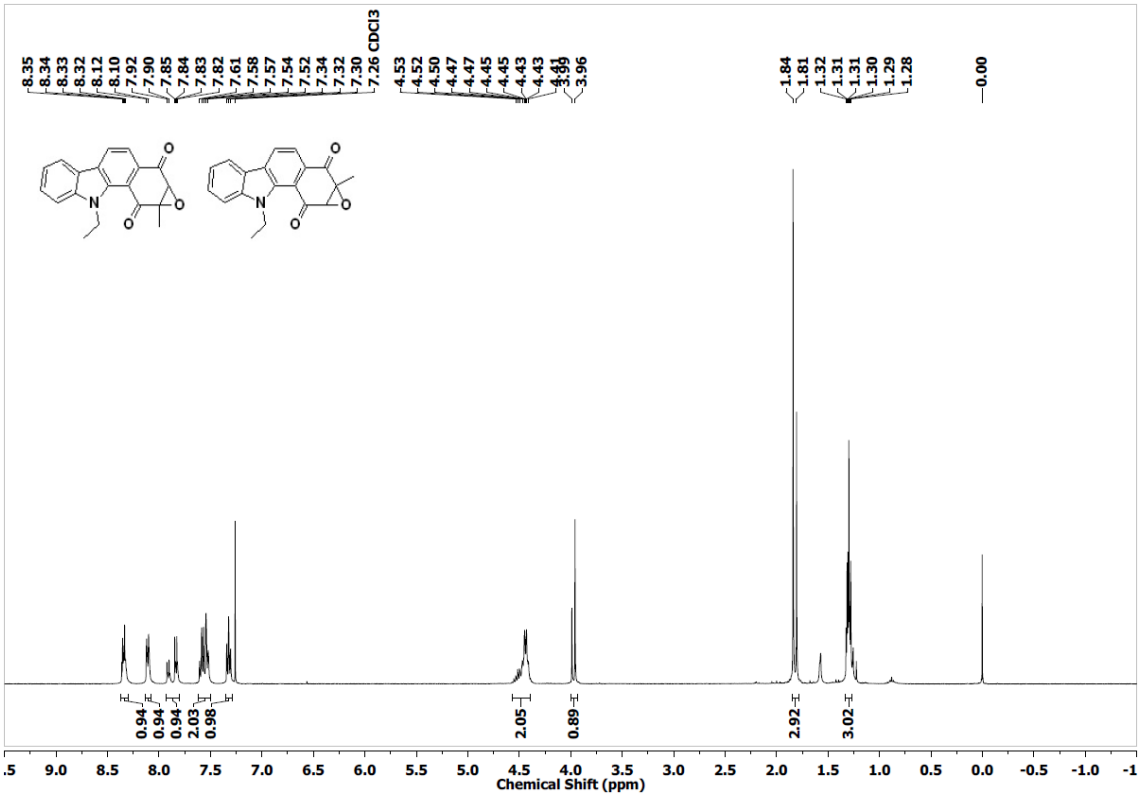

^{13}C NMR of **45, 46**

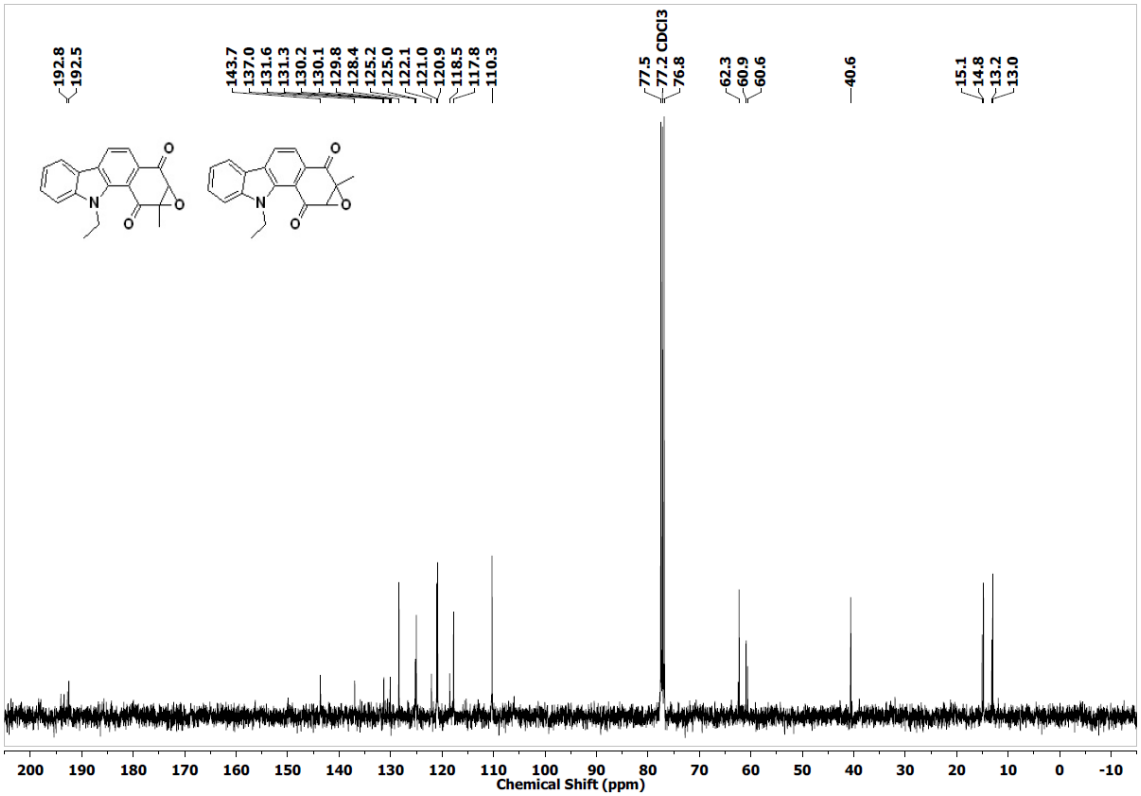

^{1}H NMR of **47**

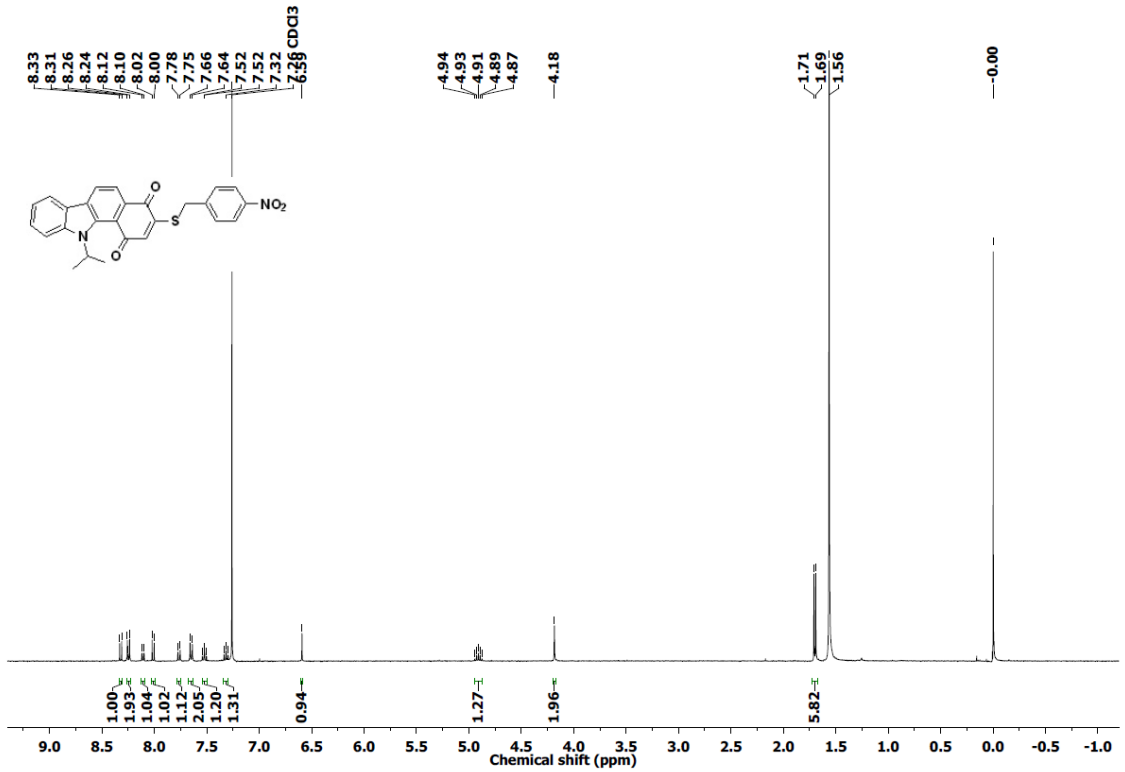

^{13}C NMR of **47**

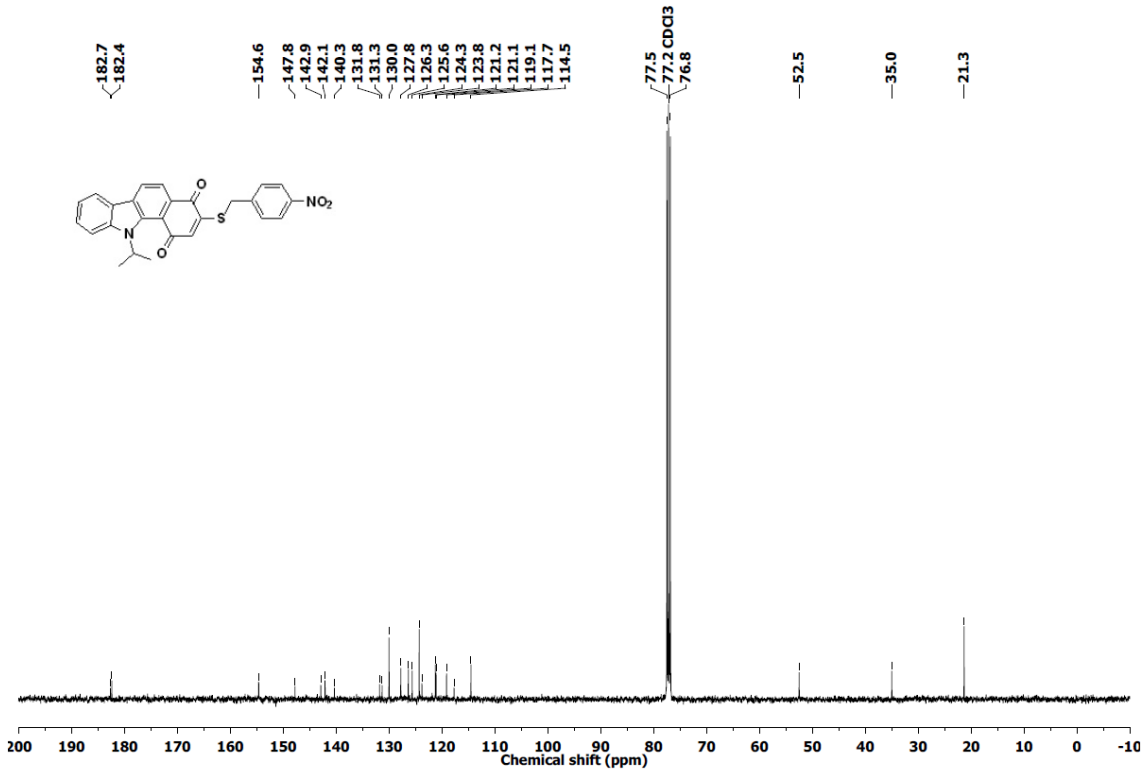

2.6. References

(1) Ellestad, G. A.; Whaley, H. A.; Patterson, E. L. The Structure of Frenolicin. *J. Am. Chem. Soc.* **1966**, *88*, 4109–4110.

(2) Feroj Hasan, A. F. M.; Furumoto, T.; Begum, S.; Fukui, H. Hydroxysesamone and 2,3-Epoxysesamone from Roots of Sesamum Indicum. *Phytochemistry* **2001**, *58*, 1225–1228.

(3) Furumoto, T. Biosynthetic Origin of 2,3-Epoxysesamone in a Sesamum Indicum Hairy Root Culture. *Biosci., Biotechnol., Biochem.* **2009**, *73*, 2535–2537.

(4) Westhofen, P.; Watzka, M.; Marinova, M.; Hass, M.; Kirfel, G.; Müller, J.; Bevans, C. G.; Müller, C. R.; Oldenburg, J. Human Vitamin K 2,3-Epoxide Reductase Complex Subunit 1-like 1 (VKORC1L1) Mediates Vitamin K-Dependent Intracellular Antioxidant Function. *J. Biol. Chem.* **2011**, *286* (17), 15085–15094.

(5) Kawakami, Y.; Hartman, S. E.; Kinoshita, E.; Suzuki, H.; Kitaura, J.; Yao, L.; Inagaki, N.; Franco, A.; Hata, D.; Maeda-Yamamoto, M.; et al. Terreic Acid, a Quinone Epoxide Inhibitor of Bruton's Tyrosine Kinase. *Proc. Natl Acad. Sci. U S A* **1999**, *96* (5), 2227–2232.

(6) Olesen, S. H.; Ingles, D. J.; Yang, Y.; Schönbrunn, E. Differential Antibacterial Properties of the MurA Inhibitors Terreic Acid and Fosfomycin. *J. Basic Microbiol.* **2014**, *54* (4), 322–326.

(7) Mandl, F. A.; Kirsch, V. C.; Ugur, I.; Kunold, E.; Vomacka, J.; Fetzer, C.; Schneider, S.; Richter, K.; Fuchs, T. M.; Antes, I.; et al. Natural-Product-Inspired Aminoepoxybenzoquinones Kill Members of the Gram-Negative Pathogen Salmonella by Attenuating Cellular Stress Response. *Angew. Chem. Int. Ed.* **2016**, *55* (47), 14852–14857.

(8) Drechsel, J.; Mandl, F. A.; Sieber, S. A. Chemical Probe To Monitor the Parkinsonism-Associated Protein DJ-1 in Live Cells. *ACS Chem. Biol.* **2018**, *13* (8), 2016–2019.

(9) Aoyama, A.; Murai, M.; Ichimaru, N.; Aburaya, S.; Aoki, W.; Miyoshi, H. Epoxycyclohexenedione-Type Compounds Make Up a New Class of Inhibitors of the Bovine Mitochondrial ADP/ATP Carrier. *Biochemistry* **2018**, *57* (6), 1031–1044.

(10) Dharmaraja, A. T.; Dash, T. K.; Konkimalla, V. B.; Chakrapani, H. Synthesis, Thiol-Mediated Reactive Oxygen Species Generation Profiles and Anti-Proliferative Activities of 2,3-Epoxy-1,4-Naphthoquinones. *Med. Chem. Commun.* **2012**, *3* (2), 219–224.

(11) Dharmaraja, A. T. Synthesis and Evaluation of Small Molecule Based Reactive Oxygen Species (ROS) Generators. *Thesis* **2015**.

(12) Welsch, M. E.; Snyder, S. A.; Stockwell, B. R. Privileged Scaffolds for Library Design and Drug Discovery. *Curr. Opin. Chem. Bio.* **2010**, *14* (3), 347–361.

(13) *Inorganic Chemistry, 4th Edition by Catherine Housecroft, Alan G. Sharpe*.

(14) Brunmark, A.; Cadenas, E. 1,4-Reductive Addition of Glutathione to Quinone Epoxides. Mechanistic Studies with h.p.l.c. with Electrochemical Detection under Anaerobic and Aerobic Conditions. Evaluation of Chemical Reactivity in Terms of Autoxidation Reactions. *Free Radic. Bio. Med.* **1989**, *6* (2), 149–165.

(15) Evans, M. G.; Polanyi, M. Some Applications of the Transition State Method to the Calculation of Reaction Velocities, Especially in Solution. *J. Chem. Soc. Faraday Trans.* **1935**, *31* (0), 875.

(16) Eyring, H. The Activated Complex in Chemical Reactions. *J. Chem. Phys.* **1935**, *3* (2), 107–115.

(17) Kosower, N. S.; Kosower, E. M. Thiol Labeling with Bromobimanes. *Methods Enzym.* **1987**, *143*, 76–84.

(18) Chakrabarty, M.; Basak, R.; Harigaya, Y.; Takayanagi, H. Reaction of 3/2-Formylindoles with TOSMIC: Formation of Indolyloxazoles and Stable Indolyl Primary Enamines. *Tetrahedron* **2005**, *61* (7), 1793–1801.

(19) Gioia, C.; Hauville, A.; Bernardi, L.; Fini, F.; Ricci, A. Organocatalytic Asymmetric Diels–Alder Reactions of 3-Vinylindoles. *Angew. Chem. Int. Ed.* **2008**, *47* (48), 9236–9239.

(20) Tandon, V. K.; Singh, R. V.; Yadav, D. B. Synthesis and Evaluation of Novel 1,4-Naphthoquinone Derivatives as Antiviral, Antifungal and Anticancer Agents. *Bioorg.*

Med. Chem. Lett. **2004**, *14* (11), 2901–2904.

(21) *M07-A10 Methods for Dilution Antimicrobial Susceptibility Tests for Bacteria That Grow Aerobically; Approved Standard-Tenth Edition*; 2015.

CHAPTER 3. Chemoproteomic profiling of the thiol proteome of *S. aureus* and identification of probable protein targets of INDQE compounds

3.1. Introduction

In Chapter 2, the INDQE scaffold was studied, and the SAR of different analogues was established by changing the groups on the epoxide followed by evaluation for their antibacterial potency. Lead compounds **25** and **27** were identified from this study. Due to the relative synthetic ease for compound **25**, it was chosen for further biological experiments. The cytotoxicity of these compounds was tested against Vero cells (lineage of cells used in cell culture isolated from kidney epithelial cells extracted from an African green monkey) and the assay gave a very good selectivity index of 200. Compound **25** was not found to adversely affect human erythrocytes as no evidence was found for hemolysis, even at elevated concentrations of 100 μg/mL. Compound **25** was potent against multi-drug resistant strains of *S. aureus* including VRSA. A time-kill analysis study was conducted with VRSA strain HIP 11714 which suggested that the lead compound **25** showed potent bactericidal activity comparable to that of Daptomycin. Daptomycin is the clinically used drug of last resort against severe infections caused by drug-resistant bacteria like VRSA.[1]

Having established the potency of the lead compound **25**, and a favourable therapeutic window, the next challenge was to elucidate the mechanism of action of these compounds, and find out their targets. INDQE scaffold was designed to be thiol-reactive, and hence, it is likely that these compounds react with the cellular thiol pool. This was also shown using mBBr assay in Chapter 2, where the lead compounds depleted cellular thiols in MRSA. But, as all the compounds were found to be reacting with thiols at varying rates, depletion of cellular thiols may not be the sole reason for their antibacterial potency. Hence, the lead compounds could probably be targeting certain key cysteine residues on proteins inside cells. This hypothesis has previous literature precedence, where targeting cysteines on protein surfaces has been utilised extensively for drug development purposes.[2–6] The importance of cysteine in the cell and its various biological roles were discussed in Chapter 1. Thus, the antibacterial effect of INDQE compounds was hypothesized to be due to hitting certain key cysteine residues on cellular proteins.

Literature reports suggest use of activity-based protein profiling (ABPP) technique as an important tool in drug discovery programmes.[12–14] ABPP was elaborately discussed in Chapter

1. Sieber and co-workers have used this technique effectively to identify important targets in pathogenic bacteria. In one study, they have screened a library of alkyne-tagged α-methylene-γ-butyrolactones against *S. aureus* and using chemoproteomics, have identified inhibitors of virulence factor α-hemolysin (Hla).[15] These compounds are Michael acceptors and may be hitting certain cysteine residues on cellular proteins. They have been shown to covalently bind to certain key transcriptional regulators like SarA, SarR and MgrA. In another study, they have identified certain redox-active proteins such as Glutaredoxin 2 and Thioredoxin-1 as potent targets in *S. typhimurium*, using scaffolds inspired from natural products aminoepoxycyclohexenones (AECs).[16]

Now, in order to identify the probable targets of INDQE compounds in *S. aureus*, a chemoproteomics approach was employed. Here, the epoxide is the reactive functional group that can react with a cysteine residue on the proteins of *S. aureus*. This reactive group can further be linked with either an alkyne or an azide functionality as an analytical handle. These functional groups can then be used for the bio-orthogonal click chemistry using a reporter molecule. Hence, the proteome can then be resolved and visualized using SDS-PAGE. LC-MS/MS based proteomics can further be employed to pull-down probable protein targets.

3.2. Results and Discussion

In Chapter 2, compound **25** was identified as the lead compound and its chemistry and biology was extensively studied. It was hypothesized that key proteins with reactive cysteine residues could be the probable targets in *S. aureus*. In order to identify them using ABPP technique, an ABP (Activity-Based Probe) of the INDQE scaffold first needed to be synthesized. Thus, synthesis of an INDQE probe appended with an alkyne handle was planned. This probe had to be synthesized without compromising on its reactivity with a thiol as well as the antibacterial potency.

3.2.1. Synthesis

Choosing lead compound **25** as a template, a probe with an alkyne handle was designed. A similar synthetic scheme as used for compound **25** was used, and compound **51** was obtained following Scheme 3.1.

Scheme 3.1. Synthesis of probe 51

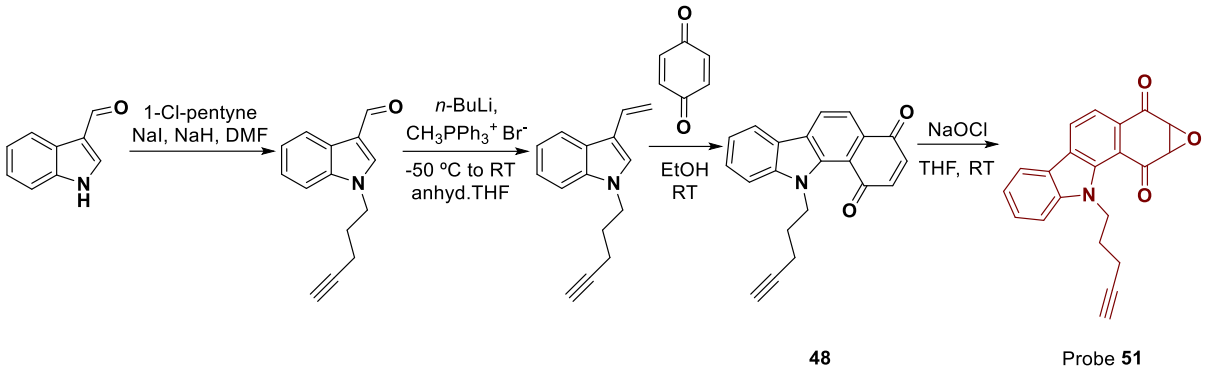

First, 5-chloropentyne was reacted with sodium iodide in DMF to displace chloride, which is not known to be a very good leaving group. Thus using sodium iodide, chloride can be displaced by iodide, to obtain a good leaving group of iodide. To this mixture, was added commercially available indole-3-carboxaldehyde, followed by the addition of NaH. This *N*-alkylation reaction was found to be very slow, possibly due to slow displacement of chloride by the iodide, which should further drive the reaction to completion. Next, following similar scheme as for compound **25**, this *N*-alkylated product was then subjected to a Wittig olefination reaction using methyltriphenylphosphonium bromide in presence of *n*-butyl lithium. The Wittig adduct was found to be very unstable and hence was not isolated, but subjected to the Diels-Alder cycloaddition reaction with 1,4 benzoquinone, followed by an aerobic oxidation in ethanol giving **48** in 27% yield. This quinone **48** was then epoxidized to the final INDQE alkyne probe **51** using sodium hypochlorite, and was obtained in 46% yield.

On a similar premise of the work done in Chapter 2, synthesis of probes with phenyl group on the epoxide was planned, choosing the compounds **27** and **28** as templates. A similar synthesis scheme was followed (Scheme 3.2). In this case however, a pure adduct could not be obtained after the Diels-Alder reaction, as was observed for compounds **17-20** in Chapter 2. The crude mixture of regioisomers **49-50** was directly used for the next reaction. Surprisingly, a single isomer, compound **52**, was obtained for the epoxide in 72% yield. This result had previous precedence, as single isomers **41** and **42** were obtained in Chapter 2.

Scheme 3.2. Synthesis of probe 52

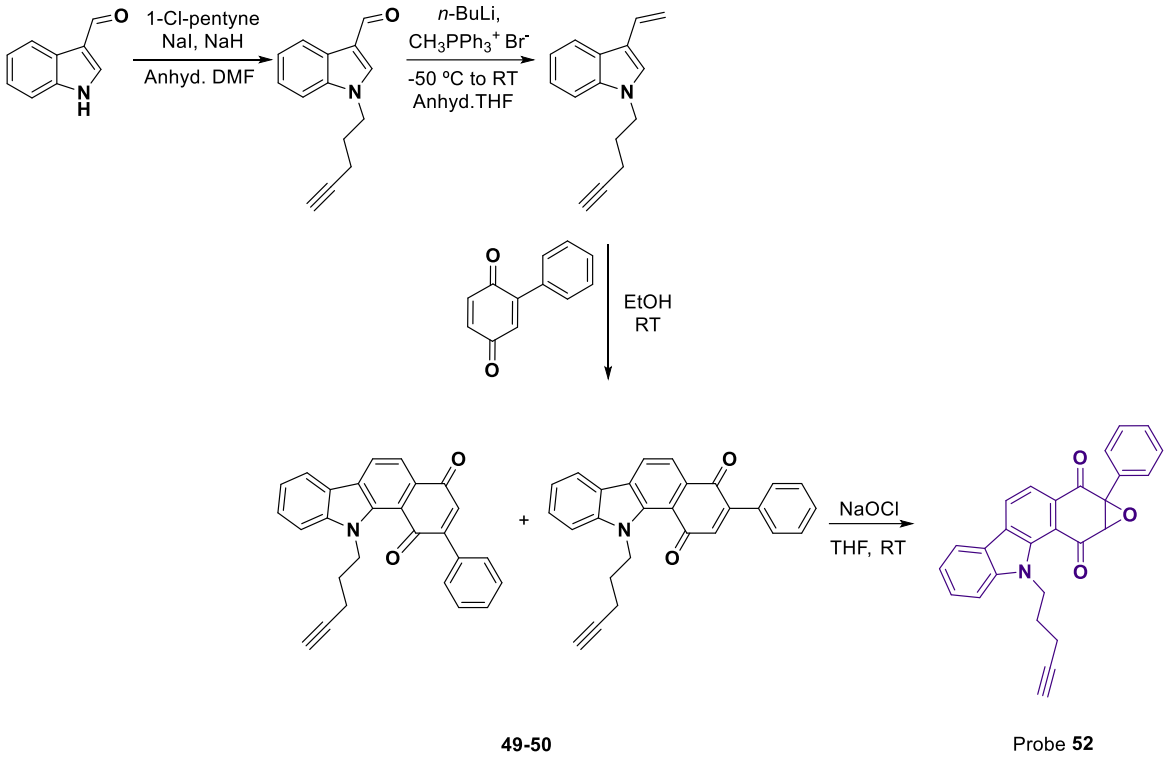

This compound was analysed using techniques such as ^{1}H, ^{13}C NMR and X-ray diffraction analysis. The crystal structure of this compound could be obtained and its regiochemistry could be assigned (Fig. 3.1). The obtained isomer was the '1' isomer. Again, this was according to the earlier observations made in the case of single isomers **41** and **42** in Chapter 2.

Figure 3.1. ORTEP diagram for probe 52

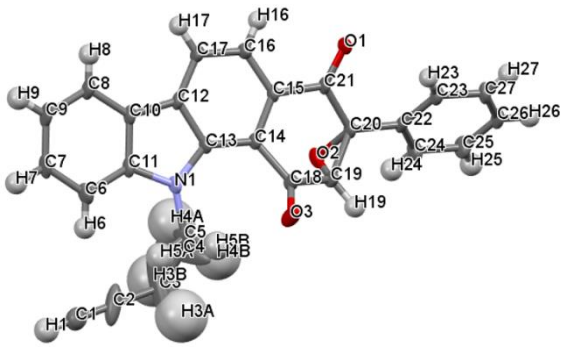

Table 3.1. Synthesis of INDQE alkyne probes

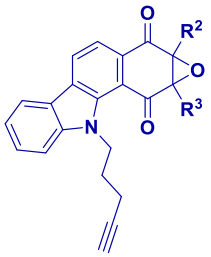

Entry	Quinone	% Yield[a]	Epoxide	R^2	R^3	% Yield[a]
1	**48**	27	**51**	H	H	72
2	**49[b], 50[b]**	-	**52**	Ph	H	46

[a]Crude yield reported; [b]not isolated, crude taken forward for next reaction

Thus, two INDQE alkyne probes **51** and **52** were synthesized based on lead compound **25** and inactive compound **28** as templates. Based on their structures and earlier evidence from SAR studies, it was hypothesized that these two probes will show variation in reactivity with a thiol. Probe **51**, modelled on active compound **25**, should be reactive with a thiol, whereas probe **52**, modelled on inactive compound **28**, should be unreactive towards a thiol. Hence, reactivity with a thiol was evaluated for these two probes and compared with their parent compounds.

3.2.2. Reactivity of INDQE probes with thiol - mBBr assay

An *in vitro* mBBr assay[17] was conducted to investigate the ability of the INDQE alkyne probes in reacting with a thiol. *L*-cysteine (10 eq.) was first reacted with a fixed concentration of the compound (100 μM) in Buffer-ACN (1:1, v/v), and at different time points of every 1 h (0-4 h), an aliquot was reacted further with mBBr reagent for 30 min in the dark. Then, the aliquot was subjected to a fluorescence measurement and the readout was further analysed. Along with alkyne probes **51** and **52**, the assay was simultaneously conducted with compounds **25**, **27** and **28** (Fig. 3.3). As discussed in Chapter 2, mBBr (monobromobimane) is a non-fluorescent molecule. On reaction with a thiol, the bromide gets displaced and generates a thiol adduct which is fluorescent in nature (Scheme 3.3). Thus, if a compound reacts with thiol, it will deplete the available thiol pool for the reaction with mBBr and will generate a lower readout value.

Scheme 3.3. Reaction of mBBr with a thiol

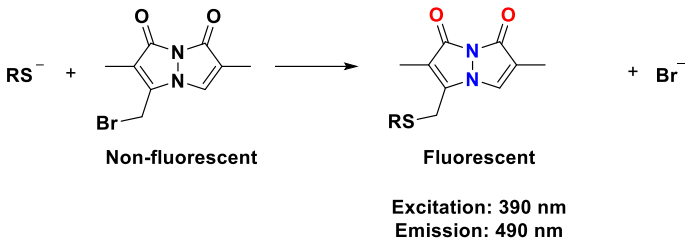

At a time point of 1 h, it was found that, probe **51** shows similar reactivity profile as compound **25**, and probe **52** shows similar reactivity profile as compound **28** (Fig. 3.3). Thus, these two probes were ideal representatives of lead compound **25** and inactive compound **28** in terms of reactivity with thiol. When assessed further, it was found that the reactivity profiles with thiol are comparable at time points of 2 h and 3 h. However, at 4 h, it was observed that compound **25** is far more reactive than probe **51**. But, as the reactivity with thiol and antibacterial activity correlation was kinetically driven, this difference at 4 h time point may not have a drastic impact in the probes' utility for the ABPP studies. The readout obtained for compound **28** and probe **52** was still comparable at 4 h.

In the same assay, the reactivity with thiol of different thiol-reactive electrophiles was analysed and compared with that of probe **51**. Thiol-reactive scaffolds such as *N*-methyl maleimide (NMM), Iodoacetamide (IAM), 4-chloro-7-nitrobenzofurazan (NBD-Cl) and 1-Fluoro-2,4-dinitrobenzene (FDNB) were chosen (Fig. 3.2). These compounds are extensively used in biochemical assays as thiol-reactive electrophiles for thiol-blocking, cysteine-modification and their alkyne or azide-tagged probes are used in various ABPP studies.[18]

Figure 3.2. Structures of all compounds used in the mBBr assay

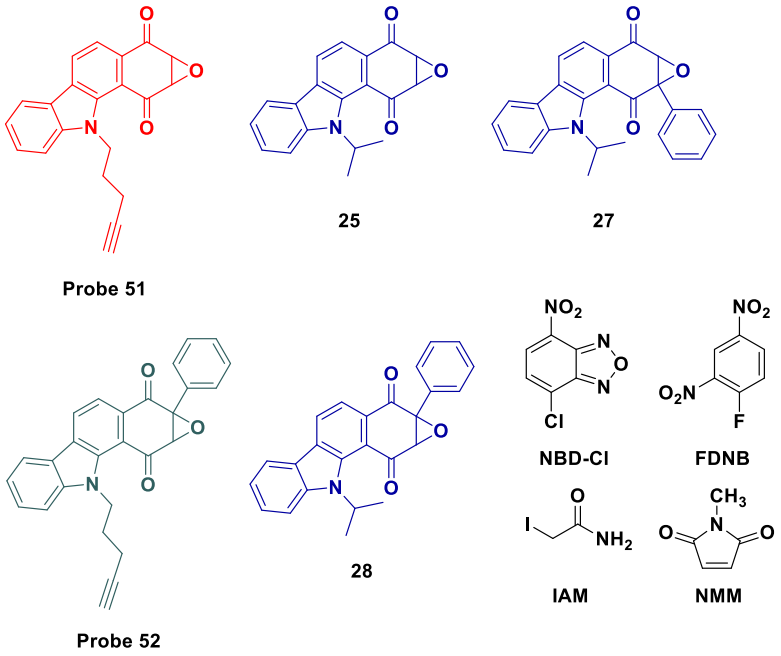

At the concentrations tested (100 μM), IAM and NMM were found to be less reactive with thiol when compared with the untreated control as well as with compounds **25** and **51** (Fig. 3.3). Whereas, NBD-Cl was found to be extremely reactive with thiol. FDNB showed moderate reactivity, which was comparable to both the compounds **25** and **51**. These results strongly suggested that the reactive probe **51** compared favourably with reported thiol-reactive electrophiles, and in fact was found to be better than NMM and IAM at the concentrations tested. This assay also suggested that these two INDQE alkyne probes **51** and **52** are well suited for use as thiol-reactive probes for profiling in *S. aureus*, **51** being the reactive probe and **52** as a non-reactive or less reactive probe.

Figure 3.3. mBBr assay with probes 51 and 52

(reproduced with permission from *J. Med. Chem.* <https://pubs.acs.org/doi/10.1021/acs.jmedchem.9b00774>)

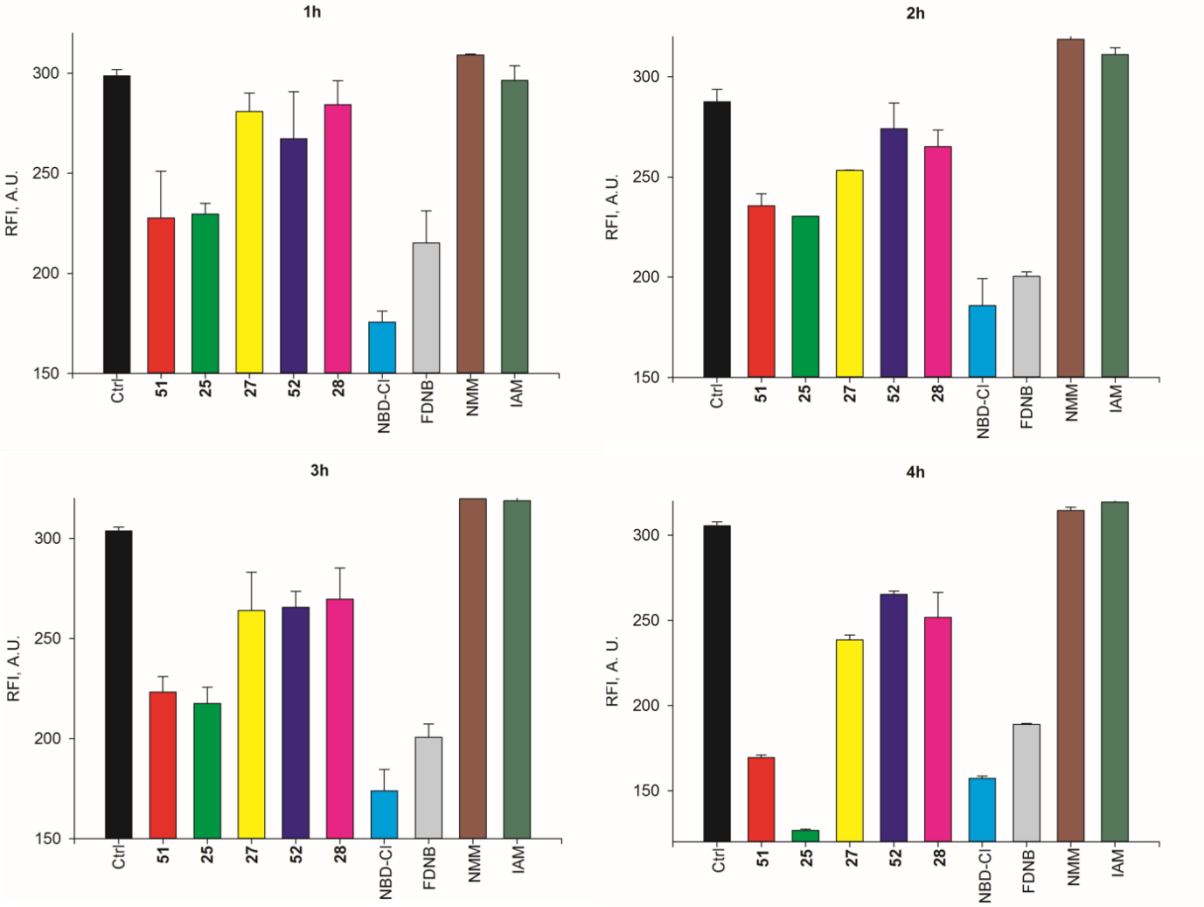

3.2.3. Antibacterial activity against ESKAPE pathogens

Having established the reactivity with thiol for the two INDQE alkyne probes, their antibacterial activity was next assessed against a panel of ESKAPE pathogens. Compound **51** was found to be selectively active against *S. aureus* (MIC 1 µg/mL, Table 3.2), as observed for all the hits of the INDQE series. Compound **52** was found to be completely inactive against all pathogens. These two results were in accordance of the results of the reactivity with thiol assessed using mBBr assay. Thus, compound **51** now could be used as an 'active' probe, whereas, compound **52** could be used as an 'inactive' probe.

Table 3.2. Antibacterial activity of INDQE alkyne probes against ESKAPE pathogens

Probe	MIC (μg/mL)						
	E. coli	*S. aureus*	*K. pnemoniae*	*A. baumannii*	*P. aeruginosa*	*E. faecalis*	*E. faecium*
51	64	1	64	64	64	64	64
52	64	64	64	64	64	64	64

E. coli ATCC 25922, *S. aureus* ATCC 29213, *K. pnemoniae* BAA 1705, *A. baumannii* BAA 1605, *P. aeruginosa* ATCC 27853, *E. faecalis* Strain B3119, *E. faecium* Strain Patient #1-1; (Data courtesy: Dr. Sidharth Chopra Lab, CDRI Lucknow)

3.2.4. Activity-based Protein profiling (ABPP) in *S. aureus*

The thiol-reactivity and the antibacterial activity of the two INDQE alkyne probes suggested their utility for use as ABPs in an ABPP experiment, with the epoxide as the electrophilic warhead and alkyne as the analytical handle. Thus, the thiol proteome of *S. aureus* was next profiled using these two probes. *S. aureus* ATCC 29213 was first cultured in MHB media. The cells were then lysed and fractionated into soluble and membrane fractions. Protein concentrations were estimated using a standard Bradford® assay and a fixed concentration was used for all the experiments. The protein fractions were then treated with probes **51** and **52** in a dose-dependent manner (0 - 100 μM). In Chapter 2, it was shown that the lead compound **25**, forms a covalent adduct with a thiol. Thus, when a protein pool was treated with INDQE probes, it was hypothesized that the probes would react covalently with one or more cysteine residues on the protein surface *via* the opening of the epoxide ring. Thus, this covalently attached INDQE probe on the protein surface, now has an alkyne group appended on it which is available for a 'Click' reaction. Thus, this was followed by CuAAC (Copper-catalysed Alkyne-Azide Cycloaddition) using Rhodamine azide (Alexa fluor 488) as the reporter fluorophore. The proteomes were then resolved and visualized by sodium dodecyl sulphate-polyacrylamide gel electrophoresis (SDS-PAGE) analysis using standard gel-based ABPP protocols.[19] Both the probes showed a dose-dependent labelling of the protein residues. For both the compounds, it was observed that the soluble fraction (Fig. 3.4) showed higher intensities of labelling as compared to the membrane fraction (Fig. 3.5).

Figure 3.4. Dose-dependent protein modification in soluble fractions of *S. aureus* lysates using probes 51 and 52

(reproduced with permission from *J. Med. Chem.* <https://pubs.acs.org/doi/10.1021/acs.jmedchem.9b00774>)

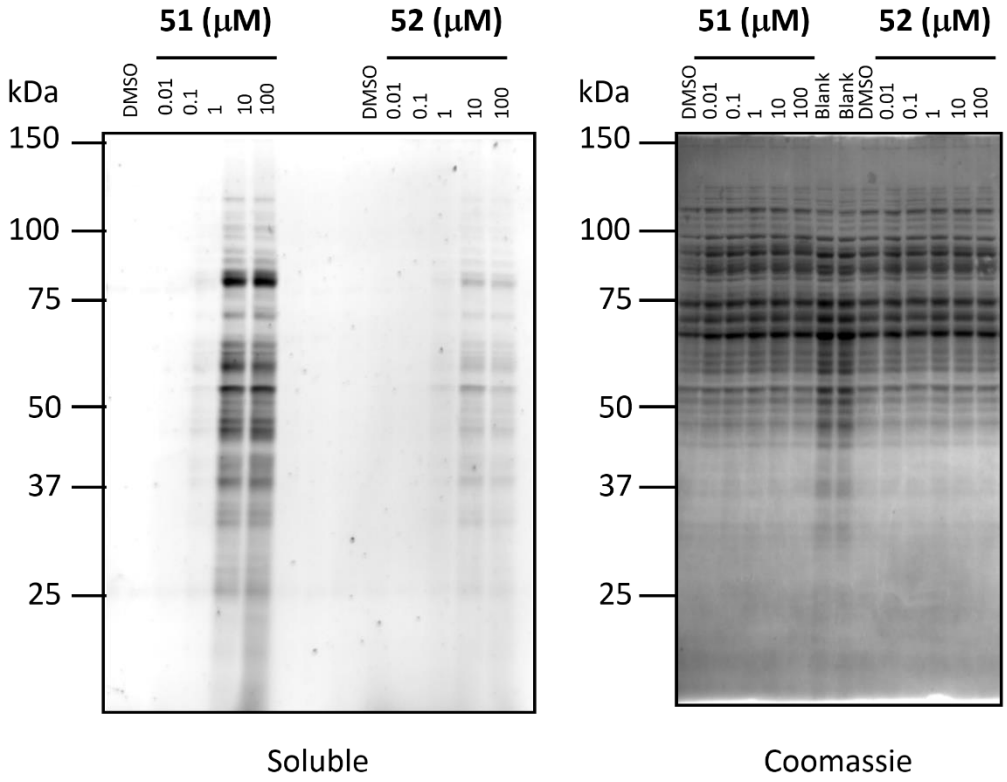

When compared between the two probes, probe **51** showed higher intensities of protein labelling than by probe **52**. Again, this was in accordance to the reactivity with thiol of these compounds as found out from the mBBr assay. Also, this suggested that *in vitro* reactivity with thiol of these compounds gets translated to reactivity in the lysates. It was observed that probe **51** could label the proteins in the lysates efficiently at 10 μM concentration. Hence, this concentration of probe **51** was used for all further experiments.

Figure 3.5. Dose-dependent protein modification in membrane fractions of *S. aureus* lysates using probes 51 and 52

(reproduced with permission from *J. Med. Chem.* <https://pubs.acs.org/doi/10.1021/acs.jmedchem.9b00774>)

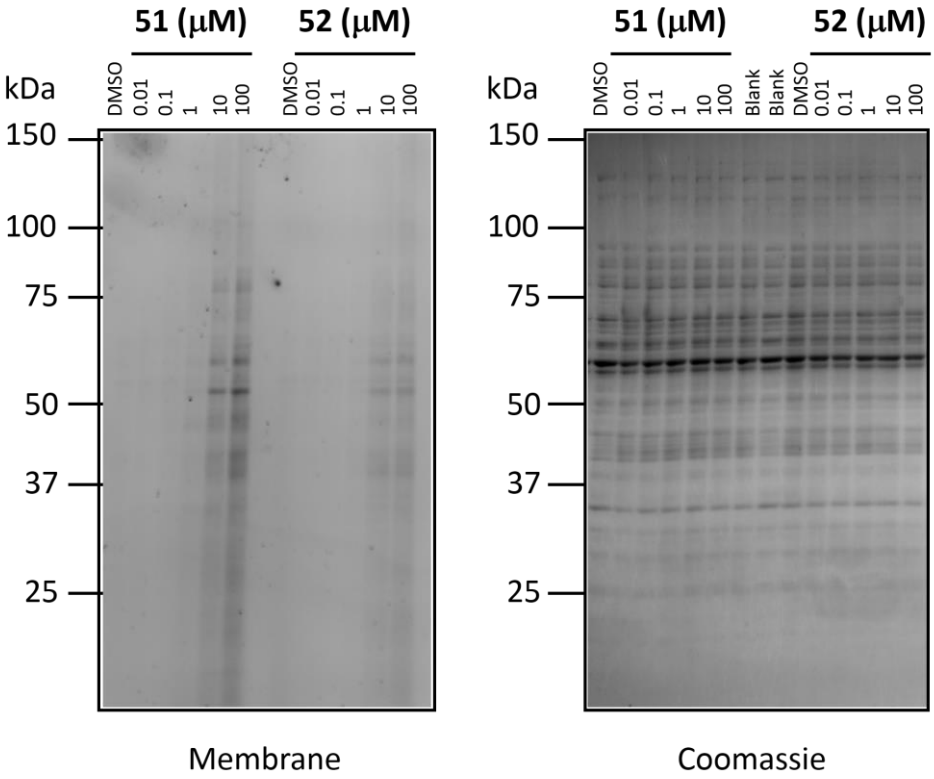

Next, a similar experiment was conducted *in situ*. Here, *S. aureus* was treated with 10 μM each of probes **51** and **52** for 1h. Then the cells were lysed and fractionated into soluble and membrane fractions, CuAAC performed with Rhodamine azide, and the proteins were resolved and visualized using a SDS-PAGE analysis. As observed for the lysates, it was found that the soluble fractions show better labelling as compared to membrane fractions (Fig. 3.6). Also, probe **51** extensively labelled the proteins whereas diminished intensities were observed for treatment with probe **52**. This reiterated the fact that reactivity with thiol gets translated to the cellular level and could possibly be the major driving force for antibacterial activity of the INDQE compounds. These two experiments also suggested that the soluble fraction could be an ideal hunting ground for the probable targets of these compounds, especially our lead compound **25**.

Figure 3.6. Protein modification *in situ* in *S. aureus* with probes 51 and 52

(reproduced with permission from *J. Med. Chem.* <https://pubs.acs.org/doi/10.1021/acs.jmedchem.9b00774>)

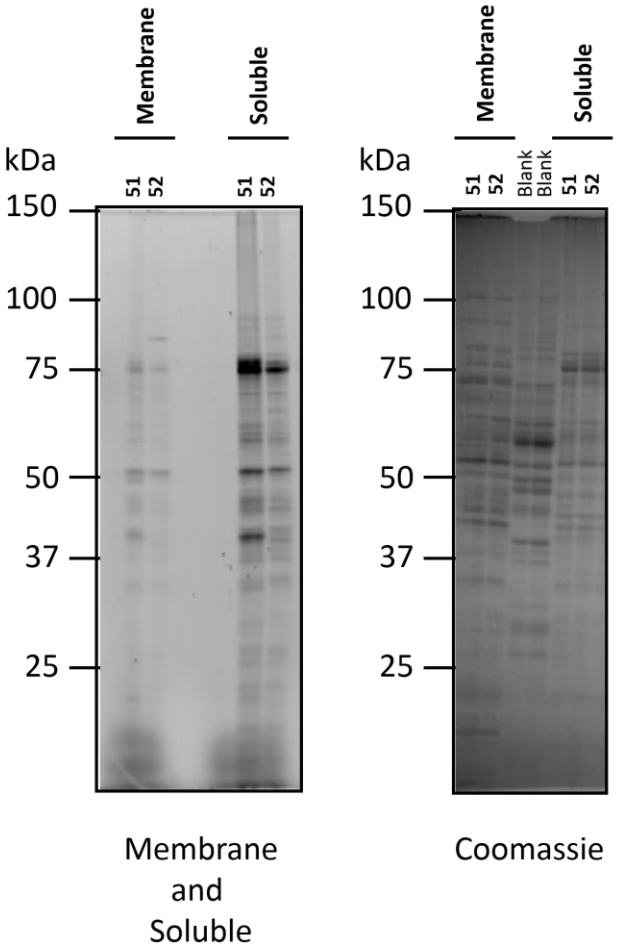

Having got these results, probe **51** was chosen for further studies due to the promising labelling of the proteome it displayed, and also due to the fact that it was found to be an active inhibitor of *S. aureus*. Next, in order to test the selectivity of probe **51** towards protein thiols, the proteome was profiled with probe **51** with an iodoacetamide (IAM) pretreatment. Iodoacetamide is known to react exclusively with thiols, and is generally used as a thiol blocking agent.[20] Hence, in this experiment, IAM, which was used in excess (10 mM), should completely block the thiols in the proteome. This IAM treatment, when followed by the treatment of probe **51** (10 μM), a complete ablation of signal was observed, as compared to the fractions without an IAM pretreatment. This result suggested that probe **51** was selective in reacting with thiols that is the cysteine residues on proteins (Fig. 3.7).

Figure 3.7. Protein modification using probe 51 in *S. aureus* with IAM pretreatment

(reproduced with permission from *J. Med. Chem.* <https://pubs.acs.org/doi/10.1021/acs.jmedchem.9b00774>)

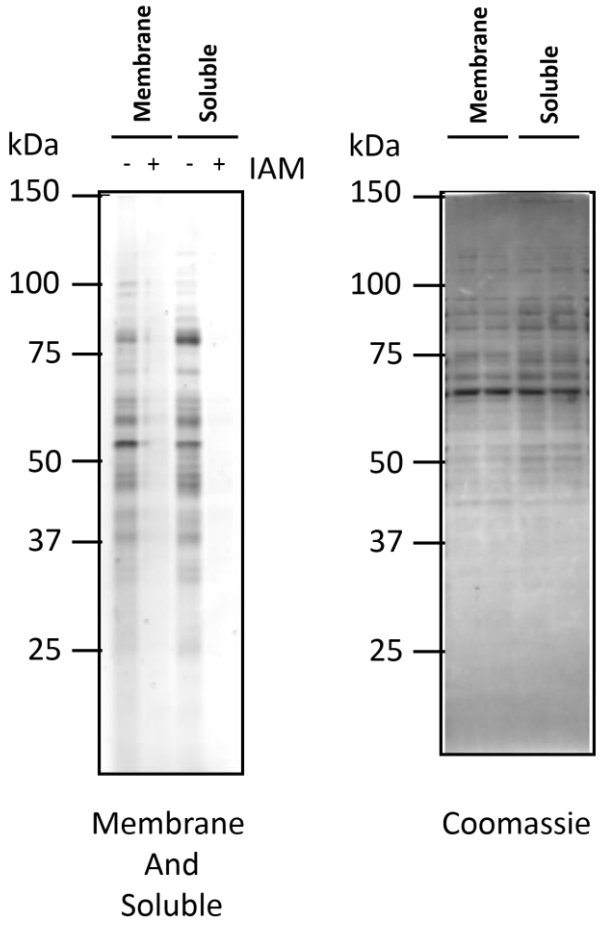

In Chapter 2, a subset of INDQE compounds were tested against ESKAPE pathogens, and were found to be inactive against all other pathogens except for *S. aureus*. The probes as well, when tested against ESKAPE pathogens, were found to be inactive, except **51** being active against *S. aureus*. Since INDQE compounds were found to be selectively inhibiting *S. aureus*, it was evident to inspect whether the INDQE probes could profile the thiol proteome of other bacteria. Thus, Gram-negative *E. coli* was first chosen. The thiol proteome of *E. coli* was profiled with the active probe **51**. First, *E. coli* ATCC 25922 cells were cultured, lysed and fractionated in soluble and insoluble protein fractions. After determination of the protein concentrations, these were then treated with probe **51** (10 μM). Following the click reaction, the proteins were resolved and visualized using a SDS-PAGE analysis (Fig. 3.8). It was found that probe **51** labels the *E. coli* thiol proteome in lysates, both in the soluble and membrane fractions, the labelling in the soluble fractions being more intense than in the membrane fractions, as also observed in the case of *S. aureus.*

Figure 3.8. Protein modification with probe 51 in *E. coli* lysates

(reproduced with permission from *J. Med. Chem.* <https://pubs.acs.org/doi/10.1021/acs.jmedchem.9b00774>)

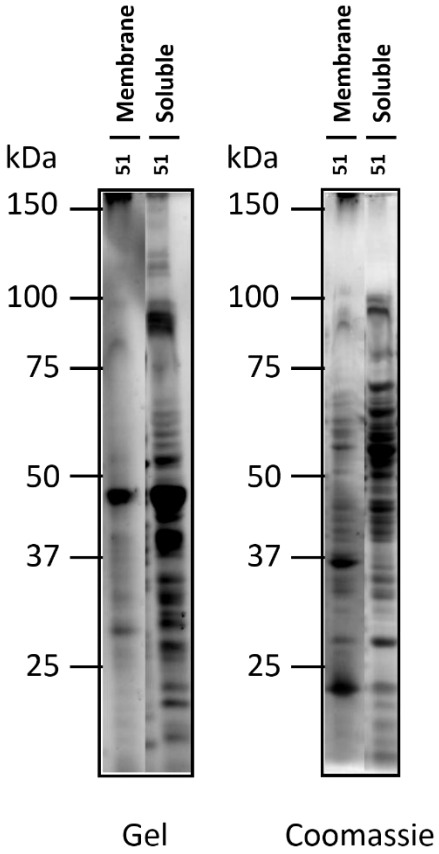

To further inspect and validate the observations made in the *in vitro* experiment, a similar experiment was conducted *in situ* in *E. coli*. The bacteria was incubated with probe **51** (10 μM) for 1h, following which they were lysed and eventually fractionated. The fractionated lysates were then subjected to Click reaction, and the proteins resolved and visualized using a SDS-PAGE analysis. Surprisingly, the signal was found to be completely ablated (Fig. 3.9). This result suggested that the INDQE compounds may not be permeable in *E. coli* and possibly even in other Gram-negative pathogens. Gram-negative bacteria have an extra Lipopolysaccharide (LPS) layer in the outer membrane along with Porins that are selective towards passage of certain molecules only. These limit the entry of a number of potential antibacterial agents majorly due to their lower permeability. The inactivity of INDQE compounds against Gram-negative pathogens may majorly due to their impermeability across the membrane and thus, in order to inhibit Gram-negative bacteria, it would be essential to improve the permeability of these compounds.

Figure 3.9. Protein modification with probe 51 *in situ* in *E. coli*

(reproduced with permission from *J. Med. Chem.* <https://pubs.acs.org/doi/10.1021/acs.jmedchem.9b00774>)

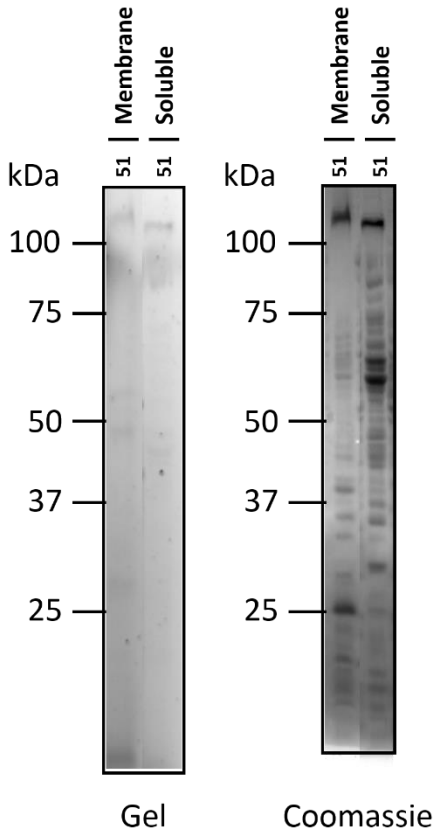

3.2.5. Competitive ABPP - Chase experiments

In the earlier experiments, it was very well established that the 'active' probe **51** profiles the *S. aureus* thiol proteome extensively, at a low concentration of 10 μM. Also, this probe was unable to penetrate into *E. coli* as suggested by the *in situ* ABPP experiments. Probe **51** was next utilized in a chase experiment in order to fish out the proteins that may be the probable targets of the lead compound **25**. The competitive ABPP experiment was set up as discussed in Chapter 1. Here, the fractionated lysates were first treated with an INDQE compound without an alkyne handle, for e.g. the lead compound **25**. This was followed by the treatment of the active alkyne probe **51**. This acts as a chase for the lead compound **25**. This was followed by the CuAAC (click reaction) and resolution and visualization of the proteins using a SDS-PAGE analysis. Now, in this experiment, compound **25** is expected to react extensively with the thiols (cysteines) on the proteins and bind covalently to them. Hence, a major subset of the total cysteine pool on the proteins will not be available to react with the active probe (chase),

as they are blocked by the lead compound **25**. Thus, after CuAAC, when these proteins are resolved and visualized using a SDS-PAGE analysis, a lower signal or labelling with respect to probe **51** is expected, as compared to the untreated control. The untreated control (DMSO), which is chased by probe **51**, will label cysteine residues according to the reactivity of the probe **51** (Fig. 3.10). This experiment will help in finding out the subset of proteins that are hit by the lead compound **25**.

Figure 3.10. Schematic of a gel for competitive ABPP - chase experiment

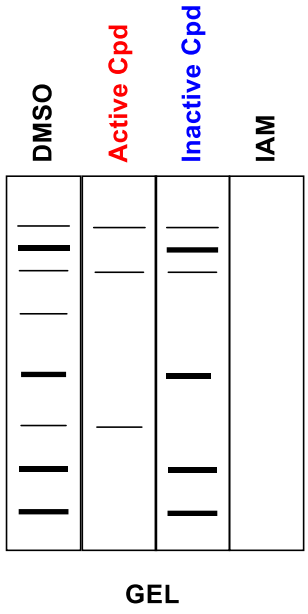

When this experiment was conducted with the lysates, it was observed, that there is a substantial signal ablation for the fractions treated with **25** as compared to the DMSO control (Fig. 3.11), and the difference distinctly visible in the soluble fraction. Similarly, when the lysates were treated with the inactive compound **28**, it was hypothesized that significantly diminished labelling would take place. Thus, the chase with probe **51**, will then differentiate between cysteine residues hit by **28** from the total set of cysteine pool. This subset may not include any probable targets of **25** that are important from the point-of-view of bacterial inhibition as compound **28** is inactive. Indeed, when treated with **28**, the signals were comparable to that obtained for the untreated fractions (Fig. 3.11). This was observed for both the membrane and soluble fractions.

Finally, when the lysates were treated with IAM, it was expected that IAM, which is used in excess, will react with all possible cysteine residues in the lysates. Thus, with the chase experiment, one would expect to see a complete ablation of the signal for probe **51**. This set of

cysteines should effectively fill up for the total cysteine pool in the lysate. The complete ablation was observed in both the cases in membrane and soluble fractions (Fig. 3.11).

Figure 3.11. Chase experiment - *In vitro* modification of proteins with INDQE compounds (membrane and soluble)

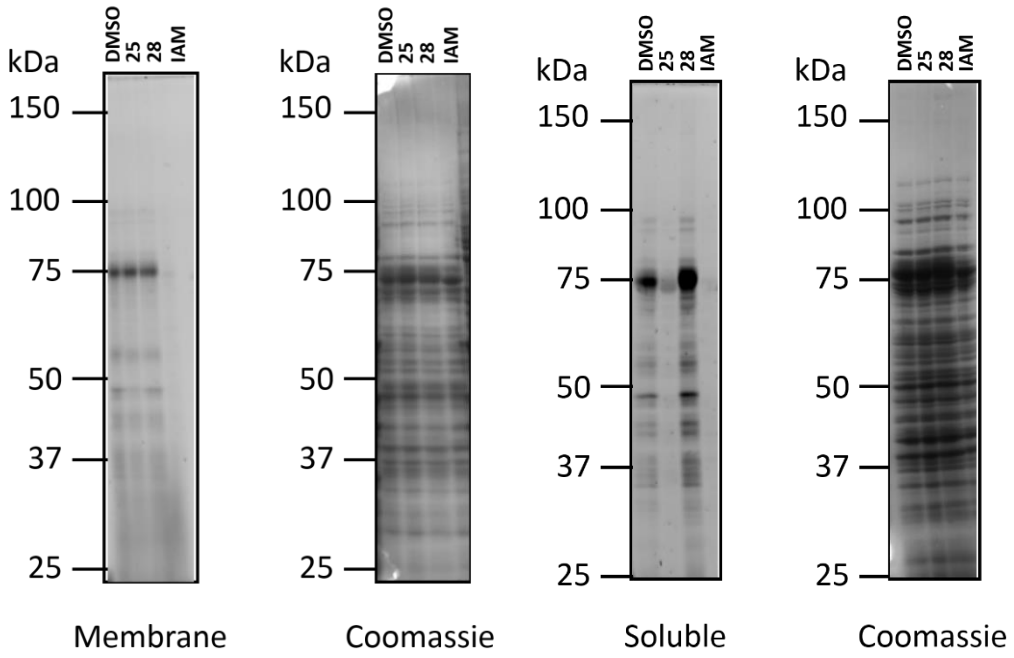

This chase experiment was next conducted *in situ* in *S. aureus*. Here, again compounds **25** and **28** were chosen. The bacteria were pre-incubated with these compounds for 1 h. Then they were lysed and fractionated. This was followed by probe **51** treatment, click reaction and finally the proteins were resolved and visualized using a SDS-PAGE analysis. Similar to the results obtained for the *in vitro* chase experiments, diminished signals were observed for the chase post compound **25** treatment, whereas comparable intensities were observed with respect to the untreated control post compound **28** treatment (Fig. 3.12). However, *in situ* studies were not as promising as the *in vitro* studies. This may be a result of some permeability differences between compounds and also the *in situ* reactivity.

Figure 3.12. Chase experiment - *in situ* modification of proteins with INDQE compounds (membrane and soluble)

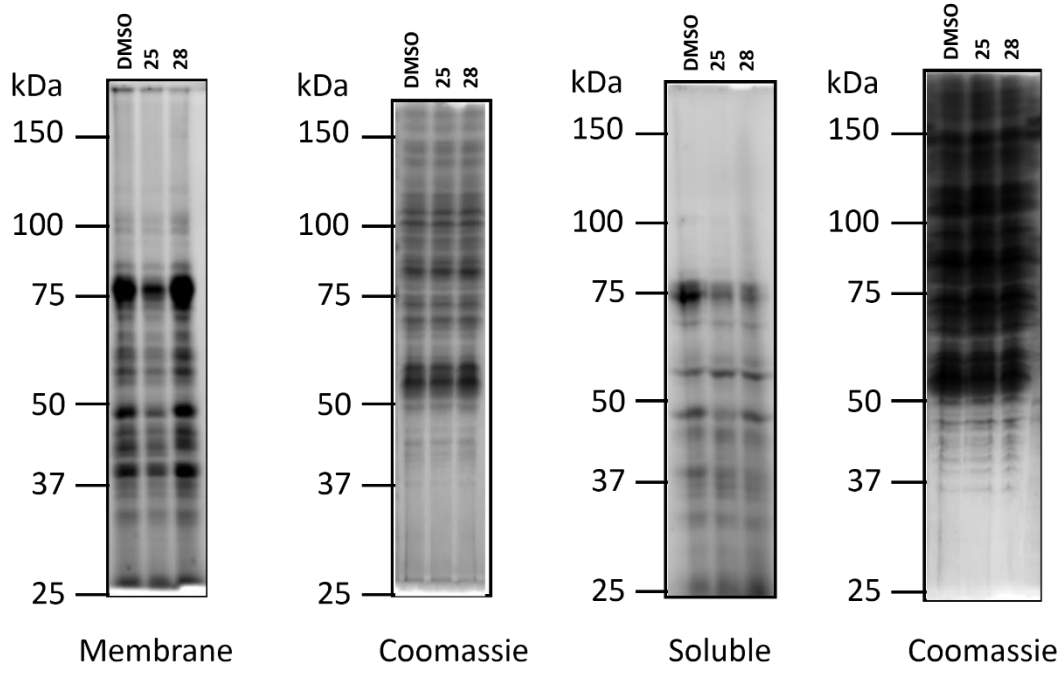

3.2.6. Competitive LC-MS/MS-based ABPP experiment for identification of targets of lead compound 25

The ABPP experiments strongly suggested that the probable targets of the lead compound **25** may be in the soluble fraction of the lysates, as the labelling was considerably more intense when compared with that obtained in the membrane fractions. Thus, in order to identify these protein targets a competitive LC-MS/MS-based ABPP experiment was conducted. Here, *S. aureus* soluble proteome was first treated with DMSO or **25** (10 μM) or **28** (10 μM) or IAM (10 mM) for 1 h. This was followed by a chase with probe **51** (10 μM) for 1 h. Then, a click reaction was conducted with biotin azide.

Biotin is a water-soluble B-vitamin and has strong affinity towards streptavidin.[20] Streptavidin is a tetramer protein purified from the bacterium *Streptomyces avidinii*. The non-covalent binding between biotin and streptavidin is one of the strongest interactions known in nature, and is thus used extensively in molecular biology. Mass spectrometry-based chemoproteomics has comprehensively used biotin-avidin affinity to fish out target proteins.

Thus, in the present experiment, the proteins of interest were tagged by the probe **51**, and followed by biotinylation. These biotinylated proteins were then enriched with avidin-agarose beads. This was then followed by on bead trypsin digestion overnight (~ 14h). Trypsin digestion helps in chopping down the proteins into smaller peptides, which could further be analysed. The tryptic peptides obtained were then subjected to LC-MS/MS based analysis to identify the respective proteins enriched in every treatment group (Fig. 3.13).

Figure 3.13. Schematic for proteomics using probe 51

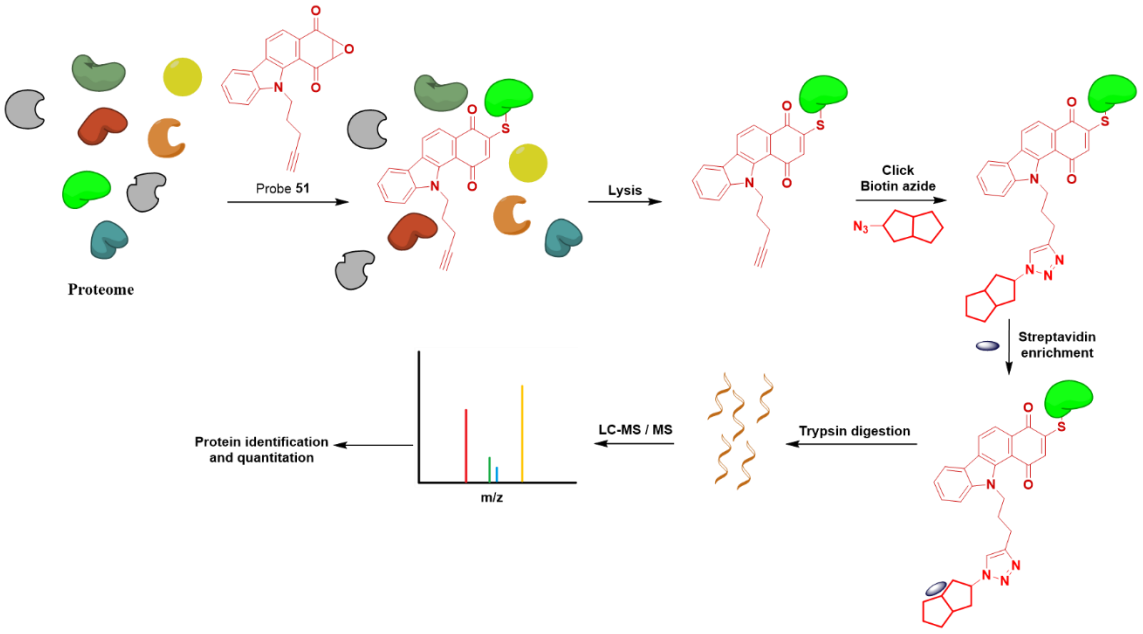

It was hypothesized that proteins absent (or largely competed) in the **25** and IAM treatment groups (ratio relative to DMSO group ≤ 0.1), but present comparable to control in the **28** treatment group (ratio relative to DMSO group ~ 1), were likely targets of **25**. Using these filtering criteria, around 17 proteins were listed out as probable targets of **25** out of the 435 proteins identified by LC-MS/MS (Table 3.3).

Table 3.3. List of probable targets from the soluble fraction with ratios identified from *in vitro* experiment

Protein IDs	Description	25 /DMSO	28 /DMSO	IAM /DMSO
AKN43_12840	MarR family transcriptional regulator	0.0	0.5	0.0
AKN43_06580	hypothetical protein	0.0	0.5	0.0
AKN43_05815	MarR family transcriptional regulator	0.0	0.5	0.1
AKN43_09265	transcriptional regulator	0.0	0.6	0.2
AKN43_05455	2-dehydropantoate 2-reductase	0.0	0.7	0.0
AKN43_07040	arsenate reductase	0.0	0.7	0.0
AKN43_06325	heme peroxidase	0.0	0.8	0.0
AKN43_04595	DNA polymerase III subunit beta	0.0	0.8	0.0
AKN43_08910	Thioredoxin	0.0	1.0	0.2
AKN43_06805	hypothetical protein	0.0	1.1	0.0
AKN43_02070; AKN43_02050	2-C-methyl-D-erythritol 4-phosphate cytidylyltransferase	0.0	1.2	0.1
AKN43_07890	catabolite control protein A	0.2	1.3	0.1
AKN43_13295	methionine aminopeptidase	0.0	1.4	0.0
AKN43_10975	hydroxyethylthiazole kinase	0.1	1.4	0.0
AKN43_12125	diaminopimelate decarboxylase	0.0	1.7	0.0
AKN43_10815	HxlR family transcriptional regulator	0.0	2.3	0.0
AKN43_04505	PhoP family transcriptional regulator	0.0	3.7	0.0

Data provided by Dr. Dhanashree Kelkar, Dr. Siddhesh Kamat Lab, IISER Pune

Out of 17 identified targets, 6 were found to be transcriptional factors or virulence factors. Identifying these as probable targets was of great significance as transcriptional factors (or virulence factors) play an important role in generating antibiotic resistance[11,21–23] and are also important from the point-of-view of fitness cost for the bacteria.[24] Having got these 17 probable

targets, a subset of 5 proteins was chosen further for validation (Table 3.4). This process would involve cloning and protein purification. This would be elaborately discussed in Chapter 4.

Table 3.4. Transcriptional factors identified as targets

	Transcriptional or Virulence factors
1.	MarR family transcriptional regulator_12840
2.	MarR family transcriptional regulator_05815
3.	Catabolite control protein A (CcpA)
4.	HxlR family transcriptional regulator
5.	PhoP family transcriptional regulator

3.3. Summary

In Chapter 2, lead compounds **25** and **27** were identified that inhibit extremely drug-resistant *S. aureus* including a number of clinical isolates of VRSA. These compounds were selectively targeting cysteine residues possibly on some key proteins of the bacteria. In this chapter, chemoproteomic profiling of the thiol proteome of *S. aureus* was undertaken in order to find out the probable targets. For this, firstly INDQE probes were synthesized with an alkyne handle, so that CuAAC can be utilised to CLICK a reporter azide onto the INDQE probe after cysteine modification through the opening of the epoxide. Probe **51**, modelled on the lead compound **25** was first synthesized. It was found that this probe reacts with a thiol and shows comparable reactivity to that of the lead compound **25**. Also, it was found to be selectively active against *S. aureus*. Another probe, compound **52**, was synthesized modelled on the compound **28**, which was found to be comparatively less reactive with a thiol. Also, it was found to be inactive against *S. aureus*. Thus, probe **51** was identified as the active probe, whereas probe **52** was identified as the inactive probe. Using these two probes, thiol proteome in the lysates of *S. aureus* was profiled, and the results suggested that reactivity with a thiol gets translated to the protein level as **51** labelled a number of cysteine residues but **52** showed diminished labelling. Similar results were obtained from an *in situ* setting for both the probes suggesting translation of reactivity with a thiol at the cellular level as well. Selectivity of probe **51** towards cysteine residues was demonstrated using IAM. To investigate lack of activity of INDQE compounds against Gram-negative pathogens, the thiol proteome of *E. coli* was

profiled using probe **51**. The probe labelled a number of protein residues in the lysates but almost none in an *in situ* setting, suggesting that the probe, and in general INDQE compounds may not be permeable in Gram-negative bacteria, which possibly may be the reason for their inactivity against these pathogens. Next, ABPP chase experiments were conducted to identify targets of lead compound **25**. This was followed with LC-MS/MS based analysis using biotin-avidin enrichment followed by trypsin digestion. From these experiments, a subset of proteins was filtered out as probable targets of lead compound **25**. The list majorly consisted of transcriptional factors (or virulent factors), which were very important probable targets as these proteins play key roles in antibiotic resistance.

Thus, having identified the probable targets, their validation was important and was planned as the next set of experiments. Cloning and purification of proteins followed by ABPP experiments with active probe **51**, would corroborate the modification of cysteine residues on these proteins. Also, further studies may include mutating out the cysteine residues on these proteins followed by ABPP experiments to validate that the activity disappears and is selective to cysteine only. These studies would be discussed in Chapter 4.

3.4. Experimental and characterization data

3.4.1. Characterization of compounds

11-(pent-4-yn-1-yl)-1H-benzo[a]carbazole-1,4(11H)-dione (48).

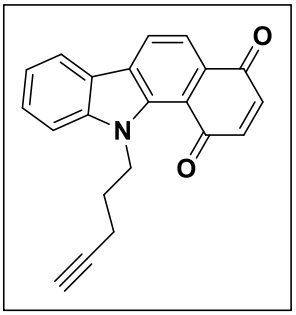

Starting from *N*-(pent-4-yn-1-yl)-indole-3-carboxaldehyde (1 g, 4.66 mmol), **48** was isolated as dark red-brown solid (264 mg, 27%). FT-IR (ν_{max}, cm^{-1}): 3280, 2922, 2857, 1658, 1615, 1465, 1378, 1292, 1182, 1122, 835, 747; ^{1}H-NMR (400 MHz, $CDCl_3$): δ 8.35 (d, *J* = 8.0 Hz, 1H), 8.09 (dt, *J* = 7.8, 0.8 Hz, 1H), 8.04 (d, *J* = 8.0 Hz, 1H), 7.62-7.56 (m, 2H), 7.35-7.31 (m, 1H), 6.94 (dd, *J* = 15.3, 10.1 Hz, 2H), 4.78 (t, *J* = 7.3 Hz, 2H), 2.13-2.08 (m, 2H), 2.05-2.03 (m, 1H), 2.00 (t, *J* = 2.6 Hz, 2H); ^{13}C NMR (100 MHz, $CDCl_3$): δ 186.1, 185.6, 144.5, 140.3, 138.1, 137.0, 131.6, 131.5, 128.5, 125.3, 122.2, 121.2, 120.9, 118.9, 118.5, 111.1, 83.5, 69.4, 46.3, 27.8, 16.1; HRMS (ESI) for $C_{21}H_{15}NO_2$ $[M+H]^+$: Calculated: 314.1181, Found: 314.1178

9-(pent-4-yn-1-yl)-1a,10a-dihydro-2H-oxireno[2′,3′:4,5]benzo[1,2-a]carbazole-2,10(9H)-dione (51).

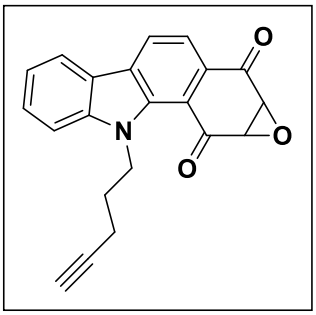

Starting from **48** (150 mg, 0.479 mmol), compound **51** was isolated as a bright yellow solid (73 mg, 46%). FT-IR (ν_{max}, cm^{-1}): 3291, 2924, 2855, 1687, 1564, 1468, 1425, 1334, 1287, 1216, 1183, 865, 742; ^{1}H NMR (400 MHz, $CDCl_3$): δ 8.36 (d, *J* = 8.0 Hz, 1H), 8.10 (d, *J* = 7.7 Hz, 1H), 7.88 (d, *J* = 8.0 Hz, 1H), 7.60 (t, *J* = 6.0 Hz, 2H), 7.35-7.32 (m, 1H), 4.68-4.61 (m, 1H), 4.57-4.49 (m, 1H), 4.14 (dd, *J* = 6.5, 4.2 Hz, 2H), 2.18-2.01 (m, 3H), 1.97-1.88 (m, 2H); ^{13}C NMR (100 MHz, $CDCl_3$): δ 192.5, 191.4, 143.9, 136.9, 131.3, 130.2, 128.6, 125.4, 121.8, 121.1, 121.0, 118.4, 117.7, 110.6, 83.2, 69.7, 56.1, 54.8, 44.4, 26.6, 16.0.; HRMS (ESI): for $C_{21}H_{15}NO_3$ $[M+H]^+$: Calculated: 330.1130, Found: 330.1131

9-(pent-4-yn-1-yl)-1a-phenyl-1a,10a-dihydro-2H-oxireno[2′,3′:4,5]benzo[1,2-a]carbazole-2,10(9H)-dione (52).

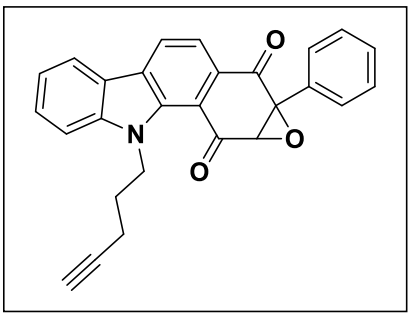

Starting from the mixture of **49, 50** (116 mg, 0.152 mmol), compound **52** was isolated as a bright yellow solid (85 mg, 70%). FT-IR (ν_{max}, cm^{-1}): 2922, 2861, 1687, 1465, 1335, 1287, 1205, 1126, 1066, 739; ^{1}H-NMR (400 MHz, $CDCl_3$): δ 8.34 (d, *J* = 8.2 Hz, 1H), 8.11 (d, *J* = 7.8 Hz, 1H), 7.97 (d, *J* = 7.9 Hz, 1H), 7.62-7.56 (m, 4H), 7.49-7.46 (m, 3H), 7.37-7.33 (m, 1H), 4.74-4.68 (m, 1H), 4.60-4.52 (m, 1H), 4.10 (s, 1H), 2.18-2.08 (m, 2H), 2.06 (t, *J* = 2.2 Hz, 1H), 1.98-1.90 (m, 2H).; ^{13}C NMR (100 MHz, $CDCl_3$): δ 192.4, 191.0, 143.9, 136.7, 131.1, 131.0, 131.0, 129.4, 128.6, 128.5, 127.9, 125.3, 121.9, 121.1, 121.0, 119.1, 117.9, 110.6, 83.2, 69.7, 65.5, 62.4, 44.4, 26.7, 16.0.; HRMS (ESI): for $C_{27}H_{19}NO_3$ $[M+H]^+$: Calculated: 406.1443, Found: 406.1443

3.4.2. X-ray diffraction analysis

52: Crystals of **52** were grown by slow evaporation from a solution of chloroform. A single crystal was mounted in a loop with a small amount of the mother liquor. The X-ray data were collected at 296 K temperature on a Bruker AXS SMART APEX CCD diffractometer using

Cu Kα radiation (λ = 1.54178 Å), ω-scans (2θ= 52.52^o), for a total number of 3398 independent reflections. Space group *P-1*, *a* = 8.0243(3), *b* = 8.6749(4), *c* = 15.0422(6) Å, α = 102.405(2), β = 95.011(2), γ = 107.124(2), *V*= 964.47(7) Å^3, monoclinic *P-1*, Z=2 for chemical formula C_{27} H_{19} N O_3.ρ calcd =1.396 g cm^{-3}, μ= 0.731 mm^{-1}, *F*(000)=424.0, R_{int} =0.0909. The structure was obtained by direct methods using SHELXS-97. All non-hydrogen atoms were refined anisotropically. The hydrogen atoms were fixed geometrically in the idealized position and refined in the final cycle of refinement as riding over the atoms to which they are bonded. The final *R* value was 0.0.0909 (*wR2*= 0.2408) for 3398, *S* = 1.095. (CCDC 1894427)

3.4.3. mBBr assay for assessing reactivity with thiol

Compound (100 µM) was reacted with *L*-cysteine (10 mM, 10 eq.) in pH 7.4 phosphate buffer (10 mM): ACN (1:1 v/v) (1 mL volume in microcentrifuge tubes) at 37 ºC. At time point of 1 h, 100 µL aliquots were taken from every tube into a 96-well microtiter plate. 2 µL of a solution of *mono*-Bromobimane (mBBr, 5 mM stock in DMSO, final concentration 100 µM, 1:1 ratio) was added to every well of the 96-well microtiter plate and then incubated for 30 min at 37 ºC in an incubator. The fluorescence (excitation at 390 nm; emission at 490 nm) was measured after 30 min using a microtiter plate reader. Each assay was conducted in duplicate and an average is reported.

3.4.4. Preparation of proteomic fractions

S. aureus (MSSA 29213) was cultured in Mueller Hinton Broth (CA-MHB) while *E. coli* (ATCC 25922) was cultured in Luria Bertani Broth medium, both at 37 ºC overnight with shaking. The cells were pelleted by centrifugation at 3220 g for 20 min, and subsequently re-suspended in 1X PBS, lysed by sonication, and eventually centrifuged at 100,000 g, at 4 ºC for 1 hour to separate the proteomic fractions. The supernatant (soluble fraction) was separated from the remaining pellet by pipetting, and the pellet were washed (3 times with 1X PBS), followed by re-suspension in 1X PBS by sonication to yield the membrane proteomic fraction. The protein concentrations were estimated by Bradford assay (Bio-rad) or BCA assay using BSA as a standard and lysate protein concentrations were adjusted to 1 mg/mL with 1X PBS, for all subsequent experiments.

3.4.5. Gel based chemoproteomics experiment

100 µL of 1 mg/mL protein for both membrane and soluble fractions was taken in a 1.5 mL microcentrifuge tube. The proteomic fractions were treated with varying concentrations of the probes (**51** or **52**, 0 – 100 µM) or DMSO at 37 ºC for 1 hour with constant shaking (700 rpm). To these tubes, was added, 11 µL of a 'click' mixture consisting of 6 µL TBTA (1.7 mM in 4:1 DMSO-^{t}BuOH), 2 µL $CuSO_4.5H_2O$ (50 mM in water), 2 µL TCEP (50 mM in DPBS - Dulbecco´s PBS 1X) and 1 µL Rhodamine azide (Alexa Fluor 488, 10 mM in DMSO), and the reaction was incubated for a further 60 min at 25 ºC. The reactions were quenched by adding 40 µL of 4X loading dye and the samples were resolved and visualized on a SDS-PAGE gel using established protocols.

For the iodoacetamide (IAM) competition experiments, the lysates (membrane and soluble) were first pre-treated with 10 mM IAM or DMSO at 25 ºC for 1 hour following which they were treated with **51** (10 µM at 37 ºC for 1 hour). Thereafter, the click reaction was performed as described above, the reactions quenched and visualized by SDS-PAGE gels. For the *in situ* cell treatments, *S. aureus* and *E. coli* cultures (25 mL at OD_{600} ~ 1.5) were treated with 10 µM **51** or **52** for 1 h, following which the cells were harvested, the proteomic fractions (soluble and membrane) prepared, click reaction performed, and the reactions visualized by SDS-PAGE gel analysis as described above.

3.4.6. Mass spectrometry based chemoproteomics

S. aureus cells were lysed in 1X DPBS by sonication and fractionated into membrane bound and soluble fractions by ultracentrifugation (100,000 g for 1 hour at 4 ˚C). The soluble fraction was incubated with **25**, or **28**, or IAM or vehicle (DMSO) at 10 µM final concentration for 1 hour at 37 ºC while constantly shaking (700 rpm). Each group contained three biological replicates. The compound or vehicle treated soluble proteomes were chased with **51** (10 µM, 1 hour at 37 ºC, shaking). The click reaction was done as described earlier with the exception that biotin-azide was used instead of rhodamine azide. Post-biotinylation, the proteomes were denatured and precipitated using 4:1 methanol: chloroform at 4 ºC, and re-suspended in 0.5 mL 6 M urea in DPBS by sonication. Reduction and alkylation was carried out with TCEP (10 mM) and K_2CO_3 (30 mM) for 30 mins at 37 ºC with constant shaking, and IAM (50 mM) for 30 mins at room temperature (25 ºC) in the dark, respectively. The biotinylated proteins were enriched using avidin-agarose beads (100 µL, Sigma-Aldrich) by shaking at room temperature for 2 hours in DPBS containing 0.2% (w/v) SDS in a final volume of 6 mL. The beads were

pelleted by centrifugation at 1000 g for 5 mins, and sequentially washed using 10 mL of 0.2% (w/v) SDS in DPBS (3X), 10 mL of DPBS (3X) and 10 mL of deionized water (3X). The beads were transferred to a Protein LoBind 1.5 mL microcentrifuge tube. On-bead protein digestion was performed using sequence grade trypsin (1.5 µg, Promega) in 200 µL of 100 mM TEAB buffer containing 2 M urea at 37 ^{o}C with constant shaking for 14 hours. Reaction was quenched by adding TFA to final concentration of 1% (v/v). Peptides were cleaned on C18 Stage tips and subjected to LC-MS/MS analysis on Agilent 6540 Accurate-Mass Q-ToF mass spectrometer coupled with Agilent HPLC-Chip Cube system. Peptides were separated on Agilent HPLC-Chip consisting of C18 enrichment and analytical column (75 µm, 10 cm) system. The LC run was a 2 hours long linear acetonitrile gradient (5% to 50%). Mass spectrometry data was collected in an information dependent acquisition (IDA) mode over a mass range of 300 – 2000 m/z, and each full MS survey scan was followed by 10 fragment scans. Dynamic exclusion was enabled for all experiments (repeat count 1, exclusion duration 30 s). Protein identification and quantitation was carried out using MaxQuant software (version 1.6). Spectral data was searched against *S. aureus* NCTC 8325 protein database downloaded from Ensembl FTP server. Precursor mass tolerance of 0.01 Da and fragment mass tolerance of 40 p.p.m. was allowed. Carbamidomethylation of cysteine was used as fixed modification and oxidation of methionine was used as variable modification. Peptides and proteins were filtered at 1 % false discovery rate. Label free quantitation was performed using LFQ option in the MaxQuant. Protein LFQ intensity value was accepted only when two or more quantifiable peptides were identified in more than 2 replicates per experimental group. Quantitation was performed by taking a ratio of the average intensity with respect to control sample (DMSO treated).

3.5. Spectral charts

^{1}H NMR of **48**

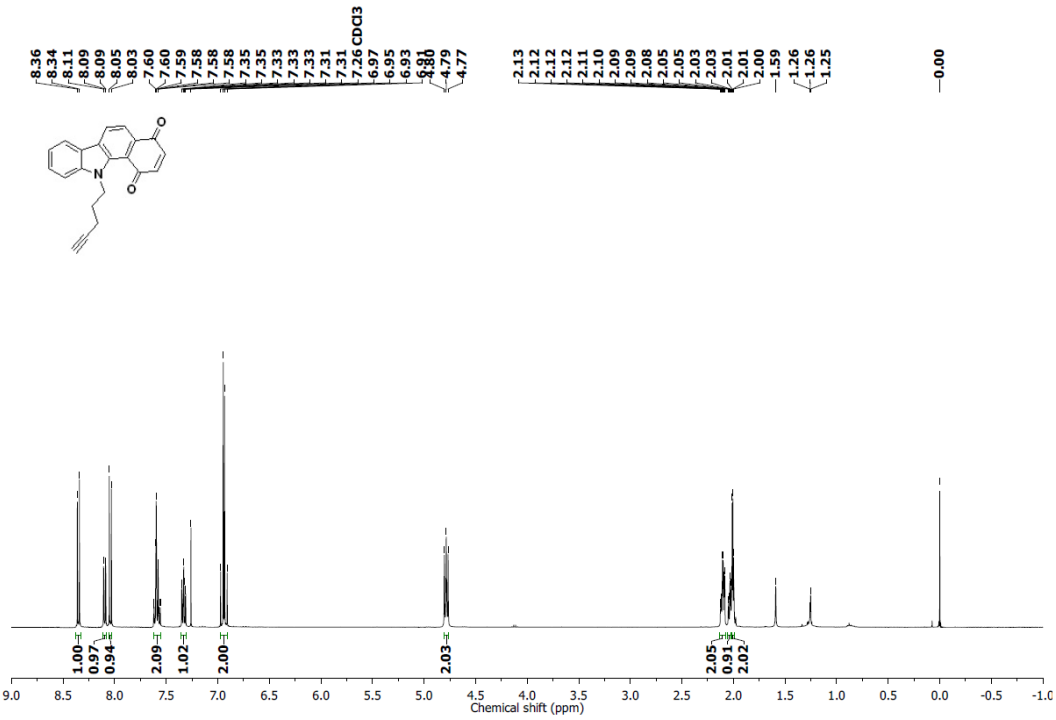

^{13}C NMR of **48**

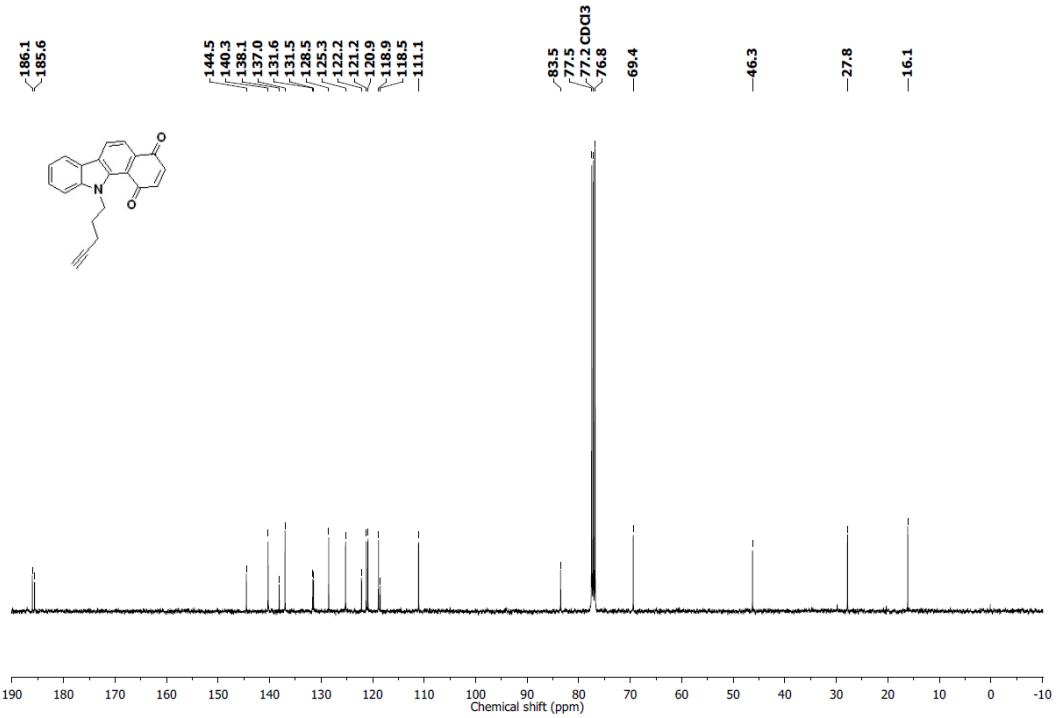

^{1}H NMR of **51**

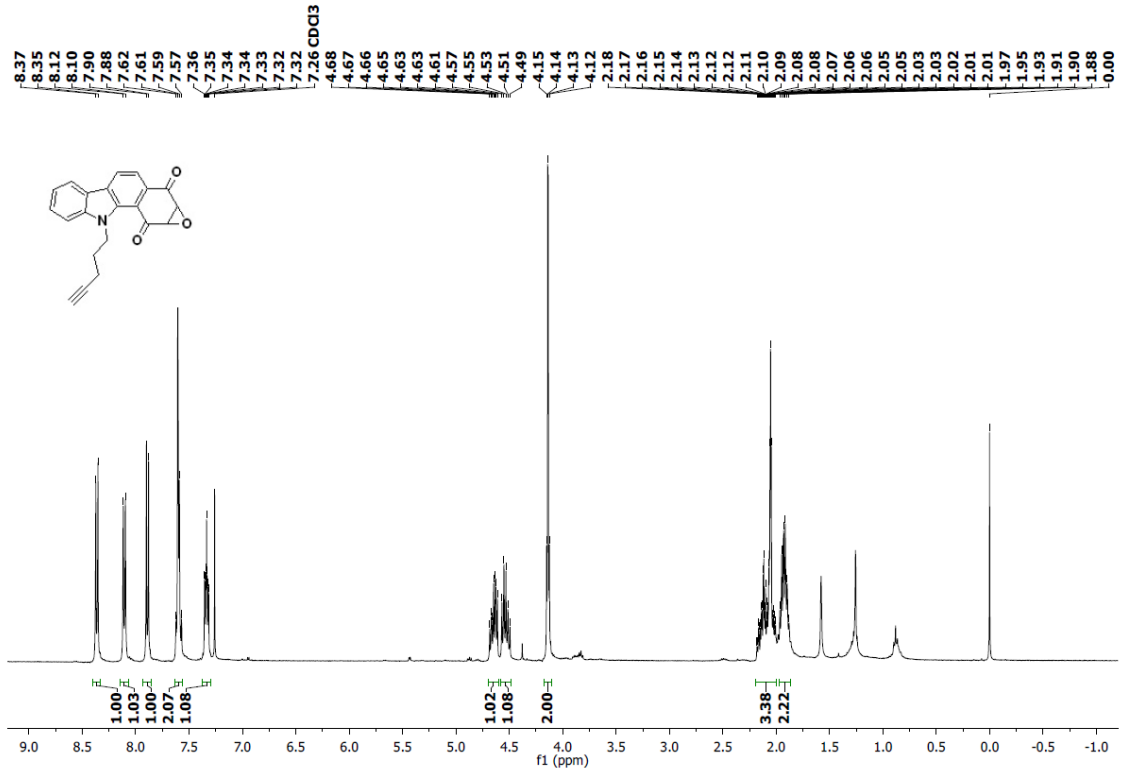

^{13}C NMR of **51**

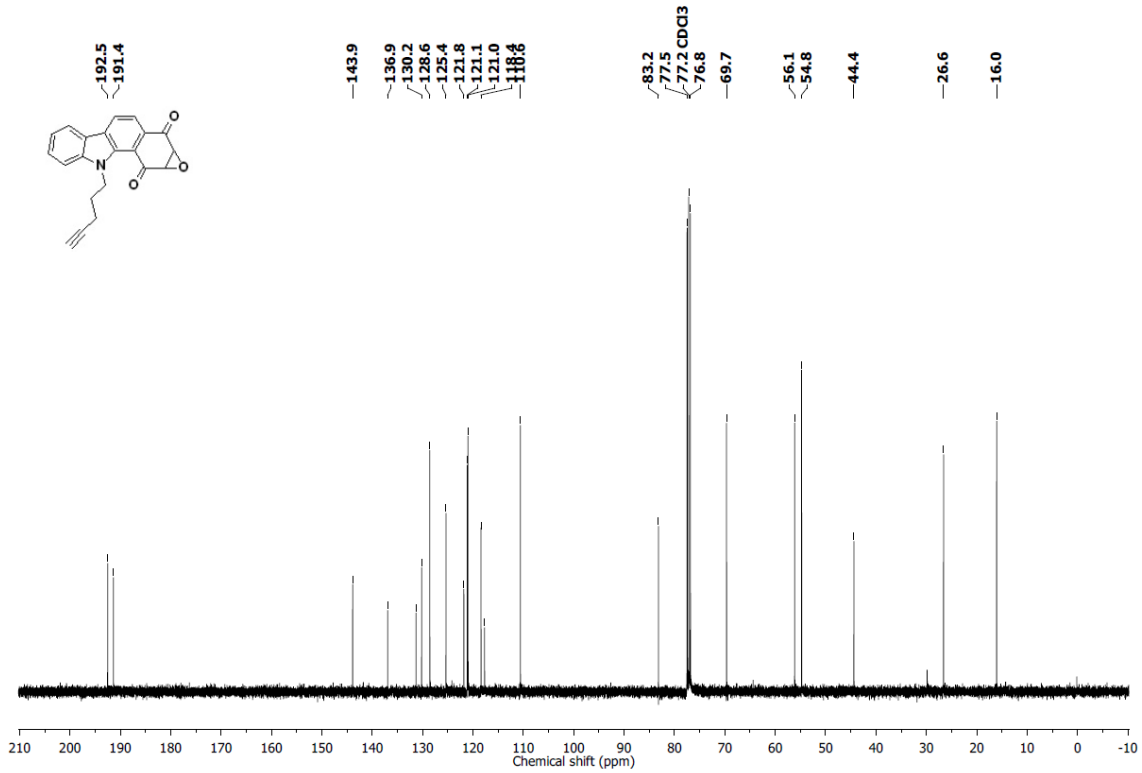

^{1}H NMR of **52**

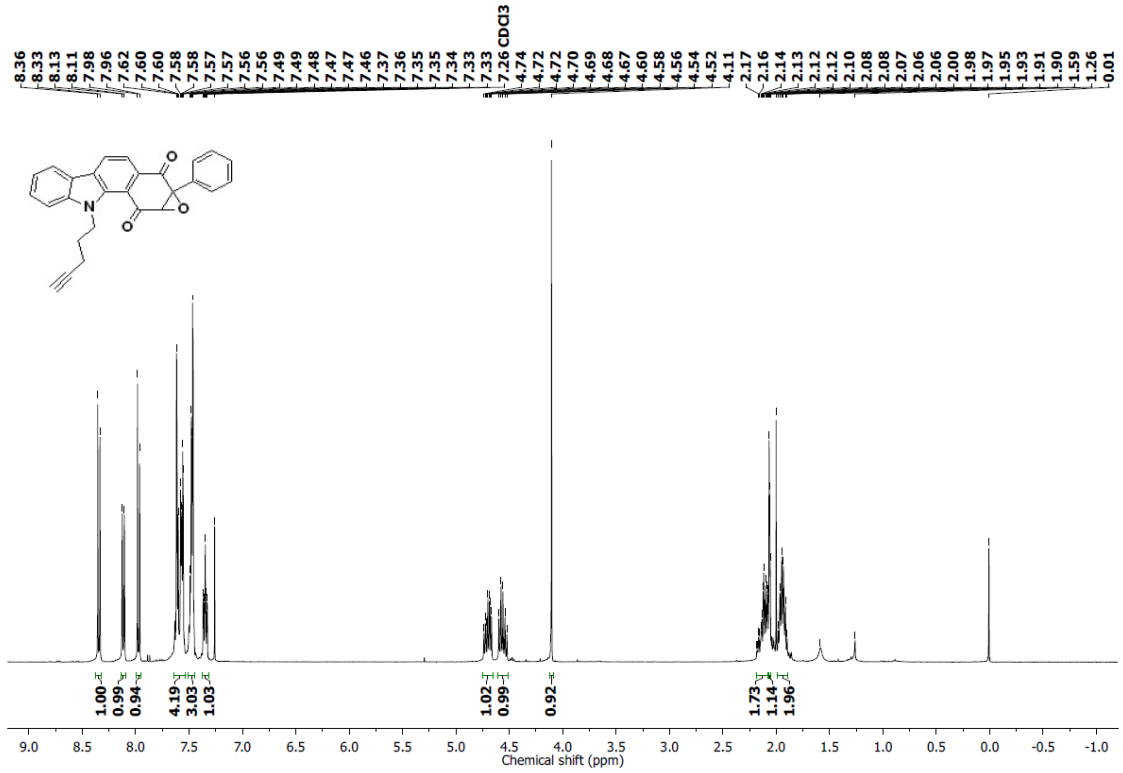

^{13}C NMR of **52**

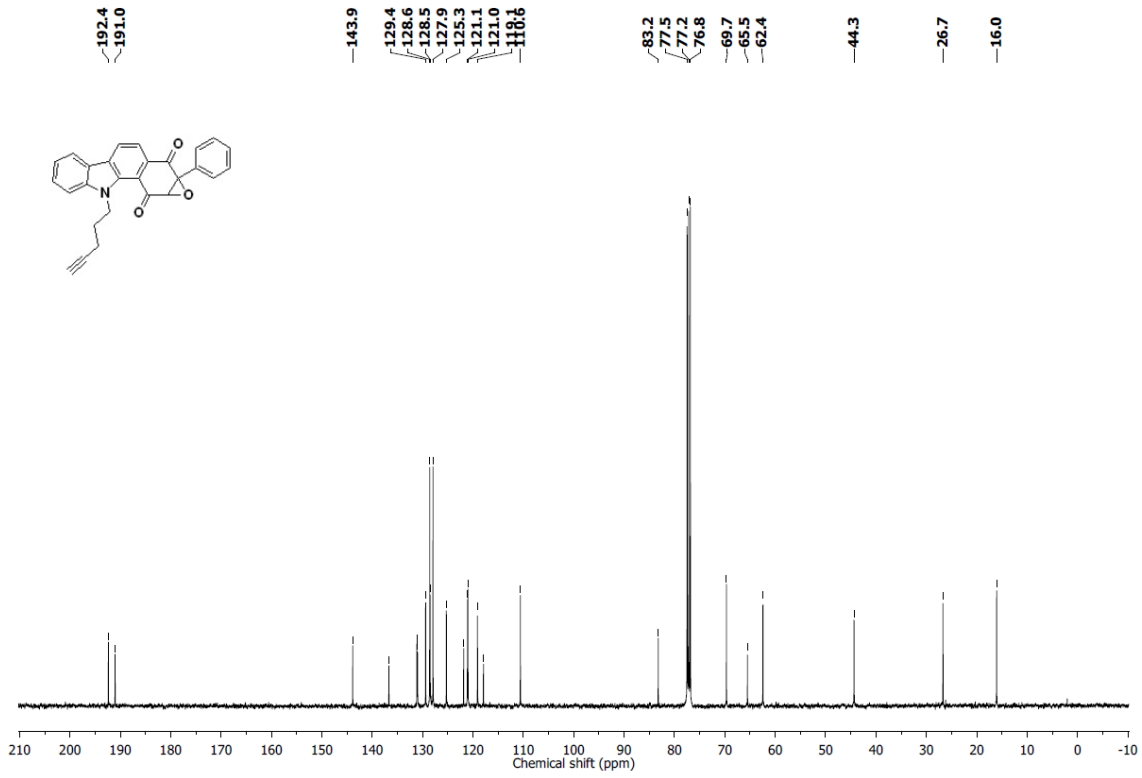

3.6. References

(1) Cha, R.; Brown, W. J.; Rybak, M. J. Bactericidal Activities of Daptomycin, Quinupristin-Dalfopristin, and Linezolid against Vancomycin-Resistant Staphylococcus Aureus in an in Vitro Pharmacodynamic Model with Simulated Endocardial Vegetations. *Antimicrob. agents chemother.* **2003**, *47* (12), 3960–3963.

(2) Casini, A.; Scozzafava, A.; Supuran, C. T. Cysteine-Modifying Agents: A Possible Approach for Effective Anticancer and Antiviral Drugs. *Environ. Heal. Perspect.* **2002**, *110 Suppl* (Suppl 5), 801–806.

(3) Visscher, M.; Arkin, M. R.; Dansen, T. B. Covalent Targeting of Acquired Cysteines in Cancer. *Curr. Opin. Chem. Biol.* **2016**, *30*, 61–67.

(4) Kathman, S. G.; Statsyuk, A. V. Covalent Tethering of Fragments for Covalent Probe Discovery. *Medchemcomm* **2016**, *7* (4), 576–585.

(5) Hallenbeck, K. K.; Turner, D. M.; Renslo, A. R.; Arkin, M. R. Targeting Non-Catalytic Cysteine Residues Through Structure-Guided Drug Discovery. *Curr. Top. Med. Chem.* **2017**, *17* (1), 4–15.

(6) Long, M. J. C.; Aye, Y. Privileged Electrophile Sensors: A Resource for Covalent Drug Development. *Cell Chem. Biol.* **2017**, *24* (7), 787–800.

(7) Paulsen, C. E.; Carroll, K. S. Cysteine-Mediated Redox Signaling: Chemistry, Biology, and Tools for Discovery. *Chem. Rev.* **2013**, *113* (7), 4633–4679.

(8) Pace, N. J.; Weerapana, E. Diverse Functional Roles of Reactive Cysteines. *ACS Chem. Biol.* **2013**, *8* (2), 283–296.

(9) Loi, V. Van; Busche, T.; Preuß, T.; Kalinowski, J.; Bernhardt, J.; Antelmann, H. The AGXX® Antimicrobial Coating Causes a Thiol-Specific Oxidative Stress Response and Protein S-Bacillithiolation in Staphylococcus Aureus. *Front. Microbiol.* **2018**, *9*, 3037.

(10) Imber, M.; Huyen, N. T. T.; Pietrzyk-Brzezinska, A. J.; Loi, V. Van; Hillion, M.; Bernhardt, J.; Thärichen, L.; Kolšek, K.; Saleh, M.; Hamilton, C. J.; et al. Protein S - Bacillithiolation Functions in Thiol Protection and Redox Regulation of the Glyceraldehyde-3-Phosphate Dehydrogenase Gap in Staphylococcus aureus Under Hypochlorite Stress. *Antioxid. Redox Signal.* **2018**, *28* (6), 410–430.

(11) Sun, F.; Ding, Y.; Ji, Q.; Liang, Z.; Deng, X.; Wong, C. C. L.; Yi, C.; Zhang, L.; Xie,

S.; Alvarez, S.; et al. Protein Cysteine Phosphorylation of SarA/MgrA Family Transcriptional Regulators Mediates Bacterial Virulence and Antibiotic Resistance. *Proc. Natl Acad. Sci. U S A* **2012**, *109* (38), 15461–15466.

(12) Puri, A. W.; Bogyo, M. Using Small Molecules To Dissect Mechanisms of Microbial Pathogenesis. *ACS Chem. Biol.* **2009**, *4* (8), 603–616.

(13) Moellering, R. E.; Cravatt, B. F. How Chemoproteomics Can Enable Drug Discovery and Development. *Chem. Biol.* **2012**, *19* (1), 11–22.

(14) Gersch, M.; Kreuzer, J.; Sieber, S. A. Electrophilic Natural Products and Their Biological Targets. *Nat. Prod. Rep.* **2012**, *29* (6), 659–682.

(15) Kunzmann, M. H.; Bach, N. C.; Bauer, B.; Sieber, S. A. α-Methylene-γ-Butyrolactones Attenuate Staphylococcus Aureus Virulence by Inhibition of Transcriptional Regulation. *Chem. Sci.* **2014**, *5* (3), 1158.

(16) Mandl, F. A.; Kirsch, V. C.; Ugur, I.; Kunold, E.; Vomacka, J.; Fetzer, C.; Schneider, S.; Richter, K.; Fuchs, T. M.; Antes, I.; et al. Natural-Product-Inspired Aminoepoxybenzoquinones Kill Members of the Gram-Negative Pathogen Salmonella by Attenuating Cellular Stress Response. *Angew. Chem. Int. Ed.* **2016**, *55* (47), 14852–14857.

(17) Kosower, N. S.; Kosower, E. M. Thiol Labeling with Bromobimanes. *Methods Enzym.* **1987**, *143*, 76–84.

(18) Hoch, D. G.; Abegg, D.; Adibekian, A. Cysteine-Reactive Probes and Their Use in Chemical Proteomics. *Chem. Commun.* **2018**, *54* (36), 4501–4512.

(19) Anna E. Speers; Gregory C. Adam, A.; Cravatt*, B. F. Activity-Based Protein Profiling in Vivo Using a Copper(I)-Catalyzed Azide-Alkyne [3 + 2] Cycloaddition. *J. Am. Chem. Soc.* **2003**, *125* (16), 4686–4687.

(20) Weerapana, E.; Wang, C.; Simon, G. M.; Richter, F.; Khare, S.; Dillon, M. B. D.; Bachovchin, D. A.; Mowen, K.; Baker, D.; Cravatt, B. F. Quantitative Reactivity Profiling Predicts Functional Cysteines in Proteomes. *Nature* **2010**, *468* (7325), 790–795.

(21) Tiwari, S.; da Costa, M. P.; Almeida, S.; Hassan, S. S.; Jamal, S. B.; Oliveira, A.; Folador, E. L.; Rocha, F.; de Abreu, V. A. C.; Dorella, F.; et al. C. Pseudotuberculosis

Phop Confers Virulence and May Be Targeted by Natural Compounds. *Integr. Biol.* **2014**, *6* (11), 1088–1099.

(22) Miller, S. I.; Kukral, A. M.; Mekalanos, J. J. A Two-Component Regulatory System (PhoP PhoQ) Controls Salmonella Typhimurium Virulence. *Proc. Natl Acad. Sci. U S A* **1989**, *86* (13), 5054–5058.

(23) Gordon, C. P.; Williams, P.; Chan, W. C. Attenuating Staphylococcus aureus Virulence Gene Regulation: A Medicinal Chemistry Perspective. *J. Med. Chem.* **2013**, *56* (4), 1389–1404.

(24) Andersson, D. I.; Hughes, D. Antibiotic Resistance and Its Cost: Is It Possible to Reverse Resistance? *Nat. Rev. Microbiol.* **2010**, *8*, 260.

CHAPTER 4. Validation of protein targets of INDQE compounds

4.1. Introduction

In Chapter 3, two INDQE alkyne probes were synthesized and identified as 'active' and 'inactive' based upon their reactivity with thiol and antibacterial potency. Using these probes as a tool in an ABPP chemoproteomic approach, the thiol proteome of *S. aureus* was profiled and probable targets of our lead compound **25** were pulled down using avidin-enrichment and trypsin-based digestion. 17 potential targets were identified, out of which 6 proteins were found to be transcriptional factors (TF) (or virulence factors).

Transcriptional factors are proteins that bind to a specific DNA sequence and control the transcription rate.[1] Transcription rate is the rate at which genetic information is passed by a DNA onto a messenger RNA. Thus, TFs play a very crucial role in the cell. In bacteria such as *S. aureus*, regulation of virulence determination is majorly done by these DNA-binding proteins and are thus considered important for the mere survival of these bacteria.[2,3] A perspective on the identified targets suggested a number of literature reports showcasing the importance of these proteins across different pathogens. For example, Mar R family of proteins are named for *E. coli* that regulate an operon that encodes a drug efflux pump.[4] Also, Mar R has been reported as a copper sensor in *E. coli*[5] and is also important from the point-of-view of controlling DNA repair and maintaining cell membrane integrity.[6] In other reports, protein cysteine phosphorylation of SarA-MgrA family of transcriptional regulators was found to be very crucial for mediating bacterial virulence and antibiotic resistance.[7] Another report suggested the importance of the two-component regulatory system of PhoP-PhoQ in controlling virulence in *S. typhimurium*.[8] In *M. tuberculosis*, PhoP plays an important role as a response regulator for the DNA sequence recognition.[9] CcpA was reported recently as a target of silver ions in *S. aureus* and the binding takes place *via* its two cysteines.[10] Thus, considering these reports, TFs are attractive targets from an antimicrobial perspective.

Number of studies have been reported where these proteins or their homologs have been targeted for the inhibition of bacteria. As already discussed in Chapters 2 and 3, Sieber and co-workers have reported small molecules that covalently bind to transcriptional regulators like SarA, SarS and MgrA to inhibit Gram-negative pathogen *S. typhimurium*.[11] The PhoP-PhoQ system has been targeted by various approaches[12] such as by inhibiting PhoQ Histidine kinases in *S. flexneri*,[13] by using natural products to target PhoP to inhibit *C. pseudotuberculosis*,[14] and using small molecule inhibitors of PhoP response regulator in *S.*

enterica.[15] Although, not directly targeting the identified transcriptional factors, there are reports where targeting the transcription regulatory system has resulted in inhibition of bacteria.[16–18] Giedroc and co-workers report the importance of cysteine sulfur chemistry in transcriptional regulators at the Host-Bacterial pathogen interface that highlights the possibility of targeting cysteine residues on such proteins for bacterial inhibition.[19]

With these useful insights in the literature of transcriptional factors, it is easy to understand the importance of hitting these targets in pathogenic bacteria like *S. aureus* for the development of better antibacterial agents.

4.2. Results and Discussion

Using chemoproteomics, a subset of proteins were pulled down as probable targets of the lead compound **25**, which were further subjected to a validation process. Out of the filtered list of 17 proteins identified as probable targets, 5 proteins were chosen namely Mar R 05815, Mar R 12840, HxlR, Pho P and CcpA. The two Mar R (Multiple Antibiotic Resistance regulator) proteins belong to the family of proteins which are known, as the name suggests, to regulate the antibiotic resistance in pathogenic bacteria, and were of more interest as these were novel targets. First, a Bioinformatic assay or sequence alignment study was conducted for all the five probable targets. Interestingly, all the identified proteins were found to have at least one conserved cysteine residue across all ESKAPE pathogens (Table 4.1). This was an important finding as it reinforced our hypothesis that lead compound **25** targets a protein cysteine residue.

Table 4.1. Bioinformatics assay

	Transcriptional or Virulence factors	Cysteine residue(s)	Conserved Cysteine residue(s)
1	MarR family transcriptional regulator_12840	C12	C12
2	MarR family transcriptional regulator_05815	C61	C61
3	Catabolite control protein A (Ccpa)	C216, C242	C242
4	HxlR family transcriptional regulator	C4, C29, C32	C4
5	PhoP family transcriptional regulator	C31, C65	C31, C65

For validation of these identified targets, cloning, expression and purification of the wild type proteins was planned using *E. coli* bacteria as the model organism. Generating the cysteine point mutants of the target proteins would help further in the validation of targets.

Figure 4.1. General scheme depicting the process of cloning and protein purification

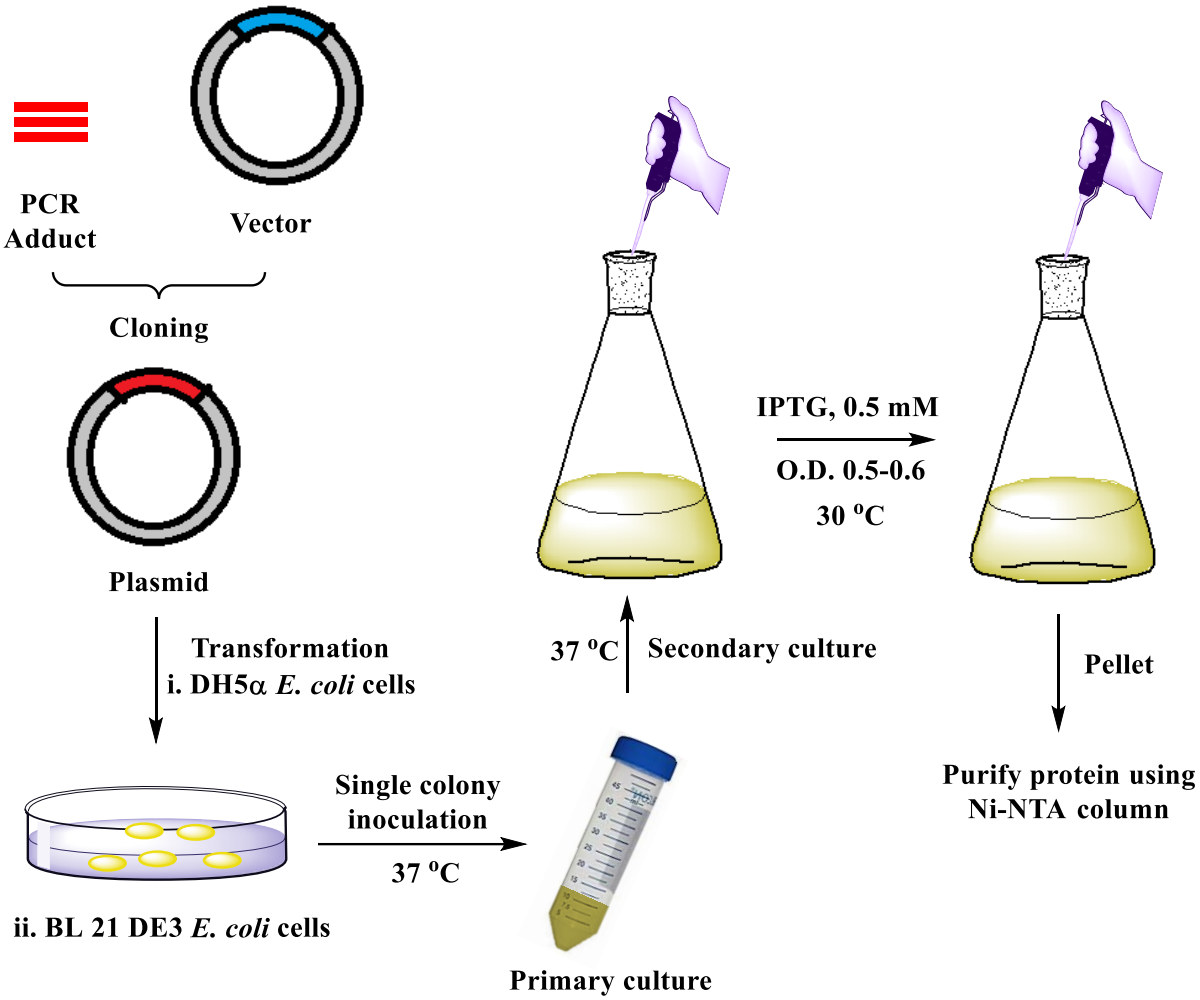

4.2.1. Plasmid isolation

S. aureus ATCC 29213 cells were incubated in MHB at 37 °C overnight. The genomic DNA was extracted and concentration adjusted to 59.2 ng/µL. This plasmid was then used as a template for the amplification of the genes that would further be used for expression of the target proteins.

4.2.2. Polymerase Chain Reaction (PCR)

The genes which would clone the 5 target proteins were amplified using PCR techniques. The forward and reverse primers were designed with their respective restriction sites (Table 4.2).

Table 4.2. Primers and restriction sites

Name	Sequence	Length	% GC	T_m	T_m of gene portion	Restriction site
Mar R 05815 Fwd-pET-30b+	gccgcaagcttgtcgaATTTTTCCTTTGTTTCATCA	36	42	63	42	SalI
MarR 05815 Rvs-pET-30b+	ttaagaaggagatatacataATGTCTGATCAACATAATTT	40	25	58	42	NdeI
MarR 12840_pET-30b+ Fwd	ggccgcaagcttgtcgaATTCAAAAACAAGATG	33	45	63	33	NdeI
MarR 12840_pET-30b+ Rev	gaaggagatatacataATGAAATATAATAACCATG	35	26	56	38	SalI
ccp a_pET-22b+ Fwd	ttgtcgacggagctcgaattTTTTGTAGTTCCTCGG	36	66	47	41	NdeI
ccp a_pET-22b+ Rev	ttaagaaggagatatacataATGACAGTTACTATATATG	39	58	26	40	EcoRI
HxlR_pET-22b+ Fwd	acggagctcgaattcggatcTTTAGCAGTACGTTGATCTG	40	68	48	48	NdeI
HxlR_pET-22b+ Rev	ttaagaaggagatatacataATGGAAGTATGTCCGTATC	39	61	33	47	BamHI
PhoP 04505_pET-22b+ Fwd	gtggtggtggtggtgctcgaACTCATGTTGTTGGAGG	37	57	70	45	XhoI
PhoP 04505_pET-22b+ Rev	ttcgagctccgtcgaATGGCTAGAAAAGTTGTTGT	34	47	64	46	SalI

*Primers designed by Abinaya Rajendran, Dr. Siddhesh Kamat Lab, IISER Pune

The PCR products were run on agarose gels, checked for the correct amplicon size and extracted from the gel. The extraction was done using Qiagen gel extraction kit. The extracted amplicons were run on agarose gel again to check for purity (Fig. 4.2).

Figure 4.2. PCR Amplification

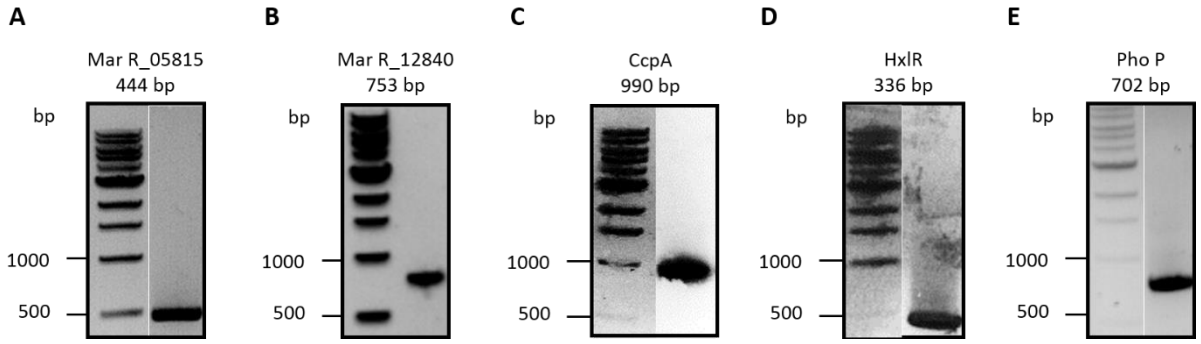

*Done by Abinaya Rajendran and Sharvari Tamhankar, Dr. Siddhesh Kamat Lab, IISER Pune

4.2.3. Restriction digestion

These plasmids were digested at their respective restriction sites using restriction enzymes. *marR* 12840 and *marR* 05815 were cloned into pET-30b(+) bacterial expression vector between NdeI and SalI sites. *phoP*, *hxlR* and *ccpA* genes were cloned in pET-22b(+) bacterial expression vector between XhoI and SalI (*phoP*), NdeI and BamHI (*hxlR*), and NdeI and EcoRI (*ccpA*) sites. All the genes were cloned using SLIC (sequence- and ligation-independent cloning) method[20] keeping the His-tag at the C-terminal. These plasmids were then further used for transformation into DH5α *E. coli* cells.

4.2.4. Transformation into *E. coli* DH5α cells

DH5α *E. coli* cells are competent engineered cells prepared for enhancing transformation efficiency. These are often used with calcium chloride transformation to insert the plasmid. These cells lack endonucleases and thus are useful in generating multiple copies of the plasmid. The PCR product were transformed in the cells using a heat shock method (42 ^{o}C, 45 sec). The cells were grown in LB broth for 1 h and finally plated onto an LB agar plate. The agar plate was preloaded with an antibiotic for avoiding contamination. The plasmids bear antibiotic resistant genes (Table 4.3).

Table 4.3. Antibiotics used for respective vectors

Vector	Genes	Resistance against
pET 22b+	Ccpa, HxlR, Pho P	Ampicillin
pET 30b+	Mar R_05815, Mar R_12840	Kanamycin

4.2.5. Sequencing

Isolated 2-3 colonies were obtained in each case. The bacteria were grown in LB broth and plasmids were extracted using regular Mini-Prep kit. These samples were then submitted for sequencing analysis to confirm the presence of the cloned gene.

4.2.6. Overexpression in BL21 (DE3) cells

After confirming from the sequencing analysis, the plasmids were then transformed into BL21 (DE3) cells for the overexpression of the proteins of interest. BL21 (DE3) are protease deficient competent cells routinely used for overexpression using the T7 promoter. Using IPTG induced overexpression, proteins of interest were overexpressed in these cells. Isopropyl-β-D-1-thiogalactopyranoside (IPTG) is a molecular mimic of allolactose. Allolactose is a lactose metabolite that triggers transcription of the *lac* operon. Hence, it is used to induce gene expression where the gene is under the control of the *lac* operon. IPTG does not get hydrolysed by β-galactosidase like allolactose, and hence is extensively used for induction procedures (for pET vector systems).

4.2.7. Purification of proteins

The cells with overexpression of the proteins of interest were fractionated and both the membrane and soluble fractions were evaluated for the overexpression. SDS-PAGE analysis of the soluble fractions suggested high levels of overexpression and hence were chosen for purification process as purifying a protein from the soluble fraction is more feasible than that from the membrane fraction. The Histidine-tagged proteins were next purified using Ni-NTA affinity chromatography. Histidine derivatives play the role of ligands to metal ions such as nickel (Ni^{2+}) by means of which the protein ligates to the Ni-NTA complex. Imidazole is used as a competitor that can displace the His-tagged protein. Imidazole has greater affinity to Nickel. The protein was eluted out, fractions collected and the purity of the protein was

confirmed using SDS-PAGE. Following this, the fractions were combined and desalted using a dialysis membrane. The concentrations of the proteins were measured using a standard Bradford assay and aliquots were stored at -80 ^{o}C till further use.

4.2.8. ABPP Chase experiment for validation of targets

Cysteine residues on proteins in the cellular environment are not always in their reduced form. They may be present in their dimer form i.e. disulfide. For the thiol-epoxide reaction (Scheme 4.1) to work efficiently, it is a prerequisite that the cysteine residue is in its reduced form.

Scheme 4.1. Reaction between cysteine thiol on a protein and quinone-epoxide

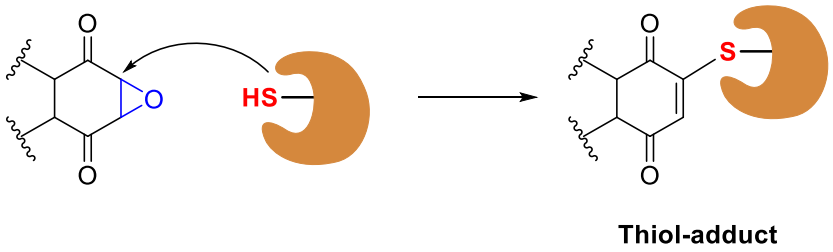

Thus, a test experiment was conducted to investigate the labelling of the cysteine residue of the protein Ccpa by probe **51** in the presence and absence of two commonly used reducing agents namely DTT and β-ME. Also, literature reports suggested that DMSO can catalyse the formation of the disulfide bond between two cysteine residues on the protein surface. Hence, permutations and combinations of DMSO were also incorporated in this assay. (Fig. 4.3).

Figure 4.3. Test experiment to investigate the reduced form of cysteine residue in Ccpa

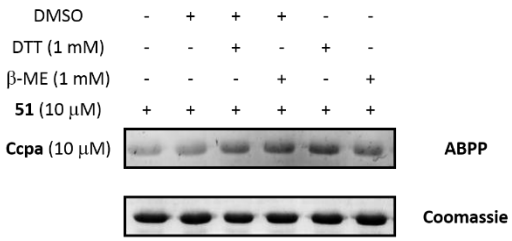

Diminished intensities for probe **51** were observed for the reaction without any additives (lane 1). It was observed that the intensities of the labelling were indeed affected by the presence of DMSO in the reaction (lanes 2-4), although addition of a reducing agent, either DTT (lane 3) or β-ME (lane 4) did improve the intensities of the labelling. However, when

the reaction mixture was pretreated only by a reducing agent (lanes 5-6), the labelling intensities were not found to be substantially improved.

Having got this understanding, a chase experiment was next conducted with the wild-type proteins as was performed with the *S. aureus* lysates in Chapter 3. Here, a fixed concentration (10 μM) of each protein was used. Aliquots were treated with fixed concentrations of compounds **25** (5×, 50μM), **28** (5×, 50μM) and IAM (10×, 100μM, in the dark) for 1 h. These were further treated (chased) with probe **51** (1×, 10μM) for 1 h. Finally, click reaction was conducted and the protein(s) visualized using a SDS-PAGE setup. As was hypothesized for the chase experiment in Chapter 3, labelling with respect to the probe **51** was expected for the untreated control. The active compound **25** treated aliquot was expected to show diminished signals for probe **51**. Similarly, inactive compound **28** treated aliquot was expected to show signal comparable to the untreated control. Finally, IAM treated aliquot was expected to show a complete aberration of signal for probe **51**.

With this hypothesis, the assay was first conducted with Ccpa. Surprisingly, diminished signals were observed for the untreated control when compared with the ones treated with compounds **25** and **28** (Fig. 4.4. A). However, the comparison between **25** treated and **28** treated aliquots was found to be as expected, where the latter showed a more intense signal after chased by probe **51**. Also, as expected IAM pre-treated aliquot showed complete aberration of the signal for probe **51**. Similar results were obtained for other proteins Mar R_05815 and Mar R_12840 (Fig. 4.4. B and C). In the case of HxlR, no inference could be made due to poor visualization of the bands on the gel (Fig. 4.4. D). Lastly, with Pho P, diminished signals were observed for all 4 lanes suggesting poor labelling or reactivity of probe **51** with cysteine residues on the protein surface. (Fig. 4.4. E).

Figure 4.4. ABPP chase experiment with wild-type proteins (targets)

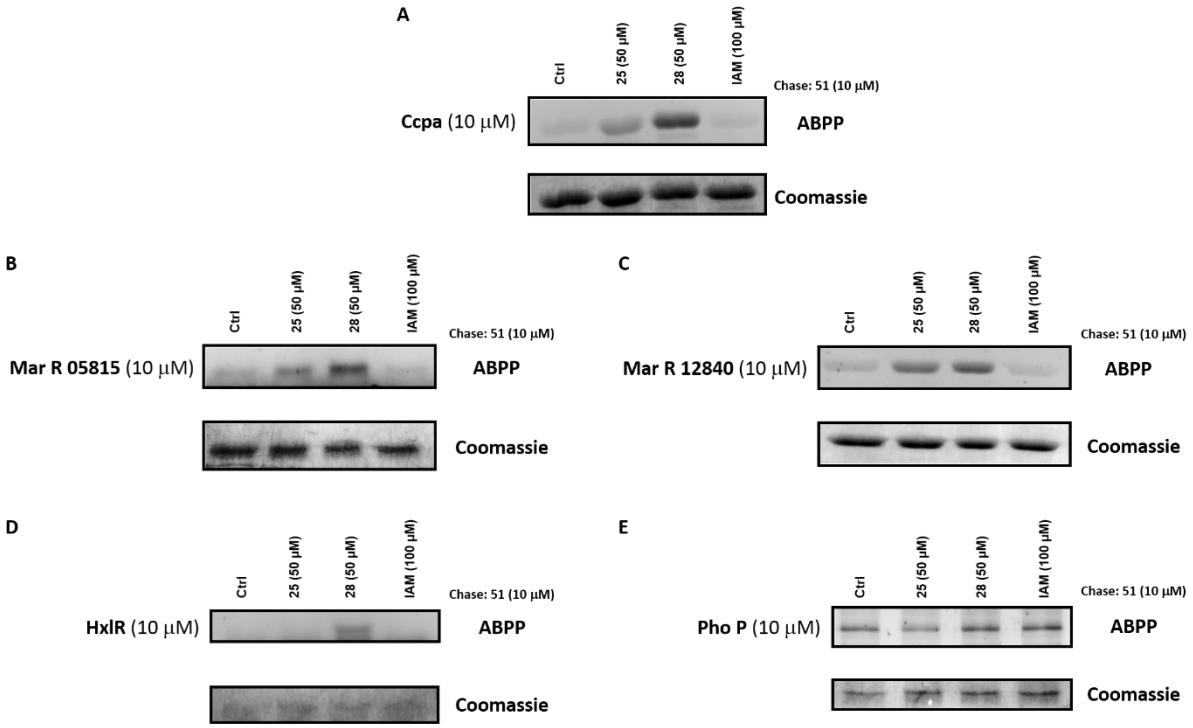

4.2.9. Cloning, expression and purification of cysteine point mutants of all wild-type proteins (targets): Site-directed mutagenesis

A subset of 5 transcriptional factors was chosen for validation out of the filtered list of 17 probable targets of lead compound **25**. As discussed earlier, Mar R_05815 and Mar R_12840 both had 1 cysteine residue each. Ccpa had 2 cysteines, whereas both HxlR and Pho P had 3 cysteine residues each. In order to validate the targets, it was evident to obtain cysteine point mutants for all these proteins. According to the hypothesis, if cysteine is mutated in the probable targets, ABPP studies should generate concrete evidence wherein labelling with active probe **51** would show no signal due to absence of a cysteine residue. To begin, it was important to first investigate whether the cysteine residues of the target proteins are conserved across the *Staphylococcus* species, which was confirmed from the Bioinformatics study conducted, as discussed earlier. Interestingly, the cysteines on the two Mar R proteins were found to be conserved and one cysteine on each Ccpa and HxlR and two cysteines on Pho P were found to be conserved. (Table 4.1).

PCR amplification was used for amplifying the genes for cloning of the cysteine point mutants. Only the conserved Cysteines were mutated to Alanine.

For mutants of Mar R_05815, Mar R_12840, Ccpa and HxlR, which involved single mutations, the PCR amplification was successful. However, for the mutant of Pho P, which involved double mutations, the PCR was not successful, possibly due to overlapping primers.

4.2.10. Dpn1 digestion

Dpn1 is a Type IIM restriction enzyme that cleaves the DNA at the methylated Adenine position. Using DpnI allows to selectively have only the artificial plasmid made in the PCR to be transformed (since it is not methylated, and everything else coming naturally from any cell would be methylated). This gives a good 'signal to noise ratio'.

4.2.11. IPTG induction

First, the plasmids were transformed into DH5α *E. coli* cells. The plasmids were extracted using a Mini-prep kit protocol and submitted for sequencing. After confirming the sequence, using IPTG induced overexpression, cysteine point mutants were overexpressed in BL21 (DE3) cells. To optimize the conditions for the overexpression of mutant proteins, a titration experiment was conducted with Mar R_12840 by varying different concentrations of IPTG (100-800 μM) at two different induction temperatures (Fig. 4.5). For this, the BL21 DE3 colonies were grown in LB media with Kanamycin in different falcons. After growing to O.D. ~0.5-0.6, each culture was induced by adding different concentrations of IPTG. These cultures were then incubated at different temperatures (18 ^{o}C and 25 ^{o}C). After overnight incubation (~16-18 h), the cells were lysed and fractionated into membrane and soluble fractions. Analysis for checking the overexpression was done by SDS-PAGE gels followed by coomassie staining. The membrane fractions did not provide any concrete evidence of overexpression at both the temperatures for all the concentrations of IPTG. In the case of the soluble fractions, induction of overexpression was observed at 25 ^{o}C for 800 μM IPTG concentration.

Figure 4.5. Titration with IPTG for induction for overexpression of proteins

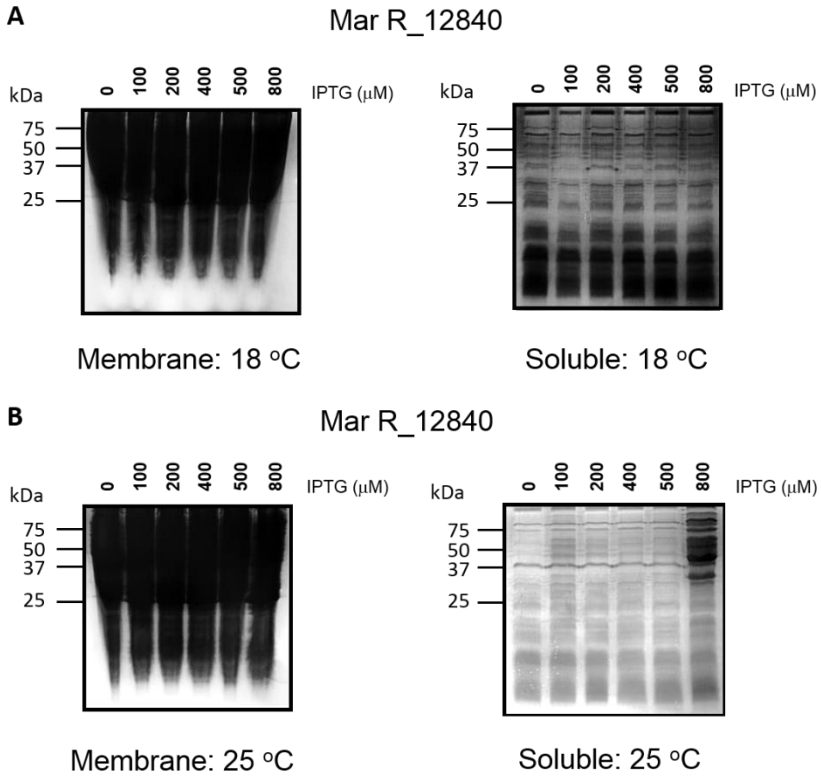

Thus, these optimized conditions (18 °C or 25 °C, 800 μM IPTG concentration for soluble fractions) were further used for induction of overexpression of the other mutant proteins. After successful induction (Fig. 4.6), the soluble lysates for the bacterial samples of the four mutant proteins were used further for protein purification.

Figure 4.6. IPTG induction of overexpression for 3 mutant proteins

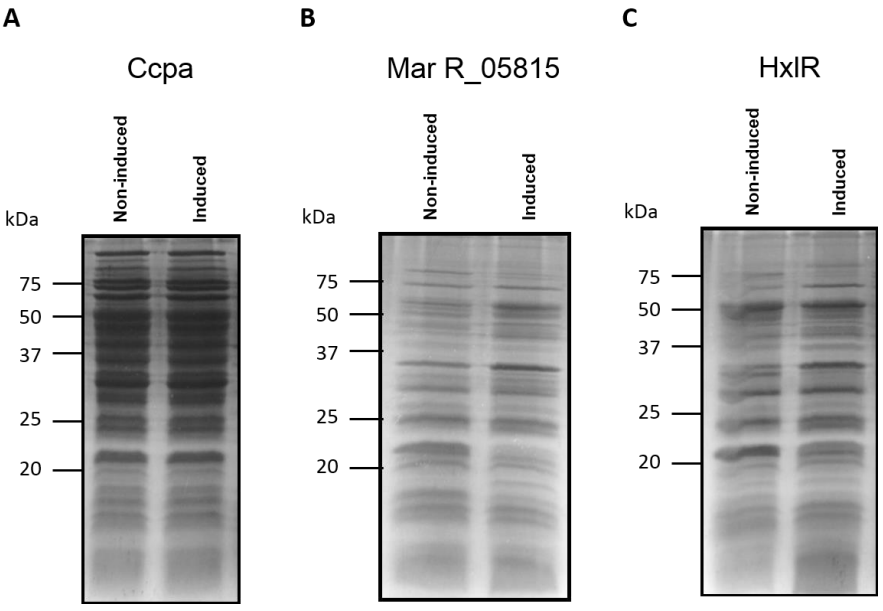

4.2.12. Protein purification using Ni-NTA Affinity Chromatography

The His-tagged proteins were next purified using Ni-NTA affinity chromatography. The proteins were purified over a FPLC system. The fractions were collected and the purity of the protein was confirmed using SDS-PAGE (Fig. 4.7). Following this, the fractions were combined and passed over a desalting column, finally concentrating them in an Amicon tube. The concentrations of the proteins were measured using a standard Bradford assay and aliquots were then stored at - 80 ^{o}C till further use.

Figure 4.7. SDS-PAGE: Purification of mutant proteins using FPLC

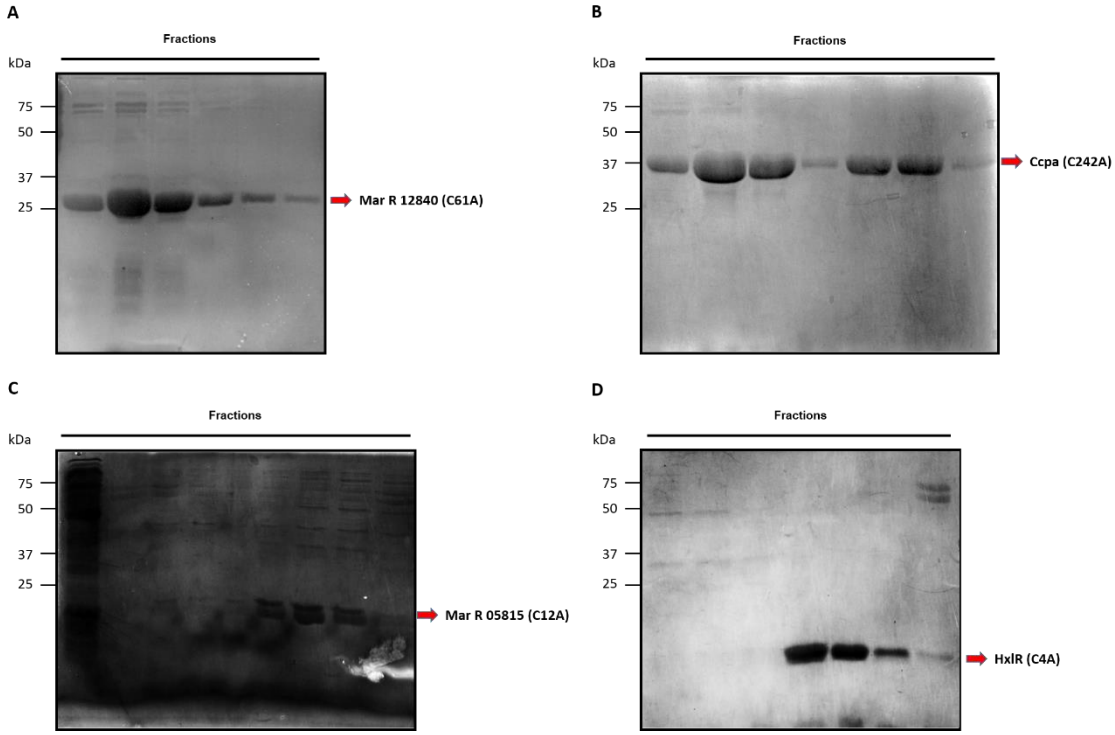

4.2.13. ABPP for the validation of protein targets

The purified cysteine point mutants were obtained and were further used for validating the targets of the lead compound **25**. Earlier, a chase experiment was conducted with the wild-type proteins wherein these were treated with the compounds **25**, **28** and IAM, followed by a chase with active probe **51**. However, conclusive evidence was not obtained. Hence, a dose-dependent experiment with active probe **51** was planned. A fixed concentration of each protein (10 μM) was treated with an increasing dosage of probe **51**. These protein samples were then clicked using Rhodamine-azide and then visualized over SDS-PAGE. In the same experiment the wild-type proteins were compared with their cysteine-point mutants. For the

three wild-type proteins namely Ccpa (Fig. 4.8. A), Mar R_05815 (Fig. 4.8. B) and Mar R_12840 (Fig. 4.8. C), a dose-dependent labelling was observed with increasing dosage of probe **51**. On the contrary, the cysteine point mutants showed no labelling at all for Mar R_05815 (C12A) and Mar R_12840 (C61A) even at the highest dose tested (100 μM). In the case of Ccpa (C242A), where 1 of the 2 Cysteines (conserved) was mutated, diminished signals were observed with probe **51** as compared to the wild-type. When conducted with HxlR, the experiment did not yield a positive result as the wild-type protein was probably denatured. However, with the cysteine point mutant of HxlR, diminished signals were observed (1 out of 3 Cysteines conserved and mutated) when treated with probe **51** (data not shown). Taken together, these ABPP experiments suggested that cysteine residue on the proteins identified as targets of **25** were indeed labelled by INDQE compounds (probe **51**, as the representative compound) and this was possibly the only mechanism of action for inhibiting drug-resistant bacteria like VRSA, as further validated by the diminished signals for the cysteine point mutants.

As these validated targets were all transcriptional factors, it suggested that lead compound **25** and in general the INDQE class of compounds could potently inhibit *S. aureus* by covalently and irreversibly targeting cysteine thiols on these key proteins. This modification possibly leads to the dysfunctioning of these proteins which ultimately deters the cellular functions in these bacteria ultimately leading to death.

Figure 4.8. ABPP for validation wild-type target proteins using cysteine point mutants

(adapted with permission from *J. Med. Chem.* <https://pubs.acs.org/doi/10.1021/acs.jmedchem.9b00774>)

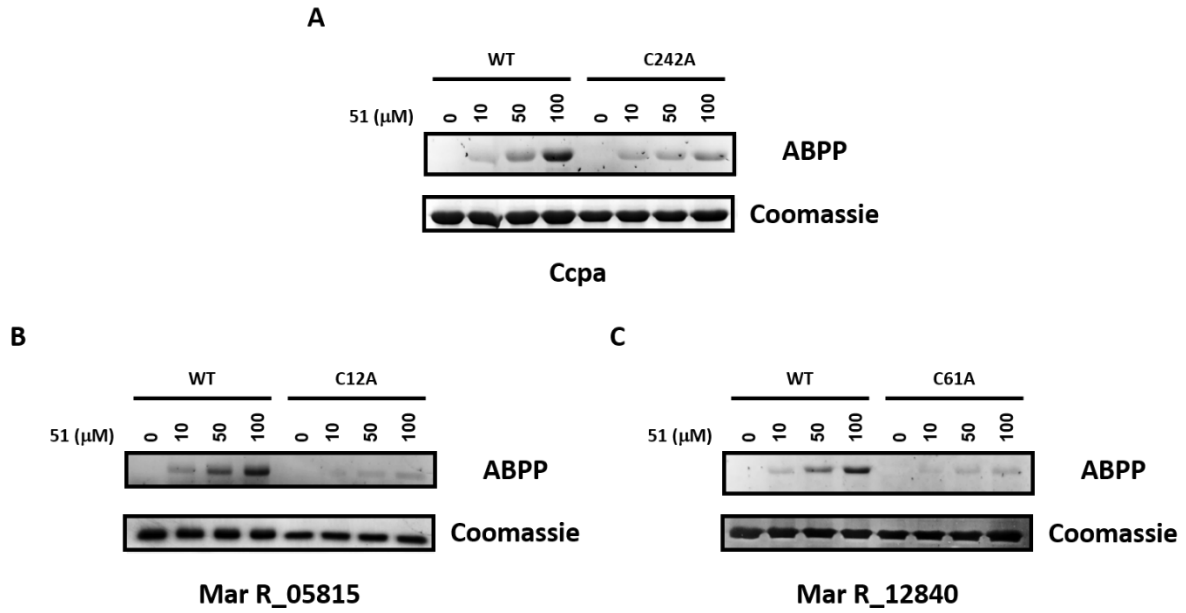

4.3. ROS generation from 25 and 27

INDQE compounds were previously shown to generate reactive oxygen species (ROS) triggered by a thiol attack.[21] The epoxide opens up and generates a quinone which enolises finally reacting with molecular oxygen to generate ROS (Scheme 4.2. A). ROS, in high concentrations are detrimental for the survival of the cell.[22] They can damage biomacromolecules such as DNA, lipids and carbohydrates extensively that can rupture various cell processes and can hence lead to death. Compound **25** was shown to react with cellular thiols and generate ROS. Albesa and co-workers have reported that ROS levels are enhanced during antibacterial action of different antibiotics against sensitive strains of *S. aureus*. However, resistant strains do not show significant increase when co-incubated with the antibiotic.[23–25] This suggests major role played by ROS in defining the antibiotic activity. Thus, it was hypothesized that simultaneous depletion (modification) of cellular thiols and generation of ROS was responsible for the antibacterial activity of potent INDQE analogues (Scheme 4.2. B). However, a good correlation between ROS generating ability and antibacterial activity of these compounds could not be established.

Scheme 4.2. A) Thiol-activated ROS generation from INDQE compounds; B) Probable dual mechanism of inducing stress - Thiol modification and ROS generation

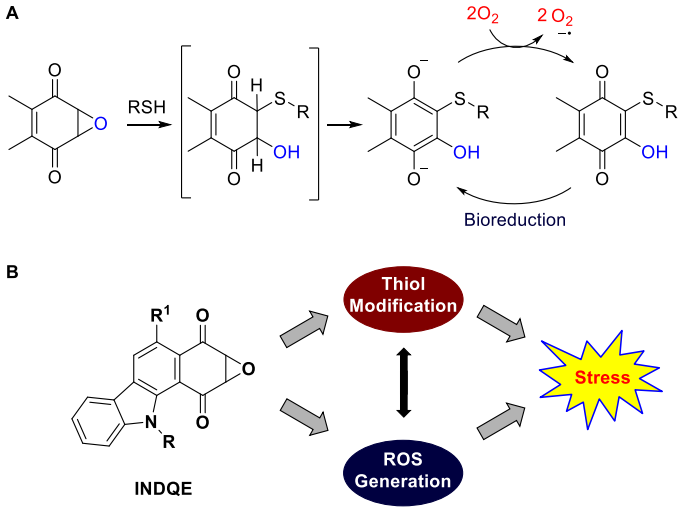

Hence, the ability of potent compound **27** in generating ROS was next investigated and compared with that of lead compound **25**. Amplex Red fluorescence assay[26] was conducted, which is used for the detection of extracellular hydrogen peroxide. First, the compound was incubated with *S. aureus* for 1 h. Then, freshly prepared Amplex Red reagent was added to this and further incubated for 25 min in the dark, following which the fluorescence measurement was undertaken to give a readout corresponding to the extracellular hydrogen peroxide. Amplex Red reagent is an *N*-acetyl protected analogue of resorufin. On reaction with hydrogen peroxide, in the presence of Horse Radish peroxidase enzyme (HRP), it gets converted to Resorufin which is fluorescent (Scheme 4.3). As expected, compound **25** was found to generate ROS significantly as compared to the untreated control, however, compound **27** was not found to generate substantial amounts of ROS (Fig. 4.9. A). Menadione was used as the positive control (Fig. 4.10).

Scheme 4.3. Amplex Red assay

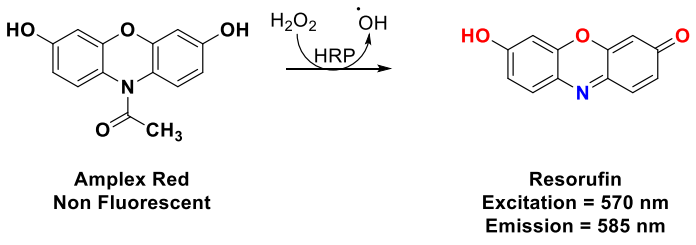

Next, H_2-DCF-DA assay[27] was conducted, which is used in the detection of intracellular superoxide. First, H_2-DCF-DA dye was incubated with *S. aureus* for 1 h in the dark. Then,

the bacterial pellet was washed, following which, it was incubated with the compound for 1 h. The fluorescence was then recorded giving the readout for the intracellular superoxide generated. H_2-DCF-DA dye is a non-fluorescent molecule which on reaction with ROS gets converted to fluorescent DCF, whose fluorescence can then be recorded (Scheme 4.4). Similar to the results obtained in the Amplex Red assay, compared to compound **25**, compound **27** was found to generate negligible amounts of ROS, and was comparable to the untreated control (Fig. 4.9. B). Menadione was used as a positive control (Fig. 4.10).

Scheme 4.4. H_2-DCF-DA assay

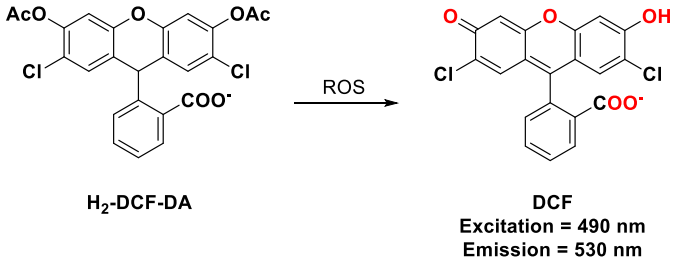

H_2-DCF-DA

DCF
Excitation = 490 nm
Emission = 530 nm

Thus, both these assays demonstrated that unlike lead compound **25**, compound **27** does not generate a burst of ROS. This observation had previous literature precedence, where a substituted 2,3-epoxy naphthoquinone molecule was shown, on thiol activation, to generate negligible amounts of ROS as compared to an unsubstituted one.[28,29] Together, these results suggested that generation of ROS *in situ* may not be playing a very important role in the inhibition of bacteria by these compounds, whereas, reaction with a cellular thiol in a kinetic manner is crucial for inhibition. More recent studies from Imlay and co-workers[30] and Lewis and co-workers,[31] independently suggest that ROS does not have a direct involvement in the killing of bacteria by antibiotics.

Figure 4.9. ROS assays: A) Amplex red assay, B) DCF assay

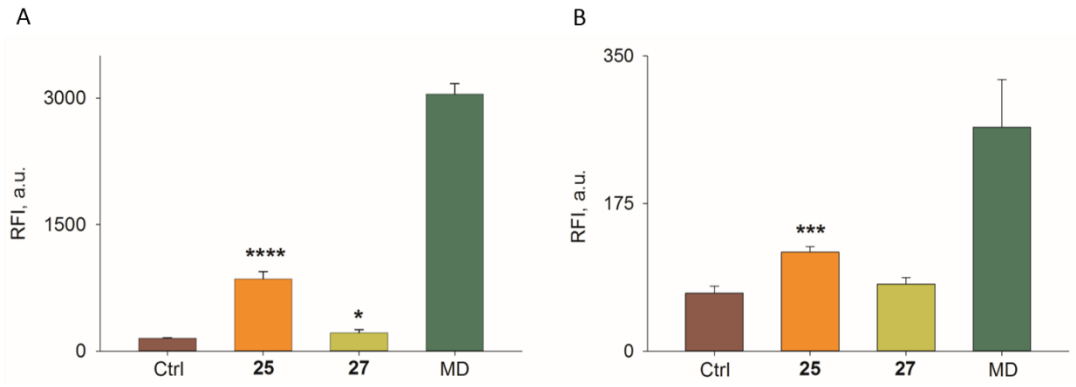

Figure 4.10. Structures of lead compounds 25 and 27 and control compound Menadione

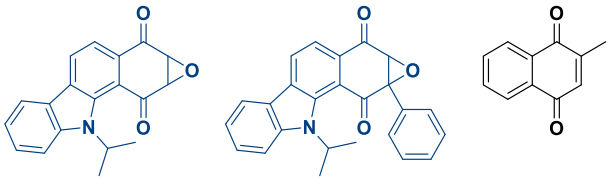

4.4. Summary

In Chapter 3, a set of 17 proteins was identified as probable targets of the lead compound **25**. Out of these 17 proteins, a subset of 5 proteins was selected for validation. These were all transcriptional factors, Ccpa, Mar R_05815, Mar R_12840, HxlR, Pho P. The wild-type proteins were cloned, overexpressed and purified from *E. coli* BL21 DE3 cells. ABPP-based chase experiments were conducted for these purified proteins using probe **51** as a chaser, but the results obtained were not conclusive enough for the validation. It was hypothesized that on compound treatment, there is transformation in the native structure of the wild-type protein which changes the reaction dynamics with the probe **51**, which is used as a chaser. This could contribute to getting diminished signals for labelling with **51**. To solve this problem, cysteine point mutants of these proteins were generated using site-directed mutagenesis, wherein the cysteine residue on the protein was replaced by alanine. The conservation of the cysteine residues across species for these proteins was studied. Only the conserved cysteines were mutated. After successfully generating the cysteine point mutants for both Mar R proteins, Ccpa and HxlR, ABPP was employed to study the reaction of these cysteine point mutants with the active probe **51** and was compared with that of the wild-type proteins. A dose-dependent modification of the wild-type proteins with **51** was observed, whereas the mutants were not labelled even at the highest concentration tested. This result confirmed that the INDQE scaffold selectively hits the cysteine residue of its target proteins. Thus, taken together, it can be concluded that INDQE compounds selectively hit the cysteine residues of a number of transcriptional factors in *S. aureus*. This bonding is covalent in nature and kinetically driven as shown in Chapter 2. The combined effect of this covalent modification in a kinetic manner leads to the inhibition of highly drug-resistant VRSA. Considering the grandeur scale of the problem of antibiotic resistance on the global level, this strategy could possibly add crucial information to combat it and to further propagate similar strategies in tackling antibiotic resistance.

In another study for detection of ROS generation, unlike **25**, compound **27** was not found to generate ROS inside cells, and hence it suggested that the reaction with a cysteine residue on a protein is crucial for the antibacterial activity of these compounds.

4.5. Experimental Section

4.5.1. Expression and purification of recombinant proteins

To overexpress the C-terminal His-tagged genes, the aforementioned vectors were transformed into *E. coli* BL21 (DE3) and the cells were grown in Luria-Bertani (LB) broth with 100 µg/mL kanamycin (pET-30b(+)) or ampicillin (pET-22b(+)) at 37 ^{o}C until the OD_{600} reached 0.6. The culture was shifted to 30 ^{o}C for 1 hour and 0.5 mM IPTG was added to induce the overexpression of the genes.16 hours post-induction at 30 ^{o}C, the cells were harvested by centrifugation at 6000 rpm for 15 min at 4 ^{o}C. The cells were resuspended in lysis buffer comprising 50 mM Tris pH 8 at room temperature (RT), 150 mM NaCl, and 5 mM β mercaptoethanol and lysed by sonication (60% amplitude, 5 s ON, 10 s OFF for 20 min). The lysate was then centrifuged at 18,000 g for 45 min at 4 ^{o}C to separate the soluble fraction from the insoluble inclusion bodies and membranes. Overexpression and solubility of ABHD14B were confirmed by SDS-PAGE gel. The soluble fraction was passed through a pre-packed Ni-NTA column (5 mL, GE Life Sciences) pre-washed with 10 column volumes (CV) of lysis buffer. The column was then washed with 10 CV of wash buffer comprising 50 mM Tris pH 8 at RT, 150 mM NaCl, 5 mM β mercaptoethanol, and 25 mM Imidazole. The protein was eluted with elution buffer comprising 50 mM Tris pH 8 at RT, 150 mM NaCl, 5 mM β mercaptoethanol, and 25 mM Imidazole and dialyzed against 50 mM Tris pH 8 at RT, 150 mM NaCl, 5 mM β mercaptoethanol, and 10 % glycerol. Aliquots of the purified proteins were flash frozen in liquid nitrogen and stored at -80 $^{\circ}$C until further use.

4.5.2. Gene and Protein sequences

Protein	Mar R 05815
Gene sequence	ATGTCTGATCAACATAATTTAAAAGAACAGCTATGCTTTAGTTTGT ACAATGCTCAAAGACAAGTTAATCGCTACTACTCTAACAAAGTTTT TAAGAAGTACAATCTAACATACCCACAATTTCTTGTCTTAACAATT TTATGGGATGAATCTCCTGTAAACGTCAAGAAAGTCGTAACTGAA TTAGCACTCGATACTGGTACAGTATCACCATTATTAAAACGAATGG

	AACAAGTAGACTTAATTAAGCGTGAACGTTCCGAAGTCGATCAAC GTGAAGTATTTATTCACTTGACTGACAAAAGTGAAACTATTAGACC AGAATTAAGTAATGCATCTGACAAAGTCGCTTCAGCTTCTTCTTTA TCTCAAGATGAAGTTAAAGAACTTAATCGCTTATTAGGTAAAGTCA TTCATGCATTTGATGAAACAAAGGAAAAAT
Protein sequence	MSDQHNLKEQL**C**FSLYNAQRQVNRYYSNKVFKKYNLTYPQFLVLTIL WDESPVNVKKVVTELALDTGTVSPLLKRMEQVDLIKRERSEVDQREV FIHLTDKSETIRPELSNASDKVASASSLSQDEVKELNRLLGKVIHAFDE TKEKFDKLAAALE (1 Cysteine at number 12 from start, marked in red)

Protein	Mar R 12840
Gene sequence	ATGAAATATAATAACCATGACAAAATTAGAGATTTTATAATCATTG AAGCATATATGTTTCGTTTTAAGAAAAAAGTCAAGCCTGAAGTCG ATATGACTATAAAAGAATTTATATTACTGACTTATTTATTTCATCA GCAAGAAAACACACTTCCATTTAAGAAGATTGTTTCAGATTTATGT TATAAACAATCGGATTTAGTACAGCATATAAAAGTACTTGTGAAA CATTCATATATTAGTAAAGTTCGAAGTAAAATTGATGAGCGTAATA CTTACATTTCAATATCTGAAGAACAACGAGAGAAAATTGCAGAAC GTGTTACATTGTTTGATCAAATCATTAAACAATTTAACCTTGCAGA TCAAAGTGAATCACAGATGATACCAAAAGATAGTAAAGAATTTCT AAACTTGATGATGTATACAATGTATTTCAAGAATATTATCAAAAAA CATCTAACATTAAGTTTTGTAGAATTCACAATTCTAGCTATTATCA CTTCTCAAAATAAAAACATCGTTCTTCTTAAAGATTTAATTGAAAC AATCCACCATAAATACCCTCAAACTGTTAGAGCTCTCAATAATTTA AAAAAGCAAGGCTATCTAATAAAAGAACGCTCAACTGAAGATGAA AGAAAAATTTTAATTCATATGGATGACGCGCAGCAAGACCATGCT GAACAATTATTAGCTCAAGTGAATCAATTATTAGCAGATAAAGAT CATTTACATCTTGTTTTTGAATAA
Protein sequence	MKYNNHDKIRDFIIIEAYMFRFKKKVKPEVDMTIKEFILLTYLFHQQE NTLPFKKIVSDL**C**YKQSDLVQHIKVLVKHSYISKVRSKIDERNTYISISE EQREKIAERVTLFDQIIKQFNLADQSESQMIPKDSKEFLNLMMYTMYF KNIIKKHLTLSFVEFTILAIITSQNKNIVLLKDLIETIHHKYPQTVRALNN

	LKKQGYLIKERSTEDERKILIHMDDAQQDHAEQLLAQVNQLLADKDH LHLVFE (1 Cysteine at number 61 from start, marked in red)

Protein	CcpA
Gene sequence	ATGACAGTTACTATATATGATGTAGCAAGAGAAGCGCGTGTCTCT ATGGCCACAGTGTCGCGTGTTGTTAATGGGAACCAAAATGTTAAA GCAGAAACTAAAAATAAAGTTAACGAAGTCATTAAGCGTTTGAAT TATCGTCCAAATGCTGTTGCTAGAGGTTTAGCTAGTAAAAAGACA ACAACAGTAGGTGTGATCATTCCAGATATATCTAATATCTATTATT CACAACTTGCTCGTGGACTTGAAGATATTGCAACAATGTATAAATA TCACTCAATTATTTCAAATTCAGATAACGATCCTGAAAAGGAAAA AGAAATTTTTAATAACTTATTAAGTAAACAGGTTGATGGTATTATT TTCCTTGGTGGTACAATTACTGAAGAAATGAAAGAATTGATAAAT CAATCATCTGTACCTGTAGTAGTATCAGGAACAAATGGTAAGGAT GCACATATAGCATCAGTTAATATTGATTTTACTGAAGCTGCGAAAG AAATTACGGGAGAATTAATTGAAAAAGGCGCTAAATCATTTGCTT TAGTAGGTGGAGAACATTCTAAAAAAGCTCAAGAAGATGTTTTAG AAGGTTTAACTGAAGTGTTAAATAAAAATGGCATTCAATTAGGTG ATACATTGAATTGTTCTGGTGCTGAAAGTTATAAAGAAGGCGTAA AAGCTTTTGCTAAAATGAAAGGCAATTTGCCAGATGCCATTTTATG TATCAGCGACGAAGAAGCAATTGGTATTATGCATAGTGCAATGGA TGCTGGTATTAAAGTTCCAGAGGAATTACAAATTATTAGTTTCAAT AATACACGATTAGTTGAGATGGTTAGACCACAACTTTCTAGTGTTA TTCAACCATTATATGATATCGGTGCAGTAGGGATGCGCTTATTAAC AAAATATATGAACGATGAAAAGATAGAAGAACCAAATGTAGTTTT ACCTCACAGAATTGAATACCGAGGAACTACAAAATAA
Protein sequence	MTVTIYDVAREARVSMATVSRVVNGNQNVKAETKNKVNEVIKRLNY RPNAVARGLASKKTTTVGVIIPDISNIYYSQLARGLEDIATMYKYHSIIS NSDNDPEKEKEIFNNLLSKQVDGIIFLGGTITEEMKELINQSSVPVVVS GTNGKDAHIASVNIDFTEAAKEITGELIEKGAKSFALVGGEHSKKAQE DVLEGLTEVLNKNGIQLGDTLN**C**SGAESYKEGVKAFAKMKGNLPDAI L**C**ISDEEAIGIMHSAMDAGIKVPEELQIISFNNTRLVEMVRPQLSSVIQP

	LYDIGAVGMRLLTKYMNDEKIEEPNVVLPHRIEYRGTTK (2 Cysteines at number 216 and 242 from start, marked in red)

Protein	HxlR
Gene sequence	ATGGAAGTATGTCCGTATCTCGAAGAAACTTTTAAAATACTTGGTA GAAGTTGGAATGGATTAATCATTAATTATCTCTCAAGATGTAATGA CTGTTCAGCACACTTTTCCGATATGAAAAGAGATTTGAAAACAATA ACACCACGTGCTTTAAGTCTTAAGTTGTCAGAGCTTGCACAATGGA AGTTAGTTGAGAAGCAAATCATTTCTACGAGTCCAGTACAAATTAT TTATGTGCTAACTGAAAAAGGTAAAGCGTTAGCAGAGGCTTTACA TCCAATTGAAGCATGGGCGCAATCATATGTCGATTTAACAGATCA ACGTACTGCTAAATAA
Protein sequence	MEV**C**PYLEETFKILGRSWNGLIINYLSR**C**ND**C**SAHFSDMKRDLKTITP RALSLKLSELAQWKLVEKQIISTSPVQIIYVLTEKGKALAEALHPIEAW AQSYVDLTDQRTAK (3 Cysteines at number 4, 29 and 32 from start, marked in red)

Protein	Pho P
Gene sequence	ATGGCTAGAAAAGTTGTTGTAGTTGATGATGAAAAACCGATTGCTGA TATTTTAGAATTTAACTTAAAAAAAGAAGGATACGATGTGTACTGTG CATACGATGGTAATGATGCAGTCGACTTAATTTATGAAGAAGAACCA GACATCGTATTACTAGATATCATGTTACCTGGTCGTGATGGTATGGA AGTATGTCGTGAAGTGCGCAAAAAATACGAAATGCCAATTATAATGC TTACTGCTAAAGATTCAGAAATTGATAAAGTGCTTGGTTTAGAACTA GGTGCAGATGACTATGTAACGAAACCGTTTAGTACGCGTGAATTAAT CGCACGTGTGAAAGCGAACTTACGTCGTCATTACTCACAACCAGCAC AAGACACTGGAAATGTAACGAATGAAATCACAATTAAAGATATTGT GATTTATCCAGACGCATATTCTATTAAAAAACGTGGCGAAGATATTG AATTAACACATCGTGAATTTGAATTGTTCCATTATTTGTCAAAACATA TGGGACAAGTAATGACACGTGAACATTTATTACAAACAGTATGGGGC TATGATTACTTTGGCGATGTACGTACAGTCGATGTAACGATTCGTCGT TTACGTGAAAAGATTGAAGATGATCCGTCACATCCTGAATATATTGT

	GACGCGTAGAGGCGTTGGATATTTCCTCCAACAACATGAGTAG
Protein sequence	MARKVVVVDDEKPIADILEFNLKKEGYDVY**C**AYDGNDAVDLIYEEEPD IVLLDIMLPGRDGMEV**C**REVRKKYEMPIIMLTAKDSEIDKVLGLELGAD DYVTKPFSTRELIARVKANLRRHYSQPAQDTGNVTNEITIKDIVIYPDAY SIKKRGEDIELTHREFELFHYLSKHMGQVMTREHLLQTVWGYDYFGDV RTVDVTIRRLREKIEDDPSHPEYIVTRRGVGYFLQQHE (2 Cysteines at number 31 and 65 from start, marked in red)

4.5.3. Site-directed mutagenesis

Cysteines at positions 61 (of marR_12840), 12 (marR_05815), 4 (HxlR), 242 (CcpA), 31 (PhoP) and 65 (PhoP) were mutated to alanine by DpnI dependent site directed mutagenesis. Clones pET-30b(+) marR_12840, pET-30b(+) marR_05815, pET-22b(+) HxlR, pET-22b(+) CcpA and pET-22b(+) PhoP were used as template for the mutagenesis PCR for the respective mutations. Following PCR the parent templates were cleaved using DpnI at 37^{o}C for 1 hour. Mutations were confirmed by sequencing.

The mutant proteins were purified over a FPLC GE Akta Pure system. The soluble fraction was passed through a Ni-NTA column (His Trap^{TM} HP 5 mL) pre-washed with 10 column volumes (CV) of lysis buffer. The column was then washed with 10 CV of wash buffer comprising 25 mM Tris pH 8 at RT, 150 mM NaCl, 5 mM β mercaptoethanol. The protein was eluted with elution buffer comprising 25 mM Tris pH 8 at RT, 150 mM NaCl, 5 mM β mercaptoethanol, and 500 mM Imidazole with gradient 40 mM (8 CV), 60 mM (8 CV), 250 mM (5 CV) and 500 mM 5 (CV). The protein fractions were then desalted over Biorad Econo-Pac®□ 10DG 10 mL prepacked desalting column using 50 mM Tris pH 8 at RT, 150 mM NaCl, 5 mM β mercaptoethanol, and 10 % glycerol. Aliquots of the purified proteins were flash frozen in liquid nitrogen and stored at -80^{o}C until further use.

4.5.4. Target validation using ABPP

The protein concentrations for both wild-type and mutant proteins were estimated using a standard protein estimation (Bradford) assay and 10 μM stocks were prepared in dialysis buffer accordingly. 100 μL aliquots were further used for all the assays. These aliquots were treated with varying concentrations of **51** (0 – 100 μM) at 37 ^{o}C for 1 hour. Following which the click reaction was performed as described earlier, and the reactions were quenched by

adding 40 µL of 4X loading dye. The samples were resolved and activity was visualized using a 20% SDS-PAGE gel using established protocols.

4.5.5. Extracellular hydrogen peroxide estimation. (Amplex Red assay)

S. aureus (MSSA 29213) was cultured in 5 mL of Mueller Hinton Broth (CA-MHB) medium at 37 ºC for 2 h. The cultured bacteria were centrifuged to aspirate out the medium and re-suspended in fresh medium and optical density (O.D) was adjusted to 1.0. A stock solution of the compound in DMSO was added so that the final concentration was 50 µM. After incubation for 1 h, a premixed solution of 10-acetyl-3,7- dihydroxyphenoxazine or Amplex Red® (prepared by following manufacturer´s protocol from Invitrogen) was added in 1:1 ratio, and incubated in the dark for 25 min. 200 µL of this mixture was then added to each well of sterile flat bottom 96-well microtiter plate and then the fluorescence was measured using a microtiter plate reader (excitation 550 nm; emission 590 nm). A calibration curve with known concentrations of hydrogen peroxide was generated in LB medium and was used to quantify hydrogen peroxide produced during incubation of test analytes.

4.5.6. Intracellular oxidative species estimation ($DCFH_2$-DA assay)

S. aureus (MSSA 29213) was cultured in 5 mL of Mueller Hinton Broth (CA-MHB) medium at 37 ºC for 2 h. The cultured bacteria were centrifuged to aspirate out the medium and re-suspended in fresh medium and optical density (O.D) was adjusted to 1.0. The bacterial medium was incubated with 200 µM of 2′,7′-dichlorodihydrofluorescein diacetate ($DCFH_2$-DA), a weakly fluorescent dye for 60 min. Next, centrifugation of the bacterial suspension followed by removal of extracellular media to remove any excess $DCFH_2$-DA was carried out. The collected bacterial pellet was re-suspended with fresh medium. A final concentration of 100 µM compound in DMSO (0.5%) was added and incubated for 60 min; bacterial solution with 0.5% DMSO was used as the control. 200 µL of this mixture was then added to each well of sterile flat bottom 96-well microtiter plate and then the fluorescence of oxidized green fluorescent 2′,7′-dichlorofluorescein (DCF) was measured (excitation, 490; emission, 520 nm) using a microtiter plate reader. $DCFH_2$DA is reported to be more reactive with •OH in comparison with other ROS.

4.6. References

(1) Latchman, D. S. Transcription Factors: An Overview. *Int. J. Biochem. Cell Biol.* **1997**, *29* (12), 1305–1312.

(2) Novick, R. P. Autoinduction and Signal Transduction in the Regulation of Staphylococcal Virulence. *Mol. Microbiol.* **2003**, *48* (6), 1429–1449.

(3) Bronner, S.; Monteil, H.; Prévost, G. Regulation of Virulence Determinants in Staphylococcus Aureus : Complexity and Applications. *FEMS Microbiol. Rev.* **2004**, *28* (2), 183–200.

(4) Grove, A. MarR Family Transcription Factors. *Curr. Biol.* **2013**, *23* (4), R142-3.

(5) Hao, Z.; Lou, H.; Zhu, R.; Zhu, J.; Zhang, D.; Zhao, B. S.; Zeng, S.; Chen, X.; Chan, J.; He, C.; et al. The Multiple Antibiotic Resistance Regulator MarR Is a Copper Sensor in Escherichia Coli. *Nat. Chem. Biol.* **2014**, *10* (1), 21–28.

(6) Sharma, P.; Haycocks, J. R. J.; Middlemiss, A. D.; Kettles, R. A.; Sellars, L. E.; Ricci, V.; Piddock, L. J. V.; Grainger, D. C. The Multiple Antibiotic Resistance Operon of Enteric Bacteria Controls DNA Repair and Outer Membrane Integrity. *Nat. Commun.* **2017**, *8* (1), 1444.

(7) Sun, F.; Ding, Y.; Ji, Q.; Liang, Z.; Deng, X.; Wong, C. C. L.; Yi, C.; Zhang, L.; Xie, S.; Alvarez, S.; et al. Protein Cysteine Phosphorylation of SarA/MgrA Family Transcriptional Regulators Mediates Bacterial Virulence and Antibiotic Resistance. *Proc. Natl Acad. Sci. U S A* **2012**, *109* (38), 15461–15466.

(8) Miller, S. I.; Kukral, A. M.; Mekalanos, J. J. A Two-Component Regulatory System (PhoP PhoQ) Controls Salmonella Typhimurium Virulence. *Proc. Natl Acad. Sci. U S A* **1989**, *86* (13), 5054–5058.

(9) He, X.; Wang, L.; Wang, S. Structural Basis of DNA Sequence Recognition by the Response Regulator PhoP in Mycobacterium Tuberculosis. *Sci. Rep.* **2016**, *6*, 24442.

(10) Liao, X.; Yang, F.; Wang, R.; He, X.; Li, H.; Kao, R. Y. T.; Xia, W.; Sun, H. Identification of Catabolite Control Protein A from Staphylococcus Aureus as a Target of Silver Ions. *Chem. Sci.* **2017**, *8* (12), 8061–8066.

(11) Kunzmann, M. H.; Bach, N. C.; Bauer, B.; Sieber, S. A. α-Methylene-γ-Butyrolactones Attenuate Staphylococcus Aureus Virulence by Inhibition of

Transcriptional Regulation. *Chem. Sci.* **2014**, *5* (3), 1158–1167.

(12) Tiwari, S.; Jamal, S. B.; Hassan, S. S.; Carvalho, P. V. S. D.; Almeida, S.; Barh, D.; Ghosh, P.; Silva, A.; Castro, T. L. P.; Azevedo, V. Two-Component Signal Transduction Systems of Pathogenic Bacteria As Targets for Antimicrobial Therapy: An Overview. *Front. Microbiol.* **2017**, *8*, 1878.

(13) Cai, X.; Zhang, J.; Chen, M.; Wu, Y.; Wang, X.; Chen, J.; Zhang, J.; Shen, X.; Qu, D.; Jiang, H. The Effect of the Potential PhoQ Histidine Kinase Inhibitors on Shigella Flexneri Virulence. *PLoS One* **2011**, *6* (8), e23100.

(14) Tiwari, S.; da Costa, M. P.; Almeida, S.; Hassan, S. S.; Jamal, S. B.; Oliveira, A.; Folador, E. L.; Rocha, F.; de Abreu, V. A. C.; Dorella, F.; et al. C. Pseudotuberculosis Phop Confers Virulence and May Be Targeted by Natural Compounds. *Integr. Biol.* **2014**, *6* (11), 1088–1099.

(15) Tang, Y. T.; Gao, R.; Havranek, J. J.; Groisman, E. A.; Stock, A. M.; Marshall, G. R. Inhibition of Bacterial Virulence: Drug-Like Molecules Targeting the Salmonella Enterica PhoP Response Regulator. *Chem. Biol. Drug Des.* **2012**, *79* (6), 1007–1017.

(16) Haebich, D.; von Nussbaum, F. Lost in Transcription-Inhibition of RNA Polymerase. *Angew. Chem. Int. Ed.* **2009**, *48* (19), 3397–3400.

(17) Yang, X.; Luo, M. J.; Yeung, A. C. M.; Lewis, P. J.; Chan, P. K. S.; Ip, M.; Ma, C. First-In-Class Inhibitor of Ribosomal RNA Synthesis with Antimicrobial Activity against *Staphylococcus Aureus*. *Biochemistry* **2017**, *56* (38), 5049–5052.

(18) Vermote, A.; Van Calenbergh, S. Small-Molecule Potentiators for Conventional Antibiotics against Staphylococcus Aureus. *ACS Infect. Dis.* **2017**, *3* (11), 780–796.

(19) Luebke, J. L.; Giedroc, D. P. Cysteine Sulfur Chemistry in Transcriptional Regulators at the Host–Bacterial Pathogen Interface. *Biochemistry* **2015**, *54* (21), 3235–3249.

(20) Li, M. Z.; Elledge, S. J. SLIC: A Method for Sequence- and Ligation-Independent Cloning; Humana Press, 2012; pp 51–59.

(21) Dharmaraja, A. T. Synthesis and Evaluation of Small Molecule Based Reactive Oxygen Species (ROS) Generators. *Thesis* **2015**.

(22) Fang, F. C. Antimicrobial Reactive Oxygen and Nitrogen Species: Concepts and

Controversies. *Nat. Rev. Micro.* **2004**, *2* (10), 820–832.

(23) Páez, P. L.; Becerra, M. C.; Albesa, I. Antioxidative Mechanisms Protect Resistant Strains of Staphylococcus Aureus against Ciprofloxacin Oxidative Damage. *Fundam. Clin. Pharmacol.* **2010**, *24* (6), 771–776.

(24) Albesa, I.; Becerra, M. C.; Battán, P. C.; Páez, P. L. Oxidative Stress Involved in the Antibacterial Action of Different Antibiotics. *Biochem. Biophys.Res. Commun.* **2004**, *317* (2), 605–609.

(25) Becerra, M. C.; Albesa, I. Oxidative Stress Induced by Ciprofloxacin in Staphylococcus Aureus. *Biochem. Biophys.Res. Commun.* **2002**, *297* (4), 1003–1007.

(26) Zhou, M.; Diwu, Z.; Panchuk-Voloshina, N.; Haugland, R. P. A Stable Nonfluorescent Derivative of Resorufin for the Fluorometric Determination of Trace Hydrogen Peroxide: Applications in Detecting the Activity of Phagocyte NADPH Oxidase and Other Oxidases. *Anal. Biochem.* **1997**, *253* (2), 162–168.

(27) Kalyanaraman, B.; Darley-Usmar, V.; Davies, K. J. A.; Dennery, P. A.; Forman, H. J.; Grisham, M. B.; Mann, G. E.; Moore, K.; Roberts, L. J.; Ischiropoulos, H. Measuring Reactive Oxygen and Nitrogen Species with Fluorescent Probes: Challenges and Limitations. *Free Radic. Biol. Med.* **2012**, *52* (1), 1–6.

(28) Brunmark, A.; Cadenas, E. 1,4-Reductive Addition of Glutathione to Quinone Epoxides. Mechanistic Studies with h.p.l.c. with Electrochemical Detection under Anaerobic and Aerobic Conditions. Evaluation of Chemical Reactivity in Terms of Autoxidation Reactions. *Free Radic. Bio. Med.* **1989**, *6* (2), 149–165.

(29) Dharmaraja, A. T.; Dash, T. K.; Konkimalla, V. B.; Chakrapani, H. Synthesis, Thiol-Mediated Reactive Oxygen Species Generation Profiles and Anti-Proliferative Activities of 2,3-Epoxy-1,4-Naphthoquinones. *Med. Chem. Commun.* **2012**, *3* (2), 219–224.

(30) Liu, Y.; Imlay, J. A. Cell Death from Antibiotics Without the Involvement of Reactive Oxygen Species. *Science (80-.).* **2013**, *339* (6124), 1210–1213.

(31) Keren, I.; Wu, Y.; Inocencio, J.; Mulcahy, L. R.; Lewis, K. Killing by Bactericidal Antibiotics Does Not Depend on Reactive Oxygen Species. *Science (80-.).* **2013**, *339* (6124), 1213–1216.

Appendix I - Future Perspectives

AI.1. Targeting Mar R in other bacteria

To extrapolate the antibacterial potency of INDQE class of compounds against Gram-negative bacteria, the structure needs modifications in order to tune for better permeability across the outer membrane of Gram-negative bacteria. Improved designs of INDQE derivatives were proposed and will need further evaluation to effectively render Gram-negative antibacterials.

AI.1.1. Design and synthesis of INDQE derivatives for targeting Gram-negative bacteria

In Chapter 2, the challenge in targeting Gram-negative pathogens with INDQE compounds was discussed briefly. The major problem that was highlighted was the issue with permeability of these compounds across the outer membrane of Gram-negative bacteria. In Chapter 3, using INDQE alkyne probe, compound **51**, it was shown that this class of compounds labels the thiol proteome of Gram-negative bacteria like *E. coli* in an *in vitro* setting. However, no labelling was observed in an *in situ* setting possibly owing to the lack of permeability of these compounds in Gram-negative bacteria.[1] Recently, Hergenrother and coworkers put forth a set of empirical rules, by means of which one can predict the permeability of antibacterial compounds inside Gram-negative bacteria. These rules suggest that a compound should have an amine functional group, should be amphiphilic and rigid, and have a low globularity. Using these empirical rules, they were successful in converting deoxynybomycin, a natural product active against Gram-positive bacteria, into a Gram-negative antibacterial agent. Taking inspiration from their work, it was hypothesized that structural modifications to improve the solubility of the present INDQE scaffold can tune and improve its permeability inside Gram-negative bacteria. However, in doing this, it was evident that the reactivity of the epoxide from the understanding obtained through the SAR studies, needed to be taken care of.

To start, active probe **51** was chosen for modification, which had potent antibacterial activity (1 μg/mL against *S. aureus*). Using click chemistry a peg (polyethylene glycol) chain was linked with this compound (Scheme 4.1) and compound **53** was obtained in 29% yield. Peg chains are routinely used to improve aqueous solubility of any molecule. Thus, it was hypothesized that bearing the peg chain, compound **53** would be able to permeate Gram-negative bacteria and lead to inhibitory activity as its parent compound **51** was active against *S. aureus*.

Scheme AI.1. Synthesis of pegylated derivative of INDQE scaffold

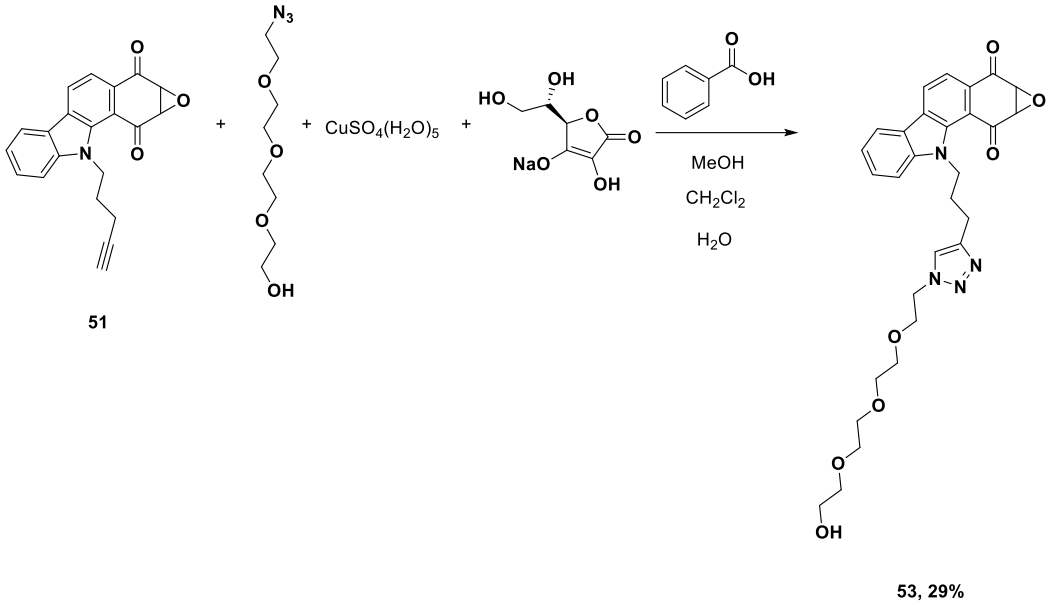

Compound **53** was next evaluated for its antibacterial potency and was tested against a panel of ESKAPE pathogens. Surprisingly it was found that this compound was not active against the Gram-negative pathogens like *E. coli*, *K. pnemoniae, A. baumannii* and *P. aeruginosa* and MIC values against Gram-positive pathogens like *S. aureus* were high (Table 4.4). This suggested that appending a peg chain could not improve the permeability of INDQE compounds in Gram-negative bacteria.

Table AI.1. Antibacterial activity of **53** against ESKAPE pathogens

	MIC (μg/mL)						
Cpd	*E. coli*	*S. aureus*	*K. pnemoniae*	*A. baumannii*	*P. aeruginosa*	*E. faecalis*	*E. faecium*
53	>64	32	>64	>64	>64	32	32

E. coli ATCC 25922, *S. aureus* ATCC 29213, *K. pnemoniae* BAA 1705, *A. baumannii* BAA 1605, *P. aeruginosa* ATCC 27853, *E. faecalis* Strain B3119, *E. faecium* Strain Patient #1-1; (Data courtesy: Dr. Sidharth Chopra Lab, CDRI Lucknow)

Hence, in order to further facilitate the design of INDQE derivatives targeted against Gram-negative bacteria, a hybrid molecule combining Pyrazinamide with active probe **51** using an ester linkage was designed. Pyrazinamide is a first line anti-TB drug used in the clinical setup. Making hybrid molecules may enhance the antibacterial efficacy of these INDQE compounds and widen the scope to target other pathogenic bacteria including *M. tuberculosis*. The following scheme was proposed for the synthesis of some of these molecules.

Scheme AI.2. Proposed synthetic scheme for synthesis of INDQE derivatives hitting Gram-negative bacteria

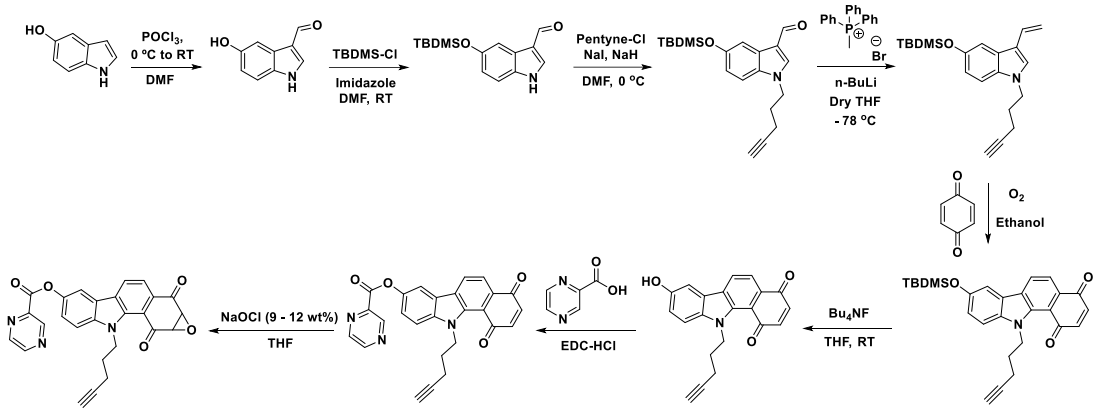

These molecules will then be evaluated for their antibacterial activity against ESKAPE pathogens.

AI.1.2. Synthesis and characterization of compounds:

Procedure for synthesis of compound **53**:[2] Compound **51** (50 mg), Peg-N_3 (prepared by lab colleague) (50 mg), Copper Sulphate pentahydrate (41.7 mg), Sodium ascorbate (36.1 mg), Benzoic acid (37.1 mg) were all added in a 25 mL RB flask. To this was added 3 mL methanol, 2 mL dichloromethane, 2 mL water. The reaction mixture was then stirred at room temperature for 10 min. (TLC analysis). All the solvents from the reaction mixture were then evaporated under reduced pressure. The organic product was then extracted in DCM, washed with brine, dried over Na_2SO_4. And solvent evaporated under reduced pressure to get the crude compound. The crude product was then purified on a Prep HPLC Column Kromasil C18 (21.5 mm x 250 mm 10 μm) with water and acetonitrile as the eluting solvents. The pure product was obtained at 52% ACN-water eluting system.

9-(3-(1-(2-(2-(2-(2-hydroxyethoxy)ethoxy)ethoxy)ethyl)-1H-1,2,3-triazol-4-yl)propyl)-1a,10a-dihydro-2H-oxireno[2',3':4,5]benzo[1,2-a]carbazole-2,10(9H)-dione (53).

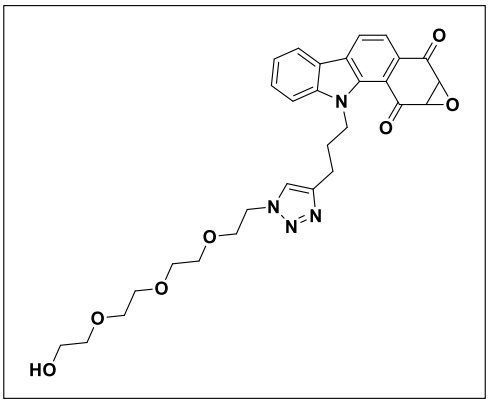

Starting from **51** (50 mg, 0.152 mmol), the click adduct **53** was isolated as a red-brown dark solid (24 mg, 29%). FT-IR (ν_{max}, cm^{-1}): 2922, 2861, 1687, 1465, 1335, 1287, 1205, 1126, 1066, 739; ^{1}H-NMR (400 MHz, $CDCl_3$): δ 8.34 (d, *J* = 8.0 Hz, 1H), 8.08 (d, *J* = 7.8 Hz, 1H), 7.86 (d, *J* = 8.0 Hz, 1H), 7.58-7.49 (m, 2H), 7.43 (s, 1H), 7.30 (t, *J* = 7.3 Hz, 1H), 4.56-4.47 (m, 5H), 4.13 (dd, *J* = 12.7, 4.2 Hz, 2H), 3.84 (t, *J* = 5.0 Hz, 2H), 3.67 (t, *J* = 4.2 Hz, 2H), 3.59-3.52 (m, 11H), 2.61 (t, *J* = 6.1 Hz, 2H).; ^{13}C NMR (100 MHz, $CDCl_3$): δ 192.5, 191.5, 143.9, 136.8, 131.3, 130.1, 128.6, 125.3, 121.8, 121.0, 120.9, 118.2, 117.8, 110.6, 72.5, 70.6, 70.5, 70.4, 70.2, 69.7, 61.7, 56.1, 54.7, 50.2, 45.0, 27.2, 22.9.; HRMS (ESI): for $[C_{29}H_{32}N_4O_7+H]^+$: Calculated: 549.2349, Found: 549.2352

AI.1.3. Spectral charts

^{1}H NMR of **53**

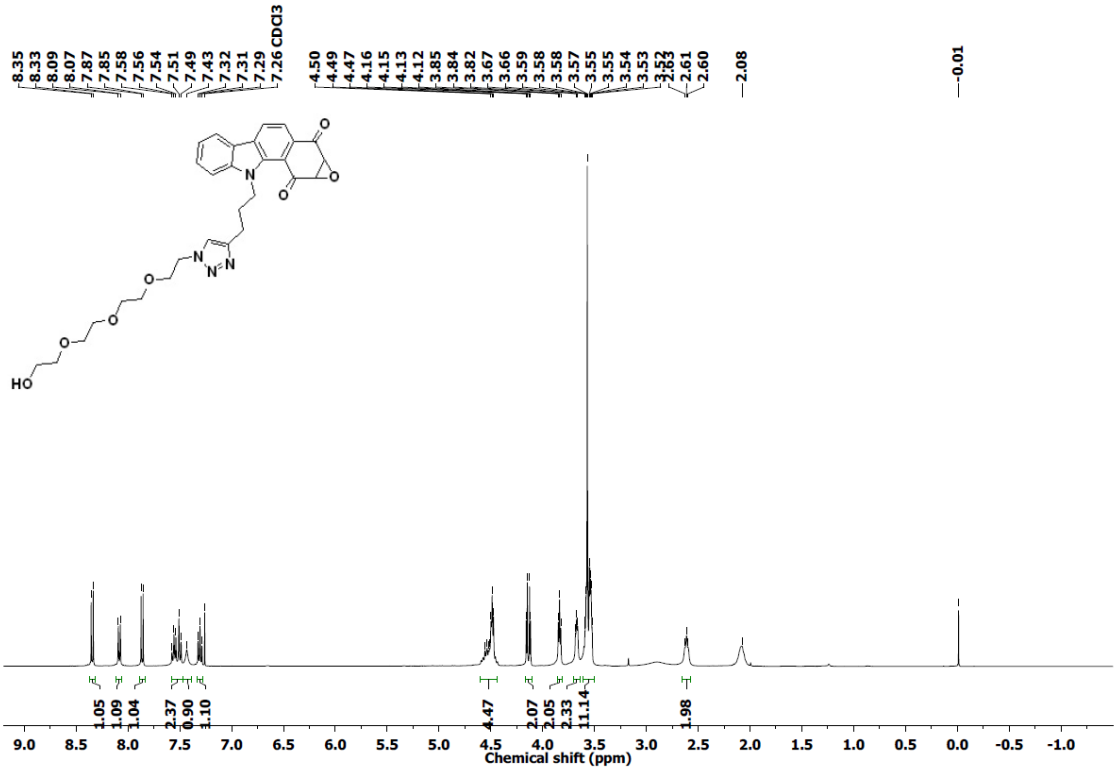

^{13}C NMR of **53**

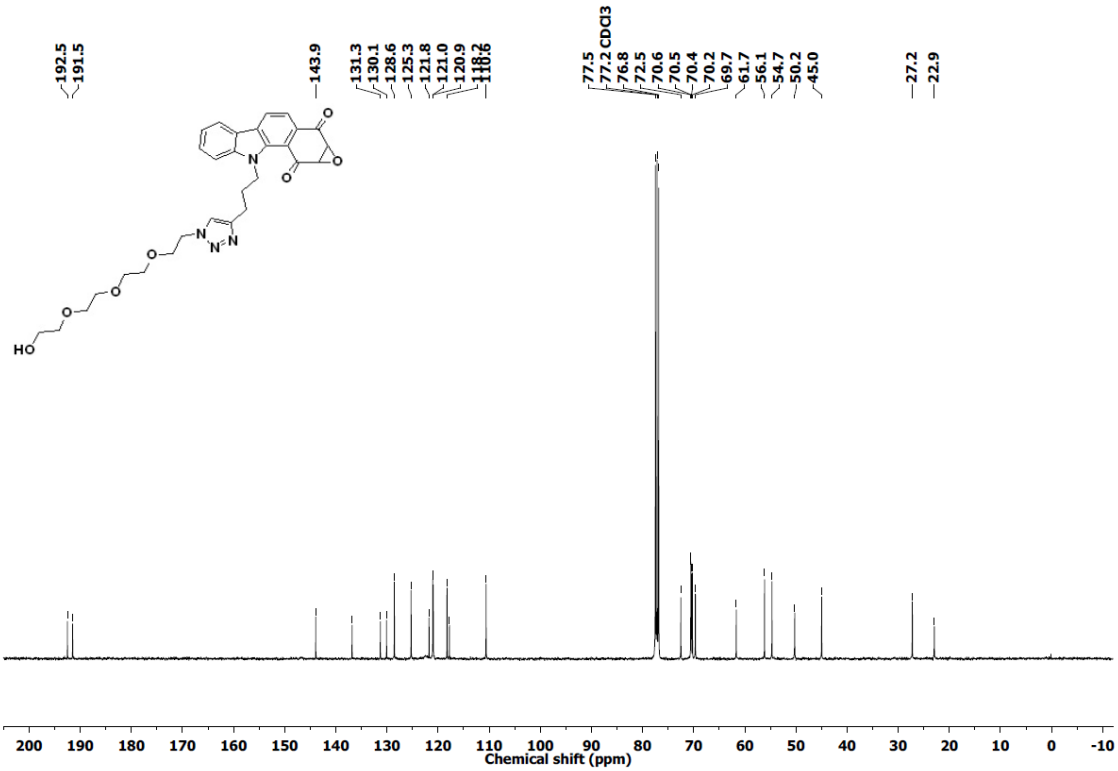

AI.1.4. References:

(1) Richter, M. F.; Drown, B. S.; Riley, A. P.; Garcia, A.; Shirai, T.; Svec, R. L.; Hergenrother, P. J. Predictive Compound Accumulation Rules Yield a Broad-Spectrum Antibiotic. *Nature* **2017**, *545* (7654), 299–304.

(2) Sharma, A. K.; Nair, M.; Chauhan, P.; Gupta, K.; Saini, D. K.; Chakrapani, H. Visible-Light-Triggered Uncaging of Carbonyl Sulfide for Hydrogen Sulfide (H 2 S) Release. *Org. Lett.* **2017**, *19* (18), 4822–4825.

Appendix II - Synopsis

Design, Synthesis and Evaluation of Small Molecules for Profiling Thiol Proteome of Microbes

Chapter 1: Introduction

Thiols are organic compounds with a 'sulfhydryl' group as the main functional group. As much as they are an important class of compounds in chemistry, they are vital molecules in a biological system. Cysteine is one of the most important biological thiol. It is an amino acid, and as a residue, is highly underrepresented on the protein sequence (3.3%).[1] Interestingly, it is involved in numerous biochemical processes (Figure 1) and conserved on the proteome suggesting its extraordinary importance. Cysteines are redox-active groups[2] and are important in a number of post-translational modifications (PTMs)[3] which are responsible in protecting the integrity of the cell. For example, in certain bacteria, *S*-glutathionation takes place in order to protect the active site cysteine in certain enzymes from getting oxidized to an irreversible sulfur oxidation state. *S*-bacillithiolation[4,5] and *S*-mycothiolation are also important defense strategies in *B. subtilis*, *S. aureus* and *M. tuberculosis*. In *S. aureus*, cysteine-phosphorylation, which is a rare PTM, of certain transcriptional factors (TFs), is important for virulence development and generating resistance against vancomycin.[6] Disulfide bond formation is important from the point-of-view of maintenance of the structural stability of the protein.

Figure 1. Schematic showing the important roles of Cysteine residues of proteins

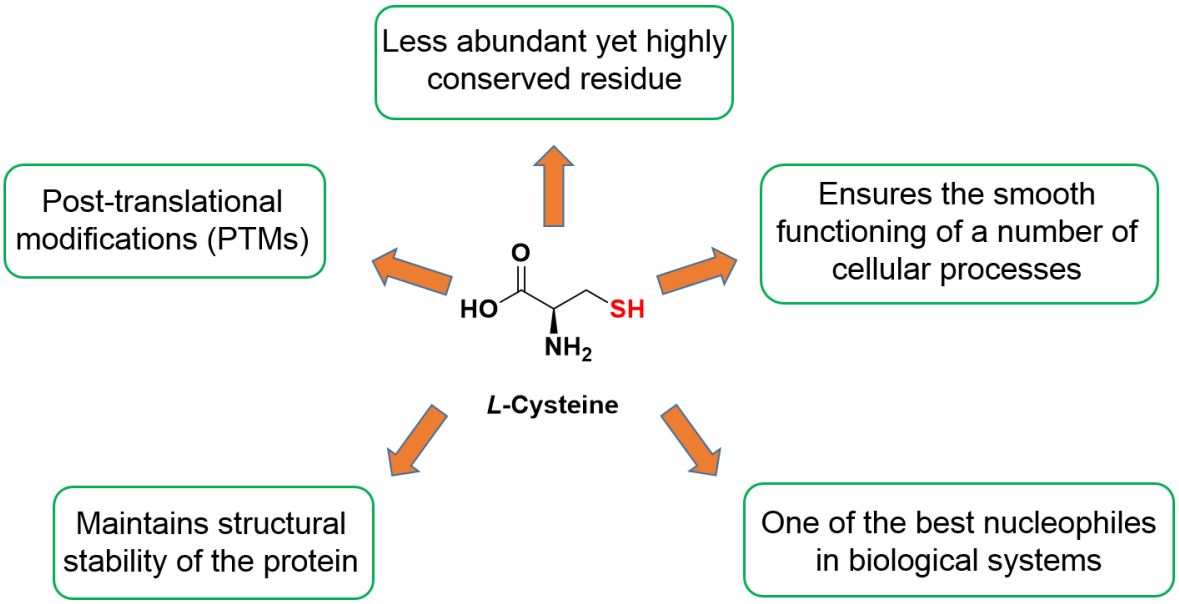

Oxidised forms of cysteine such as sulfenic acid, are important in redox homeostasis and cellular signalling. Glutathione (Figure 2), a tripeptide containing cysteine, essays the role of antioxidant in mammalian cells and bacteria like *E. coli*.[7] Similarly, Bacillithiol (Figure 2) plays an important role in redox homeostasis in *S. aureus*.[4,8,9]

Figure 2. Low molecular weight reduced thiols found in cells

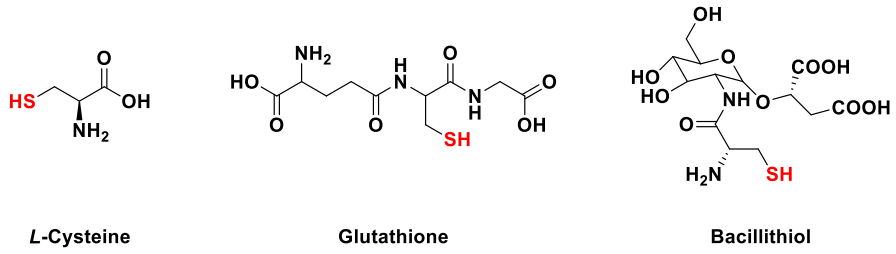

L-Cysteine Glutathione Bacillithiol

Given these important roles that cysteine essays in biological systems, it is indeed a very attractive target especially from the therapeutic and diagnostic point-of-view. A number of compounds have been developed that have been used as probes and sensors for the detection of thiols.[10–12] These include maleimides, haloacetamides, Michael acceptors, vinyl sulfones, propargyl amides, epoxides, *etc.* Targeting important cysteine residues on key proteins has generated significant therapeutic interest that has resulted in inhibition of bacterial infections, cancers and other deadly diseases.[1,13–15] Amongst the scaffolds studied, epoxides are of significant importance. These are found as constituents of natural products with therapeutic importance. Fosfomycin (Figure 3), a clinically used antibiotic against drug-resistant *S. aureus* infections, covalently reacts with a cysteine residue on the *MurA* protein, which is important for cell wall biosynthesis. E64 (Figure 3) is another natural product which is a good inhibitor of cysteine proteases including cathepsin.[16]. Derivatives of E64 have been found to be active against *S. epidermis*,[17] *C. difficile*,[18] and *S. typhimurium*.[19]

Figure 3. Structures of Fosfomycin and E64

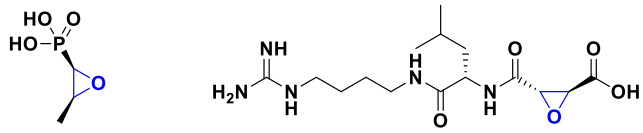

Fosfomycin E64

Another thiol-reactive scaffold bearing the epoxide functional group is 2,3-epoxy-1,4-benzoquinone. Natural products bearing this scaffold have been found to have medicinal properties. For example, 2,3-epoxysesamone,[20,21] Frenolicin[22] have antibacterial, antifungal properties respectively. Recent reported examples further suggest the therapeutic importance

of this scaffold. For example, Terreic acid, a fungal metabolite, is an inhibitor of Bruton's tyrosine kinase (BTK) (Figure 4A).[23] Sieber and co-workers have reported the amino-2,3-epoxy-1,4-naphthoquinone scaffold (AEC-FM233, Figure 4B) to be reactive with cellular thiols, targeting certain redox-active proteins, and proving to be detrimental to the growth of Gram-negative *S. typhimurium*.[24] This study was followed up by another, where the same group reported a similar scaffold to monitor Parkinsonism-associated protein DJ-1 (PARK7) in live cells.[25] The molecule **AEC-FM247** (Figure 4C) could effectively label the cysteine residue on this protein in its reduced state *via* the epoxide warhead. Recently, Miyoshi and co-workers have reported epoxycyclohexenedione-type compounds (ECHD-AMM-59, Figure 4D) as potent inhibitors of bovine mitochondrial ADP/ATP carrier.[26] Chakrapani and co-workers have reported Naphthoquinone epoxides (NQEs, Figure 4E) as potent inhibitors of human leukemia (THP1) cell proliferation.[27] These compounds were potent Reactive Oxygen Species (ROS) generators, activated by their reaction with a cellular thiol. Thus, overall, this scaffold showed therapeutic potential that could further be utilized for developing antibacterial and anticancer agents.

Figure 4. Reported examples with quinone-epoxide as reactive moiety

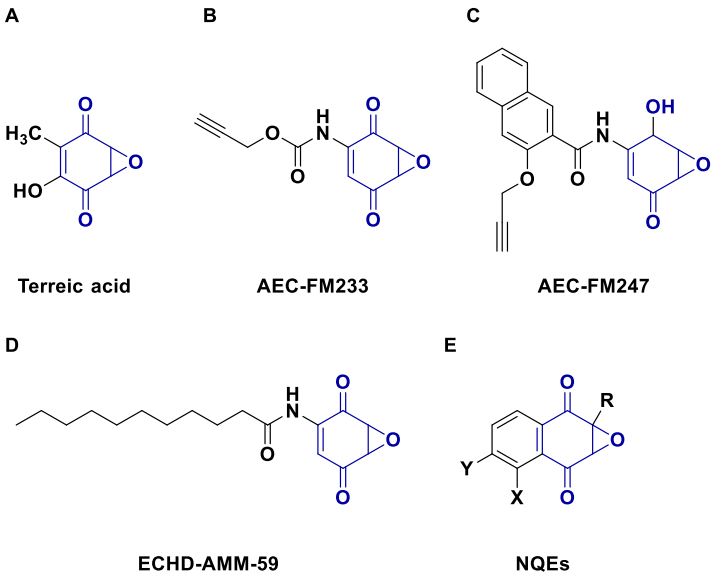

Antimicrobial resistance has been a taxing world health problem today and remedies that could lower this burden are in urgent need. Especially, infections caused by drug-resistant pathogenic bacteria like *S. aureus* are day-by-day becoming difficult to treat. A part of the resistance timeline is shown in Figure 5. Initially, treated by antibiotics of the penicillin family such as Methicillin, the bacteria generated resistance against it. Methicillin-resistant *S. aureus* (MRSA) infections have since created terrible health issues across world population causing sepsis,

endocarditis, osteomyelitis *etc.* resulting in a number of fatalities.[28] Vancomycin is a clinically used antibiotic as the last resort for the treatment of MRSA infections. However, in the last two decades, a steep rise has been seen in Vancomycin-intermediate *S. aureus* (VISA) and Vancomycin-resistant *S. aureus* (VRSA) infections that have posed severe challenges on our health care systems.[29,30] These have resulted in severe community-acquired infections that are now almost untreatable, as this pathogen is found extensively in hospital settings. Cross-resistance observed for VRSA to Daptomycin,[31] the antibiotic of last resort to treat a number of drug-resistant *S. aureus* infections, has narrowed down the fight against antibiotic resistance substantially. Thus, new antibacterial agents and that too, with a novel mechanism of action are in urgent need.

Figure 5. AMR Timeline for *Staphylococcus aureus*

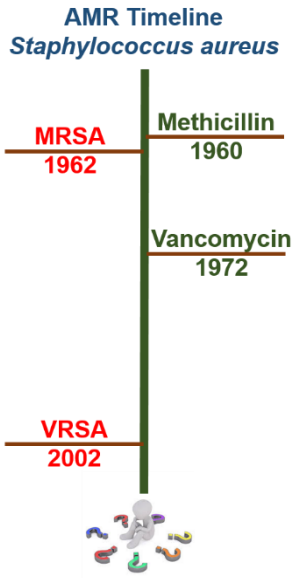

Thus, in order to develop a potent antibacterial agent targeting cysteine residues using the said scaffold, following were the challenges posed:

1) Cell permeability

2) Tunability in reactivity with thiol

3) Inhibition of bacteria at low concentrations

4) No significant cytotoxicity

5) Novel drug target

Now, in order to develop a new antibacterial agent and to identify its target, a technique known as Activity-Based Protein Profiling (ABPP) was employed. ABPP or chemoproteomics has been extensively used in the process of drug discovery and development.[32] ABPP is a technique established about two decades ago,[33] to study the complex proteomes in various biological systems especially cancer cells[34] and pathogenic bacteria.[35] The aim of the study is either from a diagnostic or therapeutic point-of-view, where reactivity of certain important protein residues is utilized to interrogate diverse biological processes. A typical ABPP experiment involves a probe called Activity-based probe (ABP). Generally, an ABP comprises of three parts. First, a reactive or a binding group where the protein residue will react, second, an analytical handle comprising of an alkyne, an azide or a biotin tag which can guide in obtaining a readout, and thirdly, a linker that connects the binding group to the analytical handle (Figure 6).[36] Thus, this technique can be used for identifying targets of novel antibacterial agents.

Figure 6. Design of Activity Based Probe (ABP)

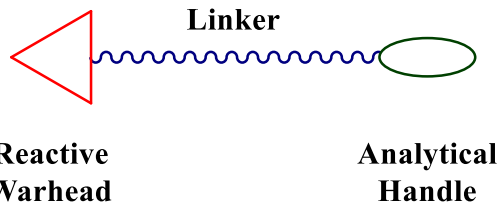

The development of INDQE analogues as potent antibacterial agents would be discussed in Chapter 2. Here, the tunability in reactivity with thiol utilising structural modifications around the epoxide will also be discussed. Identification of lead compounds, inhibition of drug-resistant VRSA, followed by cytotoxicity studies will be discussed. Chemoproteomic profiling of the thiol proteome of *S. aureus*using INDQE alkyne probes and identification of probable targets of the lead compound will be discussed in Chapter 3. Finally, validation of the identified targets using ABPP experiments will be discussed in Chapter 4. Here, a subset of the identified targets, the transcriptional factors, were cloned, expressed and purified. Site-directed mutagenesis yielded cysteine-point mutants which were further utilised for validation.

Chapter 2: Design, synthesis and evaluation of INDQE compounds as thiol targeting probes with potent antibacterial activity

Earlier, 2,3-epoxy-1,4-naphthoquinones were reported as thiol-reactive molecules showing antiproliferative properties.[27] When tested against drug-resistant Gram-positive bacteria, such

as *S. aureus*, they were found to be good inhibitors, inhibiting the resistant strain MRSA with MIC values of 16 µg/mL.[37] However, permeability and tunability with reactivity with thiol could not be further tuned with the said scaffold, and hence, the design was further modified. Indole, a constituent of the core scaffold structure of a number of natural products and drugs, is known to improve the pharmacological properties of the drug, and is thus considered as a privileged scaffold.[38] Hence, indole was added to the revised design (Figure 7).

Figure 7. Revised design - From NQEs to INDQEs

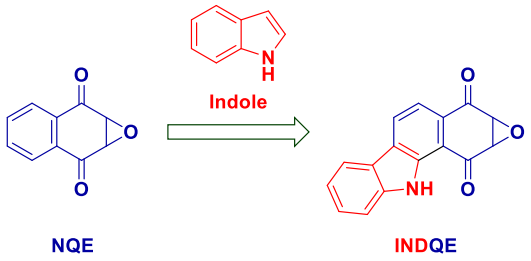

The INDQE scaffold was explored and a small library of molecules was synthesized (Scheme 1) and evaluated for reactivity with thiol and antibacterial potency. From this preliminary study, it was found that the reactivity with thiol is in good correlation with antibacterial potency of these compounds, and substitution at the '3' position deters the reactivity with thiol substantially.[37]

Scheme 1. Synthesis of INDQE scaffold

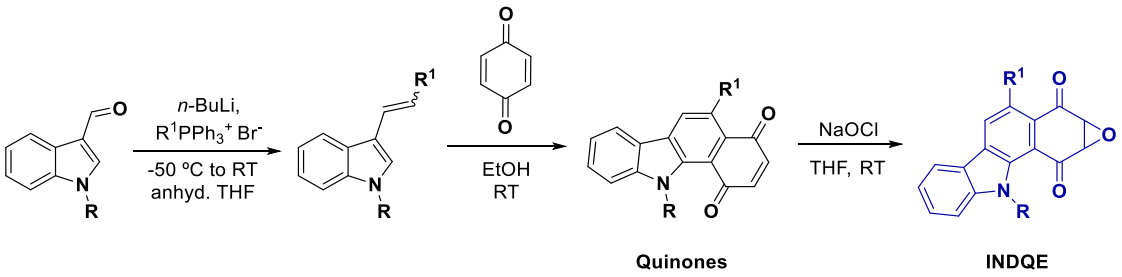

Compound **25** was identified as the lead compound with potent inhibitory activity against Gram-positive *S. aureus* (MIC = 0.125-0.5 µg/mL). Further, in this study, another analogue, compound **26**, with a bulkier substituent 'ethyl' at the '3' position was synthesized. This compound followed the trend and was found to be less reactive with thiol and inactive against *S. aureus*. Further, analogues with substitutions on the epoxide, were synthesized (Scheme 2). Epoxide, being the reactive group in the molecule, substitutions on the epoxide were expected to help modulate the reactivity with thiol. Here, due to the substitution on the benzoquinone used in the reaction scheme, a set of regioisomers were obtained in the Diels-Alder reaction

(Scheme 3). These regioisomers were further converted to the respective epoxides. Some of the regioisomers were separated using preparative-HPLC.

Scheme 2. General synthesis scheme for INDQE compounds with substitution at the epoxide

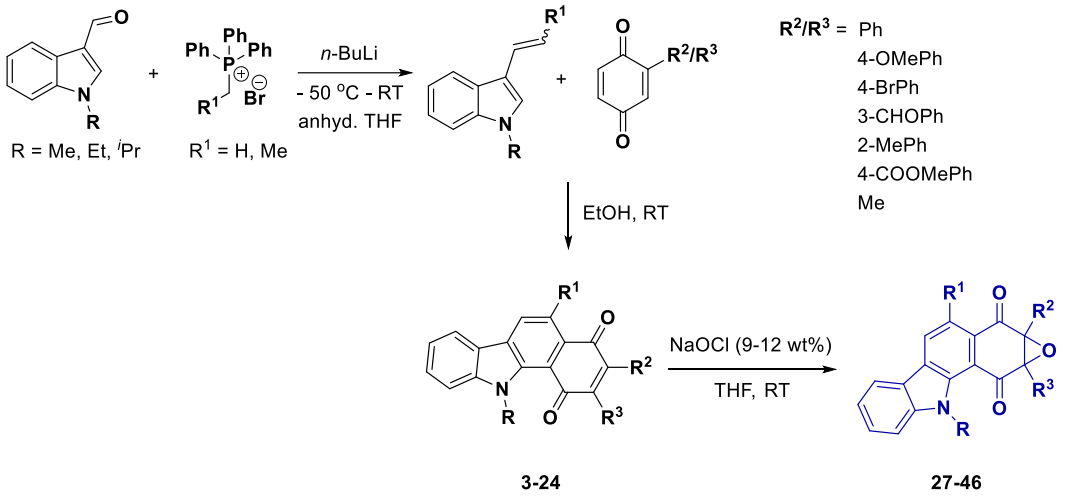

Scheme 3. Two possible orientations of the dienophile in the Diels-Alder reaction

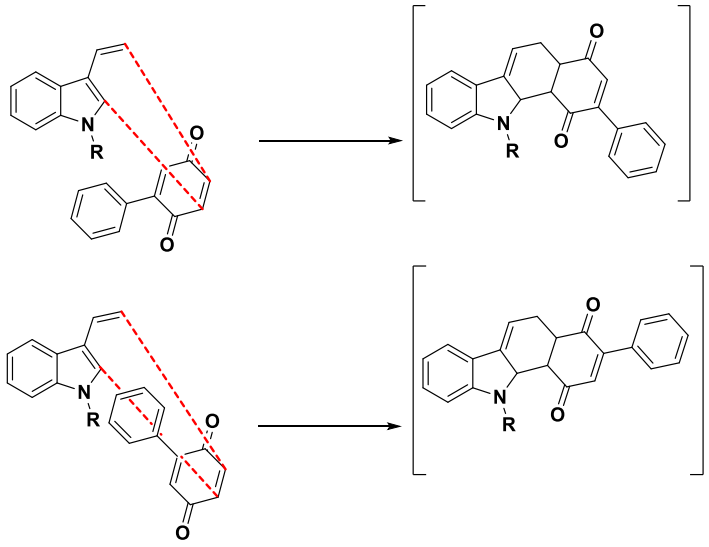

The set of regioisomers were further evaluated for their reactivity with thiol and antibacterial potency. Upon analysis, a contrasting behaviour was observed for every set of regioisomer, where one regioisomer (‘10’ isomer) was found to be more reactive with thiol and an active inhibitor of *S. aureus*. On the other hand, the other regioisomer (‘1’ isomer) was found to be comparatively less reactive with thiol, and did not inhibit the bacteria even at the highest concentration tested (Figure 8, for compounds **27** (MIC = 0.0625 μg/mL) and **28** (MIC > 64 μg/mL) with phenyl substituent).

Figure 8. Reactivity difference between regioisomers **27** (‘10’ isomer) and **28** (‘1’ isomer) (Phenyl substituent) with thiol

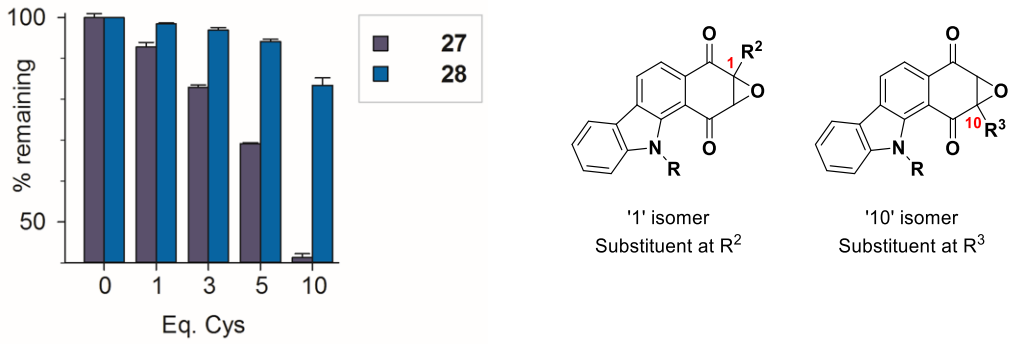

The crystal structures of compounds **25**, **27** and **28** suggested a boat-like conformation of the quinone epoxide (Figure 9). Analysis of the overlap of the van der waals radii between key groups neighbouring the epoxide suggested that the ‘1’ position was possibly more favoured for thiol attack as compared to ‘10’ position. This was because of the impact of the overlap of carbonyl oxygen with the substituent at the ‘3’ position, which would possibly hinder the carbonyl group approaching planarity after a thiol attack. This was also in accordance to the earlier observations where bulkier substituents at ‘3’ position deterred reactivity with thiol.Thus, these observations explained, to a certain level, the possible reason for the contrasting behaviour of the two regioisomers towards reacting with a thiol. Also, the studies with these compounds reiterated the correlation between reactivity with thiol and antibacterial activity. A HPLC spiking experiment was conducted with compound **25** and 4-nitrobenzyl thiol that confirmed the formation of a covalent adduct.

Figure 9. Boat-like conformation for quinone epoxide - Crystal structure of **25**

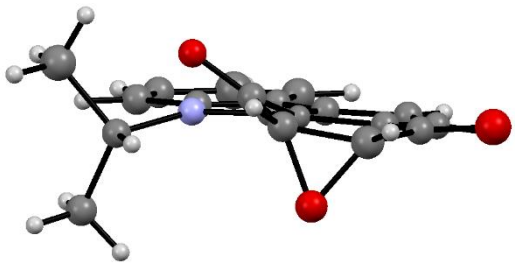

Having established the tunability of this scaffold for reactivity with thiol, next, kinetics of the reaction were studied. A subset of four compounds **25**, **26**, **27** and **28** was chosen for this study. Compounds **25** and **27**, which were reactive with a thiol and potent inhibitors of *S. aureus*, were found to have a higher rate of reaction (7.54×10^{-2} min^{-1} and 3×10^{-2} min^{-1} respectively) (Figure 10). On the contrary, compounds **26** and **28**, which were less reactive with thiol and

inactive against *S. aureus*, had lower reaction rates (1.3×10^{-2} min^{-1} and 0.78×10^{-2} min^{-1} respectively). Thus, this assay suggested the vital role of kinetics of reaction with thiol in driving the inhibitory potency of INDQE compounds.

Figure 10. Kinetics of reaction of INDQE compounds with thiol

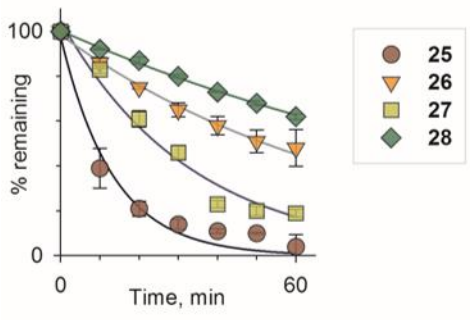

From these studies, compound **25** was identified and used further as the lead compound. It was found to be a potent inhibitor of a number of clinically isolated VRSA strains. A time-kill analysis study was conducted with VRSA strain HIP 11714 which suggested that the lead compound **25** showed potent bactericidal activity comparable to that of Daptomycin, the drug of last resort against severe infections caused by drug-resistant bacteria like VRSA.[39] The compound was further tested for its cytotoxicity against VERO cells and found to have a selective index of more than 200. Compound **25** was not found to adversely affect human erythrocytes as no evidence was found for hemolysis, even at elevated concentrations of 100 μg/mL.

Thus, this compound was a potent antibacterial agent against *S. aureus*. However, no inhibitory activity for this class of compounds was seen against any other pathogenic bacteria, including ESKAPE pathogens. Thus, further studies focused on identifying the probable targets of the lead INDQE compound.

Chapter 3: Chemoproteomic profiling of the thiol proteome of *S. aureus* and identification of probable protein targets of INDQE compounds

Literature reports suggest use of activity-based protein profiling (ABPP) technique as an important tool in drug discovery programmes.[32,35,40] Sieber and co-workers have used this technique effectively to identify important targets in pathogenic bacteria. In one study, they have screened a library of alkyne-tagged α-methylene-γ-butyrolactones against *S. aureus* and using chemoproteomics, have identified inhibitors of virulence factor α-hemolysin (Hla).[41]

These compounds are Michael acceptors and may be hitting certain cysteine residues on cellular proteins. They have been shown to covalently bind to certain key transcriptional regulators like SarA, SarR and MgrA. In another study, they have identified certain redox-active proteins such as Glutaredoxin 2 and Thioredoxin-1 as potent targets in *S. typhimurium*, using scaffolds inspired from natural products aminoepoxycyclohexenones (AECs).[24]

Thus, in order to identify the targets of INDQE lead compound **25**, two INDQE alkyne probes **51** and **52** (Figure 11) were synthesized following similar synthetic schemes. These probes were assessed further for their reactivity with thiol and antibacterial potency. It was found that probe **51** showed similar reactivity profile as lead compound **25** and comparable antibacterial potency (MIC = 1 μg/mL) against *S. aureus*. On the other hand, probe **52** showed similar reactivity as inactive compound **28** and was also found to be inactive against *S. aureus*. Thus, probe **51** was used as an active probe and probe **52** as an inactive probe.

Figure 11. Structures of INDQE alkyne probes synthesized in the study

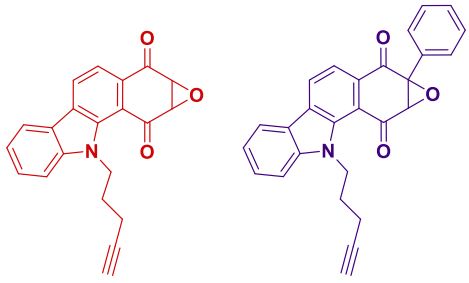

Probe 51 Probe 52

Next, these probes were utilized for profiling the thiol proteome of *S. aureus*. Click reaction was employed using Rhodamine azide as the reporter molecule. A dose-dependent study in soluble lysates suggested the utility of these probes for profiling the thiol proteome (Figure 12). Here, probe **51**, going in accordance with its reactivity with thiol, showed a dose-dependent labelling of a number of cysteine residues on the proteome. On the contrary, diminished labelling was observed for treatment with probe **52**. Similar results were obtained for *in situ* studies. These studies suggested that the reactivity with thiol was translated to the cellular level.

Figure 12. Dose-dependent protein modification in soluble fractions of *S. aureus* lysates using probes **51** and **52**

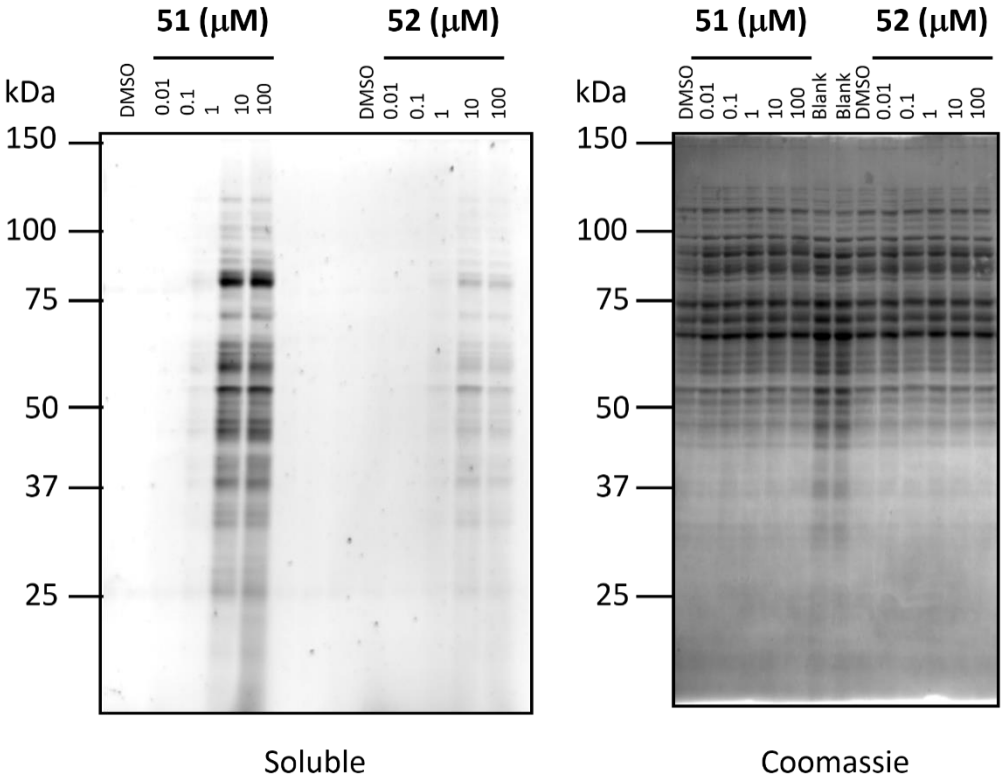

A selectivity study was conducted for probe **51** to test its selectivity with cysteine residues on proteins, and Iodoacetamide (IAM) was used in this assay. It was found that IAM pretreated lysates showed complete ablation of signal for probe **51** compared to untreated lysates (Figure 13).In another ABPP experiment, probe **51** labelled a number of residues in an *in vitro* setting in *E. coli*, whereas a complete ablation was observed in an *in vivo* experiment. This result suggested that INDQE compounds may lack permeability in Gram-negative pathogens like *E. coli*, which may be the underlying reason for the inactivity of these compounds against such bacteria.

Figure 13. Protein modification using probe **51** in *S. aureus* with IAM pretreatment

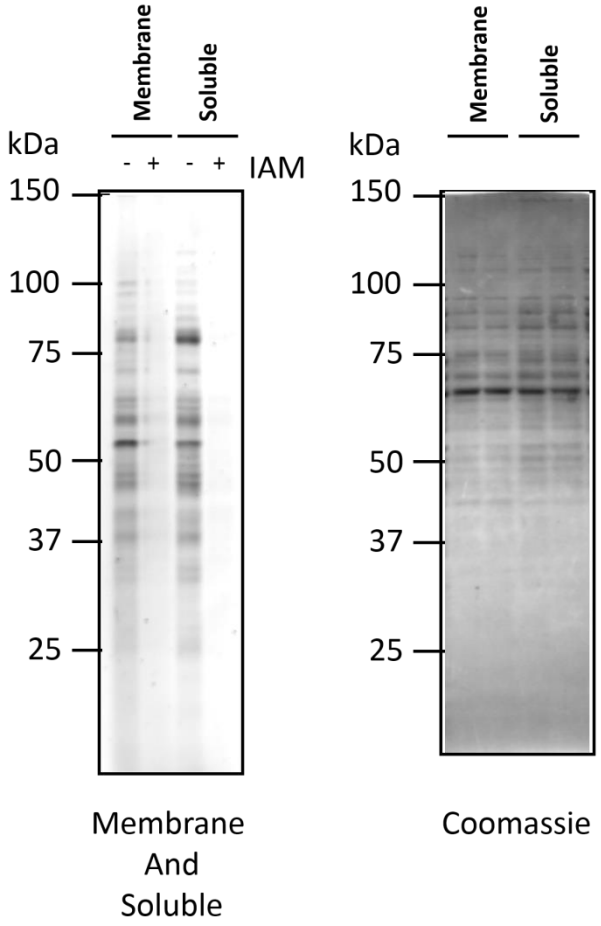

It was now well established that probe **51** is an active probe and labels a number of cysteine residues on the proteome of *S. aureus*. Thus, this probe was next chosen to conduct proteomics studies in order to find the targets of the lead compound **25**. ABPP chase experiments were conducted using probe **51** as a chaser. From the chemoproteomics assay, using biotin azide, followed by avidin enrichment and trypsin digestion, 17 potential protein targets for compound **25** were pulled down. 6 protein targets that were identified were transcriptional or virulence factors. This result was of great significance as transcriptional factors (or virulence factors) play an important role in generating antibiotic resistance.[6,42–44] Further experiments would involve validation of these identified targets.

Chapter 4: Validation of protein targets of INDQE compounds

A subset of the identified targets were transcriptional or virulence factors. Transcriptional factors are proteins that bind to a specific DNA sequence and control the transcription rate.[45]

Transcription rate is the rate at which genetic information is passed by a DNA onto a messenger RNA. Thus, TFs play a very crucial role in the cell. In bacteria such as *S. aureus*, regulation of virulence determination is majorly done by these DNA-binding proteins and are thus considered important for the mere survival of these bacteria.[46,47] Out of the filtered list of 17 proteins identified as probable targets, 5 proteins were chosen namely Mar R 05815, Mar R 12840, HxlR, Pho P and CcpA. The two Mar R (Multiple Antibiotic Resistance regulator) proteins belong to the family of proteins which are known, as the name suggests, to regulate the antibiotic resistance in pathogenic bacteria, and were of more interest as these were novel targets. Interestingly, all these identified targets were found to have at least one cysteine residue which was conserved across ESKAPE pathogens, as found out from the Bioinformatics assay (Table 1).

Table 1. Bioinformatics assay

	Transcriptional or Virulence factors	Cysteine residue(s)	Conserved Cysteine residue(s)
1	MarR family transcriptional regulator_12840	C12	C12
2	MarR family transcriptional regulator_05815	C61	C61
3	Catabolite control protein A (Ccpa)	C216, C242	C242
4	HxlR family transcriptional regulator	C4, C29, C32	C4
5	PhoP family transcriptional regulator	C31, C65	C31, C65

Thus, cloning followed by expression and purification of these proteins was conducted. Further, in order to validate that the cysteine residue on the target proteins is indeed the target of the INDQE compounds, cysteine point mutants of the wild-type proteins were generated using site-directed mutagenesis. ABPP experiments were conducted with probe **51** for both wild-type proteins and their cysteine-point mutants for validation (Figure 14). Here, probe **51** showed a dose-dependent modification of the wild-type proteins, whereas diminished or no labelling was seen for the cysteine point-mutants. The two Mar R proteins were thus, validated as targets of the INDQE compounds. Similar results were obtained for CcpA, where one conserved cysteine was mutated. Here, probe **51** labelled the wild-type protein whereas showed a diminished labelling for the cysteine point-mutant.

Figure 14. ABPP for validation wild-type target proteins using cysteine point mutants

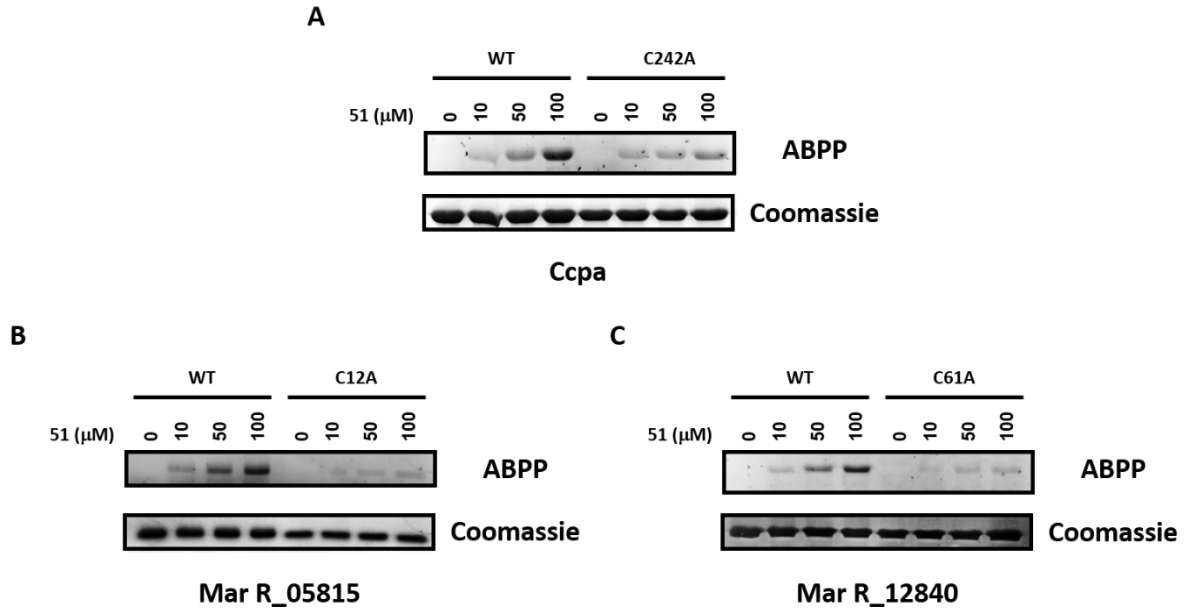

To summarize, INDQE compounds were designed and developed as a tunable thiol-reactive scaffold with potent antibacterial activity against Gram-positive pathogen *S. aureus*. A lead compound **25**, was identified, that showed a covalent-adduct formation with a thiol. This compound was found to be a potent inhibitor of a number of clinically-derived drug-resistant strains including VRSA. Chemoproteomics was conducted using two alkyne-tagged probes of the INDQE series. The active probe **51** showed selective labelling of cysteine residues in the *S. aureus* proteome and was further utilized to pull-down the probable protein targets using biotin-avidin enrichment followed by trypsin digestion. The probable targets consisted of transcriptional or virulence factors. These proteins were expressed using cloning techniques and purified. Cysteine-point mutants were generated using site-directed mutagenesis. Two novel targets, namely Mar Rs (Multiple Antibiotic Resistance Regulators) were validated as targets of lead compound **25**. Thus, this scaffold can further be utilized from the point-of-view of drug development. The scaffold can be modified further in order to improve permeability and Gram-negative pathogens could be targeted.

References:

(1) Hallenbeck, K. K.; Turner, D. M.; Renslo, A. R.; Arkin, M. R. Targeting Non-Catalytic Cysteine Residues Through Structure-Guided Drug Discovery. *Curr. Top. Med. Chem.***2017**, *17* (1), 4–15.

(2) Paulsen, C. E.; Carroll, K. S. Cysteine-Mediated Redox Signaling: Chemistry, Biology, and Tools for Discovery. *Chem. Rev.***2013**, *113* (7), 4633–4679.

(3) Pace, N. J.; Weerapana, E. Diverse Functional Roles of Reactive Cysteines. *ACS Chem. Biol.***2013**, *8* (2), 283–296.

(4) Loi, V. Van; Busche, T.; Preuß, T.; Kalinowski, J.; Bernhardt, J.; Antelmann, H. The AGXX® Antimicrobial Coating Causes a Thiol-Specific Oxidative Stress Response and Protein S-Bacillithiolation in Staphylococcus Aureus. *Front. Microbiol.***2018**, *9*, 3037.

(5) Imber, M.; Huyen, N. T. T.; Pietrzyk-Brzezinska, A. J.; Loi, V. Van; Hillion, M.; Bernhardt, J.; Thärichen, L.; Kolšek, K.; Saleh, M.; Hamilton, C. J.; et al. Protein S - Bacillithiolation Functions in Thiol Protection and Redox Regulation of the Glyceraldehyde-3-Phosphate Dehydrogenase Gap in Staphylococcus Aureus Under Hypochlorite Stress. *Antioxid. Redox Signal.***2018**, *28* (6), 410–430.

(6) Sun, F.; Ding, Y.; Ji, Q.; Liang, Z.; Deng, X.; Wong, C. C. L.; Yi, C.; Zhang, L.; Xie, S.; Alvarez, S.; et al. Protein Cysteine Phosphorylation of SarA/MgrA Family Transcriptional Regulators Mediates Bacterial Virulence and Antibiotic Resistance. *Proc. Natl Acad. Sci. U S A***2012**, *109* (38), 15461–15466.

(7) Ferguson, G. P.; Booth, I. R. Importance of Glutathione for Growth and Survival of Escherichia Coli Cells: Detoxification of Methylglyoxal and Maintenance of Intracellular K+. *J. Bacteriol.***1998**, *180* (16), 4314–4318.

(8) Newton, G. L.; Rawat, M.; La Clair, J. J.; Jothivasan, V. K.; Budiarto, T.; Hamilton, C. J.; Claiborne, A.; Helmann, J. D.; Fahey, R. C. Bacillithiol Is an Antioxidant Thiol Produced in Bacilli. *Nat. Chem. Biol.***2009**, *5* (9), 625–627.

(9) Newton, G. L.; Fahey, R. C.; Rawat, M. Detoxification of Toxins by Bacillithiol in Staphylococcus Aureus. *Microbiol.***2012**, *158* (Pt 4), 1117–1126.

(10) Chen, X.; Zhou, Y.; Peng, X.; Yoon, J. Fluorescent and Colorimetric Probes for Detection of Thiols. *Chem. Soc. Rev.***2010**, *39* (6), 2120–2135.

(11) Peng, H.; Chen, W.; Cheng, Y.; Hakuna, L.; Strongin, R.; Wang, B. Thiol Reactive Probes and Chemosensors. *Sensors (Basel).***2012**, *12* (11), 15907–15946.

(12) Wang, K.; Peng, H.; Wang, B. Recent Advances in Thiol and Sulfide Reactive Probes. *J. Cell. Biochem.***2014**, *115* (6), 1007–1022.

(13) Casini, A.; Scozzafava, A.; Supuran, C. T. Cysteine-Modifying Agents: A Possible Approach for Effective Anticancer and Antiviral Drugs. *Environ. Heal. Perspect.***2002**, *110 Suppl* (Suppl 5), 801–806.

(14) Visscher, M.; Arkin, M. R.; Dansen, T. B. Covalent Targeting of Acquired Cysteines in Cancer. *Curr. Opin. Chem. Biol.***2016**, *30*, 61–67.

(15) Belete, T. M. Novel Targets to Develop New Antibacterial Agents and Novel Alternatives to Antibacterial Agents. *Hum. Microbiome J.***2019**, *11*, 100052.

(16) Barrett, A. J.; Kembhavi, A. A.; Brown, M. A.; Kirschke, H.; Knight, C. G.; Tamai, M.; Hanada, K. L-Trans-Epoxysuccinyl-Leucylamido(4-Guanidino)Butane (E-64) and Its Analogues as Inhibitors of Cysteine Proteinases Including Cathepsins B, H and L. *Biochem. J.***1982**, *201* (1), 189–198.

(17) Oleksy, A.; Golonka, E.; Bańbula, A.; Szmyd, G.; Moon, J.; Kubica, M.; Greenbaum, D.; Bogyo, M.; Foster, T. J.; Travis, J.; et al. Growth Phase-Dependent Production of a Cell Wall-Associated Elastinolytic Cysteine Proteinase by Staphylococcus Epidermidis. *Biol. Chem.***2004**, *385* (6), 525–535.

(18) Dang, T. H. T.; Riva, L. de la; Fagan, R. P.; Storck, E. M.; Heal, W. P.; Janoir, C.; Fairweather, N. F.; Tate, E. W. Chemical Probes of Surface Layer Biogenesis in Clostridium Difficile. *ACS Chem. Biol.***2010**, *5* (3), 279–285.

(19) Hang, H. C.; Loureiro, J.; Spooner, E.; van der Velden, A. W. M.; Kim, Y.-M.; Pollington, A. M.; Maehr, R.; Starnbach, M. N.; Ploegh, H. L. Mechanism-Based Probe for the Analysis of Cathepsin Cysteine Proteases in Living Cells. *ACS Chem. Biol.***2006**, *1* (11), 713–723.

(20) Feroj Hasan, A. F. M.; Furumoto, T.; Begum, S.; Fukui, H. Hydroxysesamone and 2,3-Epoxysesamone from Roots of Sesamum Indicum. *Phytochemistry***2001**, *58*, 1225–1228.

(21) Furumoto, T. Biosynthetic Origin of 2,3-Epoxysesamone in a Sesamum Indicum Hairy

Root Culture. *Biosci., Biotechnol., Biochem.***2009**, *73*, 2535–2537.

(22) Ellestad, G. A.; Whaley, H. A.; Patterson, E. L. The Structure of Frenolicin. *J. Am. Chem. Soc.***1966**, *88*, 4109–4110.

(23) Kawakami, Y.; Hartman, S. E.; Kinoshita, E.; Suzuki, H.; Kitaura, J.; Yao, L.; Inagaki, N.; Franco, A.; Hata, D.; Maeda-Yamamoto, M.; et al. Terreic Acid, a Quinone Epoxide Inhibitor of Bruton's Tyrosine Kinase. *Proc. Natl Acad. Sci. U S A***1999**, *96* (5), 2227–2232.

(24) Mandl, F. A.; Kirsch, V. C.; Ugur, I.; Kunold, E.; Vomacka, J.; Fetzer, C.; Schneider, S.; Richter, K.; Fuchs, T. M.; Antes, I.; et al. Natural-Product-Inspired Aminoepoxybenzoquinones Kill Members of the Gram-Negative Pathogen Salmonella by Attenuating Cellular Stress Response. *Angew. Chem. Int. Ed.***2016**, *55* (47), 14852–14857.

(25) Drechsel, J.; Mandl, F. A.; Sieber, S. A. Chemical Probe To Monitor the Parkinsonism-Associated Protein DJ-1 in Live Cells. *ACS Chem. Biol.***2018**, *13* (8), 2016–2019.

(26) Aoyama, A.; Murai, M.; Ichimaru, N.; Aburaya, S.; Aoki, W.; Miyoshi, H. Epoxycyclohexenedione-Type Compounds Make Up a New Class of Inhibitors of the Bovine Mitochondrial ADP/ATP Carrier. *Biochemistry***2018**, *57* (6), 1031–1044.

(27) Dharmaraja, A. T.; Dash, T. K.; Konkimalla, V. B.; Chakrapani, H. Synthesis, Thiol-Mediated Reactive Oxygen Species Generation Profiles and Anti-Proliferative Activities of 2,3-Epoxy-1,4-Naphthoquinones. *Med. Chem. Commun.***2012**, *3* (2), 219–224.

(28) Chambers, H. F.; DeLeo, F. R. Waves of Resistance: Staphylococcus Aureus in the Antibiotic Era. *Nat. Rev. Microbiol.***2009**, *7* (9), 629–641.

(29) Hiramatsu, K.; Aritaka, N.; Hanaki, H.; Kawasaki, S.; Hosoda, Y.; Hori, S.; Fukuchi, Y.; Kobayashi, I. Dissemination in Japanese Hospitals of Strains of Staphylococcus Aureus Heterogeneously Resistant to Vancomycin. *Lancet***1997**, *350* (9092), 1670–1673.

(30) Kobayashi, S. D.; Musser, J. M.; DeLeo, F. R. Genomic Analysis of the Emergence of Vancomycin-Resistant Staphylococcus Aureus. *MBio***2012**, *3* (4).

(31) Sass, P.; Berscheid, A.; Jansen, A.; Oedenkoven, M.; Szekat, C.; Strittmatter, A.;

Gottschalk, G.; Bierbaum, G. Genome Sequence of Staphylococcus Aureus VC40, a Vancomycin- and Daptomycin-Resistant Strain, To Study the Genetics of Development of Resistance to Currently Applied Last-Resort Antibiotics. *J. Bacteriol.***2012**, *194* (8), 2107–2108.

(32) Moellering, R. E.; Cravatt, B. F. How Chemoproteomics Can Enable Drug Discovery and Development. *Chem. Biol.***2012**, *19* (1), 11–22.

(33) Liu, Y.; Patricelli, M. P.; Cravatt, B. F. Activity-Based Protein Profiling: The Serine Hydrolases. *Proc. Natl Acad. Sci. U S A***1999**, *96* (26), 14694–14699.

(34) Speers, A. E.; Cravatt, B. F. Chemical Strategies for Activity-Based Proteomics. *ChemBioChem***2004**, *5* (1), 41–47.

(35) Puri, A. W.; Bogyo, M. Using Small Molecules To Dissect Mechanisms of Microbial Pathogenesis. *ACS Chem. Biol.***2009**, *4* (8), 603–616.

(36) Evans, M. J.; Cravatt, B. F. Mechanism-Based Profiling of Enzyme Families. *Chem. Rev.***2006**, *106* (8), 3279–3301.

(37) Dharmaraja, A. T. Synthesis and Evaluation of Small Molecule Based Reactive Oxygen Species (ROS) Generators. *Thesis***2015**.

(38) Welsch, M. E.; Snyder, S. A.; Stockwell, B. R. Privileged Scaffolds for Library Design and Drug Discovery. *Curr. Opin. Chem. Bio.***2010**, *14* (3), 347–361.

(39) Cha, R.; Brown, W. J.; Rybak, M. J. Bactericidal Activities of Daptomycin, Quinupristin-Dalfopristin, and Linezolid against Vancomycin-Resistant Staphylococcus Aureus in an in Vitro Pharmacodynamic Model with Simulated Endocardial Vegetations. *Antimicrob. agents chemother.***2003**, *47* (12), 3960–3963.

(40) Gersch, M.; Kreuzer, J.; Sieber, S. A. Electrophilic Natural Products and Their Biological Targets. *Nat. Prod. Rep.***2012**, *29* (6), 659–682.

(41) Kunzmann, M. H.; Bach, N. C.; Bauer, B.; Sieber, S. A. α-Methylene-γ-Butyrolactones Attenuate Staphylococcus Aureus Virulence by Inhibition of Transcriptional Regulation. *Chem. Sci.***2014**, *5* (3), 1158.

(42) Tiwari, S.; da Costa, M. P.; Almeida, S.; Hassan, S. S.; Jamal, S. B.; Oliveira, A.; Folador, E. L.; Rocha, F.; de Abreu, V. A. C.; Dorella, F.; et al. C. Pseudotuberculosis

Phop Confers Virulence and May Be Targeted by Natural Compounds. *Integr. Biol.***2014**, *6* (11), 1088–1099.

(43) Miller, S. I.; Kukral, A. M.; Mekalanos, J. J. A Two-Component Regulatory System (PhoP PhoQ) Controls Salmonella Typhimurium Virulence. *Proc. Natl Acad. Sci. U S A***1989**, *86* (13), 5054–5058.

(44) Gordon, C. P.; Williams, P.; Chan, W. C. Attenuating Staphylococcus Aureus Virulence Gene Regulation: A Medicinal Chemistry Perspective. *J. Med. Chem.***2013**, *56* (4), 1389–1404.

(45) Latchman, D. S. Transcription Factors: An Overview. *Int. J. Biochem. Cell Biol.***1997**, *29* (12), 1305–1312.

(46) Novick, R. P. Autoinduction and Signal Transduction in the Regulation of Staphylococcal Virulence. *Mol. Microbiol.***2003**, *48* (6), 1429–1449.

(47) Bronner, S.; Monteil, H.; Prévost, G. Regulation of Virulence Determinants in Staphylococcus Aureus : Complexity and Applications. *FEMS Microbiol. Rev.***2004**, *28* (2), 183–200.

Appendix III - List of Figures

Appendix IV - List of Schemes

Appendix V - List of Tables

Appendix VI - Copyright permissions

IISER PUNE

amogh kulkarni <amogh.kulkarni@students.iiserpune.ac.in>

Request for permission to reuse some data in my Ph.D. thesis from my publication

2 messages

amogh kulkarni <amogh.kulkarni@students.iiserpune.ac.in> 30 July 2019 at 10:59
To: support@services.acs.org

Dear Sir/Madam,
I, Amogh Kulkarni, a Ph.D. student at the Indian Institute of Science Education and Research, (IISER) Pune, am writing my Ph.D. thesis. We have recently published a paper in the Journal of Medicinal Chemistry and I am the first author on this publication. I wish to use some figures and data for my thesis. I request you to kindly provide copywright permission for the same.
Following are the necessary details:

1) Publication: J. Med. Chem., 2019, 62, 6785-6795 (DOI 10.1021/acs.jmedchem.9b00774)

2) Portion of content to be reused: Figures only (2B, 4 and 6 from the Main manuscript and others from the SI)

3) Where the content will be reused: PhD Thesis

Thanks and Regards,
Amogh Kulkarni

--
With warm regards,
Amogh Kulkarni
Senior Research Fellow,
Dr. Harinath Chakrapani Lab,
Department of Chemistry,
Indian Institute of Science Education and Research (IISER), Pune

amogh.kulkarni@students.iiserpune.ac.in

support@services.acs.org <support@services.acs.org> 30 July 2019 at 11:23
To: amogh kulkarni <amogh.kulkarni@students.iiserpune.ac.in>

Dear Dr. Kulkarni,

Thank you for contacting ACS Publications Support.

Your permission request is granted and there is no fee for this reuse. In your planned reuse, you must cite the ACS article as the source, add this direct link <https://pubs.acs.org/doi/10.1021/acs.jmedchem.9b00774>, and include a notice to readers that further permissions related to the material excerpted should be directed to the ACS.

Should you need further assistance, please let us know.

Sincerely,

Noemi D. Cabalza
ACS Customer Services & Information
Website: https://help.acs.org/
[Quoted text hidden]
{CMI: MCID738453}

Appendix VII - List of Publications

1. **Amogh Kulkarni**,[a] Isha Soni,[b] Dhanashree S. Kelkar,[c] Allimuthu T. Dharmaraja,[a,d] Rathinam K. Sankar,[a,e] Gaurav Beniwal,[a] Abinaya Rajendran,[c] Sharvari Tamhankar,[c] Sidharth Chopra,[b,*] Siddhesh S. Kamat,[c,*] and Harinath Chakrapani[a,*], "Chemoproteomics of an Indole-Based Quinone-Epoxide identifies druggable vulnerabilities in Vancomycin Resistant *Staphylococcus aureus* (VRSA)" *J. Med. Chem.*, **2019**, *62*, 6785-6795
2. **Amogh Kulkarni**,‡ Ajay Kumar Sharma‡ and Harinath Chakrapani*, "Redox-Guided Small Molecule Anti-Mycobacterials" *IUBMB Life*, **2018**, *70*, 826-835 (‡ - Equal authorship)
3. Pooja Kumari, **Amogh Kulkarni**, Ajay Kumar Sharma and Harinath Chakrapani*, "Visible-Light Controlled Release of a Fluoroquinolone Antibiotic for Antimicrobial Photopharmacology" *ACS Omega*, **2018**, *3*, 2155-2160